

mRAD18Sc: a multifunctional protein in replicative damage bypass and gametogenesis

Roald van der Laan

ISBN: 90-9018032-X

DTP and graphical support: Tom de Vries Lentsch

Layout: Roald van der Laan, Tom de Vries Lentsch

Cover: Crystal Jelly, *Aequorea Victoria* the source of the green fluorescent protein
(photo by Dr Steven Haddock, Monterey, CA, USA).

Printed by: Optima Grafische Communicatie, Rotterdam

© R. van der Laan, 2004

No part of this book may be reproduced, stored in a retrieval system or transmitted in any form or by any means without permission of the author.

The copyright of the publications remains with the publishers.

The research described in this thesis was performed at the Medical Genetics Center South-West Netherlands-Department of Cell Biology and Genetics, Center for Biomedical Genetics and the Department of Reproduction and Development, within the Medical Genetics Cluster, Erasmus Medical Center Rotterdam, The Netherlands.



The printing of this thesis was financially supported by:

Carl Zeiss



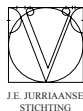
Abcam



The Dutch Cancer Society



The J.E. Juriaanse Stichting



The Dr. Ir. Van der Laar Stichting

mRAD18Sc: a multifunctional protein in replicative damage bypass and gametogenesis

mRAD18Sc: een multifunctioneel eiwit in replicative damage bypass en gametogenese

Proefschrift

ter verkrijging van de graad van doctor
aan de Erasmus Universiteit Rotterdam
op gezag van de Rector Magnificus
Prof.dr. S.W.J. Lamberts
en volgens besluit van het College voor Promoties

De openbare verdediging zal plaatsvinden op
woensdag 2 juni 2004 om 15.45 uur

door

Roald van der Laan

geboren te Tholen

Promotiecommissie

Promotor:

Prof.dr. J.H.J. Hoeijmakers

Overige leden:

Prof.dr. J.A. Grootegoed

Prof.dr. ir. A.A. van Zeeland

Dr. J.N.J. Philipsen

Co-promotoren:

Dr. H.P. Roest

Dr. W.M. Baarends

For Léonie

Contents

Scope of this thesis	7
Chapter 1. Expression and possible functions of DNA lesion bypass proteins in spermatogenesis <i>International Journal of Andrology</i> To be published, pending minor revisions	11
Chapter 2. Fluorescence microscopy techniques for live cell imaging	35
Chapter 3. Characterization of mRAD18Sc, a mouse homolog of the yeast post-replication repair gene RAD18 <i>Genomics, 69(1):86-94 (2000)</i>	53
Chapter 4. Spatio-temporal dynamics of the DNA damage replication bypass proteins mRAD18Sc and HR6B to stalled replication foci and UV-induced DNA lesions In preparation	69
Chapter 5. Ubiquitin ligase mRAD18Sc localizes to the XY body and to other chromosomal regions that are unpaired and transcriptionally silenced during male meiotic prophase <i>Journal of Cell Science</i> To be published, pending minor revisions	91
Chapter 6. Ubiquitinated H2A is associated with large silenced chromosome domains in mammalian mitotic and meiotic cells Submitted	115
Chapter 7. Concluding remarks and future prospects	135
Summary	147
Samenvatting	151
List of abbreviations	154
List of publications	155
List of presentations	156
List of meetings	157
List of courses	158
Curriculum vitae	159
Acknowledgements	160

Scope of this thesis

Integrity of the genome is of vital importance for life. DNA is constantly under attack from endogenous and exogenous DNA damaging agents. During each round of DNA replication, the replication machinery requires the presence of an intact DNA template. If a DNA lesion is encountered, progression of the replication process is at risk to be blocked. However, replicative damage bypass prevents termination of DNA replication. The proteins that act in replicative damage bypass are capable to operate as a temporary “stand-in” of the replication machinery. This process has been investigated in detail in the yeast *S. cerevisiae*, and it has become clear that the ubiquitin-conjugating enzyme RAD6 is a key factor in this process. To perform its function, RAD6 interacts with RAD18, an ubiquitin ligase. The aim of the research outlined in this thesis is to provide insight into the role of mammalian homologs of RAD6 and RAD18 in the process of replicative damage bypass (RDB) in somatic cells and during gametogenesis. The mammalian homologs are HR6A and HR6B for RAD6 and mRAD18Sc for RAD18. In this research, live cell imaging and fluorescence-based technologies are applied to study the subcellular localization and dynamics of fluorescently tagged HR6B and mRAD18Sc.

In **Chapter 1**, the origin of DNA lesions and consequences of lesions for the genome are discussed briefly. In addition, different DNA repair mechanisms involved in removal of DNA damage are described, and a detailed overview of the process of replicative damage bypass is given. The key players RAD6 and RAD18 in RDB and their mammalian homologs HR6A, HR6B and mRAD18Sc, are highlighted in the context of RDB, the ubiquitin system and gametogenesis. In this thesis several techniques are applied to study RDB proteins in living cells, and **Chapter 2** provides a schematic overview of fluorescence microscopy in living cells. In addition, advanced confocal microscopy techniques that are currently available to study the dynamics and interaction of fluorescently tagged proteins in living cells are explained. In **Chapter 3**, the identification and characterization of the mouse homolog of yeast *RAD18*, designated *mRAD18Sc*, is described. Interestingly, *mRAD18Sc* mRNA expression is highest in testis, in particular in spermatocytes and spermatids. We report the subcellular localization of fluorescently tagged mRAD18Sc protein and the chromosomal localization of the *mRAD18Sc* gene by fluorescent *in situ* hybridization. The subcellular localization throughout the cell cycle and after induction of DNA damage of fluorescently tagged HR6B and mRAD18Sc in living cells is presented in **Chapter 4**. Furthermore, association of these proteins with the replication machinery and recruitment to UV-induced DNA lesions is described. Finally, a novel technique that enables analysis of *de novo* assembly of proteins in chromatin-associated processes is presented. We studied expression of mRAD18Sc protein in spermatogenesis, as described in **Chapter 5**. This ubiquitin ligase appears to localize to unsynapsed and silenced chromosomal regions during the male meiotic prophase. This finding raised two new questions. First: is silencing of chromosomes or chromosome regions without a pairing partner during the meiotic prophase a general phenomenon that occurs in males as well as in females? Second: what is the possible function of mRAD18Sc in these silenced, unpaired chromosomal regions? These questions are addressed in **Chapter 6**. In **Chapter 7** the experimental work in this thesis and future prospects, are discussed.



Chapter 1

Expression and possible functions of DNA lesion bypass proteins in spermatogenesis

International Journal of Andrology
To be published, pending minor revisions

Expression and possible functions of DNA lesion bypass proteins in spermatogenesis

Roald van der Laan^{1,2}, Willy M. Baarends², Evelyne Wassenaar², Henk P. Roest¹, Jan H.J. Hoeijmakers¹ and J. Anton Grootegoed²

MGC-Department of Cell Biology and Genetics, Center for Biomedical Genetics¹ and Department of Reproduction and Development²
Erasmus MC, Erasmus University Rotterdam, Rotterdam, The Netherlands

Summary

In mammalian cells, there is a complex interplay of different DNA damage response and repair mechanisms. Several observations suggest that, in particular in gametogenesis, proteins involved in DNA repair play an intricate role in and outside the context of DNA repair. Here, we discuss the possible roles of proteins that take part in replicative damage bypass mechanisms (RDB), also known as postreplication DNA repair (PRR), in germ line development. In yeast, and probably also in mammalian somatic cells, replicative damage bypass (two sub-pathways: damage avoidance and translesion synthesis) prevents cessation of replication forks during the S phase of the cell cycle, in situations when the replication machinery encounters a lesion present in the template DNA. Many genes encoding key regulators of RDB and other proteins involved in RDB and its sub-pathways show an increased expression in testis, in particular in meiotic and post-meiotic spermatogenic cells. Several RDB proteins take part in protein ubiquitination, and we address relevant aspects of the ubiquitin system in spermatogenesis. RDB proteins might be required for damage avoidance and translesion synthesis of spontaneous DNA damage during gametogenesis. In addition, we consider the possible functional relation between translesion synthesis mechanism and the induction of mutations in spermatogenesis. Translesion synthesis requires the activity of highly specialized polymerases, and is an error-prone process, that may induce mutations. In evolutionary terms, controlled generation of a limited number of mutations in gametogenesis might provide a mechanism for evolvability.

DNA repair mechanisms

Defects in DNA repair mechanisms lead to an increased incidence of tumor formation, premature aging, and also in some tissues to dysregulation of development. In addition, defects in DNA repair mechanisms can cause dysregulation of gametogenesis. In the reproductive life cycle of mammalian species, DNA repair mechanisms play a role to safe-guard development of healthy offspring, which requires transmission of intact haploid genomes. However, this does not imply that germ line cells are a fully safe haven for DNA. For example,

meiotic recombination requires induction of DNA double strand breaks, and the occurrence of this type of DNA damage needs to be accorded. Also, it can be argued that there is a biological advantage for mutations to be generated in a controlled manner during gametogenesis and to be transmitted to the offspring, because this might contribute to genetic diversity among individuals of a species and thus to the evolvability of that species (Baarends et al., 2001; Friedberg et al., 2002). Taken together, in gametogenesis there needs to be an intricate balance of genome stability and instability, controlled by interplay of several DNA repair mechanisms.

The cellular DNA double helix is under constant attack by endogenous and exogenous factors that introduce a wide spectrum of DNA lesions (Figure 1). Evolution of life would not have been possible without the concurrent evolution of a variety of DNA repair mechanisms, which are found in relatively simple organisms such as bacteria and yeast, and also in virtually all cell types of mammalian organisms.

For many genes encoding proteins involved in the different complex DNA repair mechanisms, remarkable evolutionary conservation is found. Various multi-enzyme DNA repair mechanisms have been identified in eukaryotes from yeast to mammals: nucleotide excision repair (NER), base excision repair (BER), transcription-coupled repair (TCR), mismatch repair (MMR), double strand break repair either by homologous recombination (HR) or end-joining (EJ), and postreplication repair (PRR) (Hoeijmakers, 2001). The last mechanism does not repair DNA lesions, but comprises a series of events that allows DNA replication to proceed during S phase also when the replication machinery encounters a lesion. Hence, this mechanism would be aptly named: replicative damage bypass. Here, we propose the abbreviation RDB (for replicative damage byypass). The focus of this review is on possible functions of RDB proteins in gametogenesis. First, we give a very brief summary of the other DNA repair mechanisms.

NER is involved in removal of UV-induced lesions and bulky adducts. BER processes lesions induced by oxygen radicals and alkylating reagents. TCR deals with lesions that are encountered during transcription (Figure 1).

Of specific interest in relation to gametogenesis, is the mismatch repair (MMR) mechanism. This mechanism removes errors that are made during DNA replication, but which have escaped the proof-reading activity of the replicating DNA polymerase. MMR is directly coupled to DNA replication. In view of the many mitotic cell divisions that are required to produce spermatozoa, and to maintain spermatogenesis for many years during adult reproductive life (see Figure 2, and below), it is clear that MMR is important to maintain germ line genome integrity. In addition, several MMR proteins are critically involved in recombination events during the meiotic prophase. The Mlh1 protein localizes to late recombination nodules in the meiotic prophase (the so-called Mlh1 foci, see Figure 6A) (Baker et al., 1996). Mlh1 and also the protein Mlh3 are not specific for germ line cells, but deletion mutant mouse models for these two proteins are infertile, due to a meiotic arrest in oogenesis and spermatogenesis (Baker et al., 1996; Edelman et al., 1996; Lipkin et al., 2000; Lipkin et al., 2002). *Pms2* deletion only affects the male (Baker et al., 1995; de Vries et al., 1999; Edelman et al., 1999; Kneitz et al., 2000). Two meiosis-specific mammalian MMR proteins, Msh4 and Msh5, have been identified (Paquis-Flucklinger et al., 1997; Winand et al., 1998), and deletion of either the *Msh4* or the *Msh5* gene results in infertility in both males and females (Baker et al., 1995; de Vries et al., 1999; Edelman et al., 1999; Kneitz et al., 2000).

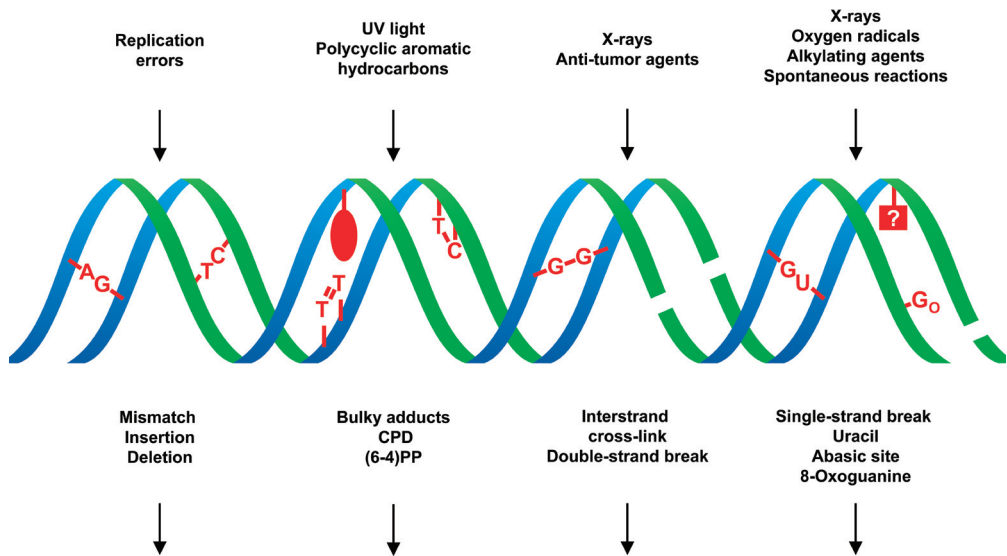


Figure 1. DNA repair mechanisms are involved in removal of a wide range of DNA lesions. The figure shows: damaging factors (top), DNA lesions (middle), and DNA repair mechanisms (bottom). The CPD (cyclobutane pyrimidine dimer) and (6-4)PP (6-4 photoproduct) are the major lesions induced by UV-C light. NER: nucleotide excision repair; BER: base excision repair; TCR: transcription-coupled repair; MMR: mismatch repair; HR: homologous recombination; EJ: end-joining. Not included in this figure are the replicative damage bypass mechanisms (RDB)

A DNA double strand break (DSB) can be repaired by a relatively simple mechanism, named non-homologous end joining. However, this mechanism is error-prone. A safer mechanism to repair DSB is based on homologous recombination. Homologous recombination repair can occur in somatic cells, and in association with meiotic recombination. DSBs are introduced by X-rays or arise from single strand breaks during DNA replication. However, during the meiotic prophase DSBs are introduced in a controlled manner by the meiosis-specific endonuclease Spo11 (Keeney et al., 1999; Keeney et al., 1997; Romanienko and Camerini-Otero, 1999). These DSBs are instrumental to effectuate meiotic recombination. DSB repair in the meiotic prophase requires homologous recombination repair, based on pairing between non-sister chromatids. This is different from what happens during DSB repair in somatic cells, where the repair involves sister chromatids. Meiosis-specific aspects of DSB repair are likely mediated by meiosis-specific variants of DSB repair proteins. One of these is Dmc1, a meiosis-specific Rad51 homolog, a protein involved in strand transfer during recombination. Deletion of the gene encoding Dmc1 in mice leads to female and male infertility, due to a defect in meiotic homologous chromosome pairing (Pittman et al., 1998; Shinohara and Ogawa, 1999; Yoshida et al., 1998). In addition, other DSB repair proteins, including Rad50, Rad51, Rad54, Rad54B, and Mre11, show increased expression in testis (Goedecke et al., 1999; Hiramoto et al., 1999; Shinohara et al., 1993; Wesloy, 2003). In meiosis, the error-prone end-joining mechanism is suppressed (Goedecke et al., 1999).

General aspects of the activity of DNA repair mechanisms in spermatogenesis are summarized in Figure 2. In females, a relatively low number of mitotic divisions occur during embryonic ovary development, preceding the

massive entry into meiosis of all oogonia present. These meiotic oocytes become arrested at the diplotene stage towards the end of the meiotic prophase, and are selectively recruited, during adult reproductive life, to grow and to proceed with the meiotic divisions in conjunction with ovulation and fertilization. Sperm production is associated with many more rounds of replication, which are necessary also in adult males for mitotic maintenance of the stem cell pool and expansion of the differentiating spermatogonia population. It has been suggested that males are the main source of germ line mutations, compared to females, and this effect would be augmented in older males (Crow, 2000; Hurst and Ellegren, 2002; Risch et al., 1987).

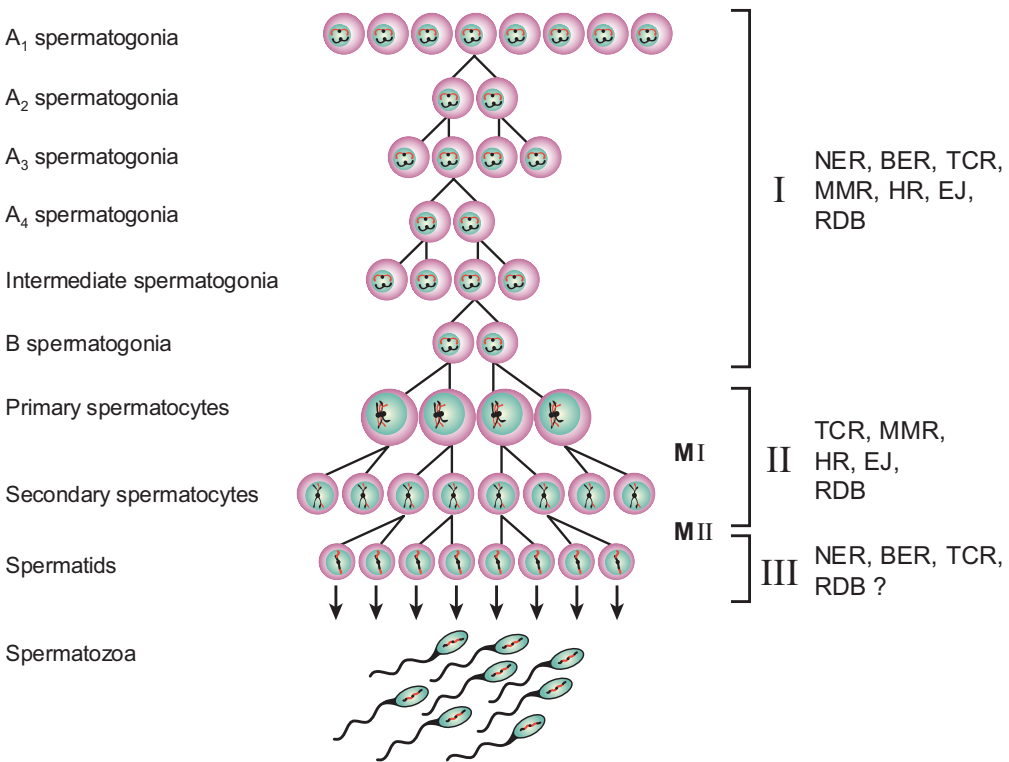


Figure 2. Schematic representation of spermatogenesis and DNA repair activities. I: Spermatogonia undergo multiple rounds of DNA replication, and DNA repair activities most likely are related to a great extent to the S phase in these cells. II: During the meiotic prophase, meiotic recombination takes place, and this process requires the activities of several enzymes that function in meiotic recombination and also in various DNA repair mechanisms. III: After completion of the meiotic divisions, post-meiotic repair might be required to remove persistent DNA lesions. In addition to DNA repair itself, progress of spermatogenesis through Phases I, II and III may also require actions of DNA repair proteins outside the context of DNA repair. MI and MII indicate the first and second meiotic divisions. NER: nucleotide excision repair; BER: base excision repair; TCR: transcription-coupled repair; MMR: mismatch repair; HR: homologous recombination; EJ: end-joining; RDB: replicative damage bypass.

For proteins that take part in meiotic homologous chromosome pairing and recombination, one would expect to see no profound functional differences between oogenesis and spermatogenesis. Yet, such differences are observed. Mouse mutants of at least 11 meiotic genes all result in remarkable sexual dimorphism in

meiotic phenotypes, indicating that sex makes a difference in meiosis (Hunt and Hassold, 2002). One important difference between the male and female meiotic prophase, is the presence of the heterologous pair of the X and Y sex chromosomes in spermatocytes. The X and Y chromosomes form a heterochromatic chromatin structure, the so-called XY body or sex body, during the meiotic prophase in spermatocytes. In this phase, the autosomes undergo homologous pairing, with the synaptonemal complex as a central element in between the chromosome cores. The sex chromosomes have only small regions of homology, the pseudoautosomal regions, and pairing between X and Y is limited to those regions. When the XY body is first formed, shortly after entry of the spermatocytes into the meiotic prophase, expression of most of the X- and Y-chromosomal genes is silenced, but re-expression of at least several of these genes occurs in haploid post-meiotic spermatids (Hendriksen et al., 1995; Monesi, 1965).

Post-meiotic development of the haploid spermatids involves many molecular and cellular processes that are absolutely unique to the male germ line. This development includes a dramatic change in chromatin structure, when histones are replaced by protamines and the nucleosomal chromatin structure is transformed into a highly compacted chromatin arrangement. This post-meiotic phase also requires activities of proteins that were identified as components of DNA damage response and repair mechanisms.

In addition to the DNA repair systems described above, several components of replicative damage bypass (RDB) appear to be implicated in control of different aspects of gametogenesis. This is discussed in the paragraphs below. In addition, some attention will be given to the ubiquitin system in relation to RDB and spermatogenesis, since several key components of RDB take part in protein ubiquitination pathways.

Key factors in RDB

The involvement of RDB mechanisms with DNA lesions starts at the very moment when the lesions block the S phase replication machinery. During duplication of the genome in the S phase of the cell cycle, the presence of lesions in the template DNA will slow down the replication machinery and interfere with cell cycle progression, eventually leading to cell death. When the number of lesions is limited, RDB is a useful mechanism to avoid arrest of the replication machinery at the site of the lesion. RDB can avoid stalling of the machinery, because it allows DNA replication to proceed over a damaged template. This is achieved by recruitment of specific polymerases to the lesion, which temporarily take over the strand elongation from the basal replication machinery (translesion synthesis) or by recombinational bypass mechanisms (damage avoidance). The actual lesion is not removed, but can be processed during the next cell cycle by other DNA repair mechanisms, such as NER or BER.

In yeast, the key genes involved in RDB encode members of the so-called RAD6 epistasis group. The *RAD6* gene codes for an ubiquitin-conjugating enzyme. Expression of the *RAD6* gene is strongly induced upon UV irradiation and during meiosis, and deletion of the gene leads to a very pleiotrophic phenotype including impaired sporulation and defects in gene silencing (Lawrence, 1994). The *RAD6* protein directly interacts with *RAD18*, another member of the *RAD6* epistasis group. Yeast *RAD18* harbors a RING-zinc-finger domain that is likely involved in protein-

protein interactions and is often found in proteins that take part in multi-protein complexes. In fact, the RING-zinc-finger is a hallmark of a group of ubiquitin ligases (Hatakeyama and Nakayama, 2003). Yeast *rad18* mutants are slightly less sensitive to UV irradiation compared to the *rad6* mutant, but do not show other obvious phenotypic characteristics outside the context of RDB. It should be noted that the process of RDB is initiated, most likely, by the key factors RAD6 and RAD18, and the RAD6-RAD18 complex is required for activity of both translesion synthesis and damage avoidance (Figure 3).

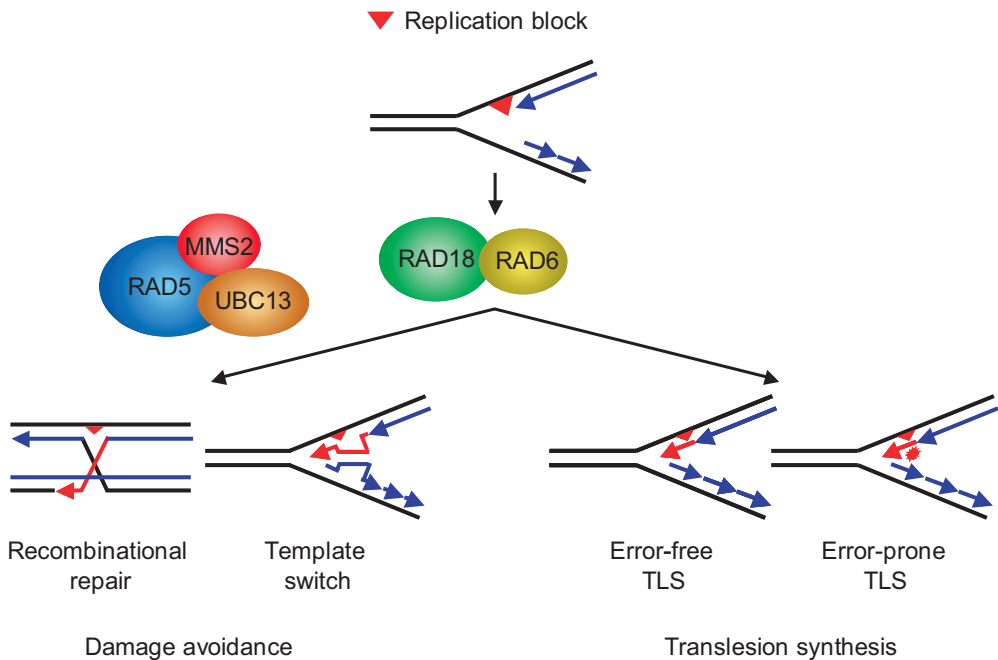


Figure 3. Lesion bypass mechanisms (RDB) during DNA replication. When a DNA lesion blocks the replication machinery, the RAD6-RAD18 complex is thought to be recruited to the site of the lesion, where it induces translesion synthesis (right) or damage avoidance (left) sub-pathways of RDB. Translesion synthesis (TLS) achieves replication past the damaged base(s) and thereby introduces a mutation (error-prone*) or insert the correct nucleotide (error-free). Damage avoidance, which requires recruitment of a MMS2-UBC13-RAD5 complex, is basically error-free, because undamaged homology from a newly synthesized daughter strand (template switch) or the other autosome (recombinational repair) is used to bypass the damaged template. The activity of the replication machinery is restored after the lesion bypass. Newly synthesized DNA is shown in blue (undamaged template) and red (damaged template).

Similar to the evolutionary conservation of other DNA repair pathways, homologs of RAD6 have been identified in higher eukaryotes (Table 1). In mammals, two highly conserved genes, *HR6A* (*Ube2a*) and *HR6B* (*Ube2b*), encode RAD6 homologs (Koken et al., 1991). Mouse models to study functional consequences of loss of *HR6A* and *HR6B* have been generated, and the single mutants do not show obvious phenotypical characteristics, besides defects in gametogenesis and early development that are described below (Roest et al., 1996; Roest et al., 2004). Complete deficiency of *HR6A/B* (double-knockout) is not a viable condition, indicating the importance of *HR6A/B* activities for essential

cellular functions (Grootegoed et al., 1998; Roest et al., 2004).

Also for yeast RAD18, homologs have been identified in higher eukaryotes (Tateishi et al., 2000; van der Laan et al., 2000; Xin et al., 2000). In human cells, overexpression of a dominant negative mutant of human RAD18, with a mutation in one of the conserved cysteine residues of the RING-finger domain, leads to increased sensitivity to various DNA damaging agents (Tateishi et al., 2000). When the *mRAD18Sc* gene is inactivated in mouse ES cells, these cells show hypersensitivity to multiple DNA damaging agents and a defect in RDB (Tateishi et al., 2003). Nothing is known about a role of mRAD18Sc in gametogenesis, because a *mRAD18Sc* knockout mouse has not been reported.

Two RDB sub-pathways: translesion synthesis and damage avoidance

Eukaryotic cells can make use of two strategies to perform DNA lesion bypass replication over a damaged template: translesion synthesis and damage avoidance (Figures 3 and 4) (Baynton and Fuchs, 2000). Translesion synthesis (TLS) involves activity of highly specialized TLS polymerases that are able to incorporate nucleotides opposite a lesion in an error-free or an error-prone manner, dependent on the specific TLS polymerase and the type of the lesion. Damage avoidance is a strategy that uses homology to bypass the lesion. Basically, this damage avoidance is an error-free mechanism, in which the homologous template is derived from the newly made daughter strand (template switch) or from the homologous chromosome (recombinational repair). However, most of the experimental data that are presently available concern the TLS sub-pathway.

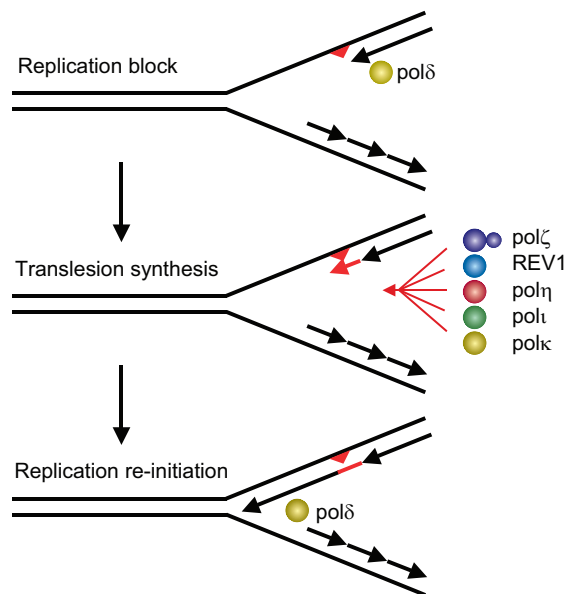


Figure 4. Translesion synthesis (TLS) in mammalian cells. The replicative DNA polymerase (pol δ) stalls at a lesion in the template, translesion synthesis is activated by RAD6-RAD18, and specialized polymerases (pol ζ , η , ι , κ and/or REV1) synthesize a DNA strand opposite and beyond the lesion, dependent on the type of lesion. The replicative DNA polymerase (pol δ) takes over again, and the replication process is continued.

Translesion synthesis (TLS) polymerases

TLS polymerases are not highly efficient in accurate DNA replication and also lack proof-reading activity (Kunkel et al., 2003). TLS is achieved by a subset of at least five TLS polymerases in higher eukaryotes (Figure 4), of which pol η , pol ι , pol κ , and REV1 are members of the Y-family of polymerases (Ohmori et al., 2001), and pol ζ is related to the classic replicative DNA polymerases (Morrison et al., 1988). Replicative DNA polymerases are not capable of bypassing lesions that cause helix distortions, because only a single unpaired template base fits into the active site of the enzymes, and these polymerases have high fidelity properties to only accept the four geometrically equivalent Watson-Crick base pairs (Doublet et al., 1998; Kunkel et al., 2003; Prakash and Prakash, 2002). The Y-family polymerases do not show a high degree of similarity at the amino acid level, but their general conformational structures harbor the characteristic finger-, thumb-, and palm domains that are also present in all known DNA polymerases (Lehmann, 2002). In addition, a fourth domain is present in the Y-family polymerases, the little finger- or polymerase-associated domain (Ling et al., 2001; Trincao et al., 2001). The pol η structure has been modeled for the protein in association with DNA, and this modeling indicates that the active site is very open and flexible, which allows altered bases in the template to be accommodated in the active site (Lehmann, 2002; Ling et al., 2001; Trincao et al., 2001). TLS polymerases have low processivity and low fidelity, dependent on the type of lesion compared to replicative DNA polymerases. For example, pol η efficiently bypasses a UV-induced cyclobutane dimer (CPD), but pol κ does not bypass CPDs and has different lesion specificity (Haracska et al., 2002b). Pol ι is able to insert a nucleotide opposite a lesion but does not extend from that point, and a second TLS polymerase, for example pol ζ , is required to complete TLS (Guo et al., 2001; Johnson et al., 2000; Prakash and Prakash, 2002; Tissier et al., 2000).

The yeast genes encoding the TLS polymerases can be listed as follows: *RAD30* codes for pol η , the *REV3* and *REV7* gene products together form pol ζ , the gene *REV1* encodes a deoxycytidyl (dCMP) transferase (Gerlach et al., 1999; Woodgate, 1999). In higher eukaryotes, two *RAD30* homologs have been identified: *RAD30A* coding for pol η and *RAD30B* coding for pol ι (Masutani et al., 1999; McDonald et al., 1999). The *RAD30A* gene is mutated in xeroderma pigmentosum variant (XPV) patients, a severe human disorder with affected individuals being prone to UV-induced skin cancer, increased incidence of internal tumors, and accelerated neurodegeneration (Hoeijmakers, 2001; Masutani et al., 1999). XPV cells have a defect in intact daughter strand synthesis after treatment with various DNA damaging agents (Boyer et al., 1990; Cordonnier et al., 1999; Lehmann, 1975; Misra and Vos, 1993; Park and Cleaver, 1979). A readily available mouse model is the 129-derived strain, in which the *RAD30B* gene appears to carry an endogenous mutation in exon 2 resulting in a premature stop codon (McDonald et al., 2003). Although recent studies suggest that pol ι is involved in somatic hypermutation of the variable regions of immunoglobulin genes, the mutation spectrum and frequency in the 129-derived mice were not found to be different from *RAD30B* proficient mice, and no human disorder or repair-related deficiency has been linked to defects in the *RAD30B* gene (Faili et al., 2002; McDonald et al., 2003). Pol η (*RAD30A*) and pol ι (*RAD30B*) associate with the replication machinery and accumulate at stalled replication forks after DNA damage induction (Kannouche et al., 2001; Kannouche et al., 2002). The two TLS polymerases physically interact

and experimental data suggest that pol η is involved in targeting pol ι to the replication machinery (Kannouche et al., 2002). Proliferating Cell Nuclear Antigen (PCNA), a DNA polymerase sliding clamp involved in DNA replication and repair, stimulates activity of both pol η and pol ι , and a PCNA binding site is located within the C-terminal part of pol η (Haracska et al., 2001a; Lehmann, 2002).

Pol κ is the mammalian homolog of the *Escherichia coli* TLS polymerase DINB (Gerlach et al., 1999; Ogi et al., 1999). This TLS polymerase, like pol η , is stimulated by PCNA, and has a different lesion specificity compared to pol η and pol ι (Haracska et al., 2002b; Zhang et al., 2000). Recent studies have shown that pol κ is an efficient extender of mispaired primer termini, and pol κ might be involved, therefore, in the extension step in TLS (Washington et al., 2002). Overexpression of pol κ in mouse cells results in an elevated spontaneous mutation frequency of the *Hprt* gene (Ogi et al., 1999). The Pol κ mRNA level is upregulated after exposure to UV, and pol κ deficient cells isolated from gene knockout mice are more sensitive to UV irradiation compared to wild type cells (Schenten et al., 2002; Velasco-Miguel et al., 2003).

REV3 is the catalytic subunit of pol ζ and is tightly associated with REV7, a protein that does not share any known domains with other proteins, but significantly stimulates the polymerase activity of REV3 (Lawrence and Hinkle, 1996; Morrison et al., 1989; Torpey et al., 1994). It has been reported that pol ζ can incorporate nucleotides opposite UV-induced lesions but with a very low efficiency (Guo et al., 2001; Nelson et al., 1996b). However, pol ζ efficiently extends from bases that are incorporated opposite lesions, including abasic sites, and is therefore likely involved in the extension step in TLS, similar to pol κ (Haracska et al., 2001b). The *REV3I* (mouse homolog of *REV3*) gene has been genetically inactivated (mouse gene knockout) by several groups, and all research groups report an embryonic lethal phenotype, but whether this is directly related to a defect in TLS or represents a functional consequence of loss of other REV3I functions, is not known (Bemark et al., 2000; Esposito et al., 2000; Van Sloun et al., 2002; Wittschieben et al., 2000). Homologs of *REV7* in higher eukaryotes have also been isolated (Murakumo et al., 2000). New findings showed that REV7 interacts not only with REV3, but also with REV1, and that it has a role in cell cycle control in *Xenopus* (Murakumo, 2002). Finally, REV1 is also required for UV-induced mutagenesis and can be considered as a member of the Y-family of polymerases. However, REV1 does not act as a template DNA polymerase, but rather is involved in inserting dCMPs opposite abasic sites *in vitro* (Haracska et al., 2002a; Lemontt, 1971; Nelson et al., 1996a). In DT40 cells, deletion of *REV1* leads to reduced growth and increased sensitivity to a wide range of lesion-inducing agents. In these mutant cells, chromosome breakage is increased after UV exposure as a result of defective gap replication (Simpson and Sale, 2003).

Damage avoidance

The current models for damage avoidance, based on studies in yeast, remain hypothetical. Several mechanistic models for damage avoidance have been proposed (Baynton and Fuchs, 2000). It appears that this error-free RDB sub-pathway requires a second ubiquitin-conjugating complex, in addition to RAD6-RAD18 (Broomfield et al., 1998). MMS2 is an Ubc-like (Ubc stands for: ubiquitin-conjugating) protein, but it lacks the essential active cysteine residue required for

ubiquitin-conjugating activity. Rather, MMS2 forms a stable complex with UBC13, which does carry ubiquitin-conjugating enzyme activity (Broomfield et al., 1998; Sancho et al., 1998). In yeast, deletion of MMS2 or UBC13 results in sensitivity to DNA damaging agents and an increased spontaneous mutation rate (Broomfield et al., 1998; Brusky et al., 2000; Hofmann and Pickart, 1999). The RING-finger protein RAD5 is required for this activity, and functions as a ubiquitin ligase for the MMS2-UBC13 complex (Hofmann and Pickart, 1999; Torres-Ramos et al., 2002). RAD5 is a DNA-dependent ATPase and recruits the MMS2-UBC13 complex to chromatin by means of its RING-finger domain (Johnson et al., 1994; Ulrich and Jentsch, 2000).

Mammalian homologs of *MMS2* and *UBC13* have been identified (Ashley et al., 2002; Franko et al., 2001; Xiao et al., 1998; Yamaguchi et al., 1996). The two mammalian *MMS2* homologs, *hMMS2* and *CROC1*, both correct the yeast *mms2* mutant regarding sensitivity to DNA damaging agents and spontaneous mutagenesis (Franko et al., 2001; Xiao et al., 1998).

Expression of RDB proteins in testis

Table 1 summarizes the mammalian homologs that have been identified for yeast proteins involved in RDB. The mRNA level and in some cases the protein level of the listed RDB components are found elevated in testis, and alternative transcripts exclusively present in testis have been detected for some RDB genes. This does not provide any direct evidence for functional importance, but contributes to our working hypothesis that there might be a special relationship between RDB proteins and spermatogenesis.

Yeast gene	Mammalian homolog	Functions of encoded proteins
<i>RAD6</i>	<i>HR6A, HR6B</i>	Ubiquitin-conjugating enzyme
<i>RAD18</i>	<i>mRAD18Sc</i>	Ubiquitin-ligase
<i>RAD5</i>		Ubiquitin-ligase
<i>UBC13</i>	<i>hUBC13</i>	Ubiquitin-conjugating enzyme
<i>MMS2</i>	<i>hMMS2</i>	Ubiquitin-conjugating enzyme-like
<i>RAD30</i>	<i>RAD30A, RAD30B</i>	Pol η (XPV), Pol ι
<i>REV1</i>	<i>hREV1</i>	Deoxycytidyl transferase
<i>REV3</i>	<i>REV3L</i>	Catalytic subunit pol ζ
<i>REV7</i>	<i>hREV7</i>	Subunit pol ζ

Table 1. Several prominent members of the yeast RAD6 epistasis group of genes involved in RDB.

All known TLS polymerases show a higher expression in testis compared to tissues that contain only somatic cells. Pol η and pol ι are highly expressed in mouse testis, and *in situ* hybridization using pol ι probes showed that the mRNA encoding this polymerase is predominantly expressed in round spermatids (McDonald et al., 1999; Yamada et al., 2000). This is surprising since DNA replication is completed in these cells. Low levels of these TLS polymerases in mitotically dividing spermatogonia could be involved in mutagenesis. The relative high levels of pol ι in

round spermatids might involve post-meiotic repair of persistent lesions or another unknown role outside the context of RDB. However, a direct and critical role for *poli* in spermatogenesis is not likely, since 129-derived mice, which were found to be deficient in functional *poli*, are normally fertile (McDonald et al., 2003). At the subcellular level, *poli* in the germ line cells may colocalize with *pol η* , as has been found for somatic cells where *pol η* shuttles *poli* to the replication machinery. The expression pattern of *polk* has been studied more extensively than those of *pol η* and *poli*, and the mRNA level is elevated in mouse testis (Velasco-Miguel et al., 2003). Both *in situ* hybridization and immunohistological staining using *polk* specific probes and antibodies, revealed that *polk* is most abundant in pachytene spermatocytes and round spermatids (Velasco-Miguel et al., 2003). *Polk* deficient mice are fertile and the overall histology of the testis from these mice is indistinguishable from wild type testis (Schenten et al., 2002). However, although analysis of the phenotype of these mice did not reveal a detectable function for *polk* in spermatogenesis, it can not be excluded that *polk* might play a yet unknown role in spermatogenesis. The two protein components of *pol ζ* , encoded by the genes *REV3* and *REV7*, are highly expressed in testis, but deletion of the *REV3l* gene in mice is a lethal condition, and the possible function of this gene in testis remains unclear (van Sloun et al., 1999; Van Sloun et al., 2002). Mouse models for the *REV7* gene have not been reported, but the *REV7* mRNA level is elevated in human testis (Murakumo et al., 2000). Finally, the *REV1* mRNA level is also very high in human testis (Murakumo et al., 2001), but also for this gene a mammalian null mutation or mouse knockout has not been reported.

Like many of the LTS polymerases discussed above, the genes that encode proteins involved in the damage avoidance sub-pathway of RDB are also markedly expressed in mammalian testis. Both *UBC13* and *MMS2* mRNA levels are elevated in mouse testis, and a testis-specific *CROC1* transcript is present in the mouse (Ashley et al., 2002; Franko et al., 2001). However, as yet we have little information about possible functions of *MMS2* and *UBC13* in spermatogenesis.

RDB and protein ubiquitination

Most likely, *RAD6-RAD18* and *MMS2-UBC13-RAD5* are essential for initiation of RDB (both sub-pathways) and for the activity of the damage avoidance sub-pathway of RDB, respectively. Since *RAD6-RAD18* and *MMS2-UBC13-RAD5* are ubiquitin-conjugating complexes, it is clear that we need to take a closer look at protein ubiquitination.

The 76 amino acid small ubiquitin moiety is present in all eukaryotic cells, and the ubiquitin system is essential to all cells. The covalent attachment of ubiquitin molecule(s) to target proteins involves a multi-step enzymatic process (Figure 5). First, ubiquitin is activated by an ubiquitin-activating enzyme (E1) (Handley et al., 1991; Stephen et al., 1997; Weissman, 2001). The activated ubiquitin is then transferred to the active cysteine residue of an ubiquitin-conjugating enzyme (E2). About 20 different E2s are known, but only two E1 enzymes have been identified, which implies that each E1 enzyme provides activated ubiquitin for multiple E2s (Hershko and Ciechanover, 1998; Weissman, 2001). The substrate specificity of the final protein ubiquitination step is determined by a specific ubiquitin ligase (E3) that interacts with the ubiquitin-bound E2 and brings it to the substrate, to allow transfer of the activated ubiquitin moiety to a lysine residue in the target protein.

However, direct transfer of activated ubiquitin to the substrate without the help of an E3 is also possible.

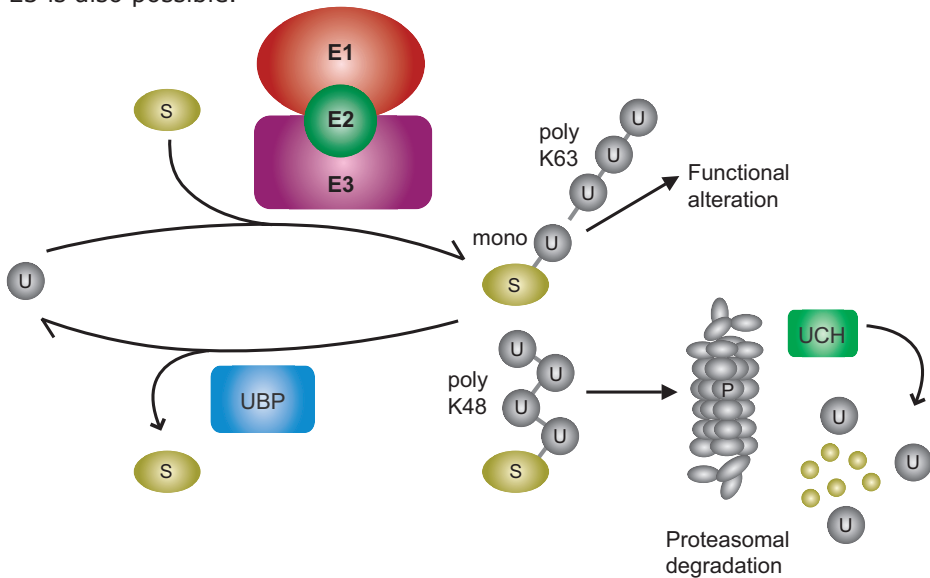


Figure 5. The ubiquitin system. Covalent attachment of ubiquitin (U) to a target substrate (S) involves successive activity of three different enzymes: ubiquitin-activating enzyme (E1), ubiquitin-conjugating enzyme (E2), and ubiquitin ligase (E3). Substrates can be poly-ubiquitinated via a Lys 48 (K48)-linked multi-chain and recognized by the proteasome (P) for degradation. Intact ubiquitin molecules can be removed from peptides by ubiquitin carboxyl-terminal hydrolases (UCH) and recycled. Mono-ubiquitination and Lys 63 (K63)-linked multi-chain poly-ubiquitination has other consequences for the target substrate, such as alteration of protein function. Ubiquitin-specific processing proteases (UBP) can remove ubiquitin moieties from intact proteins, thereby counteracting the E1-E2-E3 machinery.

The group of E3 enzymes is very large, and 3 families have been defined, composed of HECT type E3s, RING-finger type E3s, and the recently discovered U-box type E3s (Hatakeyama and Nakayama, 2003). Poly-ubiquitination (K48-linked) of substrate proteins targets these proteins for breakdown by the 26S proteasome, and mono-ubiquitination and poly-ubiquitination (K63-linked) involves targeting proteins for non-proteasome-dependent changes of their functions. These changes include direct alterations of function, changes related to endocytosis, and mediation of protein-protein interactions (Ciechanover, 1994; Hershko and Ciechanover, 1998; Pickart, 2004; Jentsch and Schlenker, 1995; Pickart, 2000; Varshavsky, 1997). Ubiquitin can be removed from poly-ubiquitin chains or small proteins by deubiquitination enzymes (DUBs) of the ubiquitin carboxyl-terminal hydrolase (UCH) type, and thereby initiate ubiquitin recycling (Wilkinson, 1997). A second family of DUBs, the ubiquitin-specific processing proteases (UBPs), have a broader specificity and several UBPs are involved in cleaving ubiquitin of intact proteins by means of editing inappropriately ubiquitinated proteins or a reverse ubiquitination process, thereby competing with the E1-E2-E3 machinery, likely for regulatory purposes (McBride et al., 2003).

When required, the ubiquitin system is quite capable of catalyzing massive breakdown of proteins, next to a multitude of roles exerted by controlled modification and/or breakdown of specific low-abundance proteins, such as proteins involved in cell cycle control (Varshavsky, 1997). In spermatogenesis, bulk protein

ubiquitination is probably required for the turnover of nuclear proteins during the post-meiotic histone-to-protamine transition, which takes place in elongating spermatids which start to undergo condensation of the haploid nucleus. Regulation of the nucleosomal structure by histone modification through ubiquitination is a general phenomenon in mammalian cells, and the amount of ubiquitinated histones is increased in spermatocytes and elongating spermatids in the mouse, where it may play a role in chromatin rearrangements (Baarends et al., 1999a; Baarends et al., 2000; Nickel et al., 1989). There are many observations on germ cell-specific or -enhanced expression of components of the ubiquitin system in spermatogenesis (Baarends et al., 2000). In fact, increased or exclusive expression of specific E2s has been found in mammalian germ line cells (Koken et al., 1996; Kovalenko et al., 1996; Wing et al., 1996; Wing and Jain, 1995; Yamaguchi et al., 1996; Yasugi and Howley, 1996).

A recently identified target for the RAD6-RAD18 and MMS2-UBC13-RAD5 complexes is the DNA polymerase clamp loader PCNA (Hoegel et al., 2002). In the presence of DNA damage, PCNA is mono-ubiquitinated at lysine residue 164 (K164) by RAD6-RAD18, and this modification also stimulates the TLS sub-pathway of RDB by pol ζ and pol η (Hoegel et al., 2002; Stelter and Ulrich, 2003). The MMS2-UBC13-RAD5 complex can form a K63-linked multi-chain of ubiquitin molecules on PCNA and induce the error-free damage avoidance pathway (Hoegel et al., 2002; Stelter and Ulrich, 2003). A small ubiquitin-related modifier (SUMO) can be conjugated to protein substrates, in a manner similar to ubiquitin conjugation (Bernier-Villamor et al., 2002; Hochstrasser, 2002). During normal DNA replication, PCNA is SUMO-modified by UBC9 (SUMO-conjugating enzyme), also at Lys 164 (Hoegel et al., 2002; Stelter and Ulrich, 2003). Another interesting finding is that pol ζ is stimulated by SUMO-modified PCNA, and therefore might be involved in generating spontaneous mutations in the absence of DNA damage (Stelter and Ulrich, 2003). Thus, three different modifications can occur at Lys 164 of PCNA (mono- or poly-ubiquitination, or SUMO-ylation). These modifications label PCNA for alternative functions and ubiquitination, and SUMO-modification appear to compete for the Lys 164 side chain, dependent on the presence or absence of DNA damage (Hoegel et al., 2002; Stelter and Ulrich, 2003). Mono-ubiquitination of PCNA has been detected after treatment of HeLa cells with the cross-linking agent mitomycin C (Hoegel et al., 2002), and poly-ubiquitination and/or SUMO-ylation of PCNA are possibly also conserved between yeast and man.

A known target for RAD6 outside the context of RDB in yeast is histone H2B. It has been reported that ubiquitination of H2B in yeast is dependent on RAD6, and that this histone modification is essential for sporulation (Dover et al., 2002; Robzyk et al., 2000). Highly specific post-translational modifications of histone proteins, by acetylation, methylation, phosphorylation, and ubiquitination of specific amino acid residues, and combinations of these, make up the so-called histone code (Strahl and Allis, 2000). This histone code is involved in rapid adjustments of gene expression as a response to developmental, physiological and environmental stimuli, and plays a major role as carrier of epigenetic information (Fischle et al., 2003a; Fischle et al., 2003b). RAD6 in yeast is essential for histone modifications in the context of the histone code. In yeast, mono-ubiquitination of H2B is a prerequisite for methylation of histone H3 at lysine residues 4 and 79, and these modifications are often associated with active or permissive chromatin (Dover et al., 2002; Fischle et al., 2003b; Ng et al., 2002; Robzyk et al., 2000; Sun and Allis, 2002). The function of RAD6 to ubiquitinate histone H2B as an important

first step in trans-histone control of some aspect of the histone code, might be conserved between yeast and mammals.

Role for RDB in spermatogenesis?

Function for the mammalian homologs of RAD6 and RAD18 outside the context of RDB?

As discussed above, RAD6-RAD18 most likely acts as the key protein complex that controls initiation of RDB. When we look at the mammalian homologs of RAD6, it is clear that both genes *HR6A* and *HR6B* are ubiquitously expressed in the mouse, but higher expression levels are found in brain and heart for both *HR6A* and *HR6B*, and *HR6B* expression is elevated in testis (Koken et al., 1996). The *HR6A* and *HR6B* proteins are 96% identical at the amino acid level, but the function of both proteins appears to be different in male and female gametogenesis, although we need to consider a possible dosage effect (Koken et al., 1991; Roest et al., 1996; Roest et al., 2004). In somatic cells the *HR6A/HR6B* protein ratio is around 1. In contrast, in spermatogenesis, in particular in the haploid spermatids that are formed by the meiotic divisions, the *HR6A/HR6B* protein ratio is <1 , and in oocytes we observed a ratio >1 (Baarends et al., 1999b; Koken et al., 1996).

Targeted disruption of *HR6A* results in infertility, related to an apparent role of *HR6A* as a maternal factor (Roest et al., 2004). Despite normal ovarian histology and ovulation in the *HR6A*-deficient mice, fertilized oocytes fail to develop beyond the two-cell stage of early embryogenesis (Roest et al., 2004). Deletion of *HR6B* on the other hand, results in impaired spermatogenesis and male infertility, and the *HR6B*-deficient female mice show normal fertility. A marked morphological sign of impaired spermatogenesis in *HR6B*-deficient testis is found during post-meiotic development of the spermatids. The nuclear elongation and condensation are severely affected, and only a limited number of highly abnormal spermatozoa are found in the epididymis (Roest et al., 1996). This aspect of the phenotype could be related to impairment of the histone-to-protamine transition that normally occurs in developing spermatids to remove the histones from the chromatin (Baarends et al., 2000). Evidently, in view of the RAD6-dependent ubiquitination of histone H2B which impacts on the histone code and sporulation in yeast (Robzyk et al., 2000), it would be relevant to look at ubiquitination of H2B in mammalian spermatogenesis. However, in mammalian cells, H2B ubiquitination is much less abundant than ubiquitination of H2A, and no information on a change in ubiquitination of H2B has been obtained. Also, no marked change in ubiquitination of histone H2A was detected, in spermatogenic cells of *HR6B*-deficient mice compared to wild type mice (Baarends et al., 1999a).

Still, a function for *HR6B* in spermatid development is likely, since the relative high level of *HR6B* protein in spermatids corresponds with a high demand for the ubiquitin system during post-meiotic development (Koken et al., 1996). However, it appears that the sequence of events is more complicated, because *HR6B* has additional functions in the meiotic prophase. We observed increased apoptosis of primary spermatocytes during the first wave of spermatogenesis in *HR6B*-deficient testis, indicating an essential role for *HR6B* in spermatocytes that are in the meiotic prophase. Major changes in the synaptonemal complex are detected in *HR6B* knockout spermatocytes (Baarends et al., 2003). The synaptonemal complex (SC) is a zipper-like structure that is assembled between homologous chromosomes in

meiotic prophase (Heyting, 1996). In HR6B-deficient cells, the structure of the SC complex appeared to be changed, resulting in lengthening of the complex and depletion of the SC protein SCP3 from near telomeric regions. Interestingly, we also found an increase (20-25%) of the crossing-over frequency in HR6B-deficient spermatocytes compared to wild type cells. These observations indicate a specific requirement for the ubiquitin-conjugating activity of HR6B in relation to chromatin dynamics and meiotic recombination in primary spermatocytes (Baarends et al., 2003).

Yeast *rad6* mutants show defective sporulation, but no evident role for RAD18, the RAD6 complex partner, in sporulation has been reported (Lawrence, 1994) (Robzyk et al., 2000). In addition, the RAD6 dependent H2B ubiquitination that is essential for sporulation seems to be RAD18 independent in yeast (Dover et al., 2002). However, when *rad18* mutant yeast strains also carry mutations in genes involved in excision repair, this results in reduced spore viability, which suggests that RAD18 might play some role in meiosis (Dowling et al., 1985).

Recently, we identified the mouse *mRAD18Sc* gene and found that this gene is highly expressed in testis, and in particular in spermatocytes (van der Laan et al., 2000). Such selective expression was not expected, because it is anticipated that *mRAD18Sc* plays a ubiquitous role in RDB in virtually all cell types. We have generated anti-*mRAD18Sc* antibodies, to study *mRAD18Sc* protein localization in mouse spermatogenesis (van der Laan et al., unpublished). Immunohistochemical staining of mouse and human testis cross sections revealed that *mRAD18Sc* is highly abundant in primary spermatocytes at the pachytene stage of the meiotic prophase (van der Laan et al., unpublished). In these primary spermatocytes, marked *mRAD18Sc* staining is observed, in particular for the XY body (Figure 6B). This is an interesting finding, and we would like to suggest that *mRAD18Sc*, in complex with HR6B (and possibly also HR6A) plays a specific role in functional aspects of the XY body. With respect to this role, several observations indicate this might be a role outside the context of RDB. To evaluate this, we studied whether or not the XY body contains other proteins, which take part in translesion synthesis or damage avoidance RDB sub-pathways. Immunocytochemical analysis using antibodies targeting several proteins involved in one of the RDB sub-pathways was applied, to study whether or not such proteins might be present at a relatively high concentration in the XY body chromatin. The results of these experiments showed that the studied proteins are much less abundant or absent from the XY body, compared to autosomal chromatin in other nuclear regions, indicating that, in the XY body, *mRAD18Sc* indeed may perform a function outside the context of RDB (van der Laan et al., unpublished).

As discussed above, in yeast, histone H2B ubiquitination is RAD6-dependent but RAD18-independent, and this histone modification is essential for changes in chromatin dynamics in relation to gene silencing and sporulation (Dover et al., 2002; Robzyk et al., 2000). However, ubiquitination of H2B is not a prevalent type of histone modification in mammalian cells, and the HR6A/B-*mRAD18Sc* complex might be involved in ubiquitination of other histones. A high level of ubiquitinated histone H2A (ubi-H2A) is present in mouse testis, and immunostaining shows that in particular the XY body contains a high concentration of ubi-H2A (Figure 6C) (Baarends et al., 1999a). This staining of the XY body is not decreased in HR6B-deficient spermatocytes, but these cells still contain HR6A. Hence, it is not excluded that ubiquitination of histone H2A in the XY body is carried out by HR6A/B-*mRAD18Sc*, and this ubiquitination might take part in regulation of chromatin

dynamics associated with formation and/or maintenance of the XY body. However, it appears more likely that the HR6A/B-mRAD18Sc complex is involved in the ubiquitination of yet unknown chromatin-associated substrates present in the XY body.

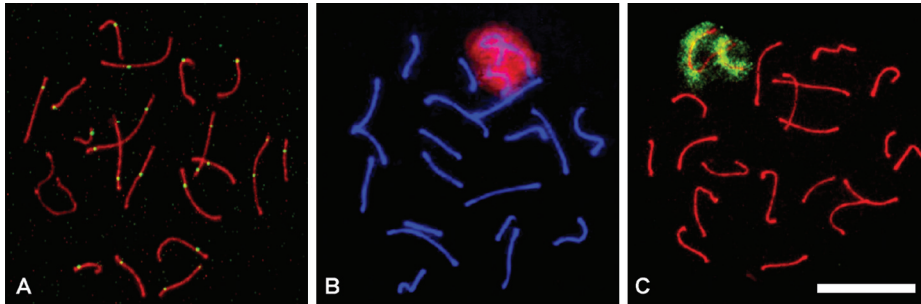


Figure 6. Immunohistochemical staining of nuclei (spread preparations) of mouse primary spermatocytes in the pachytene stage of the prophase of the meiotic divisions. The mismatch repair protein Mlh1 localizes to recombination nodules in pachytene nuclei (A). The condensed XY body, containing the X and Y chromosomes, shows marked staining for mRAD18Sc (B) and ubiquitinated histone 2A (ubi-H2A) (C). The synaptonemal complex between the paired homologous chromosomes is immunostained with anti-SCP3 (red in A and C and blue in B). The proteins Mlh1, mRAD18Sc, and ubi-H2A are immunostained with anti-Mlh1 (green), anti-mRAD18Sc (red), and anti-ubi-H2A (green), respectively. Scale bar: 20 μ m.

Translesion synthesis as a mechanism to induce mutations in the male germ line?

For a long time, the human genome was thought to harbor around 100,000 protein-coding genes, but after complete sequencing of the human genome, it became apparent that the number of genes is lower than expected. The approximate number of protein-coding genes is in the range of 25-30,000, only about 10,000 more than the nematode *Caenorhabditis elegans* (Claverie, 2001). This raises the question which mechanisms contribute to the high complexity of the most evolved species. It appears that many mammalian genes encode more than one protein. In addition, evolution can result in gene products having multiple functions in multiple pathways. When comparing yeast to mammals, at least five translesion synthesis polymerases are present in mammals and three in yeast (Table 1 and Figure 4). This is not a staggering difference. However, the mammalian TLS polymerases may perform multiple functions in different cell types, as compared to a relatively simple assignment of tasks to the yeast enzymes.

Biochemical analysis of the properties of TLS polymerases has revealed that these enzymes can repair DNA in a more or less error-prone manner, dependent on the type of lesion that is bypassed. In fact, TLS polymerases appear to be very error-prone when they operate on an undamaged template, which might be implicated in generation of mutation hotspots (Holbeck and Strathern, 1997; McGill et al., 1998). There are also indications that during the repair of double strand breaks, the invading strand is bound to TLS polymerases, with mutagenic consequences (Friedberg et al., 2002). TLS polymerases are involved in somatic hypermutation of immunoglobulin genes, where nucleotide changes are introduced in the variable regions (Gearhart and Wood, 2001; Weill et al., 2002). Pol ζ is essential for this process and inhibition of this TLS polymerase results in inhibition of somatic hypermutation (Zan et al., 2001). Interestingly, in XPV patients, lacking

functional pol η , the frequency of somatic hypermutation is unaffected but the spectrum of mutations is changed, favoring the idea of a two-polymerase affair in which two TLS polymerases collaborate by means of insertion and extension (Prakash and Prakash, 2002; Zeng et al., 2001). We feel that it is warranted to consider the possibility that TLS polymerases, highly expressed in spermatogenic cells, might play a role in mutagenic activity during the mitotic proliferation phase of spermatogenesis and in the meiotic prophase, when double strand breaks are generated to allow homologous recombination of the paired chromosomes. Alternatively, TLS polymerases might be required for TLS of spontaneous DNA lesions in spermatogenesis.

The impact of RDB and the functional implications with regard to specific aspects of spermatogenesis is still a wide open field with a lot of intriguing questions and much room for speculation. Nevertheless, the available experimental evidence provides several interesting clues for further exploration this complex field of research. Application of new technical developments, including the generation of conditional knockout animal models for RDB genes and knock-in mice expressing fluorescently-tagged RDB proteins will result in new insights in the activities of RDB proteins in spermatogenesis.

Acknowledgements

This work was supported by the Dutch Cancer Foundation (EUR 99-2003).

References

- Ashley, C., Pastushok, L., McKenna, S., Ellison, M. J., and Xiao, W. (2002). Roles of mouse UBC13 in DNA postreplication repair and Lys63-linked ubiquitination. *Gene* **285**, 183-191.
- Baarends, W. M., Hoogerbrugge, J. W., Roest, H. P., Ooms, M., Vreeburg, J., Hoeijmakers, J. H., and Grootegoed, J. A. (1999a). Histone ubiquitination and chromatin remodeling in mouse spermatogenesis. *Dev Biol* **207**, 322-333.
- Baarends, W. M., Roest, H. P., and Grootegoed, J. A. (1999b). The ubiquitin system in gametogenesis. *Mol Cell Endocrinol* **151**, 5-16.
- Baarends, W. M., van der Laan, R., and Grootegoed, J. A. (2000). Specific aspects of the ubiquitin system in spermatogenesis. *J. Endocrinol. Invest.* **23**, 597-604.
- Baarends, W. M., van der Laan, R., and Grootegoed, J. A. (2001). DNA repair mechanisms and gametogenesis. *Reproduction* **121**, 31-39.
- Baarends, W. M., Wassenaar, E., Hoogerbrugge, J. W., van Cappellen, G., Roest, H. P., Vreeburg, J., Ooms, M., Hoeijmakers, J. H., and Grootegoed, J. A. (2003). Loss of HR6B ubiquitin-conjugating activity results in damaged synaptonemal complex structure and increased crossing-over frequency during the male meiotic prophase. *Mol Cell Biol* **23**, 1151-1162.
- Baker, S. M., Bonner, C. E., Zhang, L., Plug, A. W., Robatzek, M., Warren, G., Elliott, E. A., Yu, J., Ashley, T., Arnheim, N., Flavell, R. A., and Liskay, R. M. (1995). Male mice defective in the DNA mismatch repair gene *PMS2* exhibit abnormal chromosome synapsis in meiosis. *Cell* **82**, 309-319.
- Baker, S. M., Plug, A. W., Prolla, T. A., Bronner, C. E., Harris, A. C., Yao, X., Christie, D. M., Monell, C., Arnheim, N., Bradley, A., Ashley, T., and Liskay, R. M. (1996). Involvement of mouse Mlh1 in DNA mismatch repair and meiotic crossing over. *Nat. Genet.* **13**, 336-342.
- Baynton, K., and Fuchs, R. P. (2000). Lesions in DNA: hurdles for polymerases. *Trends Biochem Sci* **25**, 74-79.
- Bemark, M., Khamlichi, A. A., Davies, S. L., and Neuberger, M. S. (2000). Disruption of mouse polymerase zeta (Rev3) leads to embryonic lethality and impairs blastocyst development in vitro. *Curr Biol* **10**, 1213-1216.
- Bernier-Villamor, V., Sampson, D. A., Matunis, M. J., and Lima, C. D. (2002). Structural basis for E2-mediated SUMO conjugation revealed by a complex between ubiquitin-conjugating enzyme Ubc9 and RanGAP1. *Cell* **108**, 345-356.

- Boyer, J. C., Kaufmann, W. K., Brylawski, B. P., and Cordeiro-Stone, M.** (1990). Defective postreplication repair in xeroderma pigmentosum variant fibroblasts. *Cancer Res* **50**, 2593-2598.
- Broomfield, S., Chow, B. L., and Xiao, W.** (1998). MMS2, encoding a ubiquitin-conjugating-enzyme-like protein, is a member of the yeast error-free postreplication repair pathway. *Proc. Natl. Acad. Sci. USA* **95**, 5678-5683.
- Brusky, J., Zhu, Y., and Xiao, W.** (2000). UBC13, a DNA-damage-inducible gene, is a member of the error-free postreplication repair pathway in *Saccharomyces cerevisiae*. *Curr Genet* **37**, 168-174.
- Ciechanover, A.** (1994). The ubiquitin-proteasome proteolytic pathway. *Cell* **79**, 13-21.
- Claverie, J. M.** (2001). Gene number. What if there are only 30,000 human genes? *Science* **291**, 1255-1257.
- Cordonnier, A. M., Lehmann, A. R., and Fuchs, R. P.** (1999). Impaired translesion synthesis in xeroderma pigmentosum variant extracts. *Mol Cell Biol* **19**, 2206-2211.
- Crow, J. F.** (2000). The origins, patterns and implications of human spontaneous mutation. *Nat Rev Genet* **1**, 40-47.
- de Vries, S. S., Baart, E. B., Dekker, M., Siezen, A., de Rooij, D. G., de Boer, P., and te Riele, H.** (1999). Mouse MutS-like protein Msh5 is required for proper chromosome synapsis in male and female meiosis. *Genes Dev* **13**, 523-531.
- Doublet, S., Tabor, S., Long, A. M., Richardson, C. C., and Ellenberger, T.** (1998). Crystal structure of a bacteriophage T7 DNA replication complex at 2.2 Å resolution. *Nature* **391**, 251-258.
- Dover, J., Schneider, J., Boateng, M. A., Wood, A., Dean, K., Johnston, M., and Shilatifard, A.** (2002). Methylation of histone H3 by COMPASS requires ubiquitination of histone H2B by RAD6. *J. Biol. Chem.* **277**, 28368-28371.
- Dowling, E. L., Maloney, D. H., and Fogel, S.** (1985). Meiotic recombination and sporulation in repair-deficient strains of yeast. *Genetics* **109**, 283-302.
- Edelmann, W., Cohen, P., Kane, M., Lau, K., Morrow, B., Bennett, S., Umar, A., Kunkel, T., Cattoretti, G., Chaganti, R., Pollard, J. W., Kolodner, R. D., and Kucherlapati, R.** (1996). Meiotic pachytene arrest in MLH1-deficient mice. *Cell* **85**, 1125-1134.
- Edelmann, W., Cohen, P. E., Kneitz, B., Winand, N., Lia, M., Heyer, J., Kolodner, R., Pollard, J. W., and Kucherlapati, R.** (1999). Mammalian MutS homologue 5 is required for chromosome pairing in meiosis. *Nat Genet* **21**, 123-127.
- Esposito, G., Godindagger, I., Klein, U., Yaspo, M. L., Cumano, A., and Rajewsky, K.** (2000). Disruption of the Rev3l-encoded catalytic subunit of polymerase zeta in mice results in early embryonic lethality. *Curr Biol* **10**, 1221-1224.
- Faili, A., Aoufouchi, S., Flatter, E., Gueranger, Q., Reynaud, C.A., Weill, J.C.** (2002). Induction of somatic hypermutation in immunoglobulin genes is dependent on DNA polymerase iota. *Nature* **419**, 944-947.
- Fischle, W., Wang, Y., and Allis, C. D.** (2003a). Binary switches and modification cassettes in histone biology and beyond. *Nature* **425**, 475-479.
- Fischle, W., Wang, Y., and Allis, C. D.** (2003b). Histone and chromatin cross-talk. *Curr Opin Cell Biol* **15**, 172-183.
- Franko, J., Ashley, C., and Xiao, W.** (2001). Molecular cloning and functional characterization of two murine cDNAs which encode Ubc variants involved in DNA repair and mutagenesis. *Biochim Biophys Acta* **1519**, 70-77.
- Friedberg, E. C., Wagner, R., and Radman, M.** (2002). Specialized DNA polymerases, cellular survival, and the genesis of mutations. *Science* **296**, 1627-1630.
- Gearhart, P. J., and Wood, R. D.** (2001). Emerging links between hypermutation of antibody genes and DNA polymerases. *Nat Rev Immunol* **1**, 187-192.
- Gerlach, V. L., Aravind, L., Gotway, G., Schultz, R. A., Koonin, E. V., and Friedberg, E. C.** (1999). Human and mouse homologs of *Escherichia coli* DinB (DNA polymerase IV), members of the UmuC/DinB superfamily. *Proc Natl Acad Sci USA* **96**, 11922-11927.
- Goedecke, W., Eijpe, M., Offenberger, H. H., van Aalderen, M., and Heyting, C.** (1999). Mre11 and Ku70 interact in somatic cells, but are differentially expressed in early meiosis. *Nat Genet* **23**, 194-198.
- Grootegoed, J. A., Baarends, W. M., Roest, H. P., and Hoeijmakers, J. H.** (1998). Knockout mouse models and gametogenic failure. *Mol. Cell. Endocrinol.* **145**, 161-166.
- Guo, D., Wu, X., Rajpal, D. K., Taylor, J. S., and Wang, Z.** (2001). Translesion synthesis by yeast DNA polymerase zeta from templates containing lesions of ultraviolet radiation and acetylaminofluorene. *Nucleic Acids Res* **29**, 2875-2883.
- Handley, P. M., Mueckler, M., Siegel, N. R., Ciechanover, A., and Schwartz, A. L.** (1991). Molecular cloning, sequence, and tissue distribution of the human ubiquitin-activating enzyme E1. *Proc. Natl. Acad. Sci. USA* **88**, 258-262.
- Haracska, L., Johnson, R. E., Unk, I., Phillips, B., Hurwitz, J., Prakash, L., and Prakash, S.** (2001a). Physical and functional interactions of human DNA polymerase eta with PCNA. *Mol Cell Biol* **21**, 7199-7206.
- Haracska, L., Prakash, S., and Prakash, L.** (2002a). Yeast Rev1 protein is a G template-specific DNA polymerase. *J Biol Chem* **277**, 15546-15551.

- Haracska, L., Unk, I., Johnson, R. E., Johansson, E., Burgers, P. M., Prakash, S., and Prakash, L.** (2001b). Roles of yeast DNA polymerases delta and zeta and of Rev1 in the bypass of abasic sites. *Genes Dev* **15**, 945-954.
- Haracska, L., Unk, I., Johnson, R. E., Phillips, B. B., Hurwitz, J., Prakash, L., and Prakash, S.** (2002b). Stimulation of DNA synthesis activity of human DNA polymerase kappa by PCNA. *Mol Cell Biol* **22**, 784-791.
- Hatakeyama, S., and Nakayama, K. I.** (2003). U-box proteins as a new family of ubiquitin ligases. *Biochem Biophys Res Commun* **302**, 635-645.
- Hendriksen, P. J., Hoogerbrugge, J. W., Themmen, A. P., Koken, M. H., Hoeijmakers, J. H., Oostra, B. A., van der Lende, T., and Grootegoed, J. A.** (1995). Postmeiotic transcription of X and Y chromosomal genes during spermatogenesis in the mouse. *Dev Biol* **170**, 730-733.
- Hershko, A., and Ciechanover, A.** (1998). The ubiquitin system. *Annu. Rev. Biochem.* **67**, 425-479.
- Heyting, C.** (1996). Synaptonemal complexes: structure and function. *Curr. Opin. Cell. Biol.* **8**, 389-396.
- Hiramoto, T., Nakanishi, T., Sumiyoshi, T., Fukuda, T., Matsuura, S., Tauchi, H., Komatsu, K., Shibasaki, Y., Inui, H., Watatani, M., Yasutomi, M., Sumii, K., Kajiyama, G., Kamada, N., Miyagawa, K., and Kamiya, K.** (1999). Mutations of a novel human RAD54 homologue, RAD54B, in primary cancer. *Oncogene* **18**, 3422-3426.
- Hochstrasser, M.** (2002). New structural clues to substrate specificity in the "ubiquitin system". *Mol Cell* **9**, 453-454.
- Hoeg, C., Pfander, B., Moldovan, G. L., Pyrowolakis, G., and Jentsch, S.** (2002). RAD6-dependent DNA repair is linked to modification of PCNA by ubiquitin and SUMO. *Nature* **419**, 135-141.
- Hoeijmakers, J. H.** (2001). Genome maintenance mechanisms for preventing cancer. *Nature* **411**, 366-374.
- Hofmann, R. M., and Pickart, C. M.** (1999). Noncanonical MMS2-encoded ubiquitin-conjugating enzyme functions in assembly of novel polyubiquitin chains for DNA repair. *Cell* **96**, 645-653.
- Holbeck, S. L., and Strathern, J. N.** (1997). A role for REV3 in mutagenesis during double-strand break repair in *Saccharomyces cerevisiae*. *Genetics* **147**, 1017-1024.
- Hunt, P. A., and Hassold, T. J.** (2002). Sex matters in meiosis. *Science* **296**, 2181-2183.
- Hurst, L. D., and Ellegren, H.** (2002). Human genetics: mystery of the mutagenic male. *Nature* **420**, 365-366.
- Jentsch, S., and Schlenker, S.** (1995). Selective protein degradation: A journey's end within the proteasome. *Cell* **82**, 881-884.
- Johnson, R. E., Prakash, S., and Prakash, L.** (1994). Yeast DNA repair protein RAD5 that promotes instability of simple repetitive sequences is a DNA-dependent ATPase. *J Biol Chem* **269**, 28259-28262.
- Johnson, R.E., Washington, M.T., Haracska, L., Prakash, S., Prakash, L.** (2000). Eukaryotic polymerases iota and zeta act sequentially to bypass DNA lesions. *Nature* **406**, 1015-1019.
- Kannouche, P., Broughton, B. C., Volker, M., Hanaoka, F., Mullenders, L. H., and Lehmann, A. R.** (2001). Domain structure, localization, and function of DNA polymerase eta, defective in xeroderma pigmentosum variant cells. *Genes Dev* **15**, 158-172.
- Kannouche, P., Fernandez de Henestrosa, A. R., Coull, B., Vidal, A. E., Gray, C., Zicha, D., Woodgate, R., and Lehmann, A. R.** (2002). Localization of DNA polymerases eta and iota to the replication machinery is tightly co-ordinated in human cells. *Embo J* **21**, 6246-6256.
- Keeney, S., Baudat, F., Angeles, M., Zhou, Z. H., Copeland, N. G., Jenkins, N. A., Manova, K., and Jasin, M.** (1999). A mouse homolog of the *Saccharomyces cerevisiae* meiotic recombination DNA transesterase Spo11p. *Genomics* **61**, 170-182.
- Keeney, S., Giroux, C. N., and Kleckner, N.** (1997). Meiosis-specific DNA double-strand breaks are catalyzed by Spo11, a member of a widely conserved protein family. *Cell* **88**, 375-384.
- Kneitz, B., Cohen, P. E., Avdievich, E., Zhu, L., Kane, M. F., Hou, H., Jr., Kolodner, R. D., Kucherlapati, R., Pollard, J. W., and Edlmann, W.** (2000). MutS homolog 4 localization to meiotic chromosomes is required for chromosome pairing during meiosis in male and female mice. *Genes Dev* **14**, 1085-1097.
- Koken, M. H., Hoogerbrugge, J. W., Jasper-Dekker, I., de Wit, J., Willemsen, R., Roest, H. P., Grootegoed, J. A., and Hoeijmakers, J. H.** (1996). Expression of the ubiquitin-conjugating DNA repair enzymes HHR6A and B suggests a role in spermatogenesis and chromatin modification. *Dev Biol* **173**, 119-132.
- Koken, M. H., Reynolds, P., Jaspers-Dekker, I., Prakash, L., Prakash, S., Bootsma, D., and Hoeijmakers, J. H.** (1991). Structural and functional conservation of two human homologs of the yeast DNA repair gene RAD6. *Proc. Natl. Acad. Sci. USA* **88**, 8865-8869.
- Kovalenko, O. V., Plug, A. W., Haaf, T., Gonda, D. K., Ashley, T., Ward, D. C., Radding, C. M., and Golub, E. I.** (1996). Mammalian ubiquitin-conjugating enzyme Ubc9 interacts with Rad51 recombination protein and localizes in synaptonemal complexes. *Proc. Natl. Acad. Sci. USA* **93**, 2958-2963.
- Kunkel, T. A., Pavlov, Y. I., and Bebenek, K.** (2003). Functions of human DNA polymerases eta, kappa and iota suggested by their properties, including fidelity with undamaged DNA templates. *DNA Repair (Amst)* **2**, 135-149.
- Lawrence, C.** (1994). The RAD6 repair pathway in *Saccharomyces cerevisiae*: what does it do, and how does it do it? *BioEssays* **16**, 253-258.

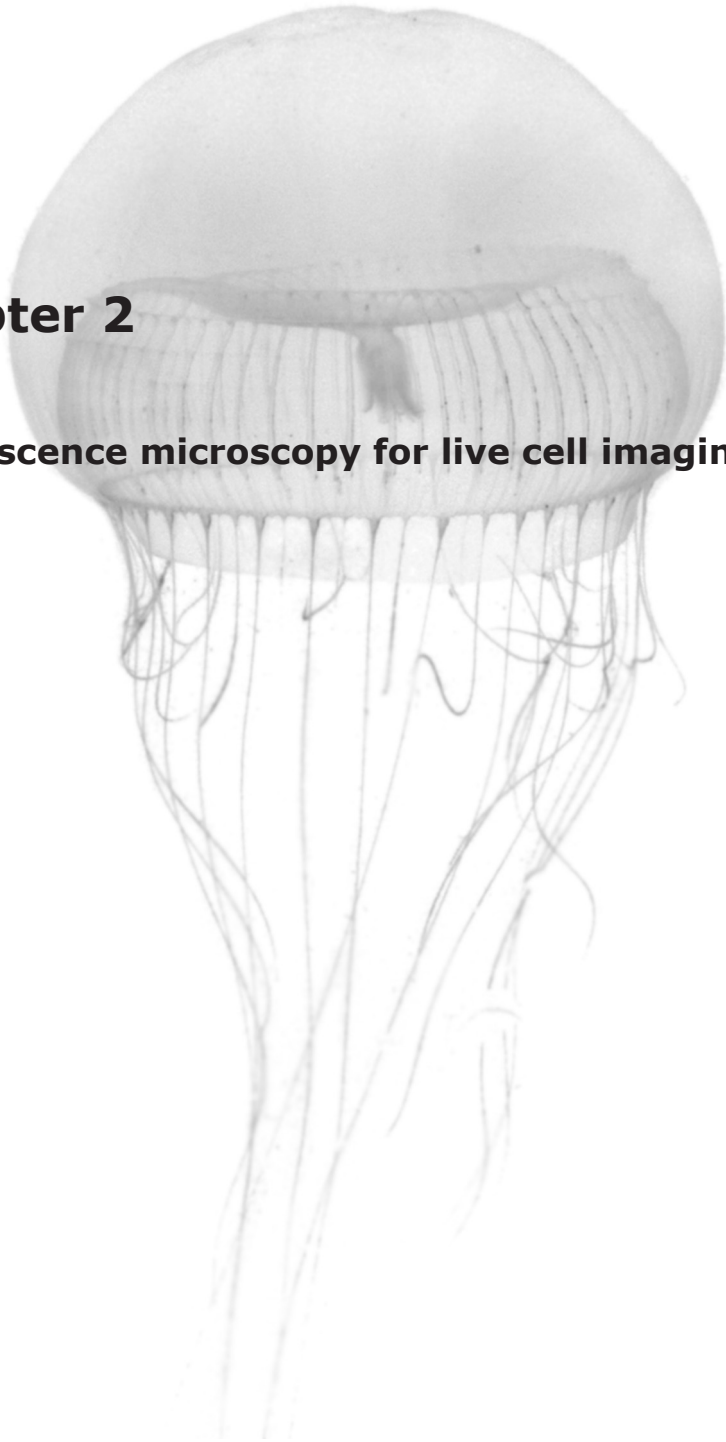
- Lawrence, C. W., and Hinkle, D. C.** (1996). DNA polymerase zeta and the control of DNA damage induced mutagenesis in eukaryotes. *Cancer Surv* **28**, 21-31.
- Lehmann, A. R.** (1975). Postreplication repair of DNA in UV-irradiated mammalian cells. *Basic Life Sci* **5B**, 617-623.
- Lehmann, A. R.** (2002). Replication of damaged DNA in mammalian cells: new solutions to an old problem. *Mutat Res* **509**, 23-34.
- Lemontt, J. F.** (1971). Pathways of ultraviolet mutability in *Saccharomyces cerevisiae*. I. Some properties of double mutants involving *uvs9* and *rev*. *Mutat Res* **13**, 311-317.
- Ling, H., Boudsocq, F., Woodgate, R., and Yang, W.** (2001). Crystal structure of a Y-family DNA polymerase in action: a mechanism for error-prone and lesion-bypass replication. *Cell* **107**, 91-102.
- Lipkin, S. M., Moens, P. B., Wang, V., Lenzi, M., Shanmugarajah, D., Gilgeous, A., Thomas, J., Cheng, J., Touchman, J. W., Green, E. D., Schwartzberg, P., Collins, F. S., and Cohen, P. E.** (2002). Meiotic arrest and aneuploidy in MLH3-deficient mice. *Nat Genet* **31**, 385-390.
- Lipkin, S. M., Wang, V., Jacoby, R., Banerjee-Basu, S., Baxevanis, A. D., Lynch, H. T., Elliott, R. M., and Collins, F. S.** (2000). MLH3: a DNA mismatch repair gene associated with mammalian microsatellite instability. *Nat Genet* **24**, 27-35.
- Masutani, C., Kusumoto, R., Yamada, A., Dohmae, N., Yokoi, M., Yuasa, M., Araki, M., Iwai, S., Takio, K., and Hanaoka, F.** (1999). The XPV (xeroderma pigmentosum variant) gene encodes human DNA polymerase eta. *Nature* **399**, 700-704.
- McBride, W. H., Iwamoto, K. S., Syljuasen, R., Pervan, M., and Pajonk, F.** (2003). The role of the ubiquitin/proteasome system in cellular responses to radiation. *Oncogene* **22**, 5755-5773.
- McDonald, J. P., Frank, E. G., Plosky, B. S., Rogozin, I. B., Masutani, C., Hanaoka, F., Woodgate, R., and Gearhart, P. J.** (2003). 129-derived strains of mice are deficient in DNA polymerase iota and have normal immunoglobulin hypermutation. *J Exp Med* **198**, 635-643.
- McDonald, J. P., Rapic-Otrin, V., Epstein, J. A., Broughton, B. C., Wang, X., Lehmann, A. R., Wolgemuth, D. J., and Woodgate, R.** (1999). Novel human and mouse homologs of *Saccharomyces cerevisiae* DNA polymerase eta. *Genomics* **60**, 20-30.
- McGill, C. B., Holbeck, S. L., and Strathern, J. N.** (1998). The chromosome bias of misincorporations during double-strand break repair is not altered in mismatch repair-defective strains of *Saccharomyces cerevisiae*. *Genetics* **148**, 1525-1533.
- Misra, R. R., and Vos, J. M.** (1993). Defective replication of psoralen adducts detected at the gene-specific level in xeroderma pigmentosum variant cells. *Mol Cell Biol* **13**, 1002-1012.
- Monesi, V.** (1965). Differential rate of ribonucleic acid synthesis in the autosomes and sex chromosomes during male meiosis in the mouse. *Chromosoma* **17**, 11-21.
- Morrison, A., Christensen, R. B., Alley, J., Beck, A. K., Bernstine, E. G., Lemontt, J. F., and Lawrence, C. W.** (1989). REV3, a *Saccharomyces cerevisiae* gene whose function is required for induced mutagenesis, is predicted to encode a nonessential DNA polymerase. *J Bacteriol* **171**, 5659-5667.
- Morrison, A., Miller, E. J., and Prakash, L.** (1988). Domain structure and functional analysis of the carboxyl-terminal polyacidic sequence of the RAD6 protein of *Saccharomyces cerevisiae*. *Mol Cell Biol* **8**, 1179-1185.
- Murakumo, Y.** (2002). The property of DNA polymerase zeta: REV7 is a putative protein involved in translesion DNA synthesis and cell cycle control. *Mutat Res* **510**, 37-44.
- Murakumo, Y., Ogura, Y., Ishii, H., Numata, S., Ichihara, M., Croce, C. M., Fishel, R., and Takahashi, M.** (2001). Interactions in the error-prone postreplication repair proteins hREV1, hREV3, and hREV7. *J Biol Chem* **276**, 35644-35651.
- Murakumo, Y., Roth, T., Ishii, H., Rasio, D., Numata, S., Croce, C. M., and Fishel, R.** (2000). A human REV7 homolog that interacts with the polymerase zeta catalytic subunit hREV3 and the spindle assembly checkpoint protein hMAD2. *J Biol Chem* **275**, 4391-4397.
- Nelson, J. R., Lawrence, C. W., and Hinkle, D. C.** (1996a). Deoxycytidyl transferase activity of yeast REV1 protein. *Nature* **382**, 729-731.
- Nelson, J. R., Lawrence, C. W., and Hinkle, D. C.** (1996b). Thymine-thymine dimer bypass by yeast DNA polymerase zeta. *Science* **272**, 1646-1649.
- Ng, H. H., Xu, R. M., Zhang, Y., and Struhl, K.** (2002). Ubiquitination of histone H2B by Rad6 is required for efficient Dot1-mediated methylation of histone H3 lysine 79. *J Biol Chem* **277**, 34655-7.
- Nickel, B. E., Allis, C. D., and Davie, J. R.** (1989). Ubiquitinated histone H2B is preferentially located in transcriptionally active chromatin. *Biochemistry* **28**, 958-963.
- Ogi, T., Kato, T., Jr., Kato, T., and Ohmori, H.** (1999). Mutation enhancement by DINB1, a mammalian homologue of the *Escherichia coli* mutagenesis protein dinB. *Genes Cells* **4**, 607-618.
- Ohmori, H., Friedberg, E. C., Fuchs, R. P., Goodman, M. F., Hanaoka, F., Hinkle, D., Kunkel, T. A., Lawrence, C. W., Livneh, Z., Nohmi, T., Prakash, L., Prakash, S., Todo, T., Walker, G. C., Wang, Z., and Woodgate, R.** (2001). The Y-family of DNA polymerases. *Mol Cell* **8**, 7-8.
- Pakis-Flucklinger, V., Santucci-Darmanin, S., Paul, R., Saunier, A., Turc-Carel, C., and Desnuelle, C.** (1997). Cloning and expression analysis of a meiosis-specific MutS homolog: the human MSH4 gene. *Genomics* **44**, 188-194.

- Park, S. D. and Cleaver, J. E.** (1979). Postreplication repair: questions of its definition and possible alteration in xeroderma pigmentosum cell strains. *Proc Natl Acad Sci USA* **76**, 3927-3931.
- Pickart, C. M.** (2000). Ubiquitin in chains. *Trends Biochem Sci* **25**, 544-548.
- Pickart, C. M.** (2004). Back to the future with ubiquitin. *Cell* **116**, 181-190.
- Pittman, D. L., Cobb, J., Schimenti, K. J., Wilson, L. A., Cooper, D. M., Brignull, E., Handel, M. A., and Schimenti, J. C.** (1998). Meiotic prophase arrest with failure of chromosome synapsis in mice deficient for Dmc1, a germline-specific RecA homolog. *Mol. Cell* **1**, 697-705.
- Prakash, S., and Prakash, L.** (2002). Translesion DNA synthesis in eukaryotes: a one- or two-polymerase affair. *Genes Dev* **16**, 1872-1883.
- Risch, N., Reich, E. W., Wishnick, M. M., and McCarthy, J. G.** (1987). Spontaneous mutation and parental age in humans. *Am J Hum Genet* **41**, 218-248.
- Robzyk, K., Recht, J., and Osley, M. A.** (2000). Rad6-dependent ubiquitination of histone H2B in yeast. *Science* **287**, 501-504.
- Roest, H. P., Klaveren van, J., Wit de, J., Gulp van, C. G., Koken, M. H. M., Vermey, M., Roijen van, J. H., Vreeburg, J. T. M., Baarends, W. M., Bootsma, D., Grootegoed, J. A., and Hoeijmakers, J. H. J.** (1996). Inactivation of the HR6B ubiquitin-conjugating DNA repair enzyme in mice causes male sterility associated with chromatin modification. *Cell* **86**, 799-810.
- Roest, H. P., Baarends, W. M., de Wit, J., van Klaveren, J. W., Wassenaar, E., Hoogerbrugge, J. W., van Cappellen, W. A., Hoeijmakers, J. A., and Grootegoed, J. A.** (2004). The Ubiquitin-conjugating DNA repair enzyme HR6A is a maternal factor essential for early embryonic development in mice. *Mol Cell Biol* in press.
- Romanienko, P. J., and Camerini-Otero, R. D.** (1999). Cloning, characterization, and localization of mouse and human SPO11. *Genomics* **61**, 156-169.
- Sancho, E., Vila, M. R., Sanchez-Pulido, L., Lozano, J. J., Paciucci, R., Nadal, M., Fox, M., Harvey, C., Bercovich, B., Loukili, N., Ciechanover, A., Lin, S. L., Sanz, F., Estivill, X., Valencia, A., and Thomson, T. M.** (1998). Role of UEV-1, an inactive variant of the E2 ubiquitin-conjugating enzymes, in in vitro differentiation and cell cycle behavior of HT-29- M6 intestinal mucosecretory cells. *Mol Cell Biol* **18**, 576-589.
- Schenten, D., Gerlach, V. L., Guo, C., Velasco-Miguel, S., Hladik, C. L., White, C. L., Friedberg, E. C., Rajewsky, K., and Esposito, G.** (2002). DNA polymerase kappa deficiency does not affect somatic hypermutation in mice. *Eur J Immunol* **32**, 3152-3160.
- Shinohara, A., Ogawa, H., Matsuda, Y., Ushio, N., Ikeo, K., and Ogawa, T.** (1993). Cloning of human, mouse and fission yeast recombination genes homologous to RAD51 and recA. *Nat Genet* **4**, 239-243.
- Shinohara, A., and Ogawa, T.** (1999). Rad51/RecA protein families and the associated proteins in eukaryotes. *Mutat Res* **435**, 13-21.
- Simpson, L. J., and Sale, J. E.** (2003). Rev1 is essential for DNA damage tolerance and non-templated immunoglobulin gene mutation in a vertebrate cell line. *Embo J* **22**, 1654-1664.
- Stelter, P., and Ulrich, H. D.** (2003). Control of spontaneous and damage-induced mutagenesis by SUMO and ubiquitin conjugation. *Nature* **425**, 188-191.
- Stephen, A. G., Trausch-Azar, J. S., Handley-Gearhart, P. M., Ciechanover, A., and Schwartz, A. L.** (1997). Identification of a region within the ubiquitin-activating enzyme required for nuclear targeting and phosphorylation. *J. Biol. Chem.* **272**, 10895-10903.
- Strahl, B. D., and Allis, C. D.** (2000). The language of covalent histone modifications. *Nature* **403**, 41-45.
- Sun, Z. W., and Allis, C. D.** (2002). Ubiquitination of histone H2B regulates H3 methylation and gene silencing in yeast. *Nature* **418**, 104-108.
- Tateishi, S., Niwa, H., Miyazaki, J., Fujimoto, S., Inoue, H., and Yamaizumi, M.** (2003). Enhanced genomic instability and defective postreplication repair in RAD18 knockout mouse embryonic stem cells. *Mol Cell Biol* **23**, 474-481.
- Tateishi, S., Sakuraba, Y., Masuyama, S., Inoue, H., and Yamaizumi, M.** (2000). Dysfunction of human Rad18 results in defective postreplication repair and hypersensitivity to multiple mutagens. *Proc Natl Acad Sci USA* **97**, 7927-7932.
- Tissier, A., Frank, E. G., McDonald, J. P., Iwai, S., Hanaoka, F., and Woodgate, R.** (2000). Misinsertion and bypass of thymine-thymine dimers by human DNA polymerase iota. *Embo J* **19**, 5259-5266.
- Torpey, L. E., Gibbs, P. E., Nelson, J., and Lawrence, C. W.** (1994). Cloning and sequence of REV7, a gene whose function is required for DNA damage-induced mutagenesis in *Saccharomyces cerevisiae*. *Yeast* **10**, 1503-1509.
- Torres-Ramos, C. A., Prakash, S., and Prakash, L.** (2002). Requirement of RAD5 and MMS2 for postreplication repair of UV-damaged DNA in *Saccharomyces cerevisiae*. *Mol Cell Biol* **22**, 2419-2426.
- Trincao, J., Johnson, R. E., Escalante, C. R., Prakash, S., Prakash, L., and Aggarwal, A. K.** (2001). Structure of the catalytic core of *S. cerevisiae* DNA polymerase eta: implications for translesion DNA synthesis. *Mol Cell* **8**, 417-426.
- Ulrich, H. D., and Jentsch, S.** (2000). Two RING finger proteins mediate cooperation between ubiquitin-conjugating enzymes in DNA repair. *Embo J* **19**, 3388-3397.

- van der Laan, R., Roest, H. P., Hoogerbrugge, J. W., Smit, E. M., Slater, R., Baarends, W. M., Hoeijmakers, J. H., and Grootoed, J. A. (2000). Characterization of mRAD18Sc, a mouse homolog of the yeast postreplication repair gene RAD18. *Genomics* **69**, 86-94.
- van Sloun, P. P., Romeijn, R. J., and Eeken, J. C. (1999). Molecular cloning, expression and chromosomal localisation of the mouse Rev3l gene, encoding the catalytic subunit of polymerase zeta. *Mutat Res* **433**, 109-116.
- Van Sloun, P. P., Varlet, I., Sonneveld, E., Boei, J. J., Romeijn, R. J., Eeken, J. C., and De Wind, N. (2002). Involvement of mouse Rev3 in tolerance of endogenous and exogenous DNA damage. *Mol Cell Biol* **22**, 2159-2169.
- Varshavsky, A. (1997). The ubiquitin system. *Trends Biochem. Sci.* **22**, 383-387.
- Velasco-Miguel, S., Richardson, J. A., Gerlach, V. L., Lai, W. C., Gao, T., Russell, L. D., Hladik, C. L., White, C. L., and Friedberg, E. C. (2003). Constitutive and regulated expression of the mouse Dinb (Polkappa) gene encoding DNA polymerase kappa. *DNA Repair (Amst)* **2**, 91-106.
- Washington, M. T., Johnson, R. E., Prakash, L., and Prakash, S. (2002). Human DINB1-encoded DNA polymerase kappa is a promiscuous extender of mispaired primer termini. *Proc Natl Acad Sci USA* **99**, 1910-1914.
- Weill, J. C., Bertocci, B., Faili, A., Aoufouchi, S., Frey, S., De Smet, A., Storck, S., Dahan, A., Delbos, F., Weller, S., Flatter, E., and Reynaud, C. A. (2002). Ig gene hypermutation: a mechanism is due. *Adv Immunol* **80**, 183-202.
- Weissman, A. M. (2001). Themes and variations on ubiquitylation. *Nat. Rev. Mol. Cell. Biol.* **2**, 169-78.
- Wesloy, J. (2003). Role of *Rad54*, *Rad54B* and *Snm1* in DNA Damage Repair. *PhD Thesis, Erasmus University Rotterdam*.
- Wilkinson, K. D. (1997). Regulation of ubiquitin-dependent processes by deubiquitinating enzymes. *Faseb J.* **11**, 1245-1256.
- Winand, N. J., Panzer, J. A., and Kolodner, R. D. (1998). Cloning and characterization of the human and *Caenorhabditis elegans* homologs of the *Saccharomyces cerevisiae* MSH5 gene. *Genomics* **53**, 69-80.
- Wing, S. S., Bédard, N., Morales, C., Hingamp, P., and Trasler, J. (1996). A novel rat homolog of the *Saccharomyces cerevisiae* ubiquitin-conjugating enzymes UBC4 and UBC5 with distinct biochemical features is induced during spermatogenesis. *Mol. Cell. Biol.* **16**, 4064-4072.
- Wing, S. S., and Jain, P. (1995). Molecular cloning, expression and characterization of a ubiquitin enzyme (E2_{17kd}) highly expressed in rat testis. *Biochem. J.* **305**, 125-132.
- Wittschieben, J., Shivji, M. K., Lalani, E., Jacobs, M. A., Marini, F., Gearhart, P. J., Rosewell, I., Stamp, G., and Wood, R. D. (2000). Disruption of the developmentally regulated Rev3l gene causes embryonic lethality. *Curr Biol* **10**, 1217-1220.
- Woodgate, R. (1999). A plethora of lesion-replicating DNA polymerases. *Genes Dev* **13**, 2191-5.
- Xiao, W., Lin, S. L., Broomfield, S., Chow, B. L., and Wei, Y. F. (1998). The products of the yeast MMS2 and two human homologs (hMMS2 and CROC-1) define a structurally and functionally conserved Ubc-like protein family. *Nucl. Acids Res.* **26**, 3908-3914.
- Xin, H., Lin, W., Sumanasekera, W., Zhang, Y., Wu, X., and Wang, Z. (2000). The human RAD18 gene product interacts with HHR6A and HHR6B. *Nucleic Acids Res.* **28**, 2847-2854.
- Yamada, A., Masutani, C., Iwai, S., and Hanaoka, F. (2000). Complementation of defective translesion synthesis and UV light sensitivity in xeroderma pigmentosum variant cells by human and mouse DNA polymerase eta. *Nucleic Acids Res* **28**, 2473-2480.
- Yamaguchi, T., Kim, N. S., Sekine, S., Seino, H., Osaka, F., Yamao, F., and Kato, S. (1996). Cloning and expression of cDNA encoding a human ubiquitin-conjugating enzyme similar to the *Drosophila* bendless gene product. *J. Biochem.* **120**, 494-497.
- Yasugi, T., and Howley, P. M. (1996). Identification of the structural and functional human homolog of the yeast ubiquitin-conjugating enzyme UBC9. *Nucl. Acids Res.* **24**, 2005-2010.
- Yoshida, K., Kondoh, G., Matsuda, Y., Habu, T., Nishimune, Y., and Morita, T. (1998). The mouse RecA-like gene Dmc1 is required for homologous chromosome synapsis during meiosis. *Mol. Cell* **1**, 707-718.
- Zan, H., Komori, A., Li, Z., Cerutti, A., Schaffer, A., Flajnik, M. F., Diaz, M., and Casali, P. (2001). The translesion DNA polymerase zeta plays a major role in Ig and bcl-6 somatic hypermutation. *Immunity* **14**, 643-653.
- Zeng, X., Winter, D. B., Kasmer, C., Kraemer, K. H., Lehmann, A. R., and Gearhart, P. J. (2001). DNA polymerase eta is an A-T mutator in somatic hypermutation of immunoglobulin variable genes. *Nat Immunol* **2**, 537-541.
- Zhang, Y., Yuan, F., Wu, X., Wang, M., Rechkoblit, O., Taylor, J. S., Geacintov, N. E., and Wang, Z. (2000). Error-free and error-prone lesion bypass by human DNA polymerase kappa in vitro. *Nucleic Acids Res* **28**, 4138-4146.

Chapter 2

Fluorescence microscopy for live cell imaging



Fluorescence Microscopy for Live Cell Imaging

Introduction

Biologists have been fascinated to observe cells by light microscopy, starting with the creation of the first lenses and microscopes by Antoni van Leeuwenhoek and his 17th/18th century scientific contemporaries. Later, and with an accelerated speed in the last 50 years, scientists have obtained an enormous amount of knowledge concerning the origin and maintenance of cellular organization, through biochemical and molecular genetic approaches. Modern cell biology entails synergy between microscopic and molecular approaches. Classical light microscopic photomicrographs represent static snapshots of cells. Fluorescence microscopy makes it possible to observe processes that happen inside living cells. Merging multiple ways of application of fluorescent probes with a plethora of sophisticated microscopic techniques that are currently available, provides a powerful toolbox to study dynamic aspects of biomolecules in living cells, such as changes in subcellular localization of proteins, and protein-protein interactions. In particular the discovery of the green fluorescent protein (GFP) from the jellyfish *Aequorea victoria* (Prasher et al., 1992), has led to the development of a wide range of techniques to study protein dynamics in living cells.

The original GFP was mutated into a GFP variant (enhanced GFP or EGFP), which can be excited efficiently at 488 nm. EGFP has a bright fluorescence which is very useful in studies with living cells (Heim et al., 1995; Yang et al., 1996). Subsequently, several other fluorescent proteins and spectral GFP variants, including enhanced blue, cyan, yellow fluorescent protein (Tsien, 1998), GFP2 (Perkin Elmer Inc., Dreieich, Germany), and DsRed, the latter isolated from a coral of the *Discosoma* genus, became available (Baird et al., 2000). The discovery of the applicability of these fluorescent proteins has revolutionized live cell imaging. The fluorescent proteins can be covalently linked to the N- or C-terminus of target proteins by transgenic expression of cDNAs encoding the fusion proteins in transfected cells or transgenic mice. Nowadays, expression of fluorescently tagged fusion proteins is widely used to study intracellular dynamics of biomolecules at high spatial and temporal resolution. This chapter provides a short schematic overview of the basic principles of fluorescence and its detection using wide field and confocal microscopy (single-photon and multi-photon). In addition, several advanced microscopy techniques will be described, such as fluorescent recovery after photobleaching (FRAP), fluorescence loss in photobleaching (FLIP), fluorescence energy transfer (FRET), fluorescence lifetime imaging (FLIM), and fluorescence correlation spectroscopy (FCS). Finally, suggestions for further reading and informative websites will be given.

Fluorescence

Fluorescence is a property of a molecule. Following exposure of the molecule to a certain wavelength, an electron absorbs a photon (excitation) and gets excited to a higher energy level. After some energy loss due to thermal relaxation, the electron almost immediately falls back to the initial ground state and releases the remaining energy as a fluorescent photon. The Jablonski diagram in Figure

1A displays schematically the events that take place in fluorescence, excitation, thermal relaxation and emission. The entire process occurs within a time window of 10^{-9} – 10^{-12} seconds. The duration of thermal relaxation is specific for a fluorescent molecule and determines the fluorescence lifetime. Due to loss of some energy by thermal relaxation, the emission spectrum is shifted to a longer wavelength compared to the excitation spectrum, and the wavelength difference between the peaks of these spectra is referred to as Stokes shift (Figure 1B). In recent years, many different fluorescent molecules and dyes have been discovered, and their specific excitation and emission spectra (Figure 1C) cover the electromagnetic spectrum from ultraviolet to far infrared.

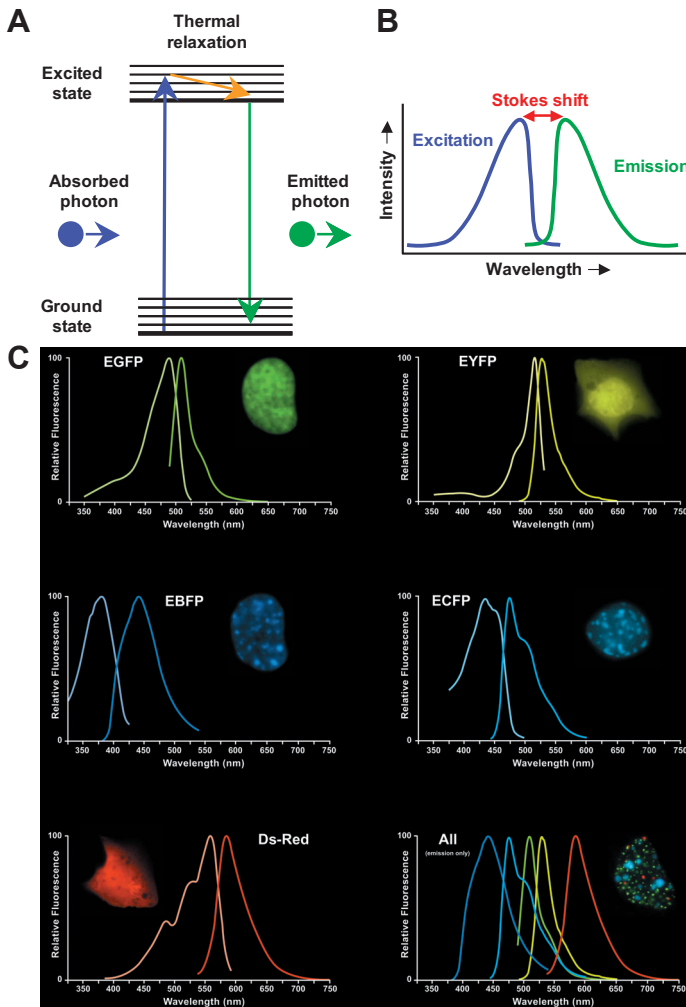


Figure 1. Basic principles of fluorescence. A: A simplified Jablonski diagram showing excitation, thermal relaxation and emission of a fluorescent dye. B: Loss of energy due to thermal relaxation results into a Stokes shift. C: Overview of excitation and emission spectra of various commonly used fluorescent proteins for live cell imaging (Patterson et al., 2001).

Wide field versus confocal fluorescence microscopy

Wide field and confocal microscopes are limited in the resolution they can achieve. Resolution is defined as the minimum separation of two point objects at a reasonable contrast. This is dependent on the wavelength (λ), numerical aperture (NA) of the optics and the specimen itself. In addition, in a wide field camera system, resolution is also limited by the number of pixels of the charge-coupled device (CCD) camera used to record the actual images. The size of the CCD chip is fixed and high magnification (100X) objectives are used to obtain high resolution images. In a confocal microscope these high magnification objectives are rarely found. The number of pixels is flexible and dependent on the settings of the scanning mirrors. Therefore, high resolution ($R_{x,y}=0.5\lambda/NA$ and $R_z=1.4\lambda/NA$) is only dependent on wavelength and the NA, and achieved using lower magnification objectives (40X, 63X) which result in a larger image field. This is advantageous when searching for regions of interest within the same field and detailed high resolution images can be obtained by increasing the zoom factor.

In thick specimens, for example larger clusters of living cells, bright fluorescence gives rise to high background and low contrast images using wide field microscopy. This is because fluorescence is emitted throughout the specimen, which makes focusing rather difficult. In a confocal system, an emission pinhole is placed in such a way in front of the detector that only light from the focus is able to pass the pinhole and reach the detector; usually a very sensitive photo multiplier tube (PMT). In addition, a focused laser point (excitation pinhole) source is used as a light source in a confocal microscope. The specimen is scanned (in x and y directions) point by point and high resolution images are created from these data points by software. The microscope focus, changed along the z-axis, will create 3-dimensional views of the specimen, referred to as optical sectioning. Optical sectioning of multiple fluorescent dyes in time-series, named five-dimensional confocal microscopy, provides high resolution images.

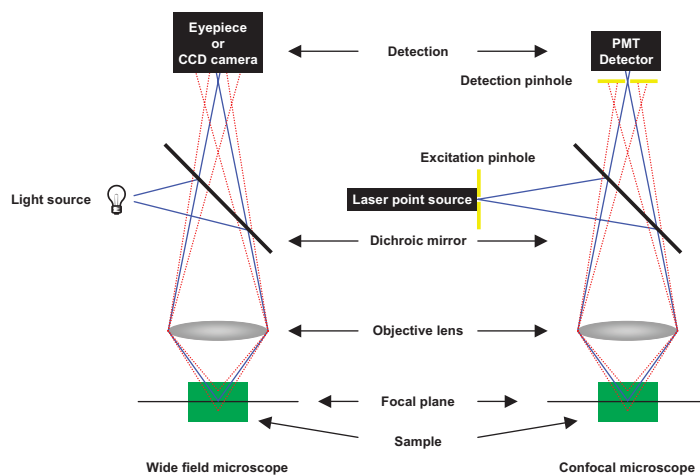


Figure 2. Wide field microscopy versus confocal fluorescence microscopy. In wide field microscopy, the excitation wavelengths come from a light source while in a confocal microscope a laser point source (excitation pinhole) is used for excitation. Some out-of-focus light will reach the detector in a wide field system (left panel). In a confocal system only a minimal of out-of-focus light reaches the detector due to the presence of a detection pinhole (right panel).

Single-photon and multi-photon microscopy

In general, a single photon can be used to excite a fluorescent molecule to a higher energy state from which emission of one fluorescent photon occurs. However, a fluorescent molecule can also be excited by absorption of multiple photons at nearly the same time (10^{-16} s). This process can only take place when the excitation photon density is very high. A pulsed infrared laser can generate the required photon densities without damaging the specimen if adjusted properly. This high photon density only occurs in the laser focus and there is no out-of-focus light is emitted, therefore, no detector pinhole is required. In addition the rate of photobleaching is also considerably reduced for the specimen as a whole. Multi-photon confocal microscopy is an especially useful imaging tool for thick specimens, since cells and tissue absorb near-infrared poorly, which results in a better penetration, and near-infrared wavelengths are less phototoxic. Therefore, analysis in tissue or in situ imaging in intact organisms benefit from this technique. In addition, the multiphoton effect only occurs in the focus which makes fluorescence based analysis possible in the femtoliter volumes. Finally, the excitation spectrum is wide and includes the excitation of dyes that are normally absorbing photons of shorter wavelengths e.g. ultraviolet (UV), without the need for an expensive UV-laser.

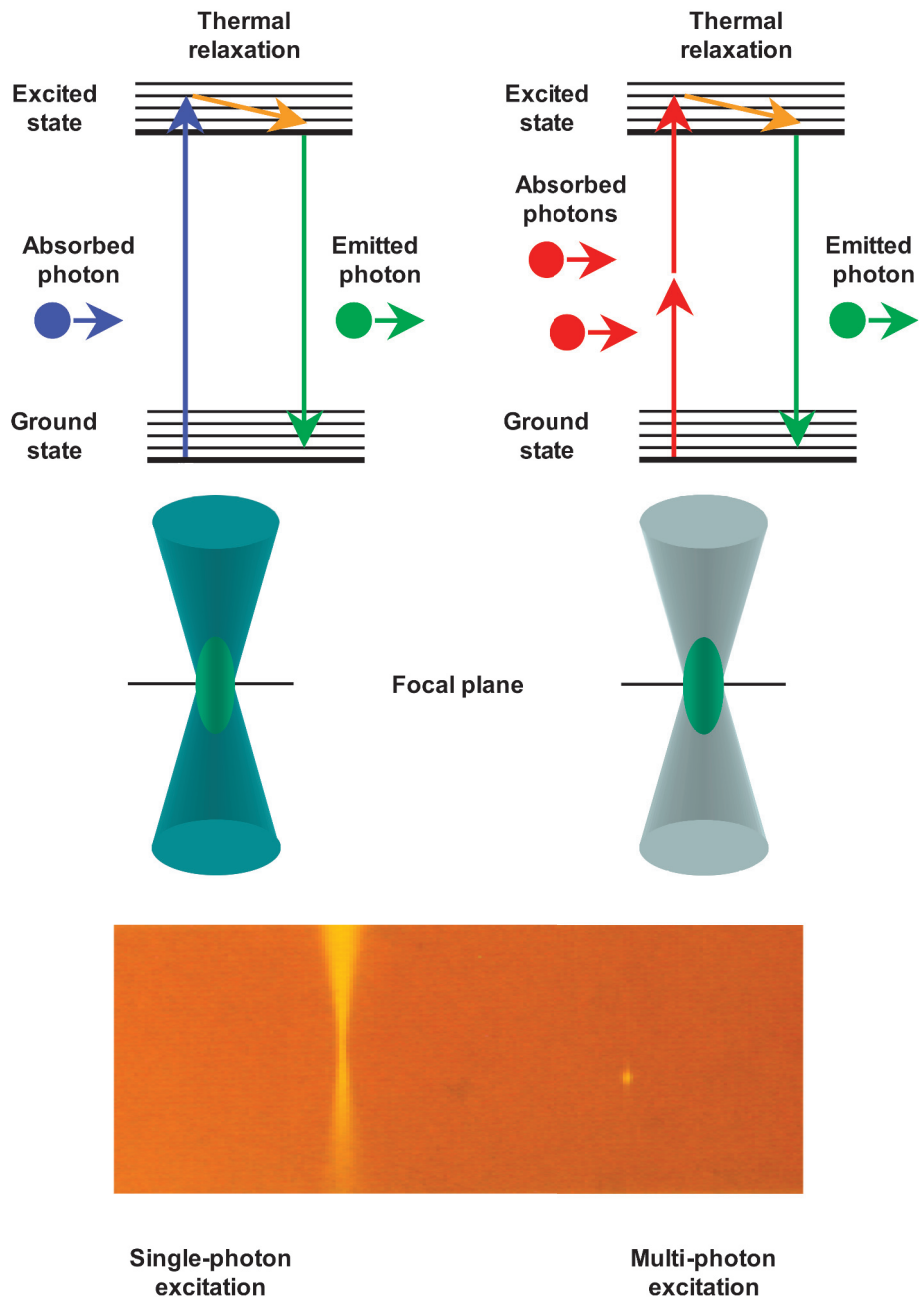


Figure 3. Single-photon and multiphoton excitation in fluorescence microscopy. A cone of emission light is formed in single-photon confocal microscope setup, but high contrast images from the focus are obtained using the emission pinhole (left panel). Multiple photons of lower energy are absorbed by fluorescent molecules in the laser focus. Subsequently, a fluorescent photon is emitted only from the laser focus (right panel). The Jablonski diagrams show single- and two-photon excitation respectively.

Band-pass detection and spectral unmixing

The commonly used fluorescent proteins, ECFP, EGFP and EYFP employed in live cell imaging have overlapping emission spectra, and sequential imaging with appropriate excitation and emission filters is required to obtain a good separation between multiple fluorescent dyes in the same sample. Colored glass or interference filters can be used to isolate specific blocks of wavelengths. They are placed between the light source (excitation filter) and the specimen for selection of appropriate excitation wavelengths, and in front of detectors (emission filters) in order to obtain fluorescence signals of selected wavelengths.

In confocal microscopes, an acousto-optic tunable filter (AOTF) is used to precisely select specific laser lines and intensity. For detection, emission filters are used with similar properties as in a wide field system. However, the scanning speed and good separation of multiple fluorescent dyes in individual channels can be achieved by measurement of spectral information in parallel channels simultaneously. Spectral imaging is implemented in the Zeiss LSM510 Meta which uses a grating for spectral dispersion, splitting the emitted light into different wavelengths and directs it onto an array of PMTs (Figure 4) (Dickinson et al., 2001; Hiraoka et al., 2002). Reference spectra are recorded for each individual fluorescent dye by taking series of fluorescent intensities at different wavelengths (λ -stack). From these references, a matrix of fluorescent dye-specific weighing factors is assembled and used to determine the contribution of each fluorescent dye to each pixel, in the image composed by combination of spectral information from multiple fluorescent probes (Tsurui et al., 2000). Spectral imaging is a very powerful method for high quality multicolor imaging and offers advantages for fast multicolor time-lapse microscopy.

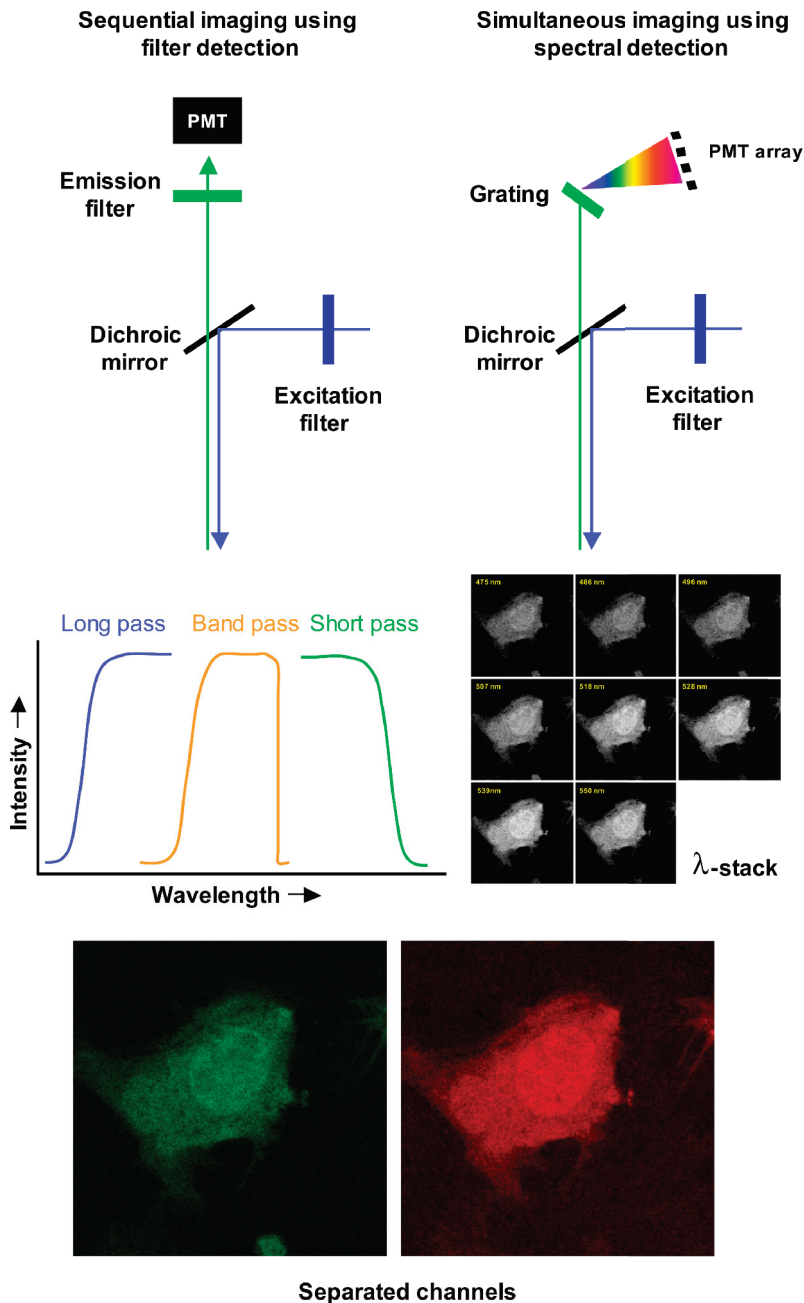


Figure 4. Comparison of conventional fluorescence microscopy with spectral unmixing. The fluorescent light is filtered by band-pass, long-pass, short-pass or combinations of them in conventional fluorescence microscopy (left panel). In spectral imaging, multiple fluorescent dyes are detected simultaneously, and a grating splits the emitted light in multiple channels detected by an array of PMTs. A wavelength stack is obtained and the contribution of each fluorescent molecule in the stack is unmixed using reference stacks of single fluorescent dyes (right panel).

FRAP and FLIP

The GFP molecule is converted into to a permanent dark state when exposed to high intensity excitation, referred to as photobleaching, a property of GFP that is widely used as a tool to study the dynamics of GFP-tagged proteins in living cells (White and Stelzer, 1999).

For example, fluorescent recovery after photobleaching (FRAP) measures recovery of fluorescence in a photobleached region by means of analyzing the influx and thereby the diffusion speed of fluorescently tagged fusion proteins in the bleached region in living cells. One way to perform FRAP is to photobleach fluorescent molecules in a small region, a strip or spot, and monitor the recovery of fluorescence within that region in time (Figure 5, upper panel). The recovery of relative fluorescence is plotted against time and used to determine the diffusion coefficient and the presence of permanent and/or transient immobile fractions of the studied GFP-tagged protein (Houtsmuller and Vermeulen, 2001). In addition, fluorescence loss in photobleaching (FLIP) is a powerful method to study residence times of a fluorescent protein in a region of interest, for example local accumulation of a GFP-tagged DNA repair protein at DNA lesion sites (Figure 5, lower panel). In FLIP analysis, an area outside the region of interest is photobleached, and the loss of fluorescence is monitored in time in the region of interest and also in a control region of the same dimensions, and at the same distance to the photobleached area. The relative fluorescence is plotted against time, and from that graph the residence time of individual molecules can be calculated by subtraction of the control distribution from the distribution in the region of interest. In FRAP and related techniques, the photobleaching properties of GFP are used to measure recovery or loss of fluorescence by diffusion in time in living cells. Recently, a GFP variant was created which is photoactivatable by a laser pulse of 413 nm (Patterson and Lippincott-Schwartz, 2002). In addition, the fluorescent protein Kaede, isolated from the stony coral *Trachyphyllia geoffroyi* is photoconvertible from green to red with a laser pulse of 300-400 nm (Ando et al., 2002). The characteristics of these new fluorescent proteins give a new dimension in the field of protein dynamics analysis in living cells and offer the possibility to track specifically activated or converted fluorescent molecules.

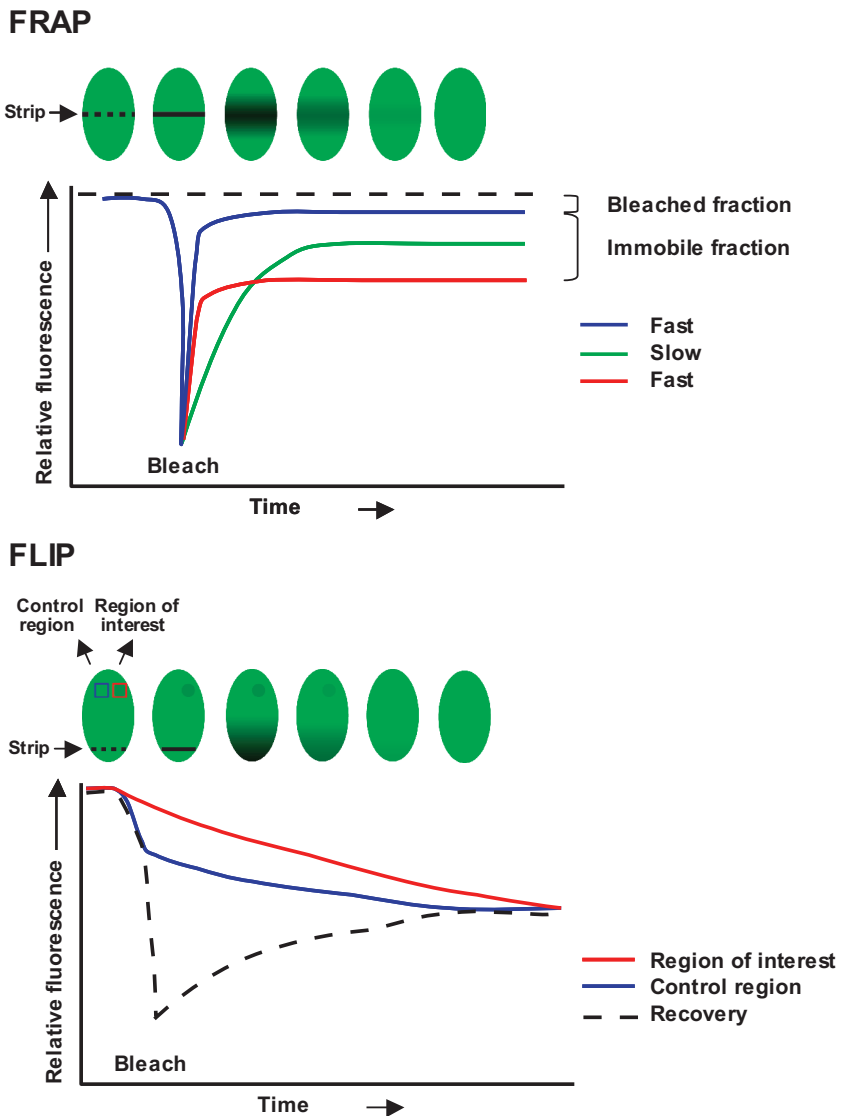


Figure 5. Protein dynamics analysis using FRAP and FLIP. A strip with a small defined volume is photobleached by a high-intensity laser pulse. Subsequently, the influx of fluorescence in the bleached strip is measured in time. The relative fluorescence is plotted against time and used to determine the diffusion coefficient and immobile fractions (upper panel). FLIP is used to calculate exchange of fluorescence between a region of interest and its surroundings. In this method, a strip distant from the region of interest is bleached, and the decrease of fluorescence is monitored in time in the region of interest and in a control region. From the relative fluorescence-time plot, residence times in the region of interest are calculated (lower panel).

FRET and FLIM

Fluorescence resonance energy transfer (FRET) is a powerful technique to study protein-protein interactions and changes in protein conformation in living cells. The FRET principle is based on intermolecular dipole-dipole coupling of donor and acceptor fluorescent molecules. After donor molecule excitement, this results in energy transfer. FRET is distance dependent and can be used as an accurate analysis method to study proximity between molecules in the range of 1-10 nm. In live cell microscopy, the CFP-YFP FRET pair is commonly used to study intracellular interactions between proteins. Usually, two fluorescently tagged fusion proteins (CFP and YFP) are expressed in living cells and used to perform interaction studies. If the fluorescent proteins are in close proximity of each other, energy can be transferred from the donor (CFP) to the acceptor (YFP) after excitation of the donor. This is referred to as sensitized emission (Figure 6, upper panel). Accurate measurement of sensitized emission can be difficult as a consequence of overlapping emission spectra of the fluorescent donor and acceptor. To circumvent these problems, acceptor photobleaching can be applied. When the acceptor is no longer capable of absorbing energy from the donor, this will result in an increase of donor emission intensity. Subsequently, FRET efficiencies can be calculated from pre- and post-bleach relative fluorescence intensities (Figure 6, upper panel).

Another method to measure FRET is fluorescence lifetime imaging (FLIM). The principle of FLIM is based on the thermal relaxation (Figure 1A) referred to as the fluorescence lifetime, a characteristic unique to a fluorescent dye. During this procedure, fluorescence lifetimes of fluorescent dyes are measured after excitation of the fluorescent dye of the donor by a laser pulse. The fluorescence lifetime of the donor decreases greatly when energy transfer from the donor to acceptor occurs (Figure 6, lower panel). A considerable advantage of FLIM in multicolor analysis is provided by different fluorescence lifetimes, despite substantially overlapping spectra, of spectrally related fluorescent molecules, such as GFP variants. Fluorescence decay is also dependent on the environmental conditions of the fluorescent dye, and FLIM can be used therefore, to monitor changes in for example intracellular pH or calcium concentration.

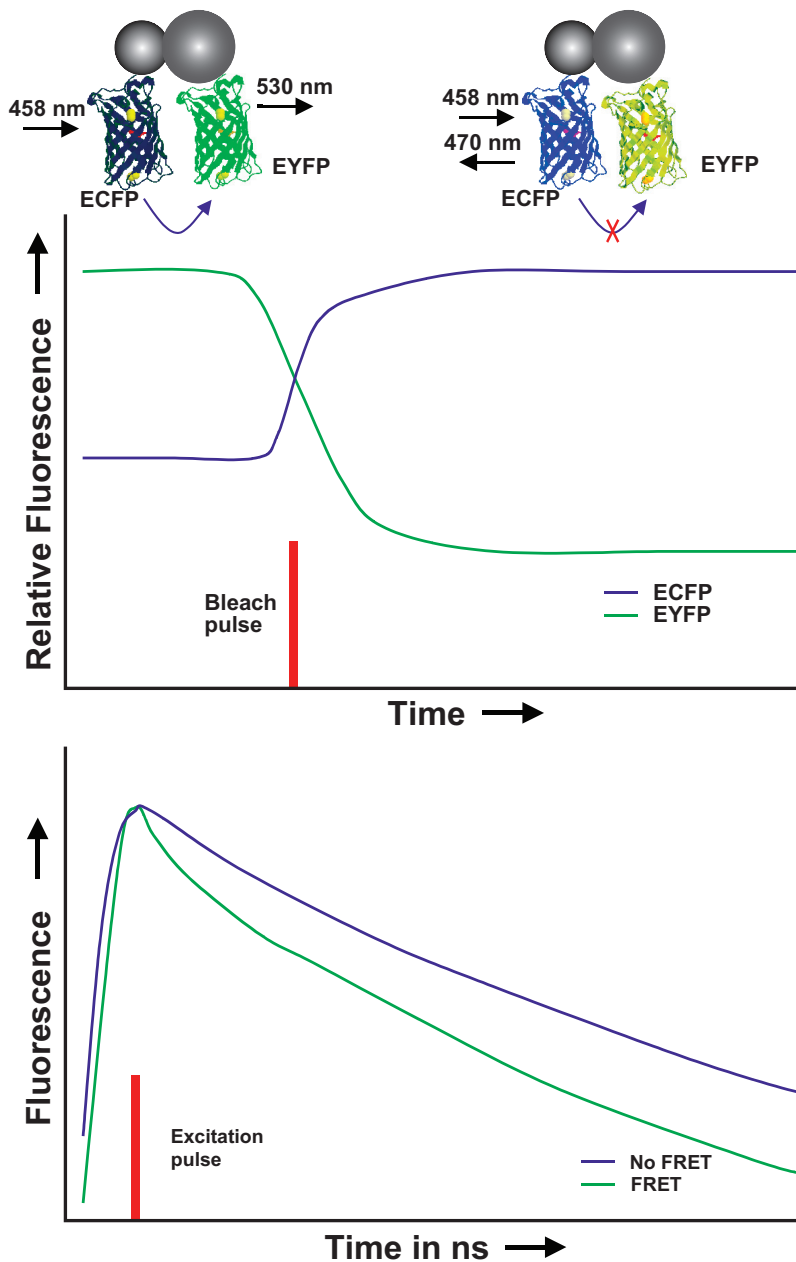


Figure 6. Protein-protein interactions in living cells analyzed by FRET and FLIM. When two fluorescent molecules are in close proximity (<10 nm), energy transfer from the donor (ECFP) to the acceptor (EYFP) can occur by excitation of the donor. Acceptor photobleaching of the acceptor abolishes energy transfer, and this results in an increase of donor fluorescence (upper panel). In FLIM analysis, interaction between molecules is analyzed by measurement of the lifetime of fluorescent molecules. The fluorescence lifetime of the donor is reduced as a result of FRET (lower panel).

FCS

Fluorescence correlation spectroscopy is a method to study diffusion of fluorescent molecules, and it yields a high temporal resolution at the single molecule level (Bacia and Schwille, 2003). A typical FCS setup is very similar to a confocal setup, but the laser beam is not moving over the sample and a very sensitive avalanche photodiode (APD) is used as detector. In combination with a confocal microscope, for example the Zeiss ConfoCor2, it is possible to define a region of interest to perform FCS (Figure 7A, white cross). The laser beam creates a very small confocal volume (0.2 femtoliter) in which the actual FCS measurement is done. During the entire measurement the laser is continuously on, but emission of photons only occurs when a fluorescent molecule travels through the excitation volume (Figure 7B). The fluctuations in fluorescence are monitored in time and are dependent on the number of molecules in the confocal volume and the time spent therein (Figure 7C). An autocorrelation function is used to separate repetitive fluorescent signals, the fluctuations coming from the emitted photons from the fluorescent molecule in the confocal volume, from the background signals. Different diffusion models can be applied to calculate concentrations and diffusion coefficients. FCS can be used to study interaction between fluorescent molecules. The fluorescent signals of two fluorescent dyes, measured in the confocal volume, are directed to separate channels, and the autocorrelation functions for each dye are calculated. A third correlation function, the cross-correlation function, represents the correlation between the two channels and thereby the degree of interaction. Interaction studies by dual-color cross-correlation FCS are not limited by a certain range of distances between the interacting molecules, like in FRET, since simultaneous diffusion of two fluorescent fusion proteins is measured. This method is much more versatile with respect to analysis of multi-protein complexes. In addition, a multiphoton laser makes it possible to excite multiple fluorescent proteins with a single laser line. FCS autocorrelation and cross-correlation provide very sensitive methods to study dynamics and concentrations of low levels of fluorescent molecules in living cells, and also interaction between fluorescent molecules at high temporal resolution.

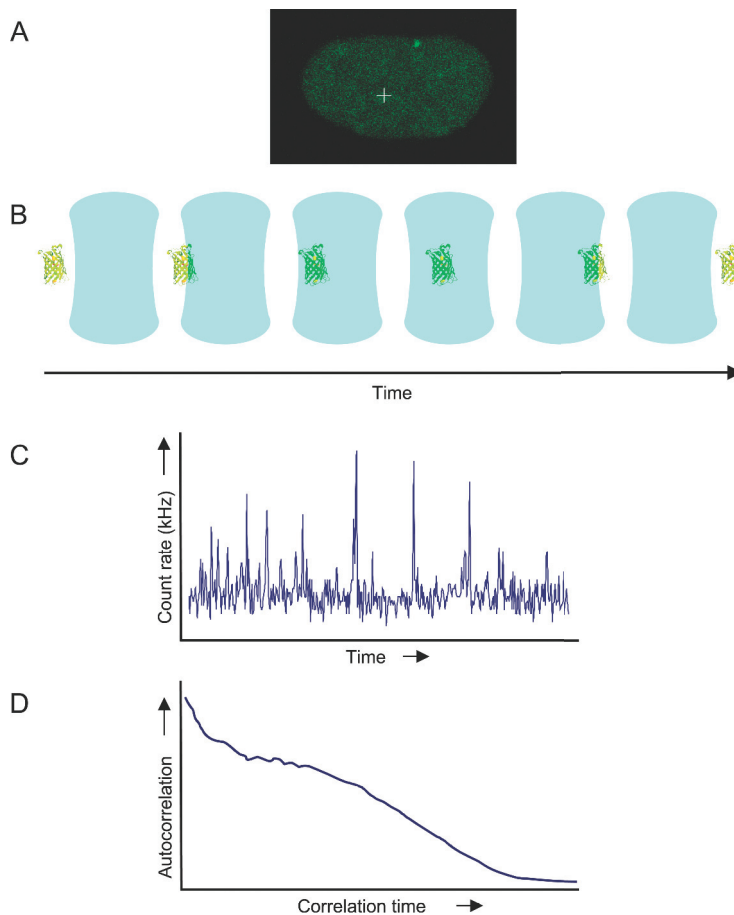


Figure 7. Fluorescence correlation spectroscopy. The FCS confocal volume can be positioned in the nucleus of cell (A, cross) and fluorescent molecules that travel through the confocal volume are excited (B). Fluorescent fluctuations result from the photons emitted by single molecules, which are counted by a very sensitive APD detector (C). The fluctuations are mathematically processed into the autocorrelation function (D).

Conclusions and perspectives

The discovery of fluorescent proteins that can be coupled to proteins of interest by genetic methods has triggered a revolution in the field of live cell microscopy. Currently, multiple techniques are available to study intracellular dynamics, conformational changes and interactions of biomolecules in living cells. However, one has to consider which technique can be applied to answer a specific question, and all techniques have intrinsic advantages and limitations that play an important role in the decision how to tackle a specific issue. For example, FRET measurement is a powerful method to study conformational changes of a molecule that harbors the donor and acceptor at opposite ends. On the other hand, interaction of multiple proteins in a complex can be studied more efficiently by

cross-correlation FCS in which distances between interacting molecules are less critical.

With the completion of the human genome project, an important task for bio-scientists is shifting towards analysis of protein structure and function, and also to find out how encoded proteins operate together in living cells. There is no doubt that fluorescence microscopy will play a central role in this ongoing and future work. In addition, application of fluorescence microscopy-related techniques becomes interesting to pharmaceutical and biotechnology industry, for developing high-throughput and high-content screening platforms for automated analysis of intracellular localization and dynamics of proteins. Finally, confocal microscopy has been coupled to endoscopy, creating diagnostic potential (Watson et al., 2002).

Further reading

Fundamentals of Light Microscopy and Electronic Imaging (2001). By **Douglas B. Murphy**; Wiley, John & Sons, Incorporated (ISBN: 047125391X).

Protein Localization by Fluorescence Microscopy: A Practical Approach (2000). By Victoria J. Allan; Oxford Press (ISBN: 0199637407).

Methods in Cellular Imaging (2001). By **Ammasi Periasamy**; Oxford University Press (ISBN: 0195139364).

Confocal and Two-Photon Microscopy: Foundations, Applications and Advances (2002). By **Alberto Diaspro**; Wiley, John & Sons, Incorporated (ISBN: 0471409200).

Methods in Cell Biology, Volume 70: Cell Biological Applications of Confocal Microscopy, Second Edition (2002). By **Brian Matsumoto**; Academic Press, Incorporated (ISBN: 012480277X).

Handbook of Biological Confocal Microscopy (1995). By **James B. Pawley**; Kluwer Academic Publishers (ISBN: 0306448262).

Confocal Microscopy Methods and Protocols (1999). By **Stephen W. Paddock**; Humana Press (ISBN: 0896035263).

Informative websites

General Information

Molecular Expressions: The Microscopy Primer	http://micro.magnet.fsu.edu/primer/index.html
Microscopy and Imaging Resources on the WWW	http://swehsc.pharmacy.arizona.edu/exppath/micro/index.html
WWW Virtual Library: Microscopy	http://www.ou.edu/research/electron/www-vl/long.shtml

Microscopy Journals

Microscopy Today	http://www.microscopy-today.com/
Microscopy Research and Technique	http://www3.interscience.wiley.com/cgi-bin/jhome/38527
Microscopy and Microanalysis	http://www.msa.microscopy.com/MM/MscopyManalysis.html
Journal of Cell Science	http://jcs.biologists.org/current.shtml

Microscopy Societies

European Microscopy Society	http://www.eurmicsoc.org
Dutch Society for Microscopy	http://www.microscopie.nl/
Royal Microscopical Society	http://www.rms.org.uk
American Microscopical Society	http://www.amicros.org
Microbeam Analysis Society	http://www.microbeamanalysis.org
Microscopy Society of America	http://www.MSA.microscopy.com

Microscope Manufacturers

Carl Zeiss Microscopy & Image Analysis	http://www.zeiss.com/
Nikon Instruments	http://www.nikon-instruments.com/
Bio-Rad Cell Science Division	http://cellscience.bio-rad.com/index.html
Olympus Microscopy	http://cf.olympus-europa.com/micro/home.cfm
Leica Microsystems	http://www.leica-microsystems.com/website/lms.nsf

References

- Ando, R., Hama, H., Yamamoto-Hino, M., Mizuno, H., and Miyawaki, A.** (2002). An optical marker based on the UV-induced green-to-red photoconversion of a fluorescent protein. *Proc Natl Acad Sci USA* **99**, 12651-12656.
- Bacia, K., and Schwille, P.** (2003). A dynamic view of cellular processes by in vivo fluorescence auto- and cross-correlation spectroscopy. *Methods* **29**, 74-85.
- Baird, G. S., Zacharias, D. A., and Tsien, R. Y.** (2000). Biochemistry, mutagenesis, and oligomerization of DsRed, a red fluorescent protein from coral. *Proc Natl Acad Sci USA* **97**, 11984-11989.
- Dickinson, M. E., Bearman, G., Tilie, S., Lansford, R., and Fraser, S. E.** (2001). Multi-spectral imaging and linear unmixing add a whole new dimension to laser scanning fluorescence microscopy. *Biotechniques* **31**, 1272, 1274-1276, 1278.
- Heim, R., Cubitt, A. B., and Tsien, R. Y.** (1995). Improved green fluorescence. *Nature* **373**, 663-664.
- Hiraoka, Y., Shimi, T., and Haraguchi, T.** (2002). Multispectral imaging fluorescence microscopy for living cells. *Cell Struct Funct* **27**, 367-374.
- Houtsmuller, A. B., and Vermeulen, W.** (2001). Macromolecular dynamics in living cell nuclei revealed by fluorescence redistribution after photobleaching. *Histochem Cell Biol* **115**, 13-21.
- Patterson, G., Day, R. N., and Piston, D.** (2001). Fluorescent protein spectra. *J Cell Sci* **114**, 837-838.
- Patterson, G. H., and Lippincott-Schwartz, J.** (2002). A photoactivatable GFP for selective photolabeling of proteins and cells. *Science* **297**, 1873-1877.
- Prasher, D. C., Eckenrode, V. K., Ward, W. W., Prendergast, F. G., and Cormier, M. J.** (1992). Primary structure of the *Aequorea victoria* green-fluorescent protein. *Gene* **111**, 229-233.
- Tsien, R. Y.** (1998). The green fluorescent protein. *Annu Rev Biochem* **67**, 509-544.
- Tsurui, H., Nishimura, H., Hattori, S., Hirose, S., Okumura, K., and Shirai, T.** (2000). Seven-color fluorescence imaging of tissue samples based on Fourier spectroscopy and singular value decomposition. *J Histochem Cytochem* **48**, 653-662.
- Watson, T. F., Neil, M. A., Juskaitis, R., Cook, R. J., and Wilson, T.** (2002). Video-rate confocal endoscopy. *J Microsc* **207**, 37-42.
- White, J., and Stelzer, E.** (1999). Photobleaching GFP reveals protein dynamics inside live cells. *Trends Cell Biol* **9**, 61-65.
- Yang, T. T., Cheng, L., and Kain, S. R.** (1996). Optimized codon usage and chromophore mutations provide enhanced sensitivity with the green fluorescent protein. *Nucleic Acids Res* **24**, 4592-4593.



Chapter 3

mRAD18Sc, a mouse homolog of the yeast post-replication repair gene RAD18

Genomics, 69(1):86-94 (2000)

Characterization of mRAD18Sc, a mouse homolog of the yeast post-replication repair gene RAD18

Roald van der Laan^{**}, Henk P. Roest^{*}, Jos W. Hoogerbrugge^{*}, Elisabeth M.E. Smit[†], Rosalyn Slater[†], Willy M. Baarends^{*}, Jan H. J. Hoeijmakers^{*1} and J. Anton Grootegeed^{*}

^{*}MGC-Department of Cell Biology and Genetics, Center for Biomedical Genetics
Erasmus University Rotterdam, P.O. Box 1738, 3000 DR Rotterdam, The Netherlands

^{*}Department of Endocrinology and Reproduction
Erasmus University Rotterdam, P.O. Box 1738, 3000 DR Rotterdam, The Netherlands

GenBank accession number AF205278

Abstract

The *RAD18* gene of the yeast *Saccharomyces cerevisiae* encodes a protein with ssDNA binding activity, that interacts with the ubiquitin-conjugating enzyme RAD6 and plays an important role in post-replication repair. We identified and characterized the putative mouse homolog of *RAD18* designated *mRAD18Sc*. The *mRAD18Sc* open reading frame encodes a 509 amino acid polypeptide that is strongly conserved in size and sequence between yeast and mammals, with specific conservation of the RING-zinc-finger and the classic zinc-finger domain. The degree of sequence conservation between mRAD18Sc and RAD18 and homologous sequences identified in other species (NuvA from *Aspergillus nidulans* and Uvs-2 from *Neurospora crassa*) is entirely consistent with the evolutionary relationship of these organisms, strongly arguing that these genes are each other's homologs. Consistent with the presence of a nuclear translocation signal in the amino acid sequence we observed nuclear localization of GFP-tagged mRAD18Sc after stable transfection to HeLa cells. mRNA expression of *mRAD18Sc* in the mouse was observed in thymus, spleen, brain and ovary, but was most pronounced in testis, the highest expression in pachytene stage primary spermatocytes, suggesting that mRAD18Sc plays a role in the meiosis of spermatogenesis. Finally, we mapped the *mRAD18Sc* gene on mouse chromosome 6F.

Introduction

At least 5 multi-enzyme DNA repair pathways are currently known; one of these is termed post-replication repair (PRR). PRR is not really a repair system, as the name suggests, but it facilitates tolerance of base damage during replication, overcoming termination of replication at the sites of damage (Lawrence *et al.*, 1994, Friedberg and Gerlach, 1999). For eukaryotes, most is known about PRR in

the yeast *Saccharomyces cerevisiae*, based numerous PRR mutants. PRR includes two distinct subpathways, error-prone repair and error-free repair (reviewed by Naegeli, 1994). In *Escherichia coli*, error-prone translesion synthesis requires the heterotrimeric UmuD'₂C DNA polymerase (Woodgate and Levine, 1996, Smith and Walker, 1998 and Tang *et al.*, 1999). In *S. cerevisiae*, the REV3 and REV7, subunits of DNA polymerase ζ , accomplish mutagenic translesion synthesis (Lawrence and Hinkle, 1996), requiring REV1 *in vivo* (Woodgate, 1999). The REV1 possesses dCTP transferase activity (Nelson *et al.*, 1996), but it has also limited DNA polymerase activity (Woodgate, 1999). The error-free subpathway is thought to involve reinitiating replication downstream of a damaged site and subsequent error-free repair of the gap, by template switching (Naegeli, 1994 and Higgins *et al.*, 1976), or usage of the newly synthesized daughter strand, involving recombinational repair (Naegeli, 1994 and Rupp *et al.*, 1971). The genes involved in PRR are placed in the very heterogeneous RAD6 epistasis group (Friedberg *et al.*, 1995). Yeast *rad6* mutants display the most severe phenotype: extreme sensitivity to UV- and ionizing radiation as well as numerous genotoxic chemical agents (Cox *et al.*, 1968, Game *et al.*, 1974), a decreased growth rate (Lawrence, 1994), and a sporulation defect (Game *et al.*, 1980, Montelone *et al.*, 1981). Other prominent members are *RAD5*, *RAD9*, *RAD18*, *REV1*, *REV3*, *REV7* (Friedberg *et al.*, 1995) and *RAD30* (McDonald *et al.*, 1997). Previously, we have cloned two mammalian homologs of the yeast *RAD6* gene (*HR6A*, *HR6B*) and determined their role in the mouse by targeted gene disruption (Roest *et al.*, 1996, Baarends *et al.*, 1999). To elaborate further in this direction, it is important to identify possible homologs of other PRR genes.

Yeast *RAD18* encodes a 55.5 kDa protein with a C₃HC₄-RING-Zn²⁺-finger and a C₂HC-Zn²⁺-finger (Chanet *et al.*, 1988). Transcription of *RAD18* remains constant during the mitotic cell cycle but increases upon UV-irradiation (Jones *et al.*, 1991). The *RAD18* has ssDNA binding ability, forms a stable complex with *RAD6* *in vivo* (Bailly *et al.*, 1994) and has been claimed to exhibit ssDNA-dependent ATPase activity (Bailly *et al.*, 1997b). *RAD18* seems to interact with both the N- and C-terminus of *RAD6* via the two acidic regions in the middle and the C-terminus of *RAD18* (Chanet *et al.*, 1988 and Bailly *et al.*, 1997a). *RAD6* is an ubiquitin-conjugating enzyme catalyzing mono- and/or poly-ubiquitination of target proteins. Poly-ubiquitinated proteins usually undergo proteasomal degradation while mono-ubiquitination may regulate stabilization, folding and/or activity of proteins (reviewed by Hochstrasser, 1996). The role of *RAD6* and *RAD18* in PRR is largely unknown. A possible function of *RAD6* is modifying chromatin structure as part of DNA repair, mutagenesis and other processes, which are affected in the *rad6* mutant (Koken *et al.*, 1991). Recently, it was reported that ubiquitination of H2B in yeast, required for optimal mitotic cell growth and meiosis, primarily depends on *RAD6* activity (Robzyk *et al.*, 2000). *Rad18* mutants are highly sensitive to UV and other genotoxic agents, but show no pronounced defect in sporulation, meiotic recombination and UV-induced mutagenesis (Haynes *et al.*, 1981, Lawrence, 1982, Quah *et al.*, 1980, Boram *et al.*, 1976). In a nucleotide excision repair-deficient background *rad18* mutants display increased UV-induced mutability, comparable to that of *rad6* mutants under the same conditions (Cassier-Chauvat *et al.*, 1991, Armstrong *et al.*, 1994). The increased mutation frequency in *rad18* mutants suggests disturbed error-free repair but still active error-prone repair (Jones *et al.*, 1991). On the other hand, two *rad18* mutants show a decreased frequency of UV-induced mutations in the *SUP4-o* gene (Armstrong *et al.*, 1994). This suggests that *RAD18* plays a more general role in the PRR, rather than being involved only in error-

free repair. The *RAD18* gene is strongly conserved in lower eukaryotes as apparent from the identification of the highly conserved homologs *NuvA* (*Neurospora crassa*) and *Uvs-2* (*Aspergillus nidulans*) (Iwanejko *et al.*, 1996, Tomita *et al.*, 1993). In the present report, we describe the cloning of the putative murine homolog, designated *mRAD18Sc*, extending the conservation to mammals and enabling studies on the function and biological impact of this gene in mammalian species.

Materials and Methods

Identification and sequencing of a cDNA sequence encoding a putative mouse RAD18 homolog.

Database (dbEST) searches were performed with the amino acid sequence of *S. cerevisiae* *RAD18* and its highly conserved homologs, *NuvA* from *Aspergillus nidulans* (*A. nidulans*) and *Uvs-2* from *Neurospora crassa* (*N. crassa*) using the TBLASTN program (Altschul *et al.*, 1990, 1994). The EST AA086742 clone obtained from ATCC (American Type Culture Collection, Rockville, MD, USA (Lennon *et al.*, 1996)) is part of a 1723 bp mouse embryonic carcinoma cDNA fragment cloned in the *EcoRI-XhoI* sites of pBluescript SK- (Stratagene, La Jolla, CA, USA). Sequence analysis was performed using the chain termination method (Sanger *et al.*, 1977) according to the manufacturer's instructions (Perkin Elmer, Norwalk, CA, USA). Fragments were separated on 6% acrylamide sequencing gels and run on an automated sequencer (Pharmacia Biotech, Uppsala, Sweden). The complete coding sequence has been deposited with GenBank identification number AF205278.

Northern blot analysis.

Total RNA was extracted from mouse tissues (C57Bl/6 and FVB) by the LiCl/urea method (Sambrook *et al.*, 1989). Mouse testes (C57Bl/6) were isolated at different days after birth (7, 14, 21 and 36 days) and RNA was extracted using TRIzol reagent (Life Technologies, Grand Island, NY, USA). Spermatocytes and round spermatids were isolated from mouse testes (C57Bl/6) after collagenase and trypsin treatment, followed by sedimentation at unit gravity (StaPut procedure) and density gradient centrifugation through Percoll (Grootegoed *et al.*, 1984) and RNA was isolated as above using LiCl/urea. The amount of RNA was measured by UV-spectrometry and 20 µg of total RNA was applied to each lane on 1% agarose gels, the separated RNA was then transferred to Hybond N+ membranes and hybridized with the labelled 1.7 kb *mRAD18Sc* cDNA probe (Sambrook *et al.*, 1989). Probes were labelled with α -³²PdATP (Amersham Lifescience Ltd., Buckinghamshire, UK) using random priming (Sambrook *et al.*, 1989). The tissue Northern blot was probed with hEF-1 α , which serves as a quantity control. In case of the testis Northern blot, the ethidium bromide-staining was used as a quantity control, since it is very difficult to select an appropriate probe for testis material of different ages which contains changing populations of different cell types.

Subcellular localization.

HeLa cells were cultured in DMEM/F12 (Life Technologies, Grand Island, NY, USA) containing 5% v/v fetal calf serum and penicillin and streptomycin, at 37° C under 5% CO₂. A monolayer of 50-80% confluency was transfected with 2 µg of Green Fluorescent Protein (GFP)-tagged *mRAD18Sc* cDNA using FuGene

(Roche, Basel, Switzerland) as the transfection reagent. The *mRAD18Sc* coding sequence was cloned into pEGFP-C2 (Clontech, Palo Alto, CA, USA) resulting in an N-terminal fusion protein. The border between the *GFP* cDNA and the *mRAD18Sc* cDNA was sequenced to confirm that *mRAD18Sc* cDNA was cloned in frame. Cells were also transfected with wild type pEGFP-C2. Stable integrants were selected using medium containing G418 (Geneticin; Life Technologies, Grand Island, NY, USA) at a final concentration of 800 µg/ml. Transfected cells were visualized using fluorescence microscopy.

Chromosomal localization.

In situ hybridization was performed on metaphase spreads of mouse E14 ES cells as described elsewhere (Pinkel *et al.*, 1988). An EMBL3 genomic clone isolated using the AA86742 cDNA was biotin-labeled and used to obtain the *mRAD18Sc* specific signal. A chromosome 6 specific telomere probe (Shi *et al.*, 1997) was dioxigenin-labeled and used to stain chromosome 6. The *mRAD18Sc* genomic probe was incubated with avidin-FITC and after amplification with biotinylated goat anti-avidin D, the signal was visualized by FISH. The dioxigenin-labeled telomere probe signal was enhanced using a Texas red-conjugated antibody. The banding pattern was visualized under the microscope using DAPI. At least 10 metaphase spreads were examined.

Results

Sequencing and characterization of the mRAD18Sc cDNA.

Regular systematic screening of public EST (the NCBI Expressed Sequence Tag) databases with *RAD18*, *NuvA* and *Uvs-2* revealed the presence of a putative murine EST (AA086742) specifying a RING-zinc-finger part of a protein with high homology to the *S. cerevisiae* *RAD18*. The amino acid sequence of the RING-zinc-finger motif is highly conserved between *RAD18*, *NuvA* and *Uvs-2*, but also shares high homology with RING-zinc-finger domains in other proteins. Interestingly, the identified EST clone harbors a possible start codon at a comparable distance from the RING-zinc-finger as in the *RAD18* amino acid sequence. The murine EST in turn was used to screen the Genbank/EMBL databases confirming and extending the homology with *RAD18*, *NuvA* and *Uvs-2*. This strengthened our presumption that the identified EST indeed represents a candidate murine homolog of *RAD18*, to which we will further refer to as *mRAD18Sc*. Sequencing of the cDNA in both directions revealed a large open reading frame of 1530 bp coding for a 509 amino acid polypeptide (Figure 1) with a calculated molecular mass of 57.3 kDa and an isoelectric point of 6.95. The 5' untranslated region (UTR) harbors the Kozak translation initiation sequence *gcgGccAtgG* (Kozak, 1987). This ATG is the first start codon in the cDNA. The stop codon TAG at position +1528 is followed by a short stretch of 3' UTR containing a poly-A tail. Surprisingly, no polyadenylation signal is found in the 3' UTR in front of the poly-A tail. It is possible that the poly-d(T) primer used for cDNA synthesis annealed to an adenosine-rich stretch upstream of the poly-A tail that resulted in a shorter 3' UTR without a polyadenylation signal sequence.


```

-29                               GGCACGAGGCGGTCTCATCAGGTGCGGCC
1  ATGGAGGTCCTGGCCGAGCCGCGATGCCCTCCGGGGTTGGCGGTGATGAAGACAATAGAT
1  M E V L A E P R C P P G L A V M K T I D
61  GACTTGTCTGCGCTGTGGGATTGCTTTGAGTATTTCAACATTGCAGTGATAATCCCCAG
21  D L L R C G I C F E Y F N I A V I I P Q
121 TGCTCTCAACATTATTGTTCACTCTGTATAAGAAAAGTTTTTATCCTATAAAAATCAGTGC
41  C S H N Y C S L C I R K F L S Y K T Q C
181 CCAACTTGTTCGCTGGCAGTAACGGAGCCAGACCTGAGAAAATAATCGCCTCTTAGATGAA
61  P T C C V A V T E P D L R N N R L L D E
241 CTGGTAAAACCATGAATTTTGCACGGACTCACCTGTGCAGTTTGCCTTAGAGTACCA
81  L V K S M N F A R T H L L Q F A L E S P
301 CCCATATCTCCTGTGTCTCCACCTCAAAGAAGGTTGTGTTAAAGTGATAATGCTGAC
101 P I S P V S S T S K K V V V K V H N A D
361 GCCGCCAACACCTGTCAAACAGGCGAACAGGTTAATGGATAAGTTAGAGAA
121 A A Q H P V K Q A N R L M D K F L I R E
421 ACTGGTGACTGTATTTGAGTTGTTGGGAAAAGAAAATGAGAGGAAAATTCAGCCPQ
141 T G D C V F E L L G K E N E R K F S P Q
481 AAAGAGCTAAGCCTCTGCTGAGATTAAAGAGACAAGTCTCCTAGGAAAAGCCGGTACTG
161 K E L S T S A E I K E T S L L G K P V L
541 GGGCTCTCGGATGCTAATGGTCTGTGACTCCCTCTACATCCACTATGAAAATGGATACT
181 G L S D A N G P V T P S T S A H K R
601 AAAGTGTCTTGTCTGTTTGTGGGGTCAGCATTCCAGAAAATCATATCAATAAGCATTTA
201 K V S C P V C G V S I P E N H I N K H L
661 GACAGTTGTTTATCACGTGAAGAGAAAAAGGAGAGCCTGCGAAGTCTCTGCACAAAAGG
221 D S C L S R E E K K E S L R S S A H K R
721 AAGCCGTTGCCAAAACGTATATAACTTGCTCTCTGATCGTGATTAAAGAAAAGCTG
241 K P L P K T V Y N L L S D R D L K K K L
781 AAACAGTATGGCTTATCTGTTCCAGGAAACAACAGCAGCTTATTTAAAGKCATCAGGAG
261 K Q Y G L S V P G N K Q Q L I K R H Q E
841 TTTGTGCACATGTATAATGCCAGTGCATGCTTTGCATCCTAAATCAGCTGCTGAAATC
281 F V H M Y N A Q C D A L H P K S A A E I
901 GTCCAAGAAATGAAAAGCATGGAGAAGACCAGGATGCGCCTTGAAGCAAGTAAACTCAAT
301 V Q E I E S M E K T R M R L E A S K L N
961 GAAAATGTCATGGTTTTTACAAAGAACCAACAGAGAAGGAAATGAGGAAGTTCACAGT
321 E N V M V F T K N Q T E K E I E V H S
1021 GAATATCGTAAAAGCACCAGAATGCATTCAGCTTCTGGTGGATCAGGCCAAAAAAGGG
341 E Y R K K H Q N A F Q L L V D Q A K K G
1081 TATAAGAAAAGTGGCAGAGTTTCACAAGCTGCACGATGAGAACAGATGAACCTGCAGAG
361 Y K K T G R V S Q A A A M R T D E P A E
1141 ACACTGCCGTCGATGAGAACAGATGAACCTGCAGAGACTGCCGTCGATGAGAACAGAT
381 T L P S M R T D E P A E T L P S M R T D
1201 GAACCTGCAGAGACTGCCGTTGATGAGAGCAGATGAACCTGCAGAAAACACTGCCGCT
401 E P A E T L P L M R A D E P A E T L P S
1261 GAGTGTATCGCACAGAAGATAATGTGAGCTTCTCAGATACTGTCTCAGTAACAACCAC
421 E C C I A Q Q E D N V S F S D T V S V G T N H
1321 TTTCTCAGACCCAGCTGGACTCGCCAGGCCCTGCGGAGCTGAGAGGCCGATGATTCT
441 F P Q P Q L D S P G P S E P E R P D D S
1381 TCTAGTTGFACTGATATCTTTTCTCCTCGGACTCAGACTCATGCAATAGAAATGATCAA
461 S S C A T D I L F S S D S D S C N R N D Q
1441 AACAGAGAAGTCAGCCACAAACAGACTCGCCGCACTAGAGCCAGTGAATGTGTTGAGATT
481 N R E V S P Q Q T R R T R A S E C V E I
1501 GAACCAAGAAACAGCGGAATAAGAATTAGTATGGGCTTTGTGCCAGCTTTCCTGACAGT
501 E P R N K R N K N *
1621 GACCTGAATATGATTTGTTATTGCCATGTATGGCTTCATATTTAAACAATATCCAAGGAA
1681 GACTTTTAAGTCTAAAn

```

Figure 1.The *mRAD18Sc* coding sequence, 3' UTR and 5' UTR and amino acid sequence. Black box: C₂HC₂-RING-Zn²⁺-finger (residues 26-63); dark gray box: C₂HC-Zn²⁺-finger (residues 204-223) [cysteines and histidines are highlighted]; bold italics: NLS (residues 257-261); light gray box: repeat amino acid sequence (residues 373-420) [1st amino acid residue is highlighted]; bold underlined: putative phosphorylation site (residues 469-474).



Figure 2. Alignment of amino acid sequences of RAD18, NuvA, Uvs-2 and mRAD18Sc. C and H: cysteines and histidines of C₃HC₄-RING-Zn²⁺-finger and C₂HC-Zn²⁺-finger; black boxes: identical residues; gray boxes: similar residues (similarity groups: STPAG, FYW, KRH, DENQ and IVLM). In addition we identified in the genome sequence of *Caenorhabditis elegans* part of the presumed worm homolog of RAD18.

The N-terminus of the protein contains a C₃HC₄-RING-Zn²⁺-finger (RING-zinc-finger), and the middle a CX₂CX₁₁HX₃C-type zinc-finger (Figure 1), both highly conserved between yeast RAD18 and the fungal homologs NuvA and Uvs-2 (Figure 2). The presence of a potential nuclear localization sequence KKKLK suggests that mRAD18Sc resides in the nucleus. Towards the C-terminus, we found a potential phosphorylation site (SSSDSDS). Finally, a 12 amino acid sequence (consensus MRTDEPAETLPS) repeat was noted, which appeared 4 times (position 372 to 420). This region is not apparent in any of the 3 other proteins and a query with the consensus sequence in the Swissprot database did not yield proteins with a similar sequence. The size of the mRAD18Sc is comparable with that of RAD18 with significant homology over the entire length (Figure 2). NuvA (*A. nidulans*) and Uvs-2 (*N. crassa*) show a similar level of homology to RAD18 as shown in Figure 3. The phylogenetic distances between the *S. cerevisiae*, *A. nidulans*, *N. crassa* and *M. musculus* proteins have been calculated, using the PHYLIP computer program (Figure 3). It is clear that *A. nidulans* and *N. crassa* proteins are most closely related, consistent with the evolutionary distance between the organisms.

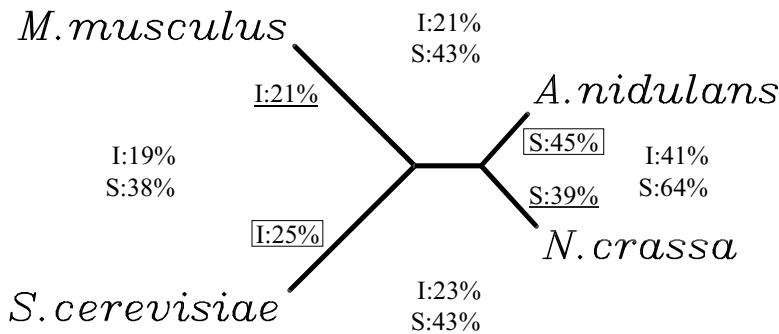


Figure 3. Phylogenetic tree (PHYLIP). Calculated phylogenetic relationship of *S. cerevisiae*, *A. nidulans*, *N. crassa* and *M. musculus* RAD18 homologs based on amino acid sequence similarity of RAD18, NuvA, Uvs-2 and *mRAD18Sc*, respectively. 'I' represents percentage identity between the proteins of 2 species and S represents percentage similarity.

Tissue-specific expression of mRAD18Sc.

RAD6 interacts with RAD18 *in vivo* (Baily *et al.*, 1994). This would predict co-expression of the mammalian homologs in certain tissues. In order to compare mRNA expression of *mRAD18Sc* with *mHR6A* and *mHR6B*, Northern blot analysis was performed on several mouse tissues revealing expression of *mRAD18Sc* in thymus and spleen at a moderate level, and lower *mRAD18Sc* expression in brain and ovary (Figure 4A). The by far highest mRNA level was observed in testis. At least 3 transcripts of 4.0, 3.1 and 1.6 kb were observed. Although our cDNA lacks a polyadenylation signal, the length of this cDNA (approximately 1.7 kb) is in the same range as that of the smallest transcript (1.6 kb transcript). As discussed below there are both parallels and differences with the expression profile of the two *HR6* genes.

The adult testis is composed of a broad range of cell types; somatic cells, notably Leydig and Sertoli cells, and germinal cells, including mitotic spermatogonia, spermatocytes going through the prophase of meiosis, and post-meiotic (round and elongating) spermatids. To find out what cell type(s) is (are) responsible for the high expression level of *mRAD18Sc* in mouse testis, we analyzed RNA of total testis of different stages of development (7, 14, 21 and 36 days after birth) and isolated cell preparations highly enriched in spermatocytes and round spermatids (Figure 4B). Developmental onset of expression of many genes in the testis occurs during postnatal life, when spermatogenesis is initiated. Testis from 21-day-old mice, displayed a marked increase of *mRAD18Sc* mRNA expression, in particular the 3.1 kb transcript. Also purified spermatocytes show a very high expression of this 3.1 kb transcript, which can explain its pronounced signal in 21-day-old testis where spermatocytes make up the largest fraction of the spermatogenic cell population. The level of *mRAD18Sc* mRNA expression in round spermatids is lower compared to the spermatocytes (Figure 4B). In testis of 36-day-old animals, the *mRAD18Sc* mRNA level is decreased, probably caused by a high number of round spermatids, which dilutes the signal from the spermatocytes.

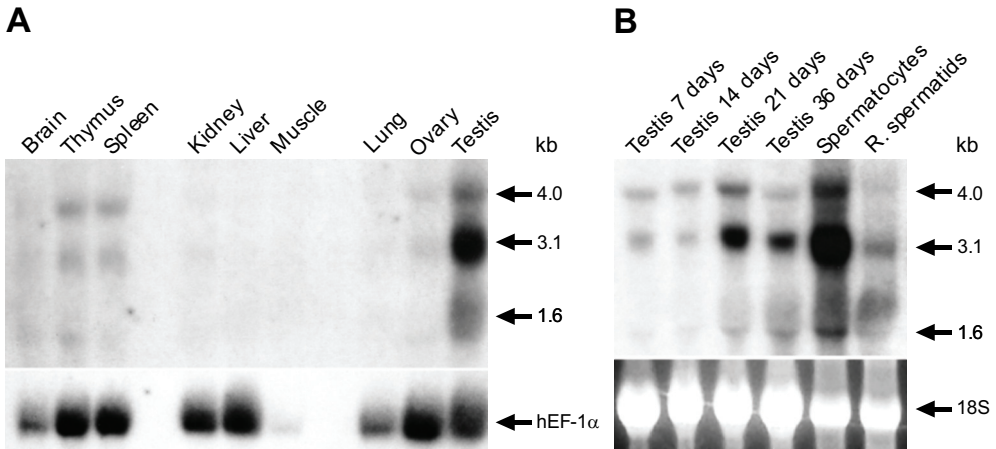


Figure 4. Northern blot analysis of various tissues from adult mice. (A), and testis from 7-36-day-old mice including purified mouse spermatocytes and round spermatids (B). The mRNA transcripts were detected using *mRAD18Sc* cDNA as a probe; hEF-1 α expression (Panel A, lower part) and 18S rRNA content (Panel B, lower part) are shown as controls for the amount of RNA.

Subcellular localization.

To investigate whether *mRAD18Sc* is a nuclear protein, suggested by the presence of a putative NLS, HeLa cells were stably transfected with a Green Fluorescent Protein (GFP)-tagged *mRAD18Sc*-coding vector. In case of vector alone, the GFP signal was observed throughout the cell while cells transfected with *mRAD18Sc*-GFP showed a fluorescence signal only in the nucleus (Figure 5). This signal was maintained in the nucleus after at least 8 passages on selective medium (G418). Similar results were observed with Cos-1 cells and CHO-9 cells (transient transfections, results not shown).

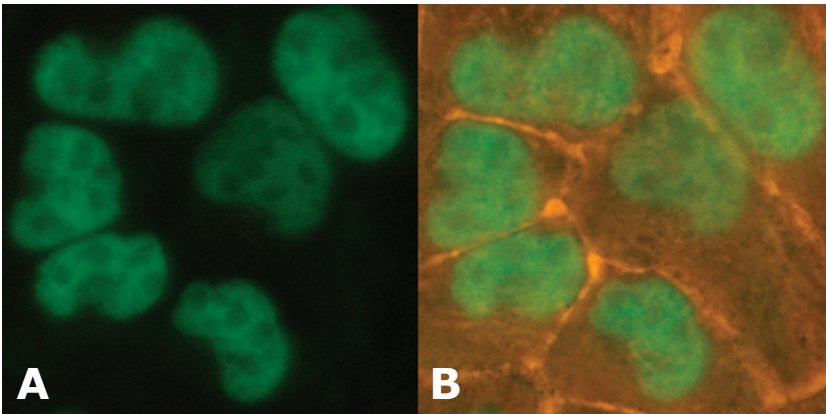


Figure 5. Subcellular localization of *mRAD18Sc* in HeLa cells. (A) Fluorescent image of stable integrants (GFP-*mRAD18Sc* fusion protein) and (B) the same cells visualized with fluorescent light combined with phase-contrast.

Chromosomal localization.

In situ hybridization was performed in order to determine the chromosomal location of the *mRAD18Sc* gene. A genomic clone representing part of *mRAD18Sc* was used as a probe for *in situ* hybridization. A *mRAD18Sc* specific signal was mapped on mouse chromosome 6F as indicated with the green arrows (Figure 6). The assignment to chromosome 6 was confirmed using a chromosome 6-specific telomere probe (indicated by the red arrows). Also a PCR-derived genomic fragment of approximately 15 kb containing the first 321 nucleotides of the coding sequence, was used for *in situ* hybridization and this confirmed the chromosomal localization of *mRAD18Sc* on mouse chromosome 6F (results not shown).

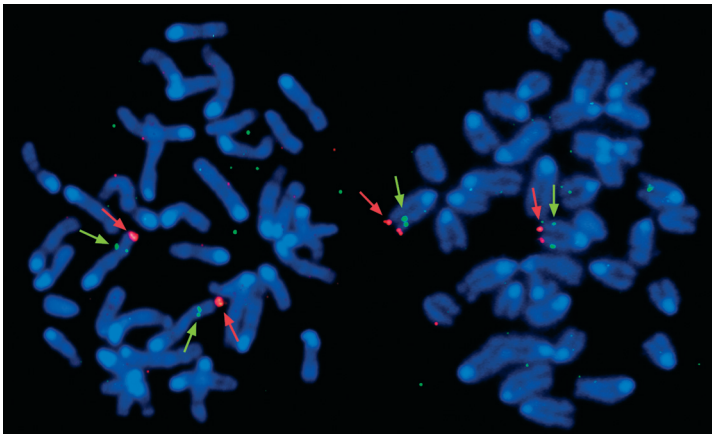


Figure 6. *In situ* hybridization of metaphase chromosomes. Biotin-labeled *mRAD18Sc* genomic probes (green arrows) visualized with FISH. Dioxigenin-labeled telomere probes visualized with Texas red were used to specifically stain chromosome 6 (red arrows). The banding pattern is visualized with DAPI.

Discussion

Despite its obvious importance for understanding the origin of mutations, the molecular mechanism of PRR in mammalian cells remains largely unknown. However, several novel DNA polymerases functioning in the translesion synthesis pathway of PRR have been identified recently (reviewed by Woodgate, 1999), among which the gene mutated in xeroderma pigmentosum variant (Masutani *et al.*, 1999). The function of RAD6 and RAD18 in this process is still unclear. This report describes the cloning of the putative mouse homolog of the yeast PRR gene *RAD18*, designated *mRAD18Sc*.

The *mRAD18Sc* gene encodes a polypeptide with two zinc-finger motifs. The RING-zinc-finger, which is situated in the N-terminal, is highly conserved between the homologs *mRAD18Sc*, *RAD18*, *Uvs-2* and *NuvA*. More to the central part there is a conserved classic zinc-finger (CX₂CX₁₁HX₃C) motif. Since *RAD18* is able to bind ssDNA (Bailey *et al.*, 1994) the C₂HC-zinc-finger could function as the DNA-binding domain in *RAD18* and its homologs. The function of RING-zinc-fingers is not very clear. The domain found recently in proteins, which take part in multi-protein complexes, and therefore the RING-zinc-finger could be involved in protein-

protein interactions (Saurin *et al.*, 1996). Recently, it has been reported that RING-zinc-finger proteins mediate ubiquitin-conjugating enzyme (E2)-dependent ubiquitination (Lorick *et al.*, 1999). Several findings suggest that RING-zinc-finger proteins can act as ubiquitin-protein ligases (E3) that recognize their target and promote ubiquitin ligation (Joazeiro *et al.*, 1999, Lorick *et al.*, 1999, Martinez-Noel *et al.*, 1999 and Waterman *et al.*, 1999). Since the RAD18 protein interacts with RAD6, which is an E2, RAD18 may play a role in ubiquitination mediated by RAD6.

It is of interest to note that mRAD18Sc lacks the sequence 'GKS' that in RAD18 (residues 365-367) has been suggested to represent a Walker A motif required for ATP binding and hydrolysis (Bailey *et al.*, 1994). Remarkably, this sequence is also absent in the other fungal homologs of RAD18 (see Figure 2), as well as in the human homolog (unpubl. observations). Close inspection of the RAD18 amino acid sequence reveals that the 'GKS' context does not obey to the general consensus for Walker A boxes and also lacks the Walker B consensus. These findings question the functional significance of the 'GKS' sequence in RAD18 and the weak ssDNA-dependent ATP-ase activity reported to be associated with a purified RAD6-RAD18 complex (Bailey *et al.*, 1997b), as it is not conserved in any of the other species.

The mRAD18Sc contains a putative nuclear localisation sequence, suggesting that mRAD18Sc can migrate to, and function in the nucleus. Indeed, transient and stable transfections to various cells yielded specific nuclear staining with mRAD18Sc-GFP but not with a vector expressing GFP alone. This indicates that mRAD18Sc acts in the nucleus, as expected for a protein involved in PRR.

The mRAD18Sc polypeptide displays a 4 times almost perfectly repeated sequence of 12 amino acids. Comparative analysis in databases did not identify other polypeptides or domains with the same or a closely related sequence that would provide a clue to its function. A recently submitted murine EST, (EST067902) derived from a different tissue has an identical sequence, ruling out that this is an artefact of cDNA synthesis. The fact that the nucleotide sequence is virtually identical for all 4 repeats indicates that the sequence has recently arisen by amplification and suggests that it may be unique to the mouse.

RAD18 interacts with RAD6 *in vivo*. To determine if *mRAD18Sc* might function in the same tissues as *mHR6A* and *mHR6B*, Northern blot analysis was performed revealing 3 distinct *mRAD18Sc* transcripts in a variety of tissues, the smallest comparable in length with the identified mouse EST. The other sized transcripts can be explained by a difference in the 5'-untranslated region as a result of multiple promoter sites, a difference in the 3'-untranslated region caused by different polyadenylation sites or alternative splice variants. If co-ordinated function of *mRAD18Sc* with *mHR6A* and/or *mHR6B* is conserved throughout evolution, combined expression of these genes is to be expected. In the mouse both *mHR6A* and *mHR6B* were found to be expressed in brain, thymus, muscle, spleen, heart, kidney, ovary and testis, with the highest level of *mHR6A* expression in brain and heart and *mHR6B* in brain, heart and testis (Koken *et al.*, 1996). For *mRAD18Sc*, we observed a different expression profile: the highest mRNA level in testis, moderate levels in thymus and spleen, and low levels in brain and ovary. Thymus and spleen are composed of mitotically active cells. Since *mRAD18Sc* mRNA levels are higher in these organs as compared to e.g. postmitotic tissue such as brain, expression of the *mRAD18Sc* gene might at least in part be proliferation-related. The low overall level of mRNA suggests that the protein is not required in large quantities.

HR6A and *HR6B* are highly expressed in various spermatogenic cell types (Koken *et al.*, 1996) and targeted disruption of *mHR6B* in the mouse results in derailment of spermatogenesis (Roest *et al.*, 1996). Therefore, we investigated *mRAD18Sc* expression in testis in more detail. The low expression of *mRAD18Sc* transcripts in testis from 7-14-day-old mice, probably presents the basal level of transcription in the somatic and mitotic components of testis. In 21-day-old testis, the progression of spermatogenesis results in a relatively high number of spermatocytes, with a very high *mRAD18Sc* expression, as observed in isolated spermatocytes. This explains the higher mRNA levels in 21-day-old testis (enrichment with spermatocytes) and the lower level in 36-day-old testis (where the abundance of spermatids dilutes the signal of *mRAD18Sc* expression in spermatocytes). Because *mRAD18Sc* expression is maximal in 21-day-old testis and in spermatocytes, we suggest that the *mRAD18Sc* gene plays an important role in the pachytene stage primary spermatocytes, which are in the prophase of meiosis.

A genomic clone was used to map the *mRAD18Sc* gene on mouse chromosome 6F. Recently, we identified part of a human cDNA highly homologous to *mRAD18Sc*. This putative human homolog of *RAD18* (*hRAD18Sc*) was localized on chromosome 21q22 (data not shown). However, no synteny between mouse chromosome 6F and human chromosome 21q22 was reported until now (Genome Informatics database, The Jackson Laboratory Bar Harbor, ME, USA).

In conclusion, a number of arguments support the idea that we have cloned the mouse homolog of yeast *RAD18*. 1.) When the *mRAD18Sc* sequence is used to screen the total yeast genome, *RAD18* stands out with the by far highest statistically significant score, implying that there is no other yeast gene with a similar high level of homology. 2.) The degree of similarity between the genes of different species is consistent with the relative evolutionary distance between them. 3.) Homology is extended over the entire protein, with specific conservation of the known functionally relevant domains. 4.) The protein resides in the nucleus, consistent with a role in PRR. The isolation of the mouse homolog provides the basis for analysis of the functions of the gene and the biological impact of the pathway in which it is involved.

Acknowledgements

This work was supported by the Dutch Cancer Society (EUR 99-2003) and the Dutch Science Foundation (NWO) through GB-MW (Medical Sciences). We thank Dr. Petra van Sloun (MGC-Department of Radiation Genetics Leiden University, The Netherlands) for providing the mouse tissue Northern blot, Jan de Wit for the CHO-9 and HeLa cells, Dr. Wim Vermeulen for the GFP-vector and assistance in fluorescence microscopy, André Eker for preparation of the phylogenetic tree and Mirko Kuit for photography. We are grateful to Dr. Jan Vreeburg and Dr. Gert van Cappellen (Department of Endocrinology and Reproduction, Erasmus University Rotterdam, The Netherlands) for helpful discussions and technical assistance.

References

- Altschul, S. F., Gish, W., Miller, W., Myers, E. W. and Lipman, D. J.** (1990). Basic local alignment search tool. *J. Mol. Biol.* **215**, 403-410.
- Altschul, S. F., Boguski, M. S., Gish, W. and Wootton, J. C.** (1994). Issues in searching molecular sequence databases. *Nat. Genet.* **6**, 119-129.
- Armstrong, J.D., Chadee, D.N. and Kunz, B.A.** (1994). Roles for the yeast RAD18 and RAD52 DNA repair genes in UV mutagenesis. *Mutat. Res.* **315**, 281-293.
- Baarends, W.M., Roest, H.P. and Grootegoed, J.A.** (1999). The ubiquitin system in gametogenesis. *Molecular and Cellular Endocrinology.* **151**, 5-16.
- Bailly, V., Lamb, J., Sung, P., Prakash, S. and Prakash, L.** (1994). Specific complex formation between yeast RAD6 and RAD18 proteins: a potential mechanism for targeting RAD6 ubiquitin-conjugating activity to DNA damage sites. *Genes Dev.* **8**, 811-820.
- Bailly, V., Prakash, S. and Prakash, L.** (1997a). Domains required for dimerization of yeast RAD6 ubiquitin-conjugating enzyme and RAD18 DNA binding protein. *Mol. Cell. Biol.* **17**, 4536-4543.
- Bailly, V., Prakash, S. and Prakash, L.** (1997b). Yeast DNA Repair Proteins RAD6 and RAD18 Form a Heterodimer That Has Ubiquitin Conjugating, DNA binding, and ATP Hydrolytic Activities. *J. Biol. Chem.* **272**, 23360-23365.
- Boram, W.R. and Roman, H.** (1976). Recombination in *Saccharomyces cerevisiae*: a DNA repair mutation associated with elevated mitotic gene conversion. *Proc. Natl. Acad. Sci. USA* **73**, 2828-2832.
- Cassier-Chauvat, C. and Fabre, F.** (1991). A similar defect in UV-induced mutagenesis conferred by the rad6 and rad18 mutations of *Saccharomyces cerevisiae*. *Mutat. Res.* **254**, 247-253.
- Chanet, R., Magana-Schwencke, N. and Fabre, F.** (1988). Potential DNA-binding domains in the RAD18 gene product of *Saccharomyces cerevisiae*. *Gene* **74**, 543-547.
- Cox, B.S. and Parry, J.M.** (1968). The isolation, genetics and survival characteristics of ultraviolet-light sensitive mutants in yeast. *Mutat. Res.* **6**, 37-55.
- Friedberg, E.C., Walker, G.C. and Siede, W.** (1995). "DNA repair and mutagenesis," ASM Press, Washington DC, USA.
- Friedberg, E.C. and Gerlach, V.L.** (1999). Novel DNA Polymerases Offer Clues to the Molecular Basis of Mutagenesis. *Cell* **98**, 413-426.
- Game, J.C. and Mortimer, R.K.** (1974). A genetic study of X-ray sensitive mutants in yeast. *Mutat. Res.* **24**, 281-292.
- Game, J.C., Lamb, T.J., Braun, R.J., Resnick, M. and Roth, R.M.** (1980). The role of radiation (rad) genes in meiotic recombination in yeast. *Genetics* **94**, 51-68.
- Grootegoed, J.A., Jansen, R. and Van der Molen, H.J.** (1984). The role of glucose, pyruvate and lactate in ATP production by rat spermatocytes and spermatids. *Biochim. Biophys. Acta* **767**, 248-256.
- Haynes, R.H. and Kunz, B.A.** (1981). "DNA repair and mutagenesis in yeast: The molecular biology of the yeast *Saccharomyces cerevisiae*: Life cycle and inheritance," Cold Spring Harbor Laboratory Press, New York.
- Higgins, N.P., Kato, K. and Strauss, B.** (1976). A model for replication repair in mammalian cells. *J. Mol. Biol.* **101**, 417-425.
- Hochstrasser, M.** (1996). Protein degradation or regulation: Ub the judge. *Cell* **89**, 813-815.
- Iwanejko, L., Cotton, C., Jones, G., Tomsett, B. and Strike, P.** (1996). *NuvA*, an *Aspergillus nidulans* gene involved in DNA repair and recombination, is a homologue of *Saccharomyces cerevisiae* RAD18 and *Neurospora crassa* *uvs-2*. *Microbiology* **142**, 505-515.
- Joazeiro, C.A., Wing, S.S., Huang, H., Levenson, J.D., Hunter, T. and Liu, Y.C.** (1999). The Tyrosine Kinase Negative Regulator c-Cbl as a RING-type, E2-dependent Ubiquitin-Protein Ligase. *Science* **286**, 309-312.
- Jones, J.S. and Prakash, L.** (1991). Transcript levels of the *Saccharomyces cerevisiae* DNA repair gene RAD18 increase in UV irradiated cells and during meiosis but not during the mitotic cell cycle. *Nucleic Acids Res.* **19**, 893-898.
- Koken, H.M., Reynolds, P., Jaspers-Dekker, I., Prakash, L., Prakash, S., Bootsma, D. and Hoeijkmakers, J.H.J.** (1991). Structural and functional conservation of two human homologs of the yeast DNA repair gene RAD6. *Proc. Natl. Acad. Sci. USA* **88**, 8865-8869.
- Koken, H.M., Hoogerbrugge, J.W., Jaspers-Dekker, I., De Wit, J., Willemsen, R., Roest, H.P., Grootegoed, J.A. and Hoeijkmakers, J.H.J.** (1996). Expression of the ubiquitin-conjugating DNA repair enzymes HHR6A and B suggests a role in spermatogenesis and chromatin modification. *Developmental Biology* **173**, 119-132.
- Kozak, M.** (1987). An analysis of 5'-noncoding sequences from 699 vertebrate messenger RNAs. *Nucleic Acids Res.* **15**, 8125-8148.
- Lawrence, C.W.** (1982). Mutagenesis in *Saccharomyces cerevisiae*. *Adv. Genetics* **21**, 173-254.
- Lawrence, C.W.** (1994). The RAD DNA repair pathway in *Saccharomyces cerevisiae*: What does it do and how does it do it? *BioAssays* **16**, 253-258.
- Lawrence, C.W. and Hinkle, D.C.** (1996). DNA polymerase ζ and the control of DNA damage induced

- mutagenesis in eukaryotes. In "Cancer Surveys: Genetic Instability in Cancer", pp. 21-31, Cold Spring Harbor Laboratory Press, Cold Spring Harbor, NY, USA.
- Lennon, G.G., Auffray, C., Polymeropoulos, M. and Soares, M.B.** (1996). The I.M.A.G.E. Consortium: An Integrated Molecular Analysis of Genomes and their Expression. *Genomics* **33**, 151-152.
- Lorick, K.L., Jensen, J.P., Fang, S., Ong, A.M., Hatakeyama, S. and Weissman, A.M.** (1999). RING-fingers mediate ubiquitin-conjugating enzyme(E2)-dependent ubiquitination. *Proc. Natl. Acad. Sci. USA* **96**, 11364-11369.
- Martinez-Noel, G., Niedenthal, R., Tamura, T. and Harbers, K.** (1999). A family of structurally related RING finger proteins interacts specifically with the ubiquitin-conjugating enzyme UbcM4. *FEBS Lett.* **454**, 257-261.
- Masutani, C., Kusumoto, R., Yamada, A., Dohmae, N., Yokoi, M., Yuasa, M., Araki, M., Iwai, S., Takio, K. and Hanaoka, F.** (1999). The XPV (xeroderma pigmentosum variant) gene encodes human DNA polymerase ϵ . *Nature* **399**, 700-704.
- McDonald, J.P., Levine, A.S., Woodgate, R.** (1997). The *Saccharomyces cerevisiae* *RAD30* gene, a homologue of *Escherichia coli* *dinB* and *umuC*, is DNA damage inducible and functions in a novel error free postreplication repair mechanism. *Genetics* **147**, 1557-1568.
- Montelone, B.A., Prakash, S. and Prakash, L.** (1981). Recombination and mutagenesis in *rad6* mutants of *Saccharomyces cerevisiae*: Evidence for multiple functions of the *RAD6* gene. *Mol. Gen. Genet.* **184**: 410-415.
- Naegeli, H.** (1994). Roadblocks and detours during DNA replication: mechanisms of mutagenesis in mammalian cells. *Bioassays* **16**, 557-564.
- Nelson, J.R., Lawrence, C.W. and Hinkle, D.C.** (1996). Deoxycytidyl transferase activity of yeast Rev1 protein. *Nature* **382**, 729-731.
- Pinkel, D., Landegent, J., Collins, C., Fuscoe, J., Segraves, R., Lucas, J., and Gray, J.W.** (1988). Fluorescence *in situ* hybridization with human chromosome-specific libraries: Detection of trisomy 21 and translocations of chromosome 4. *Proc. Natl. Acad. Sci. USA* **85**, 9138-9142.
- Quah, S.K., Von Borstel, R.C. and Hastings, P.J.** (1980). The origin of spontaneous mutation in *Saccharomyces cerevisiae*. *Genetics* **96**, 819-839.
- Robzyk K., Recht J., Osley M.A.** (2000). Rad6-dependent ubiquitination of histone H2B in yeast. *Science* **287**, 501-504.
- Roest, H.P., Van Klaveren, J., De Wit, J., Van Gurp, C.G., Koken, M.H.M., Vermey, M., Roijen, J.H., Hoogerbrugge, J.W., Vreeburg, J.T.M., Baarends, W.M., Bootsma, D., Grootegoed, J.A. and Hoeijmakers, J.H.J.** (1996). Inactivation of the HR23B ubiquitin-conjugating DNA repair enzyme in mice causes male sterility associated with chromatin modification. *Cell* **86**, 799-810.
- Rupp, W.D., Wilde, C.E. 3d, Reno, D.L. and Howard-Flanders, P.** (1971). Exchanges between DNA strands in ultraviolet-irradiated *Escherichia coli*. *J. Mol. Biol.* **61**: 25-44.
- Sambrook, J., Fritsch, E.F. and Maniatis, T. (1989). "Molecular cloning, a laboratory manual," Cold Spring Harbor Laboratory Press, New York.
- Sanger, F., Nicklen, S. and Coulson, A.R.** (1977). DNA sequencing with chain-terminating inhibitors. *Proc. Natl. Acad. Sci. USA* **74**, 5463-5467.
- Saurin, A.J., Borden, K.L., Boddy, M.N. and Freemont, P.S.** (1996). Does this have a familiar RING? *Trends Biochem. Sci.* **21**, 208-214.
- Shi, Y.P., Mohapatra, G., Miller, J., Hanahan, D., Lander, E., Gold, P., Pinkel, D. and Gray, J.** (1997). FISH Probes for Mouse Chromosome Identification. *Genomics* **45**, 42-47.
- Smith, B.T. and Walker, G.C.** (1998). Mutagenesis and more: *umuDC* and the *Escherichia coli* SOS response. *Genetics* **148**, 1599-1610.
- Tang, M., Shen, X., Frank, E.G., O'Donnell, M., Woodgate, R., Goodman, M.F.** (1999). UmuD'(2)C is an error-prone DNA polymerase, *Escherichia coli* pol V. *Proc. Natl. Acad. Sci. USA* **96**, 8919-8924.
- Tomita, H., Soshi, T. and Inoue, H.** (1993). The *Neurospora uvs-2* gene encodes a protein which has homology to yeast *RAD18*, with unique zinc finger motifs. *Mol. Gen. Genet.* **238**, 225-233.
- Waterman, H., Levkowitz, G., Alroy, I. and Yarden, Y.** (1999). The RING finger of c-Cbl mediates desensitization of the epidermal growth factor receptor. *J. Biol. Chem.* **274**, 22151-22154.
- Woodgate, R. and Levine, A.S.** (1996). Damage inducible mutagenesis: Recent insights into the activities of the Umu family of mutagenesis proteins. In "Cancer Surveys: Genetic Instability in Cancer", pp. 117-140, Cold Spring Harbor Laboratory Press, Cold Spring Harbor, NY, USA.
- Woodgate, R.** (1999). A plethora of lesion-replicating DNA polymerases. *Genes Dev.* **13**, 2191-2195.



Chapter 4

Spatio-temporal dynamics of the DNA damage replication bypass proteins mRAD18Sc and HR6B to stalled replication foci and UV-induced DNA lesions

In preparation

Spatio-temporal distribution of the replicative damage bypass proteins HR6B and mRAD18Sc to stalled replication foci and UV-induced DNA lesions

Roald van der Laan, Evert-Jan Uringa, Wiggert A. van Cappellen, Jorie Versmissen, Shehu M. Ibrahim, Harm de Waard, Adriaan B. Houtsmuller, Wim Vermeulen, Henk P. Roest, Willy M. Baarends, J. Anton Grootegoed and Jan H.J. Hoeijmakers.

Abstract

Replicative damage bypass (RDB) achieves continuation of DNA replication when lesions are encountered in the template, thereby preventing irreversible termination of DNA replication. In yeast, the key players of this system are RAD6 and RAD18. In this present study, we analyzed the dynamic distribution of fluorescently tagged mammalian orthologs, HR6B and mRAD18Sc and respectively, in HeLa cells. A clear cell cycle-dependent subnuclear distribution was observed for both fusion proteins. HR6B-GFP and GFP-mRAD18Sc colocalize with replication foci predominantly in mid-late S phase cells. UV damage-induced replication arrest caused an increase of HR6B and mRAD18Sc foci, and both proteins accumulate at local UV-damaged sites, likely reflecting the action at stalled replication forks. In addition to a complete colocalization of HR6B-CFP and YFP-mRAD18Sc the RDB proteins appear to reside in the same multi-protein complex that roams the nuclear space, as revealed by the identical nuclear mobility of HR6B-GFP and GFP-mRAD18Sc measured by photobleaching and fluorescence correlation spectroscopy. Surprisingly, both RDB factors quickly assemble on a local UV-damaged spot, in G1 and G2 cells, observed using a new method involving three-photon near-infrared absorption in subnuclear regions to locally inflict DNA damage in living cells. This powerful method allows to directly determine assembly kinetics of DNA surveillance factors to a damaged spot. The present findings suggest a new role for HR6B and mRAD18Sc in replication-independent DNA damage response.

Introduction

A large amount of DNA lesions occur in every cell of the body as a consequence of continuous exposure to exogenous agents and endogenously produced reactive metabolites that react with DNA. DNA lesions, when not properly removed, interfere with basal cellular functions including transcription and replication, and trigger cell-cycle arrest or cell death. Long-term effects of DNA damage include accumulation of irreversible mutations, which has implications for oncogenesis, accelerated aging, limited fertility, and transmission of genetic diseases if the damage occurs in the germline. Fortunately, several multi-protein DNA repair mechanisms have evolved that cooperatively maintain the integrity of the genome, in all organisms. However, if lesions are tolerated during DNA replication, the cell-cycle will not be arrested and mutations can be introduced.

In addition to direct removal of lesions, a DNA damage signaling process is operational within mammalian cells that regulates other genome surveillance pathways, including lesion-dependent cell-cycle control and a network of damage tolerance pathways. The latter allows the replication machinery to pass DNA lesions.

Replicative damage bypass (RDB; also known as PRR: post replication repair) mechanisms prevent undesirable termination of DNA replication when lesions are present in the template. At least two sub-pathways of RDB are identified. 1) Translesion synthesis (TLS) in which highly specialized TLS polymerases are utilized to bypass template damage. The fidelity of TLS depends on the type of lesion and the TLS polymerase itself. 2) Damage avoidance (DA) (Baynton and Fuchs, 2000), is generally more error-free than TLS, because sequence information is acquired from the non-damaged daughter strand created from the other template strand (template switch), or the other homologous chromosome (recombinational repair) is used to bypass the damage. Activation of DA requires the UBC13-MMS2-RAD5 complex in RDB (Broomfield et al., 1998). Although mammalian homologs of UBC13 and MMS2 have been identified, the DA mechanisms in higher eukaryotes remain unclear.

In contrast to DA, an enormous amount of data on TLS both in yeast and higher eukaryotes has been obtained recently (Woodgate, 1999). A subset of at least five TLS polymerases operates in mammalian cells: pol η (RAD30A, yeast RAD30 homolog), pol ι (RAD30B, yeast RAD30 homolog), pol ζ (REV3-REV7 complex), REV1 and pol κ (E. coli DinB homolog) (Friedberg et al., 2002; Woodgate, 1999). In contrast to replicative DNA polymerases, TLS polymerases possess a very open and flexible active site enabling them to perform replication past lesions in the template. The biological significance of TLS polymerases is underscored by the cancer prone phenotype of hereditary-defects in pol η in xeroderma pigmentosum variant (XPV) patients (Masutani et al., 1999). Pol η and pol ι have been studied in living cells by expression of proteins carrying fluorescent tags. Both TLS polymerases physically interact and associate with (stalled) replication foci in S phase cells (Kannouche et al., 2001; Kannouche et al., 2002). They are also recruited to UV-induced lesions, and pol η is involved in targeting pol ι to (stalled) replication foci (Kannouche et al., 2001; Kannouche et al., 2002).

In yeast, genes involved in RDB are members of the RAD6 epistasis group; these genes are highly conserved in mammals. The RAD6 and RAD18 genes are the key players in RDB and are required to initiate both TLS and DA (Cassier-Chauvat and Fabre, 1991; Torres-Ramos et al., 1996). RAD6 encodes an ubiquitin-conjugating enzyme and interacts with the ubiquitin ligase RAD18 (Bailly et al., 1997; Jentsch et al., 1987). RAD6 mutants show a pleiotrophic phenotype and careful analysis of these mutants revealed involvement of RAD6 in multiple pathways in addition to RDB, including: sporulation, gene silencing and mitotic recombination (Huang et al., 1997; Lawrence, 1994; Singh et al., 1998). Currently, the only known substrate in RDB for the RAD6-RAD18 complex is PCNA that is mono-ubiquitinated in response to DNA damage (Hoegge et al., 2002; Ulrich and Jentsch, 2000). Two RAD6 homologs, HR6A and HR6B, are present in mammals, and knockout mouse models have been generated (Koken et al., 1991; Roest et al., 1996; Roest et al., 2004). Single mutants of either HR6A or HR6B do not display any RDB-deficient phenotype (Roest et al., 1996), whereas double knockout animals are not born. Complete deletion of HR6A and HR6B is incompatible with cellular survival (Roest et al., 2004). Taken together, the findings indicate that HR6A and

HR6B are redundant for functions essential for mammalian somatic cell types, likely including RDB. However, the function, involved in germline cells of HR6A and HR6B might be different for male and female gametogenesis.

Yeast *rad18* mutants show similar levels of sensitivity to DNA damaging agents as the *rad6* mutant, and RAD18 is thought to be involved in RDB only. However, two reports suggest that RAD18 also might be involved in gene silencing and meiosis as well (Dowling et al., 1985; Game and Kaufman, 1999). The human homolog of RAD18, hRAD18Sc was found to interact with both HR6A and HR6B, analogous to yeast (Tateishi et al., 2000; Xin et al., 2000). Mouse mRAD18Sc-deficient ES cells were shown to be defective in RDB, and display enhanced genomic instability (Tateishi et al., 2003).

Here, we show that HR6B and mRAD18Sc colocalize and are associated with the replication machinery in living cells, using expression of proteins tagged with GFP (and spectral variants). In addition, we show that HR6B and mRAD18Sc are quickly recruited to UV-induced DNA lesions, indicating that HR6B and mRAD18Sc localize at replication foci as a result of DNA damage. Our data suggest that HR6B and mRAD18Sc proteins are involved in replicative damage bypass in response to the presence of blocking DNA lesions in mammalian cells.

Material and methods

Cell lines and culture conditions

HeLa cells were cultured in DMEM/F10 1/1 supplemented with 5% v/v fetal calf serum and antibiotics, under 5% CO₂ at 37°C. Primary mouse embryonic fibroblast were isolated from 13.5 dpc wild type C57Bl/6 mice and cultured under the same conditions (the fetal calf serum concentration was increased to 10% v/v).

Plasmids and transfections

The cDNA of mRAD18Sc was cloned into pEGFP-C2 (enhanced green fluorescent protein), (and pEYFP-C2 (enhanced yellow fluorescent protein) (BD Clontech, Palo Alto, CA, USA) and HR6B into pEGFP-N1 and pECFP-N1 (enhanced cyan fluorescent protein) (BD Clontech). Plasmids were amplified and purified according to standard molecular biology techniques.

Transfections were performed using the FuGene6 transfection reagent (Roche, Mannheim, Germany) according the manufacturer's manual. After an incubation period of 24 hours, cells were seeded at low density and grown on selective media (culture medium supplemented with 800-1200 µg/ml neomycin) to obtain individual clones. Clones with a positive fluorescence signal were picked and further cultured on selective medium. To establish a homogeneous population of stable transfectants the cells were selected by fluorescence activated cell sorting (FACS) on a FacsVantage (BD Biosciences, San Jose, CA, USA) using a 488 nm Argon laser line.

UV-C irradiation

Cells were cultured on coverslips coated with 0.1% v/v gelatin. After removal of the medium, the cells were washed with PBS and irradiated. Fresh medium was added after PBS wash step and cells were placed back in the incubator (UV-C doses and incubation times are mentioned in the result section and figure legends). Global UV irradiation was performed with a germicidal lamp (Phillips TUV lamp, 254 nm). For

introduction of UV-induced lesions in subnuclear regions, an isoporene polycarbonate membrane filter (Millipore, Billerica, MA, USA) with 8 μm pores was placed on top of the cells and irradiated from above using the same UV-C source (Mone et al., 2001). The filter shields the cells from the UV-C light and only reaches the cellular body when pores that let through the irradiation are positioned above it. The filter was removed quickly and cells were washed with PBS, fresh medium was added and cells were cultured under standard conditions.

Confocal and time lapse microscopy

For live cell microscopy, stably transfected cells were grown on 25 mm coverslips and placed in an Attofluor cell chamber (Molecular Probes, Eugene, OR, USA) that fits into a live cell microscopy chamber. The live cell chamber and the objective (Plan-Apochromat 63x/1.40 NA, oil immersion, Carl Zeiss, Jena, Germany) were kept at 37° C and the chamber was maintained in an atmosphere of 5% CO₂. Time-lapse imaging was performed using the LSM510NLO confocal microscope (Carl Zeiss). For an Argon laser line of 488 nm was used to excite GFP at an average intensity of 10-20 μW (ECFP, 458 nm and EYFP, 514 nm Argon laser lines). Images of 6 focal planes with 1 μm intervals were captured every 15 minutes from multiple locations on the coverslip after autofocusing using a Helium Neon laser line of 633 nm. The digital zoom factor was 1.5 times. Multiple images of each location were concatenated and analyzed using the LSM AIM software package (Carl Zeiss).

Fluorescence recovery after photobleaching (FRAP)

FRAP analysis was performed as described previously (Houtsmuller et al., 1999), using a LSM410 confocal microscope (Carl Zeiss). A 2 μm wide strip spanning the entire nucleus was imaged by a 40X 1.4 NA oil immersion objective using a 488 nm Argon laser line. A series of 200 pre-bleach intensities (100 ms time intervals) were recorded prior to the Photobleaching with 10 μW of laser power, the strip was bleached for 200 ms at high laser intensity (800 μW) and subsequently the fluorescence recovery was measured by recording 300 post-bleach intensities (100 ms time intervals).

Fluorescence correlation spectroscopy (FCS)

FCS measurements were carried out with a ConfoCor2 (Carl Zeiss) attached to an Axiovert inverted microscope (Carl Zeiss), using a C-Apochromat 40x /1.2 NA objective. The pinhole was 1 airy unit (70 μm) and a 488 nm laser Argon laser (2 mW) line was used to excite GFP at 1% AOTF. The confocal volume was 0.2 fL (lateral resolution 0.4 μm and axial resolution 1.9 μm). For measurement of GFP-tagged proteins, 5 time series of 30 seconds were recorded and superimposed for fitting.

Cell cycle analysis

Wild type HeLa cells were cultured in 6 cm dishes to 50% confluence and irradiated with increasing UV-C (254 nm) doses to induce DNA lesions. Cells were harvested at different time points after the UV-C treatment and fixed in 70% ethanol. The DNA was stained with propidiumiodide 2% (v/v) in PBS supplemented with 0.1% (v/v) Triton X-100 and RNase I (0.2 mg/ml). The cells were incubated 30 minutes at room temperature and placed on ice prior to FACS. The analysis was performed on a Facscalibur (BD Biosciences, San Jose, CA, USA) using Cellquest-pro software (BD Biosciences). An average of 50,000 cells was analyzed for each sample.

Immunofluorescence

Cells grown on cover slips were fixed in 2% v/v paraformaldehyde for 20 minutes at room temperature and were permeabilized for 10 minutes using PBS supplemented with 0.1% v/v Triton X-100 (Sigma Chemical CO., St. Louis, MO, USA). For immunostaining with α -PCNA, cells were fixed with methanol (100%, at -20° C), 2 times 5 minutes at 4° C. Aspecific sites were masked by blocking with 5% w/v BSA in PBS for 30 minutes at room temperature. The DNA was denatured by incubation in 0.4 M NaOH for 4 minutes at room temperature. The primary antibodies were diluted as indicated (α -mRAD18Sc 1:100, α -CPD (TDM2) (Mori et al., 1991) 1:1000, α -HA (Roche) 1:1000, α -GFP (Abcam, Cambridge, UK) 1:500 and α -PCNA (Abcam) 1/400) and incubated with the sample overnight in PBS+ (PBS with 0.5% w/v BSA and 0.15% w/v glycine) at room temperature then the excess removed by repetitive washing with PBS+. The staining pattern was amplified by incubation with Alexa350 (1:300), 488 (1:1000) and 594 (1:1000) conjugated goat anti-rabbit, -mouse and -rat antibodies (Molecular Probes). After removal of the antibody and subsequent washing steps, the cover slips were mounted on slides using Vectashield (Vector Laboratories, Burlingame CA, USA). DAPI (1:5000) (Sigma) was added for nuclear staining. The slides were analyzed by wide field fluorescence microscopy using an Axioplan (Carl Zeiss) 2 equipped with a Coolsnap-Pro digital camera (Photometrics, Waterloo, Canada).

Multi-photon DNA damage induction

Near-infrared microbeam irradiation was used to locally induce cyclobutane pyrimidine dimers (Meldrum et al., 2003) in subnuclear regions of HeLa cells. A Verdi pump laser (5W), Mira 900 multi-photon laser tunable 600-1000 nm (Coherent, Santa Clara, CA, USA), directly coupled to the LSM510NLO confocal microscope (Carl Zeiss) was used to induce CPDs. The laser was tuned in the range of 750-800 nm. A laser output of 50% (50 mW) and 5 iterations was sufficient to induce detectable amounts of CPDs in an area of 15 by 15 pixels. The presence of CPDs after the multi-photon treatment was verified using immunofluorescence with α -CPD antibodies as described above.

Results

HR6B and mRAD18Sc colocalize and show similar dynamics

To determine time resolved subcellular localization of the for RDB essential factors HR6B and RAD18Sc in living mammalian cells we tagged each of them with spectral variants of the green fluorescent protein (GFP). HR6B cDNA was tagged at the C-terminus with either GFP or CFP (for Cyan FP) and mRAD18Sc was tagged at its N-terminus with either GFP or YFP (for Yellow FP). Each of the fusion constructs either alone or in combination were transfected to HeLa cells. Stably expressing cells were isolated by G418 selection and fluorescence activated cell sorting. HR6B-CFP showed a specific nuclear localization (Figure 1A) identical to YFP-mRAD18Sc and GFP-mRAD18Sc as we have previously observed (van der Laan et al., 2000). In addition to a general homogeneous nuclear distribution, in a subfraction of the cells multiple bright foci of HR6B-CFP and YFP-mRAD18Sc were visible and appeared to significantly colocalize (Figure 1A).

Since both yeast RAD6 and RAD18 proteins are involved in RDB allowing replication over a damaged template we determined the acute effect of a high dose

of DNA damage induction on the distribution of both proteins. Cells expressing both fusion proteins were irradiated with UV-C (10 J/m^2) and incubated for 6 hours. UV-C caused the relocalization of both HR6B-CFP and YFP-mRAD18Sc into a large number of small, discrete nuclear foci with almost complete colocalization of the two proteins in the majority of the cells ($>80\%$)(Figure 1B). Immuno-fluorescent studies on UV-C irradiated wild type mouse embryonic fibroblasts (MEFs), using α -mRAD18Sc, revealed a similar distribution pattern as HeLa cells transfected with recombinant, tagged protein, indicating that endogenous mRAD18Sc responded identically (result not shown). Unfortunately, antibodies used are not suitable for detection of HR6B by Immunofluorescence. These results suggest that at least in the UV-damaged cells HR6B and mRAD18Sc co-localize within discrete nuclear foci of which the number is significantly enhanced after DNA lesion induction.

Biochemical studies revealed that the interaction between RAD6 and RAD18 is conserved from yeast to mammals. To determine whether in intact cells the mRAD18Sc interacts with or at least resides in the same complex with HR6B without DNA damage induction, we performed fluorescence recovery after photobleaching (FRAP) on HeLa cells stably expressing GFP-mRAD18Sc or HR6B. The overall nuclear mobility of GFP-mRAD18Sc and HR6B-GFP is very similar as shown by the fluorescence recovery plots and calculated effective diffusion coefficients (D_{eff})(Figure 2A and 2B). In addition, another approach to study mobility of fluorescently tagged biomolecules, fluorescent correlation spectroscopy (FCS), confirmed the FRAP results (Figure 2C). These observations strongly suggest that the colocalizing mRAD18Sc and HR6B proteins physically interact directly or indirectly. Moreover, the FRAP curves further indicate that the majority of the molecules are mobile and are not (transiently) associated to any immobile nuclear component.

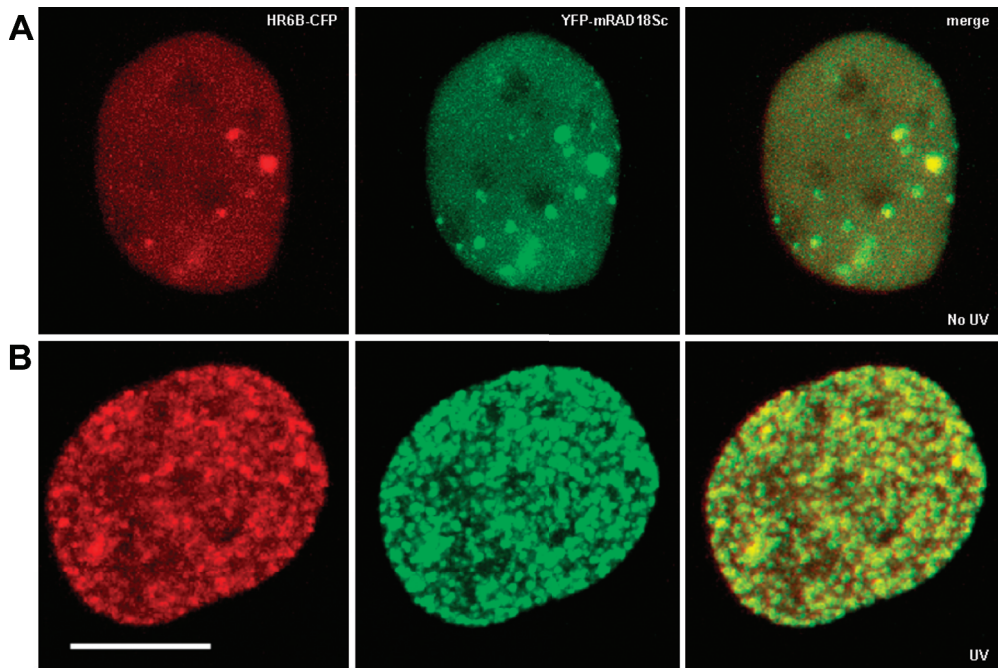


Figure 1. Colocalizes of YFP-mRAD18Sc and HR6B-CFP. A: HeLa cells stably expressing HR6B-CFP were co-transfected with cDNA coding for YFP-mRAD18Sc, and imaged by confocal microscopy twenty-four hours after the YFP-mRAD18Sc transfection. B: Cells described in A were irradiated with UV-C light (10 J/m^2) and imaged by confocal microscopy 6 hours after the UV-C irradiation. HR6B-CFP (red), YFP-mRAD18Sc (green, middle) and merged images (yellow) are shown. 6 optical slices with $1 \mu\text{m}$ intervals of live cells were imaged and processed into maximum projections. Scale bar, $10 \mu\text{m}$.

HR6B and mRAD18Sc distribution changes throughout the cell cycle

In untreated HR6B-CFP and YFP-mRAD18Sc co-expressing HeLa cells nuclear foci are present in a subpopulation of the cells, indicative for a cell cycle stage-dependent distribution. To further test this, we studied the subcellular localization HR6B-GFP and GFP-mRAD18Sc in real time. Time lapse confocal recording of untreated individual cells showed significant changes in the distribution of GFP-mRAD18Sc within the nucleus throughout the cell cycle (Figure 3A). Imaging started with a nucleus containing a large number of small homogeneously distributed foci. Over time, many of the GFP foci enlarged and move to the periphery of the nucleus and adjacent to nucleoli. Subsequently, large aggregates of GFP-mRAD18Sc were observed throughout the nucleus, which dispersed into a homogeneously distributed fluorescence just prior to cell division. In total 10 individual cells were monitored, each displaying a rather similar time-dependent nuclear redistribution as shown in Figure 3A. Next, we irradiated the samples with UV-C (10 J/m^2) and followed the GFP-mRAD18Sc derived fluorescent signal in time. After UV-C, GFP-mRAD18Sc relocated into numerous small nuclear foci, however these foci persist for at least 15 hours after DNA damage (Figure 3B). A very low number of cell divisions occurred in the population of UV-damaged cells and those that did occurred only at the beginning of the time-lapse recording, shortly after the UV irradiation. The same time series were captured with both untreated and UV-C irradiated HeLa cells expressing HR6B-GFP resulting in a similar distribution

behavior as mRAD18Sc (Figure 3C and 3D). These findings indicate that the subcellular localization of HR6B and mRAD18Sc is cell cycle-dependent and that DNA damage arrests the cells in the phase of the cell cycle in which discrete mRAD18Sc and HR6B foci are seen, likely the S phase of the cell cycle.

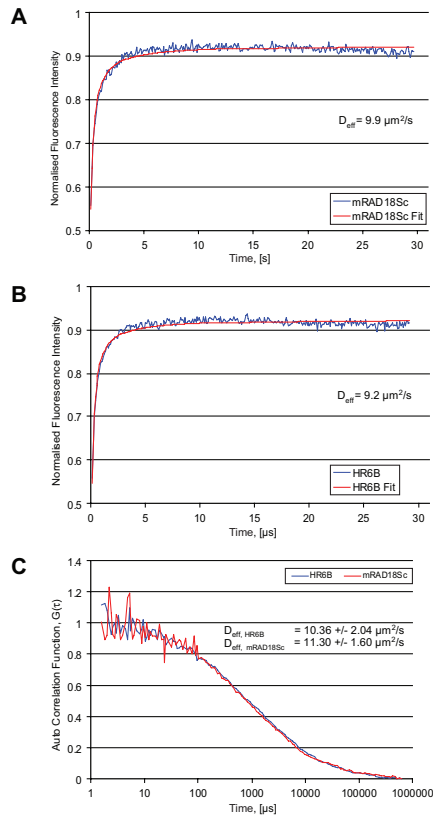


Figure 2. FRAP and FCS analysis of GFP-mRAD18Sc and HR6B-GFP nuclear mobility. A: FRAP analysis of HeLa cells ($n=20$) stably expressing GFP-mRAD18Sc and B: HR6B-GFP ($n=20$). Blue lines indicate normalized relative fluorescent intensities and the red lines show the best fit. Effective diffusion coefficients (D_{eff}) were calculated from the best fits. C: FCS analysis of HeLa cells stably expressing GFP-mRAD18Sc ($n=10$) and HR6B-GFP ($n=10$). Red line indicates fitted normalized autocorrelation of GFP-mRAD18Sc and the blue line HR6B-GFP. Effective diffusion coefficients (D_{eff}) were derived from the best fits.

To test whether the timing of the phase showing large numbers of persistent HR6B-GFP or GFP-mRAD18Sc foci after UV-C irradiation (Figure 3B and 3D) corresponds with a delay in the cell cycle, we performed cell cycle analysis by flow cytometry of wild type HeLa cells at various time points after treatment with increasing doses of UV-C. HeLa cells irradiated with 10 J/m^2 accumulated in S and G2 phase (Figure 4). At later time points after the treatment, we observed a shift from the fraction of S phase cells towards and increasing fraction of G2 and G1 phase cells. The effect was consistent, albeit less dramatic at lower doses of UV-C and the overall cell cycle profile of untreated cells was similar for all time points (results not shown). The observed UV-dependent cell cycle arrest and concomitant

HR6B and RAD18Sc persistent focal pattern in combination with the observed focal redistribution suggest that these foci represent replication foci and that the RDB proteins likely localize to stalled replication forks to activate the RDB system.

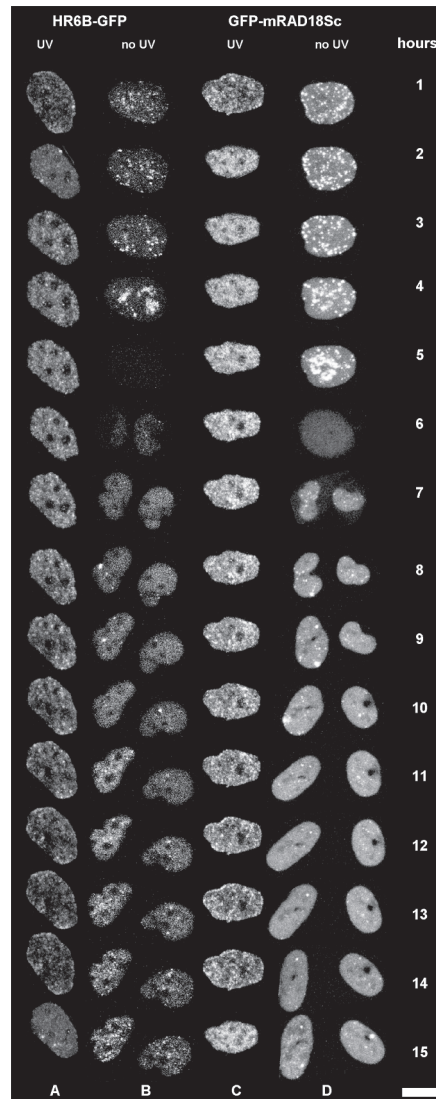


Figure 3. HR6B-GFP and GFP-mRAD18Sc show a changing nuclear pattern during the cell cycle. HeLa cells stably expressing HR6B-GFP (A) and GFP-mRAD18Sc (C) were analyzed by time-lapse confocal microscopy. B (HR6B-GFP) and D (GFP-mRAD18Sc), HeLa cells described in A and C were irradiated with UV-C (10 J/m^2) and then followed by time-lapse confocal microscopy. Time-lapse images were captured every 10 minutes for 14 hours and maximum projections of 6 optical slices with $1 \mu\text{m}$ intervals were created. Scale bar, $10 \mu\text{m}$.

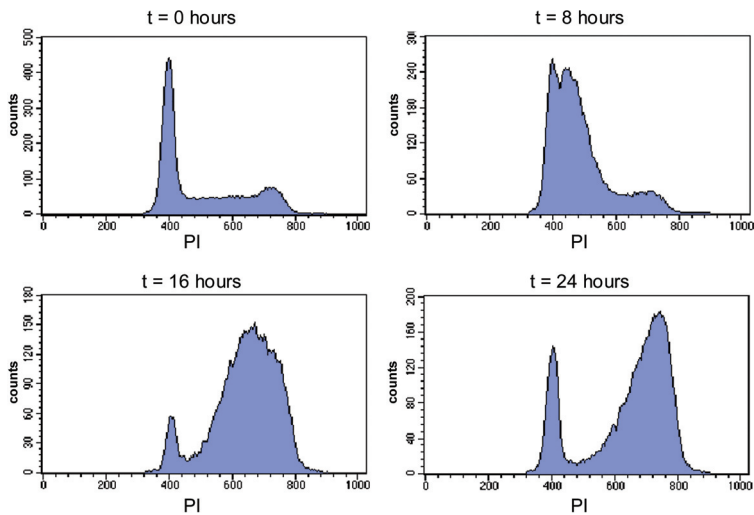


Figure 4. Flow cytometry based cell cycle profile analysis of HeLa cells irradiated with UV-C. The x-axis shows the DNA content (stained with propidium iodide, PI) and the y-axis represents the number of cells (counts). The cells were irradiated with UV-C and incubated for different time points after treatment (hours are indicated above each graph) prior to FACS analysis.

HR6B and mRAD18Sc are present in replication foci and sites of DNA damage

In S phase cells, replication takes place in discrete foci that contains proteins involved in replication including PCNA (Bravo and Macdonald-Bravo, 1987). To determine whether these HR6B and mRAD18Sc foci are S phase-specific replication foci, cells were immunostained with α -PCNA. A substantial number of both GFP-mRAD18Sc and HR6B-GFP foci colocalized with replication foci in late S phase cells (Figure 5A and 5B, respectively). However, we observed a partial colocalization of GFP-mRAD18Sc and HR6B-GFP with PCNA in early S phase cells. Previously, a similar colocalization of two translesion synthesis (TLS) polymerases, pol η and pol ι , with PCNA was observed (Kannouche et al., 2001; Kannouche et al., 2002).

To test the hypothesis that the observed mRAD18Sc and HR6B foci in UV-damaged cells represent protein accumulation at damage-induced stalled replication forks, we locally inflicted UV-C damage in subnuclear regions. HeLa cells stably expressing HR6B-GFP and transiently expressing HA-tagged mRAD18Sc were irradiated through a microporous filter (Mone et al., 2001). Treated cells were immunostained with 3 antibodies: α -CPD (Mori et al., 1991) to detect the regions containing DNA lesions, α -GFP to detect HR6B and α -HA to detect mRAD18Sc. Subnuclear regions that were exposed by the UV-C light, showed accumulation of both mRAD18Sc and HR6B indicating that both proteins are recruited to CPDs (Figure 6). Endogenously expressed mRAD18Sc in MEFs appeared also to colocalize with CPD lesions (Figure 7) and confirms the DNA damage-dependent subnuclear distribution. In conclusion, we have demonstrated that mRAD18Sc and HR6B colocalize in replication-dependent nuclear foci after DNA damage induction, likely reflecting stalled replication forks.

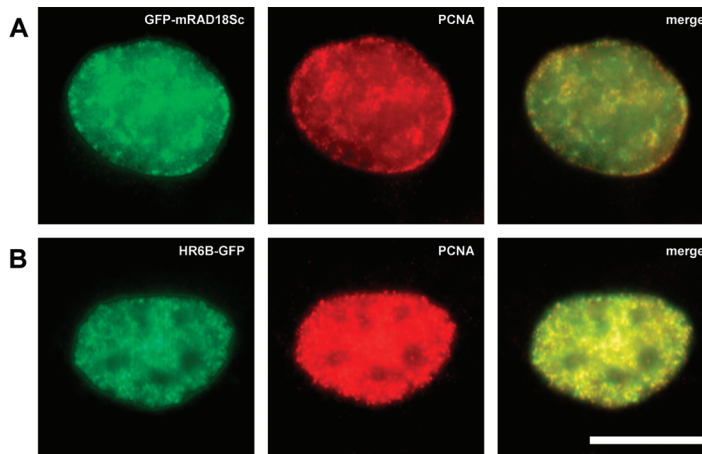


Figure 5. mRAD18Sc and HR6B are associated with the replication machinery. HeLa cells stably expressing GFP-mRAD18Sc (A, green) and HR6B-GFP (B, green) were immunostained with α -PCNA (red), and the overlaid images are shown (merge, yellow). Scale bar, 10 μ m.

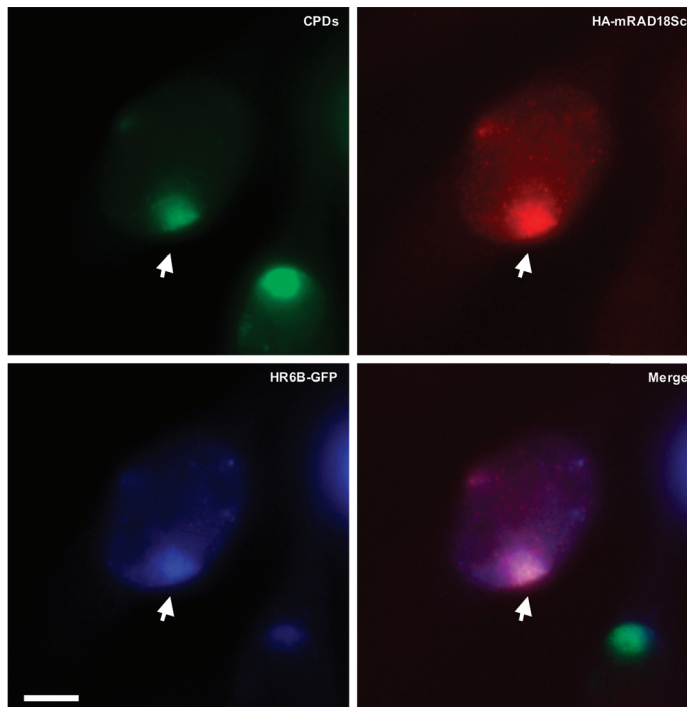


Figure 6. mRAD18Sc and HR6B are recruited to UV-induced DNA lesion. HeLa stably expressing HR6B-GFP were co-transfected with cDNA coding for amino-terminal HA-tagged mRAD18Sc. Twenty-four hours after transfection the cells were covered with polycarbonate filters (with 5 μ m micro-pores), irradiated UV-C (subnuclear local irradiation), and subsequently cultured for another 15 hours at normal conditions. Fixed cells were immunostained with α -CPD (green) to locate the DNA lesions, α -HA (red) was used to visualize mRAD18Sc and HR6B-GFP (blue) was detected using α -GFP. The overlaid image (merge) is shown, and the arrow points to local CPDs. Scale bar, 10 μ m.

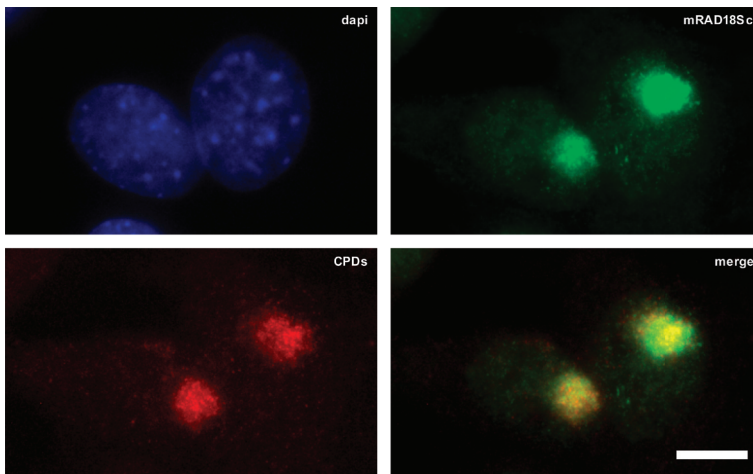


Figure 7. Endogenous mRAD18Sc localizes to CPDs in mouse embryonic fibroblasts. Wild type MEFs were locally irradiated with UV-C as described in Figure 6, and immunostained with α -mRAD18Sc (green) and α -CPD (red) to visualize the local CPDs. An overlay of the mRAD18Sc and CPD immunostaining is shown (merge) and nuclei are stained with DAPI (blue). Scale bar, 10 μ m.

HR6B and mRAD18Sc accumulate at subnuclear regions irradiated with near-infrared light

The use of filters with micropores to irradiate subnuclear regions is a very powerful tool to investigate the accumulation of DNA repair proteins to at specific sites of DNA damage within a nucleus. However, the distribution of local damage achieved with filters is very heterogeneous in size and subnuclear location, moreover time-resolved measurements of protein association to these defined sites is technically complicated. Therefore we investigated the possibility of implementing a new technique to introduce local UV damage in a cell nucleus at highly defined regions. To induce local DNA damage we applied multi-photon absorption, previously also used to introduce DNA lesions in sensitized DNA, and near-infrared multiphoton absorption induces low levels of CPDs in plasmids (Berns et al., 2000; Shafirovich et al., 1999). Furthermore, nanoscale spatial induction of CPDs by three-photon absorption is reported, and proven to be a very powerful tool to introduce DNA lesions very accurately at nanometer resolution (Meldrum et al., 2003). We used a tunable infrared laser source to induce DNA damages in subnuclear regions. The wavelength of the laser beam that is used to initiate 3-photon absorption covers a range of 750-800 nm. HeLa cells stably expressing GFP-mRAD18Sc or HR6B-GFP were imaged by confocal microscopy using a 488 nm laser line. The actual DNA damage induction was performed by a short high laser power exposure within subnuclear positions (15 by 15 pixels) using a near-infrared laser line of 750 or 800 nm. Directly after damage induction (4 ms) cells were imaged using the 488 nm laser line GFP excitation (Figure 8). The efficiency of DNA damage induction was determined using GFP-mRAD18Sc expressing cells and optimized by changing the laser power and number of iterations in the same region (i.e. 750 and 800 nm, 50 mW of laser power and 5 iterations, see Methods).

The treated cells were fixed and immunostained using α -CPD (Figure 8) and α -GFP (Figure 8). In all cases, we observed full co-localization of the GFP signal with CPD signal in areas that were irradiated (Figure 8)). The same procedure was

also performed using HeLa cells expressing HR6B-GFP with similar results (data not shown).

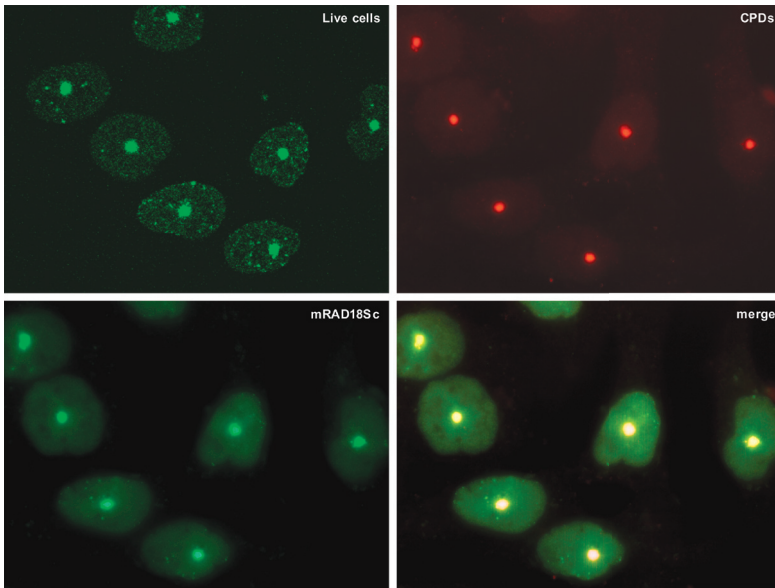


Figure 8. Induction of CPDs by three-photon absorption using an infrared laser. Living cells stably expressing GFP-mRAD18Sc were locally irradiated (15 by 15 pixels) with an infrared laser pulse (800 nm, 50 mW and 5 iterations) and imaged by confocal microscopy. Shortly after imaging the cells were fixed and immunostained with α -CPD (red) and α -GFP (green) to visualize mRAD18Sc, and imaged by wide field fluorescence microscopy. An overlay of mRAD18Sc and CPDs is shown (merge). Scale bar, 10 μ m.

We next studied the dynamics of GFP-mRAD18Sc assembly on subnuclear regions containing three-photon laser-induced DNA damage in non S phase HeLa cells with a homogeneous nuclear signal. These on the spot assembly measurements revealed that GFP-mRAD18Sc accumulated on the locally damaged area after an initial delay of approximately 1-1.5 minutes with a steady slope (Figure 9). A maximum accumulation was reached between 12 and 15 minutes, with a $t_{1/2}$ around 5 minutes (Figure 9). The sigmoidal shape of the assembly curve (including the initial delay in assembly) suggest that prior to the mRAD18Sc assembly other factors are required. The response of HR6B-GFP to local irradiation by near-infrared laser light was very similar to the GFP-mRAD18Sc response (result not shown). Surprisingly, the accumulation of mRAD18Sc and HR6B on infrared induced DNA lesions is not restricted to the S phase of the cell cycle. This indicates that these RDB proteins might be involved in DNA damage recognition or are recruited for other non-S phase related purposes, for example nucleotide excision repair.

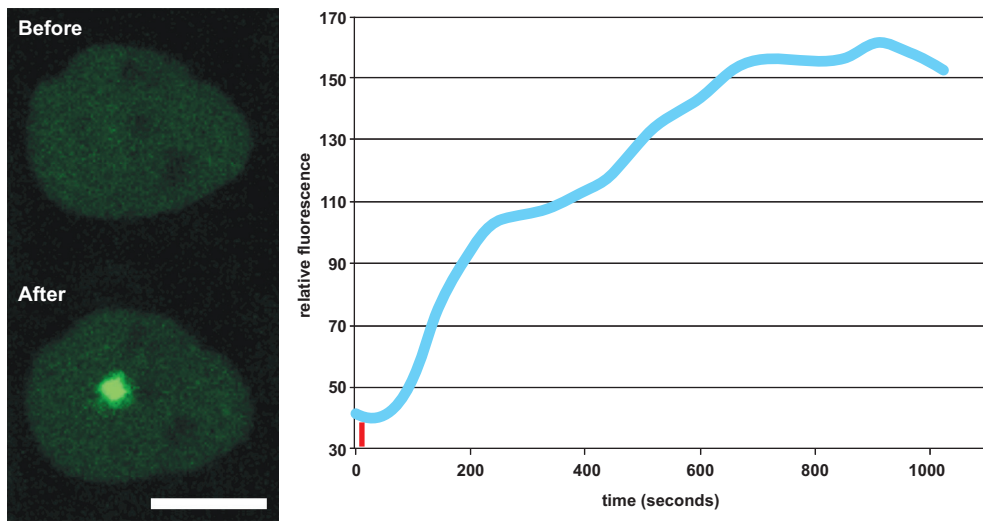


Figure 9. De novo assembly of GFP-mRAD18Sc on local CPDs. HeLa cells stably expressing GFP-mRAD18Sc were imaged by confocal microscopy (left panel). Subsequently, a subnuclear area (white rectangle, 15 by 15 pixels) was exposed to near-infrared laser light (800 nm, 50 mW and 5 iterations) and imaged every 60 seconds. A pre-exposed (top) and post-exposed (bottom) image is shown. The relative GFP fluorescence in the exposed area was quantified after subtraction of background noise and plotted in time (right panel). The red bar indicates the time point of the subnuclear near-infrared exposure (exposure time 138 ms). Scale bar, 10 μ m.

mRAD18Sc accumulates to local damage after cell division

With the protocol used to locally inflict DNA damage using multi-photon irradiation we did not observe any cell divisions, apparently is the amount of introduced lesions sufficient to induce a permanent cell cycle arrest. In order to allow cell cycle progression we decreased the amount of inflicted DNA damage, using only 1 iteration of three-photon irradiation. Under these conditions sufficient DNA lesions were introduced to allow visualization of local GFP-mRAD18Sc accumulation (Figure 10). Within the damaged region GFP-mRAD18Sc accumulated with the same kinetics as with higher doses and cells were able to divide within 14 hours post damage induction. The damaged spot remained surprisingly stable in terms of size and location. Interestingly, after cell division, redistribution of relative high levels of GFP was observed in local areas in both daughter cells. These locations very likely contain DNA lesions that have not been removed by DNA repair. In fact, in repair-proficient mammalian cells, a significant fraction of the UV-induced cyclobutane pyrimidine dimers (CPDs), persist longer than 12 hr after UV-C exposure (10 j/m^2) (van Hoffen et al., 1993). We suggest that in the daughter cells, persistent DNA lesions will block the replication machinery in subsequent rounds of DNA replication, until the lesions are repaired. Surprisingly, damaged DNA localized to only a small nuclear region after cell division, identical to the situation before cell division, this suggest that the damaged DNA localized to a similar position as before cell division and confirms the heritable relative chromosomal region positioning in the nucleus (Gerlich and Ellenberg, 2003).

The possibility of induction of local DNA damages with great precision in subnuclear regions together with the ability to image this region by confocal

microscopy within 4 milliseconds after the infrared irradiation creates a new dimension in protein dynamics analysis in living cells.

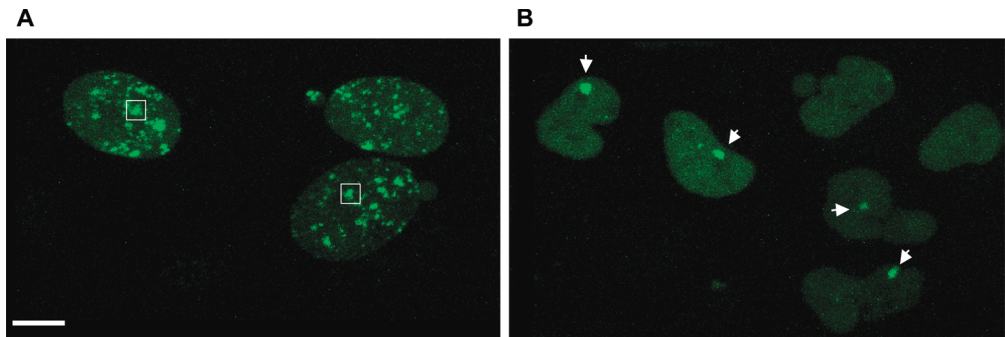


Figure 10. GFP-mRAD18Sc relocate to subnuclear regions in daughter cells after mitosis. HeLa cells stably expressing GFP-mRAD18Sc were locally (rectangles, 15 by 15 pixels) exposed to infrared light (800 nm, 50 mW and 1 iteration)(left panel). The cells were imaged by time lapse confocal microscopy and the picture shown on the right is taken 14 hours after the infrared exposure. Arrows point to local accumulation of GFP in the daughter cells. Note that the third cell in the left image was untreated as a control, and the daughter cells from this cell in the right image do not show marked re-accumulation of GFP-mRAD18Sc. Images are maximum projections of 6 optical slices with 1 μm intervals. Scale bar, 10 μm .

Discussion

Replicative damage bypass (RDB) is a system of mechanisms that function to prevent irreversible termination of the DNA replication machinery when DNA lesions are encountered that block regular elongation. In yeast, RAD6 and RAD18 proteins are the master regulators of this mechanism. In the present study we describe the subcellular localization and dynamic behavior of fluorescently tagged mammalian orthologs of RAD6 and RAD18, respectively in a normal situation and as a response to DNA damage. In addition, we describe a very powerful technique to study real time on the spot assembly, dynamic interaction of repair factors with DNA lesions and to determine reaction kinetics in living cells.

HR6B and mRAD18Sc colocalize and show different nuclear localization patterns during the cell cycle and are associated with the replication machinery

In this study we found that fluorescently tagged HR6B and mRAD18Sc each were strictly localized in nuclei of HeLa cells. Furthermore, within a sub population of the cells discrete nuclear foci of each of the proteins were observed. These bright foci contain both HR6B and mRAD18Sc and they increase in numbers when cells are exposed to UV-C light. Also the proportion of cells containing foci and the number of foci per nucleus dramatically increases. Immunostaining of locally irradiated (UV-C) cells co-transfected with HR6B-GFP and HA-mRAD18Sc revealed that both proteins are recruited to regions containing CPDs. Colocalization of each with PCNA further suggests that these foci represent stalled replication machinery at DNA lesions. The subcellular relocalization of mRAD18Sc and HR6B changes in response to DNA damage, and this is similar to the behavior of two TLS DNA polymerases, pol η and pol ι (Kannouche et al., 2001; Kannouche et al., 2002).

In yeast, the ubiquitin-conjugating complex RAD6-RAD18 is involved in ubiquitination of PCNA in the presence of DNA damage, thereby changing the structure of PCNA, enabling this clamp loader to recruit translesion synthesis and/or damage avoidance factors to allow bypass of the lesion and continuation of DNA replication (Hoege et al., 2002; Stelter and Ulrich, 2003). We propose that this function of RAD6-RAD18 is conserved in higher eukaryotes. In fact, ubiquitination of PCNA has been observed in human cells after treatment with a DNA damaging agent (Hoege et al., 2002). Furthermore, RAD6-RAD18 and their mammalian orthologs may be involved in mediating a structural change of a stalled replication process allowing access of downstream RDB factors. In yeast, it was found that RAD5 (RAD5 interacts also with RAD18) is involved in chromatin remodeling via modification of histone H2B (Martini et al., 2002; Ulrich and Jentsch, 2000). Therefore, the RAD6-RAD18 complex, possibly in cooperation with other RDB factors, might be involved in creating a more open chromatin conformation, providing a better platform for either template switching, recombination repair, or to support access of TLS polymerases.

mRAD18Sc is associated with HR6B

The high degree of colocalization between mRAD18Sc and HR6B suggests that these proteins might interact or at least reside within the same multi-protein complex. Indeed, the nuclear mobility of GFP-mRAD18Sc and HR6B-GFP as identified by FRAP and FCS revealed that both fusion proteins have similar dynamic properties. Furthermore, these measurements were performed on cells in which no large amounts of DNA damage was introduced, indicating that mRAD18Sc and HR6B reside in the same complex that roams the nuclear space. These observations further suggest that these factors load to stalled replication forks simultaneously, in a non-sequential manner. Surprisingly, GFP-mRAD18Sc and HR6B-GFP appeared to relocalize to regions irradiated with near-infrared to introduce DNA lesion, independent of the S phase. These findings suggest a yet unknown role for mRAD18Sc and HR6B proteins in non-S phase cells and a direct role in DNA damage repair. To gain more insight in possible roles for mRAD18Sc and HR6B, the assembly kinetics to DNA lesions needs to be determined in more detail, and for/or different genetic backgrounds harboring mutations in upstream or downstream RDB factors. In addition, analysis of the behavior of mRAD18Sc and HR6B in cell lines mutated for a variety of DNA repair factors might reveal a better understanding of functions of RDB proteins in DNA damage repair and response mechanisms.

Near-infrared laser light efficiently introduces local DNA lesions

Introduction of local UV-lesions using polycarbonate filters with micro pores is a powerful technique to study localization of DNA proteins to these subnuclear regions (Mone et al., 2001; Volker et al., 2001). However, this system does not allow damage infliction at any desired location and/or at any preferred time, and does not allow a semi-high throughput and statistical analysis of a large number of damaged regions. We and others have shown that irradiation with near-infrared laser light efficiently induces CPDs by three-photon absorption (Meldrum et al., 2003). The great advantages of this technique are, that the location and dimension of the lesion are definable and of high resolution, and that the actual measurement can start milliseconds after damage induction. However, it is currently not known what other effects occur as a result of near-infrared irradiation, including other

types of DNA damage. We also observed that long-term measurements of cells after near-infrared irradiation is difficult when too much laser intensity is used, so that cells are damaged and do not divide anymore. Using near-infrared irradiation we have shown that GFP-mRAD18Sc accumulation in local UV-lesions occurs within minutes after treatment. Therefore, this technique is very powerful to analyze quick responses, and multiple fluorescent proteins can be combined to study for example complex formation of DNA repair proteins at local damage. In contrast to currently used approaches such as FRAP-based techniques that study a steady-state status of a process, this new approach provides the possibility to analyze kinetics of de novo assembly of chromatin-associated processes in living cells.

The data presented here show that mRAD18Sc and HR6B are associated with the replication machinery and localize to UV-induced lesions. This localization occurs within minutes after lesions are introduced, and mRAD18Sc re-accumulates in local areas in daughter cells after the cell divisions. These latter two observations were possible by application of near-infrared irradiation, a new technique with great implications for studying dynamic aspects of DNA repair proteins in living cells in the near future. Finally, HR6B and mRAD18Sc are likely involved in activation of replicative damage bypass, probably by their ubiquitin-conjugating activity acting on PCNA, resulting in changes of the mode of action of PCNA.

Acknowledgements

The authors would like to thank Dr. Laura Niedernhofer (Pittsburgh, PA, USA) for helpful comments and Dr. Osamu Nikaido (Kanazawa, Japan) for kindly providing the α -CPD (TDM2) antibody. This work was supported by the Dutch Cancer Foundation (EUR 99-2003).

References

- Bailly, V., Prakash, S., and Prakash, L.** (1997). Domains required for dimerization of yeast Rad6 ubiquitin-conjugating enzyme and Rad18 DNA binding protein. *Mol Cell Biol* **17**, 4536-4543.
- Baynton, K., and Fuchs, R. P.** (2000). Lesions in DNA: hurdles for polymerases. *Trends Biochem Sci* **25**, 74-79.
- Berns, M. W., Wang, Z., Dunn, A., Wallace, V., and Venugopalan, V.** (2000). Gene inactivation by multiphoton-targeted photochemistry. *Proc Natl Acad Sci USA* **97**, 9504-9507.
- Bravo, R., and Macdonald-Bravo, H.** (1987). Existence of two populations of cyclin/proliferating cell nuclear antigen during the cell cycle: association with DNA replication sites. *J Cell Biol* **105**, 1549-1554.
- Broomfield, S., Chow, B. L., and Xiao, W.** (1998). MMS2, encoding a ubiquitin-conjugating-enzyme-like protein, is a member of the yeast error-free postreplication repair pathway. *Proc. Natl. Acad. Sci. USA* **95**, 5678-5683.
- Cassier-Chauvat, C., and Fabre, F.** (1991). A similar defect in UV-induced mutagenesis conferred by the rad6 and rad18 mutations of *Saccharomyces cerevisiae*. *Mutat Res* **254**, 247-253.
- Dowling, E. L., Maloney, D. H., and Fogel, S.** (1985). Meiotic recombination and sporulation in repair-deficient strains of yeast. *Genetics* **109**, 283-302.
- Friedberg, E. C., Wagner, R., and Radman, M.** (2002). Specialized DNA polymerases, cellular survival, and the genesis of mutations. *Science* **296**, 1627-1630.
- Game, J. C., and Kaufman, P. D.** (1999). Role of *Saccharomyces cerevisiae* chromatin assembly factor-I in repair of ultraviolet radiation damage in vivo. *Genetics* **151**, 485-497.
- Gerlich, D., and Ellenberg, J.** (2003). Dynamics of chromosome positioning during the cell cycle. *Curr Opin Cell Biol* **15**, 664-671.
- Hoegge, C., Pfander, B., Moldovan, G. L., Pyrowolakis, G., and Jentsch, S.** (2002). RAD6-dependent DNA repair is linked to modification of PCNA by ubiquitin and SUMO. *Nature* **419**, 135-141.

- Houtsmuller, A. B., Rademakers, S., Nigg, A. L., Hoogstraten, D., Hoeijmakers, J. H., and Vermeulen, W.** (1999). Action of DNA repair endonuclease ERCC1/XPF in living cells. *Science* **284**, 958-961.
- Huang, H., Kahana, A., Gottschling, D. E., Prakash, L., and Liebman, S. W.** (1997). The ubiquitin-conjugating enzyme Rad6 (Ubc2) is required for silencing in *Saccharomyces cerevisiae*. *Mol. Cell. Biol.* **17**, 6693-6699.
- Jentsch, S., McGrath, J. P., and Varshavsky, A.** (1987). The yeast DNA repair gene RAD6 encodes a ubiquitin-conjugating enzyme. *Nature* **329**, 131-134.
- Kannouche, P., Broughton, B. C., Volker, M., Hanaoka, F., Mullenders, L. H., and Lehmann, A. R.** (2001). Domain structure, localization, and function of DNA polymerase eta, defective in xeroderma pigmentosum variant cells. *Genes Dev* **15**, 158-172.
- Kannouche, P., Fernandez de Henestrosa, A. R., Coull, B., Vidal, A. E., Gray, C., Zicha, D., Woodgate, R., and Lehmann, A. R.** (2002). Localization of DNA polymerases eta and iota to the replication machinery is tightly co-ordinated in human cells. *Embo J* **21**, 6246-6256.
- Koken, M. H., Reynolds, P., Jaspers-Dekker, I., Prakash, L., Prakash, S., Bootsma, D., and Hoeijmakers, J. H.** (1991). Structural and functional conservation of two human homologs of the yeast DNA repair gene RAD6. *Proc. Natl. Acad. Sci. USA* **88**, 8865-8869.
- Lawrence, C.** (1994). The RAD6 repair pathway in *Saccharomyces cerevisiae*: what does it do, and how does it do it? *BioEssays* **16**, 253-258.
- Martini, E. M., Keeney, S., and Osley, M. A.** (2002). A role for histone H2B during repair of UV-induced DNA damage in *Saccharomyces cerevisiae*. *Genetics* **160**, 1375-1387.
- Masutani, C., Kusumoto, R., Yamada, A., Dohmae, N., Yokoi, M., Yuasa, M., Araki, M., Iwai, S., Takio, K., and Hanaoka, F.** (1999). The XPV (xeroderma pigmentosum variant) gene encodes human DNA polymerase eta. *Nature* **399**, 700-704.
- Meldrum, R. A., Botchway, S. W., Wharton, C. W., and Hirst, G. J.** (2003). Nanoscale spatial induction of ultraviolet photoproducts in cellular DNA by three-photon near-infrared absorption. *EMBO Rep* **4**, 1144-1149.
- Mone, M. J., Volker, M., Nikaido, O., Mullenders, L. H., van Zeeland, A. A., Verschure, P. J., Manders, E. M., and van Driel, R.** (2001). Local UV-induced DNA damage in cell nuclei results in local transcription inhibition. *EMBO Rep* **2**, 1013-1017.
- Mori, T., Nakane, M., Hattori, T., Matsunaga, T., Ihara, M., and Nikaido, O.** (1991). Simultaneous establishment of monoclonal antibodies specific for either cyclobutane pyrimidine dimer or (6-4)photoproduct from the same mouse immunized with ultraviolet-irradiated DNA. *Photochem Photobiol* **54**, 225-232.
- Roest, H. P., Klaveren van, J., Wit de, J., Gulp van, C. G., Koken, M. H. M., Vermey, M., Roijen van, J. H., Vreeburg, J. T. M., Baarends, W. M., Bootsma, D., Grootegoed, J. A., and Hoeijmakers, J. H. J.** (1996). Inactivation of the HR6B ubiquitin-conjugating DNA repair enzyme in mice causes male sterility associated with chromatin modification. *Cell* **86**, 799-810.
- Roest, H. P., Baarends, W. M., de Wit, J., van Klaveren, J. W., Wassenaar, E., Hoogerbrugge, J. W., van Cappellen, W. A., Hoeijmakers, J. A., and Grootegoed, J. A.** (2004). The Ubiquitin-conjugating DNA repair enzyme HR6A is a maternal factor essential for early embryonic development in mice. *Mol Cell Biol* **in press**.
- Shafirovich, V., Dourandin, A., Luneva, N. P., Singh, C., Kirigin, F., and Geacintov, N. E.** (1999). Multiphoton near-infrared femtosecond laser pulse-induced DNA damage with and without the photosensitizer proflavine. *Photochem Photobiol* **69**, 265-274.
- Singh, J., Goel, V., and Klar, A. J.** (1998). A novel function of the DNA repair gene rhp6 in mating-type silencing by chromatin remodeling in fission yeast. *Mol. Cell. Biol.* **18**, 5511-5522.
- Stelter, P., and Ulrich, H. D.** (2003). Control of spontaneous and damage-induced mutagenesis by SUMO and ubiquitin conjugation. *Nature* **425**, 188-191.
- Tateishi, S., Niwa, H., Miyazaki, J., Fujimoto, S., Inoue, H., and Yamaizumi, M.** (2003). Enhanced genomic instability and defective postreplication repair in RAD18 knockout mouse embryonic stem cells. *Mol Cell Biol* **23**, 474-481.
- Tateishi, S., Sakuraba, Y., Masuyama, S., Inoue, H., and Yamaizumi, M.** (2000). Dysfunction of human Rad18 results in defective postreplication repair and hypersensitivity to multiple mutagens. *Proc Natl Acad Sci USA* **97**, 7927-7932.
- Torres-Ramos, C. A., Yoder, B. L., Burgers, P. M., Prakash, S., and Prakash, L.** (1996). Requirement of proliferating cell nuclear antigen in RAD6-dependent postreplicational DNA repair. *Proc Natl Acad Sci USA* **93**, 9676-9681.
- Ulrich, H. D., and Jentsch, S.** (2000). Two RING finger proteins mediate cooperation between ubiquitin-conjugating enzymes in DNA repair. *Embo J* **19**, 3388-3397.
- van der Laan, R., Roest, H. P., Hoogerbrugge, J. W., Smit, E. M., Slater, R., Baarends, W. M., Hoeijmakers, J. H., and Grootegoed, J. A.** (2000). Characterization of mRAD18Sc, a mouse homolog of the yeast postreplication repair gene RAD18. *Genomics* **69**, 86-94.
- van Hoffen, A., Natarajan, A. T., Mayne, L. V., Van Zeeland, A. A., Mullenders, L. H. F., and Venema, J.** (1993). Deficient repair of the transcribed strand of active genes in Cockayne's syndrome cells. *Nucleic Acids Res* **21**, 5890-5895.

- Volker, M., Mone, M. J., Karmakar, P., van Hoffen, A., Schul, W., Vermeulen, W., Hoeijmakers, J. H., van Driel, R., van Zeeland, A. A., and Mullenders, L. H.** (2001). Sequential assembly of the nucleotide excision repair factors in vivo. *Mol Cell* **8**, 213-224.
- Woodgate, R.** (1999). A plethora of lesion-replicating DNA polymerases. *Genes Dev* **13**, 2191-2195.
- Xin, H., Lin, W., Sumanasekera, W., Zhang, Y., Wu, X., and Wang, Z.** (2000). The human RAD18 gene product interacts with HHR6A and HHR6B. *Nucleic Acids Res.* **28**, 2847-2854.



Chapter 5

Ubiquitin ligase mRAD18Sc localizes to the XY body and to other chromosomal regions that are unpaired and transcriptionally silenced during the male meiotic prophase

Journal of Cell Science

To be published, pending minor revisions

Ubiquitin ligase mRAD18Sc localizes to the XY body and to other chromosomal regions that are unpaired and transcriptionally silenced during the male meiotic prophase

Roald van der Laan^{1, 2}, Evert-Jan Uringa², Evelyne Wassenaar², Jos W. Hoogerbrugge², Esther Sleddens², Hanny Odijk¹, Henk P. Roest¹, Peter de Boer³, Jan H.J. Hoeijmakers¹, J. Anton Grootoeged² and Willy M. Baarends²

¹MGC-Department of Cell Biology and Genetics, Center for Biomedical Genetics, and

²Department of Reproduction and Development, Erasmus MC, Erasmus University Rotterdam, P.O. Box 1738, 3000 DR Rotterdam, The Netherlands

³Department of Obstetrics and Gynecology, UMC St. Radboud, P.O.Box 9101, 6500 HB Nijmegen, The Netherlands

Abstract

In replicative damage bypass (RDB) in yeast, the ubiquitin-conjugating enzyme RAD6 interacts with the ubiquitin ligase RAD18. In mammalian species, these enzymes are represented by two homologs of RAD6, HR6A and HR6B, and one homolog of RAD18, mRAD18Sc. Expression of these genes and the encoded proteins is ubiquitous, but there is relatively high expression in the testis. We have studied the subcellular localization of mRAD18Sc and other RDB proteins in mouse primary spermatocytes passing through the meiotic prophase in spermatogenesis by immunostaining. The highest mRAD18Sc protein level is found at pachytene and diplotene, and the protein localizes mainly to the XY body, a subnuclear region that contains the transcriptionally inactivated X and Y chromosomes. In spermatocytes that carry two semi-identical reciprocal translocations for chromosomes 1 and 13, mRAD18Sc protein concentrates on translocation bivalents that are not fully synapsed. The partly synapsed bivalents are often localized in the vicinity of the XY body, and show a very low level of RNA polymerase II, indicating that the chromatin is in a silent configuration, similar to the transcriptional silencing of the XY body. Thus, mRAD18Sc localizes to unsynapsed and silenced chromosome segments during the male meiotic prophase. All known functions of mRAD18Sc in yeast are related to RDB. However, in contrast to the relatively high level of mRAD18Sc in the XY body, expression of several other proteins known to be involved in subsequent steps of RDB, UBC13 and pol η , appears to be diminished in this heterochromatic subnuclear domain and also in regions containing the unpaired translocation bivalents. Taken together, these observations suggest that the interaction of mRAD18Sc with the XY body may involve a function outside the context of RDB. This function is likely related to a mechanism that signals the presence of unsynapsed chromosomal regions and subsequently leads to transcriptional silencing of these regions during the male meiotic prophase.

Introduction

Maintenance of the stability of the genome of an organism is essential for proper cell function and faithful transmission of genetic information to subsequent generations. However, DNA can be attacked by both exogenous and endogenous factors that introduce lesions. When not properly removed, these DNA lesions can result in disruption of transcription and replication, and in cell death or mutagenesis. When transmitted through the germline, mutations may also lead to genetic disease. Life would not be possible without various DNA repair pathways that are active in somatic and germ line cells to cope with DNA damage.

Lesions that are not removed before cells enter the S phase of the mitotic cell cycle will interfere with DNA replication. However, a set of pathways termed replicative damage bypass (RDB also known as post-replication repair), provides for mechanisms that tolerate the presence of DNA lesions during replication. The genes involved in RDB in the yeast *Saccharomyces cerevisiae* encode members of the RAD6 epistasis group, and homologs in higher eukaryotes have been identified. The RDB pathways are thought to be initiated by the RAD6-RAD18 protein complex, and two major downstream sub-pathways for RDB have been proposed: translesion synthesis (TLS) and damage avoidance (DA) (Baynton and Fuchs, 2000). Translesion synthesis is capable of bypassing a DNA lesion that blocks the replicative polymerase, by using the activity of several specialized enzymes to prevent irreversible termination of DNA replication (Friedberg and Gerlach, 1999). These TLS polymerases include RAD30A (pol η), RAD30B (pol ι), REV3-REV7 (pol ζ), and REV1 (Woodgate, 1999). These polymerases take over from the replicative DNA polymerase when a given lesion is encountered, and are capable of bypassing the lesion with incorporation of a few nucleotides. Subsequently, the activity of the replicative polymerase is reinitiated. In contrast to TLS, the DA mechanisms remain largely hypothetical. DA sub-pathways are basically error-free, because the lesion is bypassed using homology of the newly replicated strand, in a template switch mechanism. Alternatively, homology from the homologous chromosome is used to bypass the lesion, through recombinational repair (Baynton and Fuchs, 2000). Initiation of the DA sub-pathways requires activity of the UBC13-MMS2-RAD5 complex (Broomfield et al., 1998).

To study the possible role of RDB in mammalian species, a first step is the identification of mammalian homologs of genes encoding the proteins that take part in this process. Using this strategy, our laboratory has identified two mouse *RAD6* homologs, *HR6A* (*Ube2a*) and *HR6B* (*Ube2b*) (Roest et al., 1996; Kwon et al., 2001), and recently we also cloned the mouse homolog of *RAD18*, designated *mRAD18Sc* (van der Laan et al., 2000). The yeast *RAD6* gene encodes an ubiquitin-conjugating enzyme (E2 enzyme). The ubiquitin system marks target proteins with one or multiple ubiquitin moieties (mono- or poly-ubiquitination) through a multi-enzyme mechanism: ubiquitin-activating enzyme E1, ubiquitin-conjugating enzyme E2, and ubiquitin ligase E3. Ubiquitinated substrates are targeted for degradation by the proteasome or may undergo functional alterations (Pickart, 2004). The E2 enzyme *RAD6* plays a role in RDB and also in several other functions outside the context of RDB, including sporulation, gene silencing and chromatin modification (Dover et al., 2002; Lawrence, 1994; Singh et al., 1998; Sun and Allis, 2002; Sun and Hampsey, 1999). The mammalian homologs *HR6A* and *HR6B* are thought to function in conserved aspects of the RDB pathways and also in many

other processes including chromatin structure regulation (Baarends et al., 1999; Baarends et al., 2003; Roest et al., 1996).

The yeast RAD6 protein forms a stable complex *in vivo* with RAD18 (Bailly et al., 1994), and for hRAD18Sc, the human homolog of RAD18, interaction with both HR6A and HR6B has been demonstrated (Xin et al., 2000). The mRAD18Sc protein harbors a RING-zinc-finger that is conserved in all known RAD18 homologs (van der Laan et al., 2000; Xin et al., 2000). This protein domain is a hallmark of a family of ubiquitin ligases (E3 enzyme) (Martinez-Noel et al., 1999), and we proposed mRAD18Sc to act as an E3 (van der Laan et al., 2000). Recently it was reported that, in yeast and man, the RAD6-RAD18 (HR6A/B-human RAD18) complex is involved in ubiquitination of the DNA polymerase clamp loader PCNA in response to DNA damage during DNA replication (Hoegel et al., 2002).

Deletion of both *HR6A* and *HR6B* in mice is an embryonic lethal condition, and even double-knockout ES cells are not obtained (Grootegoed et al., 1998; Roest et al., 2004). Inactivation of the *HR6B* gene alone has no overall effect on viability of the mice, and at the cellular level no increased sensitivity for DNA damage was observed (Roest et al., 1996). However, the males were found to be infertile, due to derailment of spermatogenesis. The mice that are HR6A-deficient fail to display a pronounced somatic phenotype, but we observed maternal factor infertility, manifested as a two-cell block of embryonic development (Grootegoed et al., 1998; Roest et al., 2004). The absence of a somatic phenotype in the single knockout animals is most likely due to functional redundancy of the two RAD6 homologs in somatic cells. Recently, mRAD18Sc-deficient ES cells were generated, and these cells are defective in RDB as visualized by an increased sensitivity to various DNA damaging agents, including UV-C light, MMS, mitomycin C and cisplatin, but not to X-rays (Tateishi et al., 2003).

The *mRAD18Sc* gene is ubiquitously expressed in mouse tissues, but the highest level of mRNA expression is found in testis (van der Laan et al., 2000). This expression appears to be associated mainly with the gametogenic compartment, and high expression is detected in primary spermatocytes, that are in the prophase of the first meiotic division. Following DNA replication in preleptotene spermatocytes, which is the spermatogenic final round of DNA replication, the relatively long meiotic prophase I can be subdivided into 4 phases: leptotene, zygotene, pachytene and diplotene. During leptotene, the chromosomes are stretched out, meiotic double strand DNA breaks are induced, and telomere clustering, as observed by the formation of axial elements along the chromosomes, initiates homologous chromosome synapsis during zygotene. At pachytene, spermatocytes display complete synapsis of autosomal bivalents. In synapsed homologous chromosomes, the axial elements, now called lateral elements, are held together as a tripartite structure called the synaptonemal complex (SC), that is composed of these lateral elements (SCP2/Syc2p and SCP3/Syc3p proteins) and a central element (SCP1/Sycp1 protein and a 48 kDa protein) (Heyting, 1996). During the pachytene stage, crossing-overs are established that become visible as chiasmata, when disassembly of the SC starts in diplotene. Finally, the cells reach diakinesis, the stage of transition to metaphase. In the meiotic prophase, the sex chromosomes are stably synapsed only along the pseudo-autosomal regions (PARs) and form the so-called XY body. In this heterochromatic chromatin structure, the X and Y chromosomes are transcriptionally inactive (Monesi, 1965).

In the present study we analyzed the expression of the mRAD18Sc protein in mouse testis in detail, and the results show that mRAD18Sc marks unsynapsed and

inactive chromosomal regions in pachytene and diplotene primary spermatocytes, during the meiotic prophase in the male mouse.

Materials and Methods

Antibody production

Polyclonal antibodies against the mRAD18Sc protein were raised in rabbits using GST-fusion proteins. Different parts of the mRAD18Sc cDNA were fused to the GST gene (M-version: amino acid residues 192-360, and C-version: amino acid residues 428-509). These fusion proteins were purified from a 2-liter culture using a glutathione column (Sigma Chemical CO., St. Louis, MO, USA) followed by an ion exchange column (Sp-sepharose, Sigma). The purified fusion proteins were used to immunize rabbits (2 animals for each fusion protein) using Freund's (Sigma) complete adjuvant for the prime and Freund's incomplete adjuvant (Sigma) for the booster injections (intra cutaneous). Pre-immune serum and antisera were tested on an immunoblot of mouse total testis lysate. One antiserum against the M-version was affinity purified using the M-version fusion protein coupled to Affigel 10 (BioRad, La Jolla, CA, USA) and used for all the described experiments unless indicated otherwise (the C-version antibody was used to verify all results obtained with the affinity-purified antibody).

Antibodies against mouse UBC13 were generated at Eurogentec (Seraing, Belgium) according to their protocols. Rabbits were immunized with a mixture of 2 peptides (C₂₁PGIKAEPDES₃₄NARY and A₁₁₄PNPDDPLANDVAEQ₁₂₈).

Immunoblot analysis

Mouse testes were obtained from wild type FVB mice of different age, and frozen in liquid nitrogen directly after removal from the body. Cell preparations highly enriched in spermatocytes and round spermatids were isolated from mouse testes (FVB) after collagenase and trypsin treatment, followed by sedimentation at unit gravity (StaPut procedure) and density gradient centrifugation through Percoll (Grootegoed et al., 1984).

Protein extracts were prepared by 10 cycles of 10-second sonification in 0.25 M sucrose/ 1mM EDTA supplemented with complete protease inhibitor cocktail (Roche, Mannheim, Germany). Protein concentrations were determined using Coomassie Plus protein assay reagent (Pierce, Rockford IL, USA) as described by the manufacturer.

An amount of 20 µg of protein per sample was separated on 12% SDS-polyacrylamide gels and the separated proteins were transferred to nitrocellulose membranes, using the BioRad miniprotean III system and blot cells (BioRad, La Jolla CA, USA). Membranes were stained with Ponceau S (Sigma) according to the supplier's protocol.

The mRAD18Sc protein was detected using the affinity purified α -mRAD18Sc antibody described above. After blocking non-specific sites with 2.5% w/v non-fat milk in PBS/ with 0.1% v/v Tween20 (blotto) for 1 hour at room temperature, antibody was added at a 1:250 dilution in fresh blotto, and incubation was continued for an additional hour at room temperature. Subsequently, non-bound antibody was removed through several washes using PBS with 0.1% v/v Tween20. The second antibody, alkaline phosphatase (AP)-conjugated goat anti-rabbit (Biosource International, Camarillo, CA, USA) was diluted 1:1000 in blotto,

and the incubation was for 1 hour at room temperature. After washing with PBS with 0.1% v/v Tween20 the specific signal was detected by incubation with NBT/BCIP (Sigma) according to the manufacturer's manual.

In vitro transcription-translation

The mRAD18Sc cDNA was cloned into the pcDNA3 plasmid (Invitrogen, Carlsbad, CA, USA) and labeled with [³⁵S]methionine by TnT-coupled in vitro transcription-translation according to the manufacturer's protocol (Promega, Madison, WI, USA). The product was separated on 12% polyacrylamide gels, the gels were dried and the labeled protein was detected by autoradiography.

Isolation of testicular tubule fragments and immunofluorescence

Mouse testes were isolated from 21-23-day-old FVB mice, and the decapsulated testes were shaken (90 cycles/minute; amplitude 20 mm in a 200 ml Erlenmeyer flask) in 20 ml phosphate-buffered saline (PBS) supplemented with collagenase (100 µg/ml), hyaluronidase (60 µg/ml), glucose (5.6 mM) and DL-lactic acid (10 mM) at 32-34° C for 50 minutes. This treatment results in dissociation of the testis tissue into fragments of testicular tubules. After addition of DNase (1 µg/ml) and trypsin (100 µg/ml) the incubation was continued for 3 more minutes to obtain smaller tubule fragments, and this tubule preparation was then washed 3 times with PBS containing DNase (1 µg/ml) and fetal calf serum 2% v/v, using centrifugation at low speed to collect the tubule fragments. Finally, the tubule fragments were cultured on cover slips in DMEM-F12 supplemented with 2% v/v fetal calf serum and antibiotics at 33° C for 2-3 days

For immunofluorescence, all the steps were performed at room temperature. The cultured tubule fragments were fixed in 2% w/v paraformaldehyde for 20 minutes and were permeabilized for 10 minutes using PBS supplemented with 0.2% Triton X-100 (Sigma). Aspecific sites were masked by blocking in PBS/ 0.5% v/v BSA/ 0.15% v/v glycine (PBS+) for 5 minutes. Primary antibodies (α -mRAD18Sc diluted 1:100 or α -HR6A/B recognizing HR6A and HR6B diluted 1:100, both antibodies are rabbit polyclonals) were incubated overnight in PBS+ and subsequently the excess of first antibody was removed by three wash steps with PBS+. The specific signal was visualized by incubation with Alexa488 (diluted 1:1000) goat anti-rabbit antibodies (Molecular Probes, Eugene, OR, USA). After removal of the antibody and subsequent washing steps, the coverslips were mounted on slides using Vectashield (Vector Laboratories, Burlingame CA, USA). DAPI (diluted 1:5000, Sigma) was used for nuclear staining. As controls, preimmune serum was used (α -mRAD18Sc) or the first antibody was omitted during the procedure (α -HR6A/B). In addition, on meiotic spread preparations, α -HR6A/B accumulates on XY body chromatin, and the specificity of this reaction was confirmed using pre-incubation of the antibody with the N-terminal epitope of HR6A/B that was used to generate the antibody (not shown).

Immunohistochemistry

Mouse testes were isolated from wild type FVB mice and fixed in phosphate-buffered formalin (30 mM NaH₂PO₄, 45 mM Na₂HPO₄, 4% v/v formaldehyde, pH 6.8) overnight at room temperature, dehydrated and embedded in paraffin. Cross sections of 8 µm were made and mounted on 3-aminopropyltriethoxysilane coated slides (Sigma) and dried at 37° C overnight. Slides were deparaffinized and endogenous peroxidase was blocked by incubation with 3% v/v H₂O₂ for 20

minutes. After washing in tap water, the slides were incubated for 20 minutes in a microwave oven at 1000 Watts in 0.01 M citric acid, pH 6.0. After cooling down to room temperature, the slides were washed with distilled water and subsequently in PBS, and non-specific sites were blocked for 20 minutes in 0.5% w/v non-fat milk/ 0.5% w/v BSA in PBS. The slides were incubated overnight at room temperature with the mRAD18Sc antibody diluted 1:100 or with anti-PCNA diluted 1:200 (Abcam, Cambridge, UK) in 10% w/v bovine serum albumin (BSA) in PBS. The slides were washed 3 times for 20 minutes with PBS and incubated with the second antibody (biotinylated goat anti-rabbit; or biotinylated goat anti-mouse; DAKO, Glostrup, Denmark) diluted 1:200 in PBS containing 2% v/v normal goat serum for 2 hours. The antigen-antibody complexes were visualized with avidin-biotin complex reagent (DAKO) according to the manufacturer's protocol, followed by staining using 3,3'-diaminobenzidine tetrahydrochloride (DAB) metal concentrate (Pierce) as a substrate and counterstaining with hematoxylin.

Immunostaining of meiotic spread nuclei preparations

Nuclear spread preparations of mouse spermatocytes were made according to the protocol described (Peters et al., 1997b). 4-5 week-old wild type FVB mouse testes and testes of T(1;13)70H/T(1;13)Wa double-heterozygous mice (de Boer et al., 1986, Swiss random bred HsdCpb:SE,) were analyzed. The slides containing the meiotic nuclear spreads were washed with PBS/ 0.05% v/v Triton X100 extensively and nonspecific sites were blocked by incubation in PBS/ 0.05% v/v Triton X100/ 5% w/v non-fat milk (blocking solution) prior to addition of the specific antibodies. The primary antibodies (α -mRAD18Sc, rabbit polyclonal (1:100), α -UBC13, rabbit polyclonal (1:100), α -SCP3, mouse monoclonal (1:2) and rabbit polyclonal (1:500) (gift from C. Heyting, Wageningen, The Netherlands), α -Pol η , rabbit polyclonal (1:50) (gift from A. Lehman, Brighton, UK), α -PCNA mouse monoclonal (1:200) (Abcam), and mouse monoclonal α -RNA pol II (1:50) (8wg16, detects total RNA pol II; Abcam) were diluted in blocking solution and incubated overnight at room temperature. Non-bound antibodies were removed by washing in PBS and the slides were incubated with PBS/ 5% w/v non-fat milk/ 10% v/v normal goat serum for 20 minutes at room temperature. The secondary antibodies (FITC-conjugated goat anti-rabbit and TRITC-conjugated goat anti-mouse (DAKO) 1:1000) were added, and incubation was continued for 2 more hours at room temperature. Finally, after extensive washing with PBS the slides were mounted in Vectashield (Vector Laboratories, Burlingame CA, USA) containing DAPI.

RESULTS

mRAD18Sc protein is expressed in spermatocytes and spermatids

mRAD18Sc has a calculated molecular mass of 57.3 kDa. However, antibodies against the mRAD18Sc protein recognize a protein of approximately 80 kDa on immunoblots of mouse total testis lysate (Figure 1A). In addition, we performed an *in vitro* transcription-translation assay using mRAD18Sc cDNA. The assay yielded a prominent protein band around 80 kDa and several low intensity bands, possibly representing degradation products (Figure 1B). The result of the transcription-translation assay is consistent with the immunoblot. The size difference between the calculated and observed molecular mass of mRAD18Sc is presumably due to the fact that the tertiary structure of the mRAD18Sc protein is partly maintained under the denaturing conditions of gel electrophoresis. Similar results have been obtained for human RAD18 by other investigators; this protein also runs at a higher molecular mass than expected (Tateishi et al., 2000; Xin et al., 2000;).

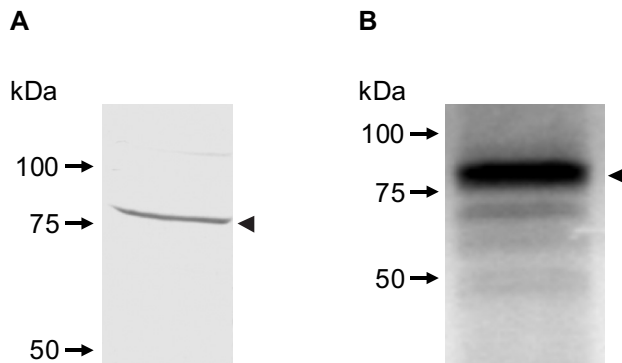


Figure 1. Detection of mRAD18Sc protein. A: On an immunoblot of proteins isolated from total testis lysate, the α -mRAD18Sc antibody recognizes a specific protein band around 80 kDa (arrowhead). B: *In vitro* transcription- translation using mRAD18Sc cDNA results in a protein band with a molecular mass of approximately 80 kDa (arrow head).

We performed immunoblot analysis on total testis proteins derived from wild type FVB mice of different age (Figure 2A), and on proteins from isolated spermatocytes and round spermatids (Figure 2B). In testis from 7- and 14-day-old mice the amount of mRAD18Sc protein is relatively low, compared to a higher level at subsequent steps of postnatal testis development. Spermatogenesis is initiated in the first week after birth, and the first wave of spermatogenesis results in population of the testis by primary spermatocytes in the period around 14 days of postnatal testis development, followed by the appearance of a large number of spermatids around day 21. A relatively high level of the mRAD18Sc protein was found to be present in spermatocytes and round spermatids (Figure 2B), which is in agreement with the developmental increase in mRAD18Sc protein level in testis (Figure 2A).

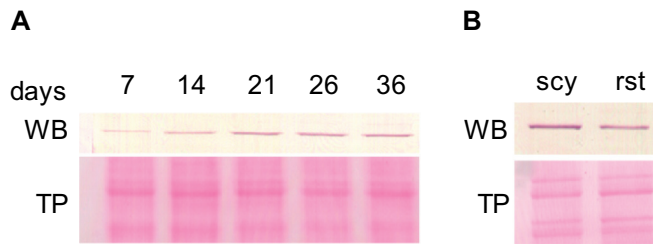


Figure 2. Relative mRAD18Sc protein level in mouse testis at different postnatal developmental time points and in isolated germinal cells. A: Total testis proteins from mice at different postnatal ages (7-36 days) were analyzed on an immunoblot (WB) using α -mRAD18Sc. The relative mRAD18Sc protein level increases after birth to a maximum at 21 days. B: The mRAD18Sc protein level in isolated spermatocytes (scy) is slightly higher than in isolated spermatids (rst). Ponceau S staining of total protein (TP) is shown as a loading control.

mRAD18Sc protein localizes to the XY body chromatin in pachytene and diplotene spermatocytes

To study subcellular localization of mRAD18Sc protein in different testicular cell types, affinity-purified polyclonal α -mRAD18Sc antibody directed against amino acid residues 192-360 was used for immunohistochemical staining of mouse testis cross-sections. In addition, an antibody against the C-terminus of mRAD18Sc was included in the experiments to verify the results, and preimmune sera were used as negative controls. mRAD18Sc protein is detected in spermatogonia, spermatocytes and round spermatids, and the highest mRAD18Sc protein level is found in the nuclei of pachytene primary spermatocytes (Figure 3A, B, C). In the nuclei of these cells, mRAD18Sc protein shows marked localization in a heterochromatic sub-nuclear region, the XY body, containing the X and Y chromosomes (Figure 3C). When the same immunohistochemistry analysis was performed on cross-sections from a human testis biopsy, we observed a strong signal in the XY body, which most likely represents high expression of human RAD18 in this subnuclear region (Figure 3D).

In view of the interaction of RAD6-RAD18 in RDB in yeast, it is of interest to study possible colocalization of HR6A/B and mRAD18Sc. The subcellular localization patterns of mRAD18Sc and HR6A/B proteins were compared using immunofluorescence on fixed testicular tubule fragments. Since both α -mRAD18Sc and α -HR6A/B were raised in rabbits, we performed the assays separately. The results indicate that the XY body chromatin in spermatocytes contains both mRAD18Sc and HR6A/B (Figure 4A and 4B). The HR6A/B protein is associated with the chromatin over the entire nucleus of the primary spermatocytes in the prophase of the meiotic divisions, and it is not clear whether the XY body chromatin is highly enriched in HR6A/B. Again, a relatively high level of mRAD18Sc protein is limited to the XY body.

The localization of mRAD18Sc to the XY body in spermatocytes was analyzed in more detail by immunostaining of meiotic spread preparations of spermatocytes, using α -mRAD18Sc antibodies in combination with an antibody against SCP3, a major protein component of the SC. SCP3 protein is present in the axial elements and lateral elements of the SC, and an antibody against SCP3 can be used to mark the stages of the meiotic prophase in nuclear spread preparations of primary spermatocytes (Dobson et al., 1994; Heyting and Dietrich 1991; Offenberget al., 1991). HR6A/B localization was not studied, since the available antibodies

against HR6A/B give non-reproducible results when used for immunostaining of meiotic spread preparations.

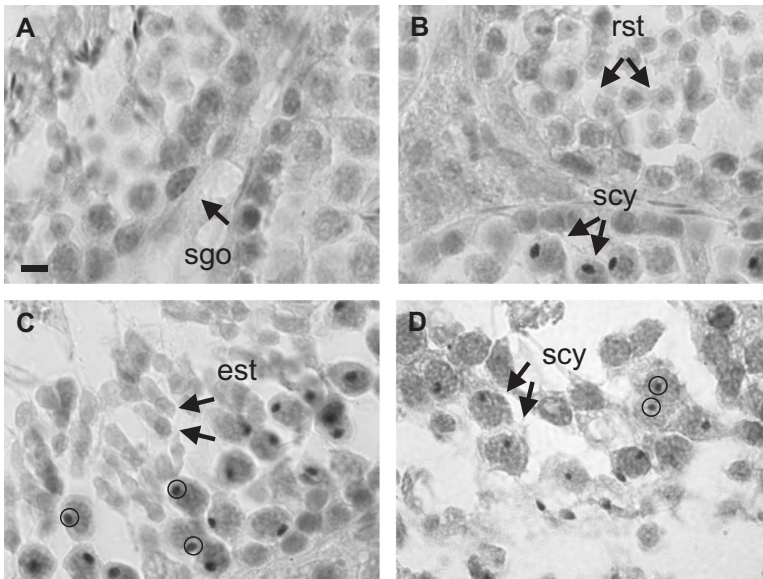


Figure 3. Localization of mRAD18Sc protein in mouse and human testis. Panels A-C: Sections of wild type mouse testis were stained with α -mRAD18Sc. A and B: a positive signal was found in spermatogonia (sgo), primary spermatocytes (scy) and round spermatids (rst). C: Hardly any mRAD18Sc was present in elongating spermatids (est). In primary spermatocytes (scy), the highest amount of mRAD18Sc was found associated with the XY body (circles). Panel D: In cross sections of human testis, α -mRAD18Sc gave marked staining of the XY body (circles) in primary spermatocytes (scy). Scale bar, 30 μ m.

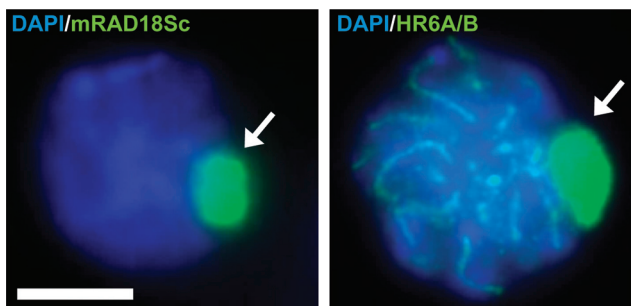


Figure 4. mRAD18Sc and HR6A/B localize to XY body chromatin in mouse primary spermatocytes. Fixed testicular tubule fragments were stained with α -mRAD18Sc (left panel) or α -HR6A/B (right panel), and the nuclei were visualized with DAPI (blue). The arrows indicate the XY body. Scale bar, 10 μ m.

AAt the zygotene stage, no clear mRAD18Sc signal is visible (Figure 5A). The XY body is formed around early pachytene, and accumulation of the mRAD18Sc protein in the XY body is clearly visible at mid-pachytene (Figure 5B). The mRAD18Sc protein localizes around the XY SC and (unsynapsed) axial elements, covering the area where the X and Y chromosomes are located in the

nucleus. Following further progression of the meiotic prophase, a high mRAD18Sc signal is still present in the XY body in early diplotene (Figure 5C), and thereafter the XY body and the mRAD18Sc signal disappear (Figure 5D).

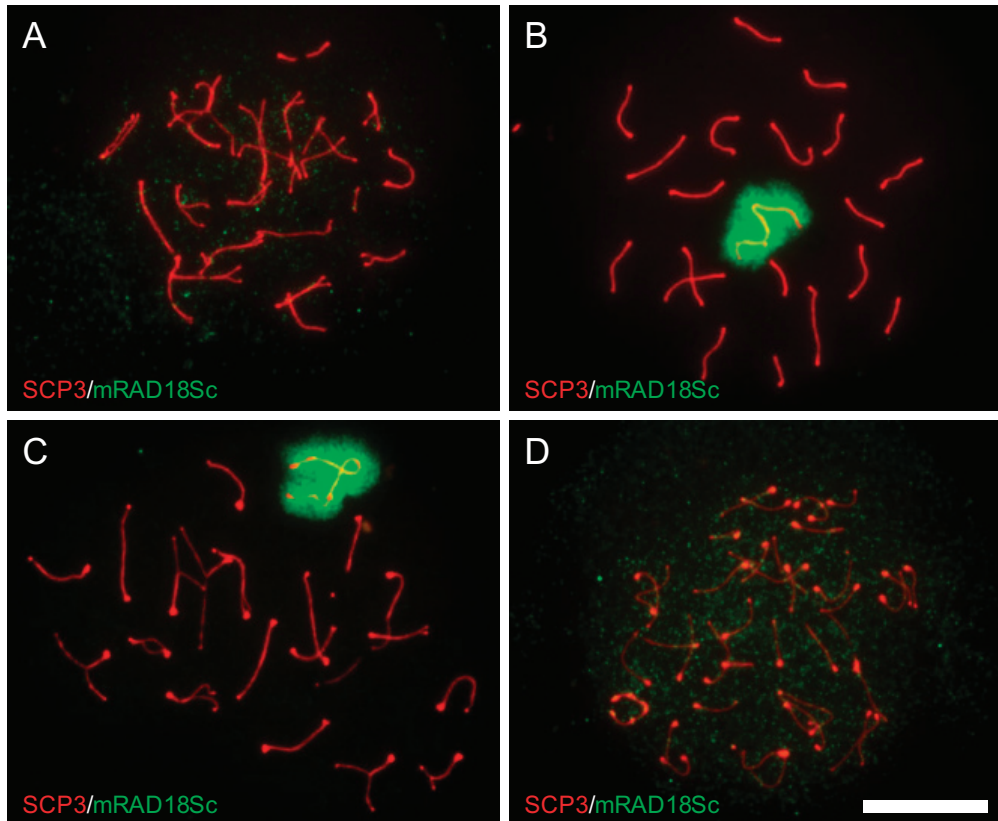


Figure 5. mRAD18Sc protein is associated with XY body chromatin of pachytene and diplotene spermatocytes. mRAD18Sc is stained using α -mRAD18Sc (green) and the axial elements and lateral elements of SC's are stained with α -SCP3 (red) in zygotene (A); pachytene (B); early diplotene (C); and diplotene (D) spermatocytes. Scale bar, 20 μ m.

mRAD18Sc protein is present at partially synapsed translocation bivalents in spermatocytes from T(1;13)70H/T(1;13)Wa double-heterozygous mice

The marked association of mRAD18Sc with XY body chromatin might be related to the fact that the large heterologous regions of the X and Y chromosomes, outside the PAR, can not undergo stable synapsis and, for the proximal Y and larger proximal part of the X, remain unpaired throughout pachytene. To investigate whether mRAD18Sc is associated also with unsynapsed autosomal regions, we used T(1;13)70H/T(1;13)Wa double-heterozygous mice (de Boer et al., 1986) in which an autosomal pairing problem occurs during spermatogenesis. This problem is caused by the presence of two different, but nearly identical, reciprocal translocations involving chromosomes 1 and 13 (de Boer et al., 1986). The presence of the translocations leads to variable impairment of spermatogenesis: 12-47% of the male mice generate offspring, the percentage being dependent

on the breeding history (Peters et al., 1997a). The mean testis weight and the sperm count of the translocation carriers are lower compared to wild type animals (Peters et al., 1997a), but a sufficient number of relatively intact spermatocytes remains present to allow the current analysis. The epididymal sperm count negatively correlates with the frequency of 1^{13} heteromorphic bivalents adjacent to the sex bivalent during pachytene (de Boer et al., 1986). During the meiotic prophase, the unsynapsed axial loop of the 13^1 translocation bivalent can be seen in early pachytene, but this loop disappears by non-homologous synapsis, in most nuclei (Moses and Poorman, 1981; Peters et al., 1997a). In contrast, resolution of the homologous 1^{13} loop is not always accomplished, and this small bivalent is often found in the vicinity of the XY body (de Boer et al., 1986, Forejt, 1996). Synaptic adjustment of bivalents increases with progression of the pachytene, but the frequency of loop configurations remains fairly constant (Baart et al., 2000; de Boer et al., 1986; Peters et al., 1997a). In nuclear spread preparations of spermatocytes from mice with these translocations, the locations of mRAD18Sc and SCP3 were visualized by immunostaining. In Figure 6, it is clearly visible that mRAD18Sc protein in pachytene spermatocytes localizes not only to the XY body, but also to the 1^{13} translocation bivalent adjacent to it. However, in some nuclei the XY body accumulates mRAD18Sc, but the translocation bivalent does not. For the 1^{13} bivalent, different configurations of the SC have been described, associated with different degrees of homologous and/or non-homologous synapsis (de Boer et al., 1986, Peters et al., 1997a).

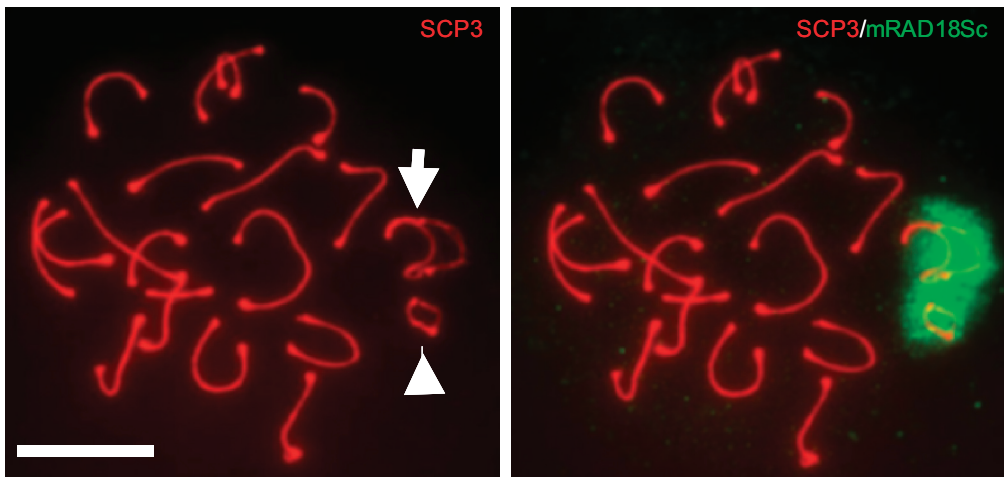
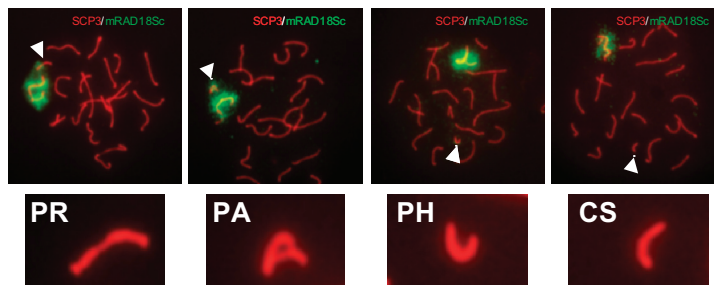


Figure 6. mRAD18Sc protein localizes to unsynapsed axial loops. Immunostaining of SCP3 (red) and mRAD18Sc (green) of T(1;13)70H/T(1;13)Wa double-heterozygous spermatocytes. The mRAD18Sc protein localizes to the XY body and also to the translocation bivalent that shows incomplete synapsis. The unsynapsed axial loop of the 1^{13} bivalent is often found close to the XY body. The arrow indicates the X and Y bivalent (XY body) and the arrowhead points to the 1^{13} translocation bivalent. Scale bar, 20 μ m.

The morphology of the SC in primary spermatocytes from T(1;13)70H/T(1;13)Wa double-heterozygous mice, immunostained with α -SCP3, also shows this variability (Baart et al., 2000). To estimate the percentage pachytene nuclei with a positive mRAD18Sc signal on the 1^{13} bivalent, we analyzed the pachytene nuclei with an overall normal SC morphology and mRAD18Sc signal covering the XY body. These

nuclei were subdivided into four groups, based on different configurations of the 1^{13} bivalent: The morphology of the 1^{13} bivalent was classified as Partially synapsed Rest (PR, low degree of synapsis), Partially synapsed A shape (PA, intermediate degree of synapsis), Partially synapsed Horsheshoe shape (PH, almost complete synapsis), and Completely Synapsed (CS). It was found that mRAD18Sc accumulates on the 1^{13} bivalent in almost all nuclei that contain unsynapsed 1^{13} segments (PR, PA, PH). In contrast, when synapsis of the 1^{13} bivalent is apparently complete (CS), the mRAD18Sc signal is very low or absent (Figure 7). In the majority of the nuclei containing the 1^{13} translocation bivalent in the PR and PA configuration, the bivalent was located in very close proximity to the XY body. In contrast, the horseshoe (PH) and paired (CS) configurations of the 1^{13} bivalent are found close to the XY body in only 30% of the nuclei that carry these configurations and mRAD18Sc associates with the 1^{13} bivalent in only 17.8% of the PH nuclei and not in the CS nuclei. Taken together, these observations indicate that the 1^{13} bivalent loses mRAD18Sc protein, and its tendency to colocalize with the XY body, when synapsis is more complete.



mRAD18Sc signal	PR	PA	PH	CS	Tot
-	0	2	4	7	13
+/-	1	5	6	0	12
+	13	10	3	0	26
Tot	14	17	13	7	51

Figure 7. The mRAD18Sc protein localizes to unsynapsed regions of the 1^{13} bivalent. The morphology of the 1^{13} bivalent was classified as Partially synapsed A shape (PA, intermediate degree of synapsis), Partially synapsed Horsheshoe shape (PH, almost complete synapsis), Partially synapsed Rest (PR, low degree of synapsis), and Completely Synapsed (CS). The accumulation of mRAD18Sc to these regions was analyzed by immunostaining (upper panel). Over groups, the number of nuclei positive for mRAD18Sc was found to be increased when the synapsis of these bivalents was less complete (lower panel). The arrowhead indicates the 1^{13} bivalent.

The XY body chromatin may not contain downstream components of the postreplication repair subpathways

In yeast, RAD6/RAD18 interaction is a key step in activation of all RDB sub-pathways. The observed colocalization of HR6A/B and mRAD18Sc on XY body chromatin might signify activation of RDB subpathways within these chromatin domains. This activation would become visible by recruitment of downstream

RDB components. In yeast, one of the downstream components is UBC13. This ubiquitin-conjugating enzyme associates with MMS2 and RAD5, and together these proteins constitute a second ubiquitin-conjugating protein complex in RDB, which is thought to initiate the damage avoidance sub-pathway of RDB (Baynton and Fuchs, 2000; Stelter and Ulrich, 2003). The mouse homolog of *UBC13* has been identified, and the mRNA is ubiquitously expressed, but with the highest level in testis (Ashley et al., 2002). After selection of candidate antigenic peptides, a polyclonal antibody against mouse UBC13 was generated, and affinity purified. The antibody specifically recognizes GST-fused mouse UBC13 on immuno blots (results not shown). Using meiotic nuclear spread preparations, UBC13 was detected in the nuclei of pachytene and diplotene spermatocytes, and UBC13 protein was also found in the post-meiotic spermatids. However, UBC13 is largely or completely excluded from the XY body chromatin (Figure 8A). Based on this observation, we suggest that the mRAD18Sc protein does not take part in a protein complex that triggers the damage avoidance pathway in XY body chromatin. To test whether mRAD18Sc in the XY body might be involved in activation of the translesion synthesis sub-pathway of RDB, we used an antibody against pol η , one of the TLS polymerases. The antibody used in this immunostaining is known to recognize human pol η , but the peptide sequence used to generate this polyclonal antibody is 100% conserved between mouse and human (Kannouche et al., 2001). Similar to what was observed for UBC13, the amount of pol η is much lower in the area of the XY body chromatin compared to the rest of the chromatin in the nuclear spread preparation (Figure 8B), and this is not observed using the pre-immune serum (result not shown). Since RDB is associated with DNA replication, we also studied PCNA localization in the testis. Using immunostaining of mouse testis cross-sections and meiotic nuclear spread preparations, we did not detect PCNA in late pachytene and diplotene nuclei (results not shown). Taken together, the present results indicate that HR6A/B and mRAD18Sc are associated with the XY body chromatin, and may perform a function outside the context of RDB.

mRAD18Sc is located in transcriptionally silenced chromatin

Yeast RAD6 exerts multiple functions, including key roles in RDB and N-end rule protein degradation, and also has an involvement in sporulation and gene silencing, and in mitotic and meiotic recombination (Freiberg et al., 2000). XY body chromatin in spermatocytes is transcriptionally inactive (Monesi, 1965). We performed an immunostaining for RNA pol II (antibody 8wg16) to visualize transcriptional activity in spermatocytes. The XY body is negative for RNA pol II in nuclear spreads prepared from wild type mouse testis (Figure 9A). In T(1;13)70H/T(1;13)Wa spermatocytes, we observed a very low RNA pol II signal in the region where the unpaired 1¹³ loop is located (Figure 9B). Co-staining of RNA pol II with mRAD18Sc in these nuclear preparations indicates that RNA pol II is largely absent from regions where the mRAD18Sc protein is abundant: the chromatin of the XY body and the unpaired 1¹³ translocation bivalent (Figure 9C).

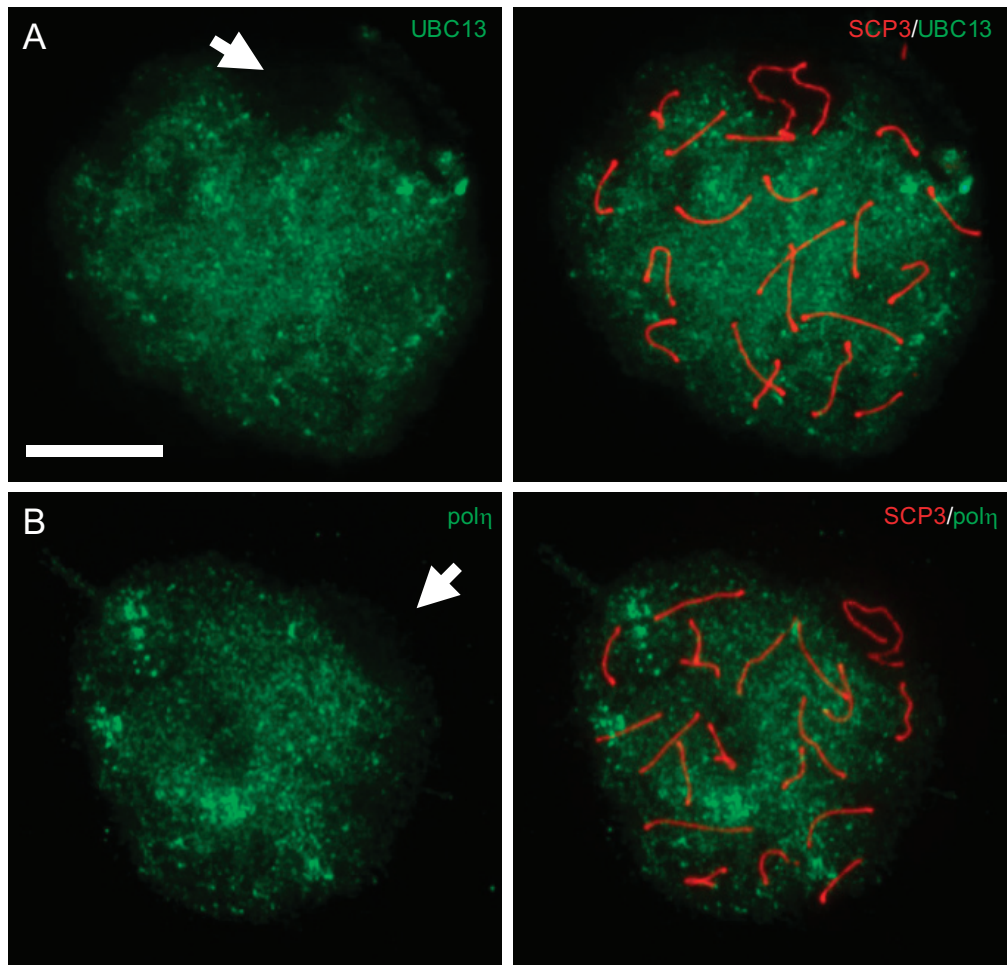


Figure 8. Immunostaining of RDB proteins downstream of HR6A/B-mRAD18Sc is low in the XY body chromatin of primary spermatocytes. A, left panel: Immunostaining of UBC13 using α -UBC13 (green) shows that the UBC13 protein is absent from a subnuclear region where the XY body is situated (arrow). Right panel: Co-immunostaining of UBC13 and SCP3 (red) to visualize the autosomes and the location of the XY body. B, left panel: Immunostaining of the TLS polymerase pol η by α -pol η (green). The level of this RDB protein is also very low in the subnuclear region where the sex chromosomes are located (arrow). Right panel: Co-immunostaining of pol η and SCP3 (red) to visualize the autosomes and the location of the XY body. Scale bar, 20 μ m.

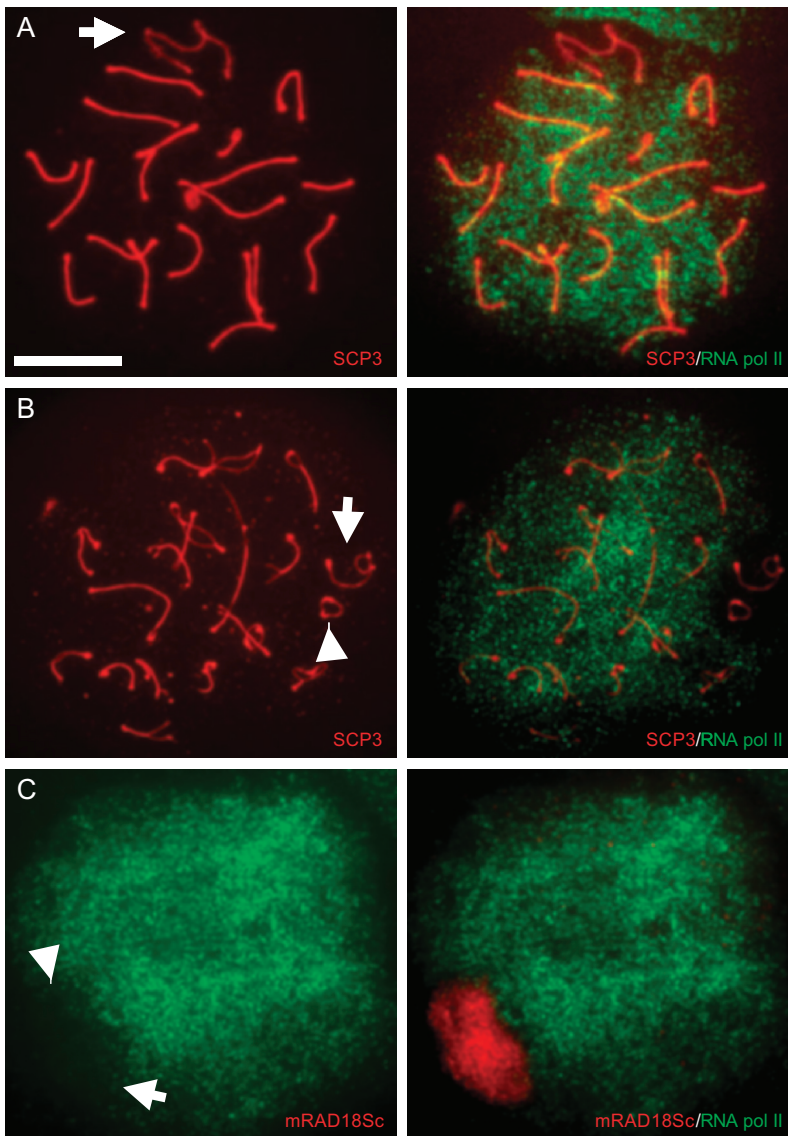


Figure 9. RNA pol II is largely excluded from nuclear regions containing mRAD18Sc associated with unsynapsed chromosomes. A, left panel: Immunostaining of the SC using α -SCP3 (red) on a wild type spermatocyte. The arrow points to the XY body. Right panel: Co-immunostaining of SCP3 and RNA polymerase II (green) showing that the RNA polymerase II staining signal is very low in the XY body. B, left panel: Immunostaining of SCP3 (red) on a T(1;13)70H/T(1;13)Wa double-heterozygous spermatocyte. The arrow points to the XY body and the arrowhead to the 1¹³ translocation bivalent. Right panel: Co-immunostaining of SCP3 and RNA polymerase II (green) shows that the RNA polymerase II staining signal is also very low in the subnuclear region of the 1¹³ translocation bivalent. C, left panel: Immunostaining on a T(1;13)70H/T(1;13)Wa double-heterozygous spermatocyte with α -RNA polymerase II (green). The subnuclear regions containing the XY body (arrow) and the 1¹³ translocation bivalent (arrowhead) have a very low level of RNA polymerase II protein. Right panel: Co-immunostaining of RNA polymerase II and mRAD18Sc shows that the regions deficient in RNA polymerase II contain a large amount of mRAD18Sc (red). Scale bar, 20 μ m.

Discussion

Replicative damage bypass (RDB) is a tolerance system that prevents irreversible termination of DNA replication in S phase cells when the basal replication machinery encounters blocking lesions in the DNA template. The key players of RDB are RAD6 and RAD18, and these two proteins have been shown to undergo functional interactions, a feature that is conserved from yeast to higher eukaryotes. The yeast RAD6 protein is involved in multiple functions, including non-RDB functions, whereas RAD18 is thought to function in RDB only. Mammalian HR6A/HR6B and mRAD18Sc mRNAs are ubiquitously expressed in mouse tissues, but the mRNA levels in testis are relatively high. In this study we have investigated the subcellular localization of mRAD18Sc and other RDB proteins in mouse testis.

RDB-associated mRAD18Sc activity in spermatogenic cells

Immunoblot analysis of postnatal mouse testis and isolated spermatogenic cell types showed a relative high mRAD18Sc protein level in primary spermatocytes, but the protein is also present in other testicular cell types, including spermatogonia which compose the mitotically active cell population that gives rise to new generations of spermatocytes entering the meiotic prophase, throughout adult reproductive life. The presence of mRAD18Sc in spermatogonia might be required for RDB in these proliferating cells. The last DNA replication during spermatogenesis occurs in preleptotene primary spermatocytes, and the relatively high mRAD18Sc level in pachytene primary spermatocytes might serve other purposes than a role in RDB related to DNA replication, although meiotic homologous recombination during the meiotic prophase is associated with some DNA strand elongation. Meiotic nuclear spread preparations of pachytene and early diplotene spermatocytes, immunostained with α -mRAD18Sc, show very clear staining of the XY body, and HR6A/B is also present in this region of the nuclei.

At male meiotic prophase, the non-homologous X and Y chromosomes can only pair in the PARs. The chromatin of the sex bivalent forms a subnuclear region that is first seen around early pachytene and persists into diplotene. During early pachytene, transcription from the X and Y chromosomes is globally repressed (Monesi, 1965), but following completion of the meiotic divisions, several X and Y chromosomal genes are re-expressed in haploid spermatids (Hendriksen et al., 1995). Possible functions of the transcriptionally inactive XY body chromatin in spermatocytes include: 1) promotion of alignment of the pseudoautosomal regions (PARs) of the X and the Y chromosomes (Turner et al., 2000), 2) prevention of non-homologous recombination between regions outside the PARs of the X and Y chromosomes, and 3) masking of unpaired chromosomal regions in the X and Y chromosomes from a synapsis checkpoint (Jablonka and Lamb, 1988).

Functional interaction of HR6A/B-mRAD18Sc, an ubiquitin-conjugating enzyme (E2) and an ubiquitin ligase (E3), would result in ubiquitination of target proteins. Mono-ubiquitination may stabilize or alter the activity of the target proteins, whereas poly-ubiquitination of target proteins leads to proteasomal degradation (Pickart, 2004). The only known substrate of the RAD6-RAD18 complex in yeast is PCNA (Hoegge et al., 2002). This protein functions as a sliding clamp during DNA replication and is also required during DNA chain elongation in connection with RDB. PCNA staining has been reported for mitotically active spermatogonia and for preleptotene spermatocytes, and persistence of some nuclear staining at later stages of the meiotic prophase (zygotene and early-mid

pachytene) might represent PCNA protein that is left over from earlier stages and/or PCNA playing some role in meiotic DNA replication associated with homologous recombination (Kamel et al., 1997; Wrobel et al., 1996). Possibly, mRAD18Sc is directly involved in ubiquitination of PCNA, in the presence of DNA damage in the S phase of spermatogonia and preleptotene primary spermatocytes. In mouse testis cross-sections, using immunostaining, we did not detect PCNA in late pachytene and diplotene spermatocytes and also not in the XY body. Therefore, HR6A/B and mRAD18Sc in spermatocytes are most likely involved in ubiquitination of other, yet unknown substrates that are possibly associated with the XY chromosomal chromatin in the male meiotic prophase.

The XY body, mRAD18Sc, and DNA repair

Apart from mRAD18Sc, several other DNA repair proteins have been found to accumulate in the XY body, including Rad50, Mre11, and Ku70, all proteins involved in double strand break repair (Eijpe et al., 2000; Goedecke et al., 1999). The function of these proteins with respect to the function of the XY body remains unclear. Expression of several XY body proteins has been investigated in female meiotic cells carrying a Y chromosome with a deletion of the sex determining gene *Sry* (XY^{Tdym1}), as well as in XO cells. Pachytene XY^{Tdym1} and XO oocytes mostly contain unsynapsed sex chromosomes, but no XY body-like structure has been observed (Turner et al. 2000; Hoyer-Fender et al., 2004). The results indicate that some of the proteins investigated also localize to unpaired sex chromosomes in female pachytene nuclei, whereas others are XY body specific (Turner et al., 2000; Hoyer-Fender et al., 2004). Using male mice double-heterozygous for the T(1;13)70H and T(1;13)Wa translocations as described in this report, it has been shown that the XY body and the 1¹³ bivalent also stain with an antibody targeting the cell cycle checkpoint protein Atr (for ataxia telangiectasia and Rad3-related) (Baart et al., 2000; Moens et al., 1999; Keegan et al., 1996). The Atr protein is most likely involved in phosphorylation of proteins, a response of the cell cycle machinery to DNA damage (Cortez et al., 1999; Keegan et al., 1996). The intensity of the Atr signal on the 1¹³ bivalent depends on the degree of pairing within this region, and the protein tends to localize to incompletely paired configurations of the bivalent (Baart et al., 2000). This protein localization pattern is similar to the present observations on mRAD18Sc staining of the 1¹³ bivalent. Possibly, Atr and/or mRAD18Sc also bind to unpaired chromosomal regions in oocytes that go through the meiotic prophase, but this remains to be investigated. These observations suggest that the localization of some proteins to the XY body is related to the presence of unsynapsed axes. In addition, the XY body may also have specific functions, as indicated by the existence of true XY body specific proteins (Turner et al., 2000). The only known XY body protein that has a proven XY body function is phosphorylated histone H2AX (γ -H2AX). γ -H2AX has important roles in DNA repair in somatic cells, and in meiotic recombination. Interestingly, phosphorylation of H2AX is enhanced in the XY body, and this process is essential for formation and transcriptional silencing of the XY body (Fernandez-Capetillo et al., 2003; Mahadevaiah et al., 2001).

The question arises why a protein involved in RDB localizes to unpaired chromosomal regions in pachytene primary spermatocytes. If mRAD18Sc functions in the XY body are related to RDB, it is to be expected that components of the RDB subpathways downstream of HR6A/B and mRAD18Sc also accumulate in the XY body. To test this hypothesis, we have selected antibodies against two proteins, mouse UBC13 and pol η , each involved in one of the RDB sub-pathways,

and studied their localization in male meiotic nuclei. Both antibodies gave very little, if any, immunostaining of the XY body, and therefore it is not likely that the observed subnuclear mRAD18Sc accumulation is indicative for activation of RDB subpathways in XY body chromatin.

mRAD18Sc functions in the testis outside the context of RDB

A possible alternative explanation for the presence of the HR6A/B-mRAD18Sc complex in the XY body is that it plays a functional role to prevent non-homologous recombination between the X and Y chromosomes. In yeast, RAD6 is implicated in control of mitotic homologous recombination and silencing (Lawrence, 1994). For mice, it has been observed that HR6B might play some role in the control of meiotic recombination frequency. In *HR6B* knockout spermatocytes, the number of meiotic recombination sites has increased from an average of 23, found in spermatocytes from wild type mice, to an average of 27 (Baarends et al., 2003). This would lead to the hypothesis that mRAD18Sc might take part in a series of molecular events, to prevent interchromosomal meiotic recombination events outside the PARs of the X and Y chromosomes.

HR6B may regulate several processes related to control of chromatin structure in the meiotic prophase. In HR6B-deficient mouse pachytene spermatocytes, we have observed marked aberrations of the synaptonemal complex, including lengthening of the SC and loss of SCP3 from near telomeric regions (Baarends et al., 2003). These aberrations point to a general role of HR6B in maintaining chromatin structure, which, for the sex chromosomes, may require interaction of HR6B with mRAD18Sc. However, in *HR6B* knockout spermatocytes mRAD18Sc can still interact with HR6A, which may be sufficient for normal function of mRAD18Sc.

A possibility that has become more apparent during the course of these investigations is that the HR6A/B-mRAD18Sc complex could be involved in a cascade of events that first signals incomplete chromosome pairing and subsequently leads to transcriptional inactivation. The XY body is transcriptionally inactive (Monesi, 1965). Using α -RNA pol II antibodies, we have shown that the incompletely paired translocation 1¹³ bivalent in pachytene nuclei of male mice carrying the double-heterozygote T(1;13)70H/T(1;13)Wa translocations also becomes transcriptionally inactivated in pachytene spermatocytes. These data are supported by results from early studies on meiotic chromosome behavior that have shown frequent association of different autosomal chromosomes with the XY body, when the presence of a translocation, or trisomic chromosome leads to meiotic pairing problems (Solari, 1971; de Boer and Groen, 1974; Forejt, 1974). In addition, such XY body associated autosomal chromosome regions often were heteropyknotic, and appeared to become incorporated in the XY body (Solari, 1971; de Boer and Groen, 1974).

As mentioned earlier, the RAD6 protein in yeast plays a role in gene silencing, at least in part through monoubiquitination of histone H2B (Robzyk et al., 2000), and this function could be conserved to higher eukaryotes. In contrast, mutation of *RAD18* does not affect gene silencing, and *RAD18* is also not required for ubiquitination of histones. Gene function of *RAD18* in yeast is thought to be limited to RDB. Still, one report describes that yeast *rad18* mutants combined with mutations in excision repair genes have reduced spore viability, indicating a role for *RAD18* in meiosis (Dowling et al., 1985). In addition, *RAD18* might be involved in regulation of gene silencing through some other ubiquitin modification, since

mutation of *Chromatin Assembly Factor I (CAF1)* combined with a $\Delta rad18$ mutation revealed a possible role of RAD18 in telomeric silencing (Game and Kaufman, 1999). CAF1 is involved in depositing histones on DNA, and when this process is impaired, RAD6 may depend on RAD18 for recruitment to the DNA (Game and Kaufman, 1999). In addition, the process of inactivation of unpaired chromosomal segments might require substantial chromatin remodeling in which the HR6A/B-mRAD18Sc complex is involved. To further investigate the precise role of this complex, we are currently searching for HR6A/B-mRAD18Sc substrates in spermatogenesis.

The present observations that the mRAD18Sc protein localizes to unpaired and transcriptionally inactive chromosomal regions in the meiotic prophase opens a new field of interest. More detailed analysis of the XY body chromatin in primary spermatocytes could give us new insights in meiotic functions of mRAD18Sc, and also in the mechanisms that drive formation of the XY body and control transcriptional silencing of specific chromatin domains.

Acknowledgements

We would like to thank dr. Andre Eker (Rotterdam, The Netherlands) for technical assistance in the antibody production. The SCP3 antibodies were kindly provided by dr. Christa Heyting (Wageningen, The Netherlands) and the antibodies targeting pol η by dr. Alan Lehmann (Brighton, UK). This work was supported by the Dutch Cancer Foundation (EUR 99-2003).

References

- Ashley, C., Pastushok, L., McKenna, S., Ellison, M. J., and Xiao, W. (2002). Roles of mouse UBC13 in DNA postreplication repair and Lys63-linked ubiquitination. *Gene* **285**, 183-191.
- Baarends, W. M., Hoogerbrugge, J. W., Roest, H. P., Ooms, M., Vreeburg, J., Hoeijmakers, J. H., and Grootegoed, J. A. (1999). Histone ubiquitination and chromatin remodeling in mouse spermatogenesis. *Dev Biol* **207**, 322-333.
- Baarends, W. M., Wassenaar, E., Hoogerbrugge, J. W., van Cappellen, G., Roest, H. P., Vreeburg, J., Ooms, M., Hoeijmakers, J. H., and Grootegoed, J. A. (2003). Loss of HR6B ubiquitin-conjugating activity results in damaged synaptonemal complex structure and increased crossing-over frequency during the male meiotic prophase. *Mol Cell Biol* **23**, 1151-1162.
- Baart, E. B., de Rooij, D. G., Keegan, K. S., and de Boer, P. (2000). Distribution of Atr protein in primary spermatocytes of a mouse chromosomal mutant: a comparison of preparation techniques. *Chromosoma* **109**, 139-147.
- Bailly, V., Lamb, J., Sung, P., Prakash, S., and Prakash, L. (1994). Specific complex formation between yeast RAD6 and RAD18 proteins: a potential mechanism for targeting RAD6 ubiquitin-conjugating activity to DNA damage sites. *Genes Dev* **8**, 811-820.
- Baynton, K., and Fuchs, R. P. (2000). Lesions in DNA: hurdles for polymerases. *Trends Biochem Sci* **25**, 74-79.
- de Boer, P. And Groen, A. (1974). Fertility and meiotic behaviour of male *T70H* tertiary trisomics of the mouse (*Mus musculus*). *Cytogenet. Cell Genet.* **13**, 489-510
- de Boer, P., Searle, A. G., van der Hoeven, F. A., de Rooij, D. G., and Beechey, C. V. (1986). Male pachytene pairing in single and double translocation heterozygotes and spermatogenic impairment in the mouse. *Chromosoma* **93**, 326-336.
- Broomfield, S., Chow, B. L., and Xiao, W. (1998). MMS2, encoding a ubiquitin-conjugating-enzyme-like protein, is a member of the yeast error-free postreplication repair pathway. *Proc Nat. Acad Sci USA* **95**, 5678-5683.
- Cortez, D., Wang, Y., Qin, J., and Elledge, S. J. (1999). Requirement of ATM-dependent phosphorylation of brca1 in the DNA damage response to double-strand breaks. *Science* **286**, 1162-1166.

- Dobson, M.J., Pearlman, R.E., Karaiskakis, A., Syropoulos, B., and Moens, P.B.** (1994). Synaptonemal complex proteins: occurrence, epitope mapping and chromosome disjunction. *J Cell Sci* **107**, 2749-2760.
- Dover, J., Schneider, J., Boateng, M. A., Wood, A., Dean, K., Johnston, M., and Shilatifard, A.** (2002). Methylation of histone H3 by COMPASS requires ubiquitination of histone H2B by RAD6. *J. Biol. Chem.* **277**, 28368-28371.
- Dowling, E. L., Maloney, D. H., and Fogel, S.** (1985). Meiotic recombination and sporulation in repair-deficient strains of yeast. *Genetics* **109**, 283-302.
- Eijpe, M., Offenbergh, H., Goedecke, W., and Heyting, C.** (2000). Localisation of RAD50 and MRE11 in spermatocyte nuclei of mouse and rat. *Chromosoma* **109**, 123-132.
- Fernandez-Capetillo, O., Mahadevaiah, S. K., Celeste, A., Romanienko, P. J., Camerini-Otero, R. D., Bonner, W. M., Manova, K., Burgoyne, P., and Nussenzweig, A.** (2003). H2AX is required for chromatin remodeling and inactivation of sex chromosomes in male mouse meiosis. *Dev Cell* **4**, 497-508.
- Forejt, J.** (1974). Nonrandom association between a specific autosome and the X chromosome in meiosis of the male mouse: possible consequence of the homologous centromeres' separation. *Cytogenet. Cell Genet.* **13**, 369-383.
- Forejt, J.** (1996). Hybrid sterility in the mouse. *Trends Genet* **12**, 412-417.
- Freiberg, G., Mesecar, A. D., Huang, H., Hong, J. Y., and Liebman, S. W.** (2000). Characterization of novel rad6/ubc2 ubiquitin-conjugating enzyme mutants in yeast. *Curr Genet* **37**, 221-233.
- Friedberg, E. C., and Gerlach, V. L.** (1999). Novel DNA polymerases offer clues to the molecular basis of mutagenesis. *Cell* **98**, 413-416.
- Game, J. C., and Kaufman, P. D.** (1999). Role of *Saccharomyces cerevisiae* chromatin assembly factor-I in repair of ultraviolet radiation damage in vivo. *Genetics* **151**, 485-497.
- Goedecke, W., Eijpe, M., Offenbergh, H. H., van Aalderen, M., and Heyting, C.** (1999). Mre11 and Ku70 interact in somatic cells, but are differentially expressed in early meiosis. *Nat Genet* **23**, 194-198.
- Grootegoed, J. A., Baarends, W. M., Roest, H. P., and Hoeijmakers, J. H.** (1998). Knockout mouse models and gametogenic failure. *Mol Cell Endocrinol* **145**, 161-166.
- Grootegoed, J. A., Jansen, R., and Van der Molen, H. J.** (1984). The role of glucose, pyruvate and lactate in ATP production by rat spermatocytes and spermatids. *Biochim Biophys Acta* **767**, 248-256.
- Hendriksen, P. J., Hoogerbrugge, J. W., Themmen, A. P., Koken, M. H., Hoeijmakers, J. H., Oostra, B. A., van der Lende, T., and Grootegoed, J. A.** (1995). Postmeiotic transcription of X and Y chromosomal genes during spermatogenesis in the mouse. *Dev Biol* **170**, 730-733.
- Heyting, C.** (1996). Synaptonemal complexes: structure and function. *Curr Opin Cell Biol.* **8**, 389-396.
- Heyting, C., and Dietrich, A.J.J.** (1991). Meiotic chromosome preparation and protein labeling. *Methods Cell Biol* **35**, 177-202.
- Hooge, C., Pfander, B., Moldovan, G. L., Pyrowolakis, G., and Jentsch, S.** (2002). RAD6-dependent DNA repair is linked to modification of PCNA by ubiquitin and SUMO. *Nature* **419**, 135-141.
- Hoyer-Fender, S., Czirr, E., Radde, R., Turner, J. M., Mahadevaiah, S. K., Pehrson, J. R., and Burgoyne, P. S.** (2004). Localisation of histone macroH2A1.2 to the XY-body is not a response to the presence of asynapsed chromosome axes. *J Cell Sci* **117**, 189-198.
- Jablonka, E., and Lamb, M. J.** (1988). Meiotic pairing constraints and the activity of sex chromosomes. *J Theor Biol* **133**, 23-36.
- Kamel, D., Mackey, Z.B., Sjoblom, T., Walter, C.A., McCarrey, J.R., Uitto, L., Palosaari, H., Lahdetie, J., Tomkinson, A.E., Syvaoja, J.E.** (1997). Role of deoxyribonucleic acid polymerase epsilon in spermatogenesis in mice. *Biol Reprod* **57**, 1367-1374.
- Kannouche, P., Broughton, B. C., Volker, M., Hanaoka, F., Mullenders, L. H., and Lehmann, A. R.** (2001). Domain structure, localization, and function of DNA polymerase eta, defective in xeroderma pigmentosum variant cells. *Genes Dev* **15**, 158-172.
- Keegan, K. S., Holtzman, D. a., Plug, A. W., Christenson, E. R., Brainerd, E. E., Flaggs, G., Bentley, N. J., Taylor, E. M., Meyn, M. S., Moss, S. B., Carr, A. M., Ashley, T., and Hoekstra, M. F.** (1996). The Atr and Atm protein kinases associate with different sites along meiotically pairing chromosomes. *Genes Dev.* **10**, 2383-2388.
- Kwon, Y. T., Xia, Z., Davydov, I. V., Lecker, S. H., and Varshavsky, A.** (2001). Construction and analysis of mouse strains lacking the ubiquitin ligase UBR1 (E3alpha) of the N-end rule pathway. *Mol. Cell. Biol.* **21**, 8007-8021.
- Lawrence, C.** (1994). The RAD6 repair pathway in *Saccharomyces cerevisiae*: what does it do, and how does it do it? *BioEssays* **16**, 253-258.
- Mahadevaiah, S. K., Turner, J. M., Baudat, F., Rogakou, E. P., de Boer, P., Blanco-Rodriguez, J., Jasin, M., Keeney, S., Bonner, W. M., and Burgoyne, P. S.** (2001). Recombinational DNA double-strand breaks in mice precede synapsis. *Nat Genet* **27**, 271-276.
- Martinez-Noel, G., Niedenthal, R., Tamura, T., and Harbers, K.** (1999). A family of structurally related RING finger proteins interacts specifically with the ubiquitin-conjugating enzyme UbcM4. *FEBS Lett* **454**, 257-261.

- Moens, P. B., Tarsounas, M., Morita, T., Habu, T., Rottinghaus, S. T., Freire, R., Jackson, S. P., Barlow, C., and Wynshaw-Boris, A.** (1999). The association of ATR protein with mouse meiotic chromosome cores. *Chromosoma* **108**, 95-102.
- Monesi V.** (1965). Differential rate of ribonucleic acid synthesis in the autosomes and sex chromosomes during male meiosis in the mouse. *Chromosoma* **17**: 11-21.
- Moses, M. J., and Poorman, P. A.** (1981). Synaptosomal complex analysis of mouse chromosomal rearrangements. II. Synaptic adjustment in a tandem duplication. *Chromosoma* **81**, 519-535.
- Offenberg, H. H., Dietrich, A. J., and Heyting, C.** (1991). Tissue distribution of two major components of synaptonemal complexes of the rat. *Chromosoma* **101**, 83-91.
- Peters, A. H., Plug, A. W., and de Boer, P.** (1997a). Meiosis in carriers of heteromorphic bivalents: sex differences and implications for male fertility. *Chromosome Res.* **5**, 313-324.
- Peters, A. H., Plug, A. W., van Vugt, M. J., and de Boer, P.** (1997b). A drying-down technique for the spreading of mammalian meocytes from the male and female germline. *Chromosome Res.* **5**, 66-68.
- Pickart, C. M.** (2004). Back to the future with ubiquitin. *Cell* **116**, 181-190.
- Robzyk, K., Recht, J., and Osley, M. A.** (2000). Rad6-dependent ubiquitination of histone H2B in yeast. *Science* **287**, 501-504.
- Roest, H. P., van Klaveren, J., de Wit, J., van Gurp, C. G., Koken, M. H., Vermeij, M., van Roijen, J. H., Hoogerbrugge, J. W., Vreeburg, J. T., Baarends, W. M., Bootsma, D., Grootegoed, J. A., and Hoeijmakers, J. H.** (1996). Inactivation of the HR6B ubiquitin-conjugating DNA repair enzyme in mice causes male sterility associated with chromatin modification. *Cell* **86**, 799-810.
- Roest, H.P., Baarends, W.M., de Wit, J., van Klaveren, J.W., Wassenaar, E., Hoogerbrugge, J.W., van Cappellen, W.A., Hoeijmakers, J.H.J., and Grootegoed, J.A.** (2004). The ubiquitin-conjugating DNA repair enzyme HR6A is a maternal factor essential for early embryonic development in mice. *Mol Cell Biol* **24**, in press.
- Singh, J., Goel, V., and Klar, A. J.** (1998). A novel function of the DNA repair gene rhp6 in mating-type silencing by chromatin remodeling in fission yeast. *Mol. Cell. Biol.* **18**, 5511-5522.
- Solari, A.J.** (1971). The behaviour of chromosomal axes in Searle's X-autosome translocation. *Chromosoma* **34**, 99-112.
- Stelter, P., and Ulrich, H. D.** (2003). Control of spontaneous and damage-induced mutagenesis by SUMO and ubiquitin conjugation. *Nature* **425**, 188-191.
- Sun, Z. W., and Allis, C. D.** (2002). Ubiquitination of histone H2B regulates H3 methylation and gene silencing in yeast. *Nature* **418**, 104-108.
- Sun, Z. W., and Hampsey, M.** (1999). A general requirement for the Sin3-Rpd3 histone deacetylase complex in regulating silencing in *Saccharomyces cerevisiae*. *Genetics* **152**, 921-932.
- Tateishi, S., Sakuraba, Y., Masuyama, S., Inoue, H., and Yamaizumi, M.** (2000). Dysfunction of human Rad18 results in defective postreplication repair and hypersensitivity to multiple mutagens. *Proc Natl Acad Sci USA* **97**, 7927-32.
- Tateishi, S., Niwa, H., Miyazaki, J., Fujimoto, S., Inoue, H., and Yamaizumi, M.** (2003). Enhanced genomic instability and defective postreplication repair in RAD18 knockout mouse embryonic stem cells. *Mol Cell Biol* **23**, 474-481.
- Turner, J. M., Mahadevaiah, S. K., Benavente, R., Offenberg, H. H., Heyting, C., and Burgoyne, P. S.** (2000). Analysis of male meiotic "XY body" proteins during XY female meiosis provides new insights into their functions. *Chromosoma* **109**, 426-432.
- van der Laan, R., Roest, H. P., Hoogerbrugge, J. W., Smit, E. M., Slater, R., Baarends, W. M., Hoeijmakers, J. H., and Grootegoed, J. A.** (2000). Characterization of mRAD18Sc, a mouse homolog of the yeast postreplication repair gene RAD18. *Genomics* **69**, 86-94.
- Woodgate, R.** (1999). A plethora of lesion-replicating DNA polymerases. *Genes Dev* **13**, 2191-2195.
- Wrobel, K.H., Bickel, D., Kujat, R.** (1996). Immunohistochemical study of seminiferous epithelium in adult bovine testis using monoclonal antibodies against Ki-67 protein and proliferating cell nuclear antigen (PCNA). *Cell Tissue Res* **283**, 191-201.
- Xin, H., Lin, W., Sumanasekera, W., Zhang, Y., Wu, X., and Wang, Z.** (2000). The human RAD18 gene product interacts with HHR6A and HHR6B. *Nucleic Acids Res* **28**, 2847-2854.



Chapter 6

Silencing of unpaired chromatin and histone H2A ubiquitination in mammalian meiosis

Submitted

Silencing of unpaired chromatin and histone H2A ubiquitination in mammalian meiosis

Willy M. Baarends*, Evelyne Wassenaar, ¹Roald van der Laan, Jos Hoogerbrugge, Esther Sleddens-Linkels, ¹Jan H.J. Hoeijmakers, ²Peter de Boer and J. Anton Grootegoed

Department of Reproduction and Development, and ¹MGC-Department of Cell Biology and Genetics, Erasmus MC, Erasmus University Rotterdam, The Netherlands, and ²Department of Obstetrics and Gynecology, University Medical Center St. Radboud, Nijmegen, The Netherlands

Abstract

During meiotic prophase in male mammals, the X and Y chromosomes are incorporated in the XY body or sex body. Chromatin in the XY body is transcriptionally silenced, and marked by increased ubiquitination of histone H2A. This led us to investigate the relation between histone H2A ubiquitination and chromatin silencing in more detail. First, we found that ubiquitinated H2A also marks the silenced X chromosome of the Barr body in female somatic cells. Next, we studied a possible relation between chromatin silencing, H2A ubiquitination, and unpaired chromatin in meiotic prophase. The mouse models used carried an unpaired autosomal chromosome region in male meiosis, or unpaired X and Y chromosomes in female meiosis. We show that ubiquitinated histone H2A is associated with transcriptional silencing of large chromatin regions. In addition, our findings on transcriptional silencing of unpaired chromatin regions in mammalian meiotic prophase cells are reminiscent of a phenomenon described in the fungus *Neurospora crassa*, named Meiotic Silencing of Unpaired DNA (MSUD).

Introduction

Chromatin remodeling is at the basis of control of cell-specific gene expression, cell determination and differentiation. The basic unit of chromatin, the nucleosome, consists of two each of the histones H2A, H2B, H3 and H4. The N-terminal ends of these core histones extend from the nucleosome, and can undergo posttranslational covalent modifications, such as methylation, acetylation, phosphorylation, and ADP-ribosylation of specific amino acid residues. Together, these modifications constitute the so-called 'histone code' (Strahl and Allis, 2000). Interaction of other nuclear proteins with chromatin, dependent on composition of the histone code present at specific chromatin regions, determines local chromatin structure, which can be open or closed. Ubiquitination of lysine residues in the C-termini of histones H2A and H2B are somewhat exceptional components of the histone code. Ubiquitin, a protein of 7 kDa, can be attached to lysine residues of a specific protein substrate through action of a multi-enzyme complex containing ubiquitin-activating (E1), ubiquitin-conjugating (E2) and ubiquitin ligase (E3) enzymes. Polyubiquitination can target proteins for degradation by the proteasome

(Pickart, 2004; Pickart and Cohen, 2004). Monoubiquitination of histones, however, is a stable modification that does not decrease the half-life of the target histone (Zhang, 2003), but plays a role in the histone code.

In the yeast *Saccharomyces cerevisiae*, histone H2A ubiquitination is not required for cell growth or sporulation (Swerdlow et al., 1990), but histone H2B ubiquitination is an essential mechanism involved in sporulation (Robzyk et al., 2000). Most importantly, recently it has been shown that ubiquitination of H2B by the ubiquitin-conjugating enzyme RAD6, interacting with the ubiquitin ligase BRE1, is a prerequisite for dimethylation of histone H3 at lysine residues 4 and 79 (Briggs et al., 2002; Dover et al., 2002; Robzyk et al., 2000; Sun and Allis, 2002). This 'trans-histone' mechanism that results in changed histone H3 methylation is thought to be associated with potentiation of gene activation.

It is not known whether this 'trans-histone' mechanism is conserved between yeast and mammals. RAD6 shows marked evolutionary conservation. The two mammalian homologs of yeast RAD6, HR6A/Ube2a and HR6B/Ube2b show approximately 70% amino acid sequence identity to yeast Rad6. Previously, we have investigated histone ubiquitination in mice deficient for HR6B/Ube2B. X-chromosomal *HR6A/Ube2a* and autosomal *HR6B/Ube2b* are functionally equivalent in somatic cells, but gametogenesis requires differential expression and/or differential functions of the two genes (Roest et al., 1996; Roest et al., 2004). *Ube2a* knockout mice show maternal factor infertility (lack of embryo development beyond the two-cell stage), whereas *Ube2b* knockout mice display male infertility (severely impaired spermatogenesis) (Roest et al., 1996; Roest et al., 2004). *Ube2a-Ube2b* double knockouts are not viable. No defect in H2A ubiquitination was observed in spermatogenic cells of *Ube2b* knockout mice, and the level of H2B ubiquitination was too low, to be detected in wild type and knockout tissues and cells (Baarends et al., 1999).

In mammalian cells, H2A ubiquitination is far more prominent than H2B ubiquitination, and the functional relevance of these modifications in higher organisms remains elusive (Zhang, 2003). Marked H2A ubiquitination was observed in meiotic prophase cells, in particular in a specific subnuclear region that contains the heterochromatic X and Y chromosomes (Baarends et al., 1999). This region is called the sex body or XY body, which is formed at the beginning of meiotic prophase, when homologous chromosomes align. This process of chromosome alignment requires development of a protein structure that holds the two chromosomes together, the synaptonemal complex (Heyting, 1996). First, axial elements attach to the chromosomal cores, and subsequently, central and transverse elements form the connection. One of the axial element proteins is Sycp3, and immunostaining for this protein is a useful tool to follow progression through meiotic prophase. Synaptonemal complex formation coincides with chromosome pairing and synapsis. The heterologous X and Y chromosomes are covered by Sycp3 along their whole length, but show synapsis only in short pseudoautosomal regions (PARs). From late zygotene onwards, the X and Y chromosomes in the XY body are transcriptionally silent (Monesi, 1965).

Localization of ubiquitinated histone H2A (ubi-H2A) to transcriptionally silent XY body chromatin may signify that H2A ubiquitination is linked to transcriptional silencing, also in other chromatin regions, and not only in meiotic prophase. The aim of the experiments presented in this manuscript was to obtain additional

information concerning a possible connection between histone H2A ubiquitination and formation or maintenance of silent chromatin regions.

Materials and Methods

Isolation of different cell types from mouse testis

For isolation of basic nuclear proteins, a cell preparation containing more than 70% spermatocytes and spermatids) was isolated from 30-day-old wild type FVB/N mice, using a shortened protocol. Iodoacetamide (10 mM) was present throughout the cell isolation procedure, to inhibit protein deubiquitination (Matsui et al., 1982), and the isolation procedure was shortened to limit negative effects of iodoacetamide on cell viability, as follows. Decapsulated testes were shaken (90 cycles/minute, amplitude 10 mm, in a siliconized 100 ml Erlenmeyer flask) at 32-34°C for 25 minutes, in 20 ml phosphate-buffered saline (PBS) with Ca²⁺ and Mg²⁺ (PBS+Ca/Mg:137 mM NaCl, 2.7 mM KCl, 1.5 mM KH₂PO₄, 6.5 mM Na₂HPO₄, 1.1 mM CaCl₂, 0.5 mM MgCl₂), containing 1 mg/ml trypsin (40-110 U/mg, Roche, Mannheim, Germany), 1 mg/ml collagenase (0.435 U/mg, Roche), and 0.5 mg/ml hyaluronidase (1000 U/mg, Roche). The tubule fragments obtained by this enzyme treatment were shaken (120 cycles/minute) at 32-34°C for 10 minutes, in 20 ml PBS without Ca²⁺ and Mg²⁺ (PBS-Ca/Mg:137 mM NaCl, 2.7 mM KCl, 1.5 mM KH₂PO₄, 8.1 mM Na₂HPO₄). Larger cell clumps were removed using a Pasteur pipette, and the cell suspension was filtered through a 60 µm nylon filter and centrifuged at 250g.

Isolation of acid soluble nuclear proteins and two-dimensional gel electrophoresis

Nuclei and acid soluble proteins were isolated from cell preparations according to Chen et al., (1998). The isolated protein fraction was precipitated with 5% (w/v) trichloroacetic acid. First dimension acetic acid-urea-triton (AUT) gels were run according to Davie (1982), and contained 0.8 M acetic acid, 6 M urea and 0.375% v/v Triton X-100. The AUT strips were placed on 15% SDS-polyacrylamide gels and blotted on nitrocellulose (0.45 µm) using BioRad mini-protean II electrophoresis and blot cells (BioRad, La Jolla, CA, USA). After equilibration of the gel for 30 minutes in 50 mM acetic acid and 0.5% w/v SDS, blotting was performed in 25 mM CAPS buffer (pH 10) and 20% v/v methanol according to the protocol described by Thiriet and Albert (1995). Ubi-H2A was detected as described by Baarends et al. (1999).

Meiotic spread nuclei preparations and immunocytochemistry

Embryonic ovaries were isolated at E18 from wild type, XO and XY^{tdym1} embryos (generated on a random bred MF1 background using stocks maintained at the National Institute for Medical Research, Mill Hill London, United Kingdom, and made available by P. Burgoyne, London, UK). Testes were obtained from 5-week-old wild type and T(1;13)70H/T(1;13)1Wa (T/T') mice (Swiss random bred), and from one adult rat (Wistar). Human testicular tissue was obtained as remnant material from a testicular biopsy. Testis and ovary tissues were processed for immunocytochemistry as described by Peters et al. (1997b). Spread nuclei of spermatocytes and oocytes were double-stained or triple-stained with rabbit polyclonal or mouse monoclonal anti-Sycp3 (gift from C. Heyting, Wageningen, The Netherlands), mouse monoclonal IgM anti-ubi-H2A (Upstate, Waltham,

MA, USA), mouse monoclonal anti-RNAPolII (the 8wg16 detects total RNA polII (Abcam, Cambridge, UK), rabbit polyclonal anti-Rad18 (as described by van der Laan et al., submitted), anti-ubiquitin (DakoCytomation, Glostrup, Denmark) and anti- γ -H2AX (Upstate). For polyclonal first antibodies, the secondary antibodies were FITC- (Sigma, St Louis, MO, USA), TRITC- (Sigma), or Alexa 350- (Molecular Probes, Eugene, OR, USA) labeled goat anti-rabbit IgG antibodies; FITC-, TRITC-, or Alexa 350-labelled goat-anti-mouse IgG and FITC-labeled goat anti-mouse IgM (Sigma) were used as secondary antibody for monoclonal anti-Sycp3 (IgG), anti-polII (IgG) and anti-uH2A (IgM). Before incubation with antibodies, slides were washed in PBS (3x10 min), and non-specific sites were blocked with 0.5% w/v BSA and 0.5% w/v milk powder in PBS. First antibodies were diluted in 10% w/v BSA in PBS, and incubations were overnight at room temperature in a humid chamber. Subsequently, slides were washed (3x10 minutes) in PBS, blocked in 10% v/v normal goat serum (Sigma) in blocking buffer (supernatant of 5% w/v milk powder in PBS centrifuged at 14000 rpm for 10 minutes), and incubated with secondary antibodies in 10% normal goat serum in blocking buffer at room temperature for 2 hours. Finally, slides were washed (3x10 min) in PBS (in the dark) and embedded in Vectashield containing DAPI to counterstain the DNA (Vector Laboratories, Burlingame, CA, USA). When Alexa 350-labelled second antibody was present on the slides, Vectashield without DAPI was used. Fluorescent images were observed using a fluorescent microscope (Axioplan 2, Carl Zeiss, Jena, Germany) equipped with a digital camera (Coolsnap-pro; Photometrics, Waterloo, Canada). Digital images were processed using Adobe Photoshop software (Adobe Systems).

FISH

Following immunocytochemistry, the position of selected nuclei on the slide was determined, and FISH was performed to detect the X or Y chromosomes using STAR*FISH mouse whole chromosome-specific paints (1200XmCy3 and 1200YmCy3; Cambio, Cambridge, UK) according to the manufacturer's protocol. All fluorescent signals obtained after immunocytochemistry had disappeared after FISH. To make sure that remaining signal from immunocytochemistry is not mistaken for a FISH signal, the color of the fluorescent dye for FISH differs from the color of the fluorescent dye coupled to the second antibody that was used to visualize ubi-H2A or Rad18. If specific signal was not obtained, the procedure was performed for a second time, and this always resulted in a positive signal in the majority of nuclei. Specificity of hybridization was confirmed using male meiotic spread nuclei preparations; positive signal colocalized with the XY body of pachytene spermatocytes (not shown). Since the X and Y chromosome probes are labeled with the same fluorescent dye, and both probes were used on the same slide in subsequent experiments (first the X chromosome probe, then the Y chromosome probe), some X-chromosomal signal remains visible after the second FISH with the Y-chromosomal probe.

To localize telomeres, a TRITC-labeled peptide nuclei acid probe directed against mouse telomeres (gift from M. Zijlmans, Rotterdam, The Netherlands) was used to identify telomeres in spread nuclei of spermatocytes. Meiotic spread nuclei preparations were denatured in 70% v/v deionized formamide in 2xSSC at 72°C for 2.5 min, followed by dehydration with ethanol. Slides were air-dried, and 20 μ l of denatured probe (0.3 μ g/ml) in hybridization mix (70% v/v deionized formamide, 10 mM Tris-HCl pH7.0, 0.25% w/v blocking reagent (DuPont/NEN, Boston, USA; stock 1% w/v in 40 mM Tris-HCl pH7.0) was applied. Hybridization

was carried out under a coverslip in a humid chamber for 2 h in the dark at room temperature, followed by sequential washing in 70% v/v formamide, 10 mM Tris-HCl pH 7.0, 0.1% w/v BSA (2x15 min) and 0.1 M Tris-HCl pH 7.0, 0.15 M NaCl, 0.08 % v/v Tween-20 (3x5 min). Subsequently, immunocytochemistry using the anti-ubi-H2A monoclonal antibody was carried out as described above. Digital images were obtained and processed as above. FISH images were combined with immunocytochemical images using Adobe Photoshop software (Adobe Systems), and alignment was obtained by alignment of non-specific signals present in both images. In addition, in some cases, the red fluorescent FISH signal was converted to white to obtain better contrast.

Immunohistochemistry

Kidney and liver tissues were isolated from male and female adult rats (Wistar) and fixed in phosphate-buffered formalin (30 mM NaH₂PO₄, 45 mM Na₂HPO₄, 4% v/v formaldehyde, pH 6.8) for 6-18 hours at 4°C, dehydrated, and embedded in paraffin. 8 µm sections were collected on 3-aminopropyltriethoxysilane-coated (Sigma) slides and dried overnight. After deparaffinization, endogenous peroxidase was blocked by incubation in 3% v/v H₂O₂ for 20 minutes, followed by a rinse with tap water. Then the slides were incubated for 20 minutes in a microwave oven at 1000 Watts in 0.01 M citric acid, pH 6.0. The slides were allowed to cool down and washed with distilled water and PBS. The slides were blocked for 20 minutes in PBS with 0.5% w/v BSA and 0.5% w/v nonfat milk, and incubated with anti-ubi-H2A (diluted 1:10 in 10% BSA in PBS) overnight at room temperature. Subsequently, the slides were washed in PBS and incubated for 1 hour at room temperature with the second antibody (biotinylated goat anti-mouse; DAKO, Glostrup, Denmark) which was diluted 1:200 in PBS containing 2% v/v normal goat serum. The antibody-antigen complexes were detected by incubation for 30 minutes with avidin-biotin complex reagent (DAKO) according to the protocol supplied by the manufacturer, followed by staining with 3,3'-diaminobenzidine tetrahydrochloride (DAB)/Metal concentrate (Pierce, Rockford, IL, USA), counterstaining with haematoxylin, and mounting.

Results

Ubi-H2A is present in the XY body of mouse, rat, and man

The monoclonal anti-ubi-H2A IgM antibody binds ubiquitinated H2A on one dimensional SDS PAGE gels (Baarends et al., 1999; Vassilev et al., 1995). To verify specificity, we performed Western blot analyses (Figure 1A). Anti-ubi-H2A recognizes one clear spot, corresponding to the expected localization of ubi-H2A, but no signal corresponding to ubi-H2B is detected.

In meiotic spread nuclei, the degree of synapsis of homologous chromosomes can be determined with an antibody that recognizes Sycp3, a component of the axial/lateral elements of the synaptonemal complex (SC) (Lammers et al., 1994). Using this marker, the leptotene, zygotene, pachytene, and diplotene substages of meiotic prophase can be detected. At pachytene, all autosomal bivalents have fully synapsed, and the XY body has become a prominent structure. These spread nuclei are prepared in such a way that only chromatin-associated proteins are maintained, and ubi-H2A shows marked localization to the XY body (Figure 1B). In addition, nuclear foci with lower signal intensity are observed in late pachytene and

early diplotene nuclei, and a significant fraction of these foci colocalize with (near) telomeric regions (Figure 1B, inserts; and 1C). As a control for specificity of the antibody on meiotic spreads nuclei of spermatocytes, we looked at colocalization between anti-ubiquitin and anti-ubiH2A. In accordance with the presence of ubi-H2A in the XY body, there is intense staining of ubiquitin in the XY body, and a lower overall staining of the nucleus, most likely due to the presence of other ubiquitinated proteins (Figure 1B, C). Ubi-H2A also marked the XY body of rat and human spermatocytes (Figure 1D), indicating that H2A ubiquitination is an evolutionary conserved feature of XY body chromatin.

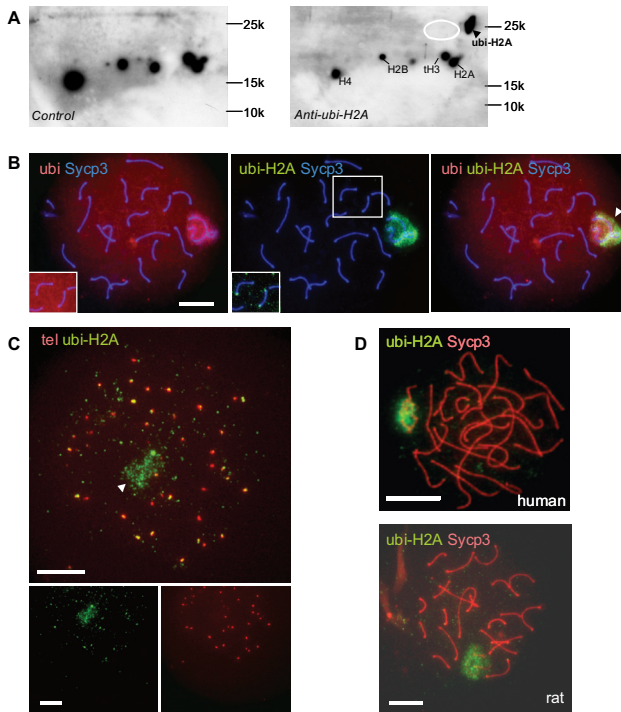


Figure 1. Ubi-H2A marks the XY body and telomeres of pachytene spermatocytes. A: Western blots of basic nuclear proteins separated on AUT SDS-PAGE 2-D gels (first dimension AUT and second dimension SDS-PAGE) were stained with anti-ubi-H2A (right panel), or with second antibody only (Control, left panel). A specific signal is detected at the expected position for ubiquitinated histone H2A (ubi-H2A; arrowhead). The approximate positions of histones H2A, H2B, th3, and H4 are indicated for reference. Positions and molecular weights (k) of marker proteins are indicated. The expected approximate position of ubi-H2B is indicated by the white ellipse, and the blots are overexposed to show that no ubi-H2B is detected. B: Spermatocyte spread nucleus from wild type mice stained with a mouse monoclonal IgG antibody against Sycp3 (blue), a rabbit polyclonal anti-ubiquitin antibody (ubi; red), and a mouse monoclonal IgM antibody against ubiquitinated H2A (ubi-H2A; green). Both ubi and ubi-H2A mark XY body chromatin (arrowhead in right panel, showing the merged signals). Anti-ubi also detects other ubiquitinated proteins associated with chromatin in the rest of the nucleus. Upon overexposure, ubi and ubi-H2A are detected at the ends of some synaptonemal complex axes (inserts). C: FISH analysis of telomeres (tel; red) followed by immunocytochemistry with anti-ubi-H2A (ubi-H2A; green) of an early diplotene cell. Diplotene is identified by presence of a low level of ubi-H2A in the XY body (arrowhead), and the high number of telomeric foci (more than 40, with double foci still attached counted as one) and splitting of telomeres. The left panel shows that around 30 telomere foci colocalize, at least partially, with ubi-H2A. A total number of approximately 100 ubi-H2A foci is observed outside the XY body area, indicating that chromatin regions other than XY body and telomeres also accumulate ubi-H2A. The right panels show lower magnification images of the single fluorescent signals. D: Spermatocyte spread nuclei from rat and human stained with anti-Sycp3 (red), and anti-ubi-H2A (ubi-H2A; green). ubi-H2A marks XY body chromatin in both species. All scale bars represent 20 μm .

Ubi-H2A marks the Barr body in female somatic cells

Since the XY body is transcriptionally silent, these data suggest that ubiquitinated H2A could be a general feature of inactive chromatin domains. In female somatic cells, one of the two X chromosomes becomes inactivated to accomplish dosage compensation. This mechanism ensures that in male as well as female cells, only one X chromosome is active. In 1949 the inactive X chromosome in female somatic cells was recognized for the first time and named "Barr body" (Barr and Bertram, 1949). We studied the accumulation of ubi-H2A in male versus female somatic cells, to determine whether ubi-H2A localized to the Barr body. Immunohistochemical staining of kidney sections from adult male and female rats revealed a marked nuclear spot of ubi-H2A accumulation, only in female cells (Figure 2A). In addition, in female liver cells, that contain many polyploid cells, we often observed two spots (Figure 2B). Finally, in meiotic spread preparations of XO, XY (sex reversed) and XX female fetal ovaries (see experiments described below), somatic pre-granulosa cells were also present, and in these preparations, we observed a single ubi-H2A spot exclusively in pre-granulosa cells from fetal XX ovaries (Figure 2C).

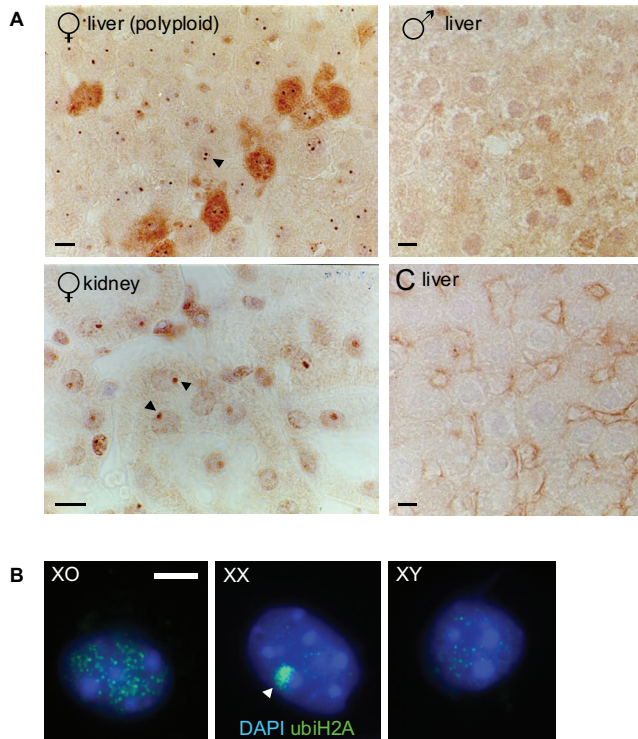


Figure 2: Ubi-H2A marks the inactive X chromosome (Barr body) in female somatic cells. A: Immunohistochemical analysis of ubi-H2A localization in rat female liver and kidney sections, and in male liver sections. Control (C liver): incubation without first antibody. In female nuclei only, high level accumulation of ubi-H2A is seen as a single nuclear spot (arrowhead). In addition, two spots are often observed in polyploid female liver nuclei (arrowhead). These spots are not observed in male tissues. Scale bars represent 10 μm . B: Immunocytochemical detection of ubi-H2A in XO, XX, and XY^{tdym1} XO pre-granulosa cells. Only the XX pre-granulosa cells accumulate ubi-H2A in a single large spot in the periphery of the nucleus (arrowhead). Scale bar represents 20 μm .

Ubi-H2A localizes to unpaired and silenced chromatin regions in male meiotic prophase

To study the relation between accumulation of ubiquitinated H2A, homologous chromosome pairing, and silencing of DNA during meiotic prophase, we studied a male mouse model that carries two different but nearly identical translocations between chromosomes 1 and 13, named T(1;13)70H/T(1;13)1Wa (abbreviated as T/T'). A small difference in the location of the translocation breakpoints causes the two 1¹³ and 13¹ homologs to be not fully identical, and this leads to a pairing problem during meiotic prophase (de Boer et al., 1986; Peters et al., 1997a). The degree of synapsis that is achieved varies among nuclei, and also between animals. The percentage of spermatocyte nuclei with complete synapsis of all bivalents positively correlates with fertility. In particular the small 1¹³ bivalent often remains only partially synapsed. To study ubi-H2A localization on the small translocation bivalent in pachytene spermatocyte nuclei, we selected the nuclei that showed normal morphology of the synaptonemal complex and accumulation of ubi-H2A in the XY body. The morphology of the 1¹³ bivalent was classified as Partially synapsed Rest (PR, low degree of synapsis), Partially synapsed A shape (PA, intermediate degree of synapsis), Partially synapsed Horseshoe shape (PH, almost complete synapsis), and Completely Synapsed (CS). On incompletely synapsed PR/PA bivalents, we found ubi-H2A accumulation in 19 out of 26 nuclei, whereas for the PH/CS bivalents only 6 out of 30 nuclei showed accumulation of ubi-H2A. Overall, the fraction of nuclei with ubi-H2A positive 1¹³ bivalents decreases with an increasing degree of synapsis (Figure 3).

RNA polymerase II immunolocalization was used as a marker for transcriptionally active chromatin. The signal to noise ratio for this antibody is optimal in late pachytene and early diplotene cells. Analysis of the RNA polymerase II signal covering the 1¹³ translocation bivalent in spermatocyte nuclei from the T/T' mice revealed a positive correlation between fluorescent signal and degree of nonhomologous synapsis. Of 23 nuclei analyzed, three 1¹³ translocation bivalents showed complete nonhomologous synapsis (CS configuration), as well as a high level of RNA polymerase II immunoexpression on chromatin covering the 1¹³ bivalent. This was also observed for one out of nine nuclei with near complete synapsis (PH configuration). The rest of the partially synapsed 1¹³ translocation bivalents (19 PH, PA and PR nuclei) showed no (11 nuclei) or a low level (8 nuclei) of RNA polymerase II immunoexpression. This indicates that the incompletely synapsed 1¹³ bivalent is at least partially transcriptionally silenced (not shown).

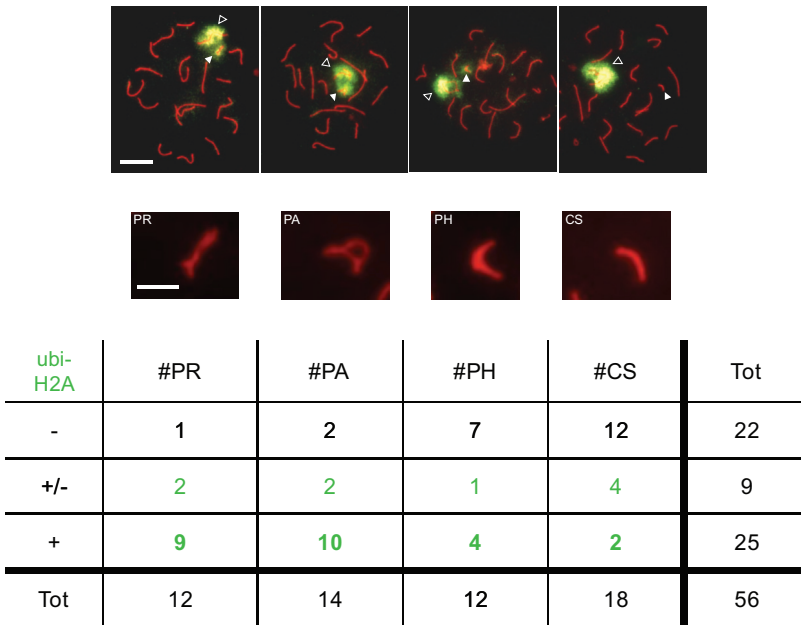


Figure 3: The ubi-H2A signal on the 1¹³ translocation bivalent of T/T' spermatocytes disappears when there is complete synapsis. The top row panels show four T/T' pachytene spermatocyte spread nuclei stained with anti-ubi-H2A (green) and anti-Sycp3 (red). The closed arrowheads indicate the location of the 1¹³ bivalent, at different positions respective to the XY body (open arrowheads). Scale bar represents 20 μ m. The images in the second row panels represent the four defined groups of 1¹³ synapsis morphologies, detected with anti-Sycp3 staining and shown at higher magnification (scale bar represents 5 μ m). PR, partially synapsed rest; PA, partially synapsed A-shape; PH, partially synapsed horseshoe shape; CS, complete synapsis. The table shows that an increasing fraction of 1¹³ bivalents is ubi-H2A negative when synapsis is more complete. Absolute numbers of scored nuclei with: no ubi-H2A signal (-), low ubi-H2A signal (+/-), or clear ubi-H2A signal (+) are indicated. Tot, total number of nuclei counted.

Another marker of transcriptionally silenced unsynapsed chromatin regions is phosphorylated H2AX (γ -H2AX). This modification occurs in response to DNA double strand breaks in somatic cells, and is also associated with meiotic double strand breaks (Mahadevaiah et al., 2001; Rogakou et al., 1998). Furthermore, it has been shown that accumulation of γ -H2AX in the chromatin of the X and Y chromosomes during male meiotic prophase in mouse is a prerequisite for XY body formation (Fernandez-Capetillo et al., 2003). Previously, it has been shown that γ -H2AX also accumulates on the partially synapsed 1¹³ bivalent in T/T' mice (Mahadevaiah et al., 2001). Triple immunostainings of meiotic nuclei from T/T' mice with anti- γ -H2AX, anti ubi-H2A, and anti-Sycp3 revealed that 1¹³ bivalents that accumulate ubi-H2A also show an increase in γ -H2AX staining (Figure 4A). However, γ -H2AX accumulation on XY body chromatin as well as on the chromatin of the 1¹³ bivalent is often observed in the absence of ubi-H2A (Figure 4B). This may be due to the fact that γ -H2AX accumulates earlier during meiotic prophase, and persists longer than ubi-H2A.

In *S. cerevisiae*, the E2 enzyme RAD6 and the E3 enzyme RAD18 are key factors in a mechanism that tolerates presence of DNA damage during DNA replication. In this so-called Replicative Damage Bypass (RDB) mechanism (Lawrence, 1994; van der Laan et al., 2004), RAD6 interacts with RAD18 (Bailey et

al., 1994). RDB does not require histone H2B ubiquitination (Robzyk et al., 2000). We have identified the mouse *Rad18* gene, and *Rad18* mRNA expression was shown to be highly elevated in mouse testis, in particular in primary spermatocytes in meiotic prophase (van der Laan et al., 2000). The Rad18 protein was found to be present in a relatively high concentration in the XY body of these primary spermatocytes, at several subsequent steps of meiotic prophase (van der Laan et al., in preparation). In addition, the ubiquitin ligase Rad18 also localizes to the unsynapsed 1^{13} bivalent in pachytene spermatocytes of T/T' mice (van der Laan et al., in preparation). Triple immunostaining with anti-ubi-H2A, anti-Rad18, and anti-Sycp3 revealed colocalization of Rad18 and ubi-H2A on the XY body and on the partially synapsed translocation bivalents in most nuclei (Figure 4D). It appears that during male meiotic prophase, Rad18 accumulation, similar to γ -H2AX, precedes that of ubi-H2A, and Rad18 also remains present in early diplotene nuclei, when ubi-H2A staining has disappeared. Overall, the immunofluorescent Rad18 signal is more intense than that of ubi-H2A. Therefore, lack of colocalization of Rad18 and ubi-H2A in some nuclei is most likely due to differences in timing and level of accumulation of the two proteins.

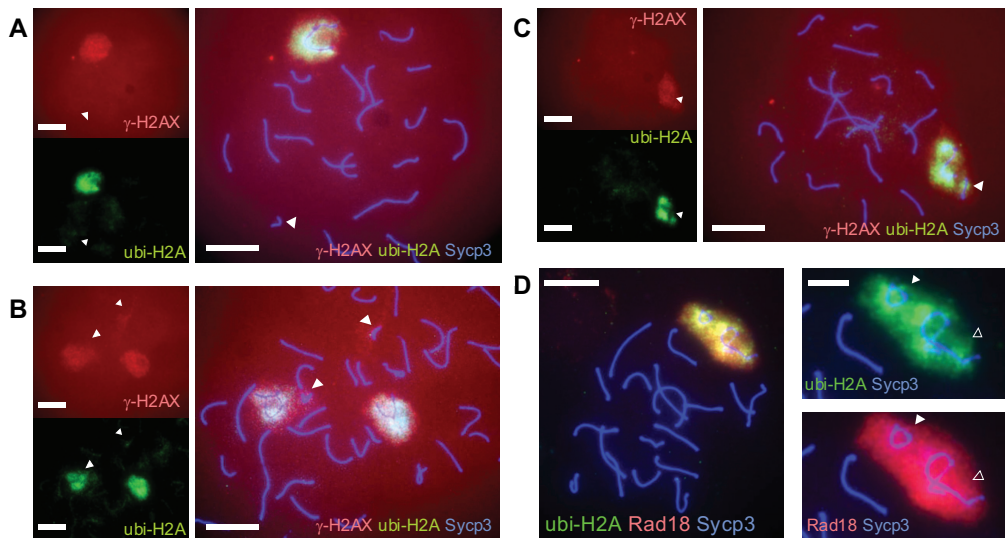


Figure 4: Ubi-H2A, γ -H2AX and Rad18 colocalize in unsynapsed chromatin regions of late pachytene spermatocytes. A: Triple immunostaining of a T/T' pachytene spermatocyte spread nucleus with anti- γ -H2AX (red), anti-ubi-H2A (green) and anti-Sycp3 (blue). Left panels show single immunostainings (lower magnification), and the right panel shows the triple immunostaining (higher magnification). Both γ -H2AX and ubi-H2A accumulate on the XY body, but not on the completely synapsed 1^{13} bivalent. B: As in A, but part of two spread nuclei is shown. γ -H2AX, but not ubi-H2A, accumulates on partially synapsed 1^{13} bivalents (PA and PH group, indicated with PA and PH). C: As in A, but this spread nucleus shows accumulation of both γ -H2AX and ubi-H2A on the partially synapsed 1^{13} bivalent (PA group). D: The left panel shows triple immunostaining of a T/T' pachytene spermatocyte spread nucleus with anti-Sycp3 (blue), anti-Rad18 (red), and anti-ubi-H2A (green). Scale bar represents 20 μ m. The right panels show a higher magnification (scale bar represents 10 μ m) of the ubi-H2A/Sycp3 and the Rad18/Sycp3 double staining of XY body and PA group 1^{13} bivalent. All scale bars represent 20 μ m, unless otherwise indicated. Open arrowheads point to the XY body and closed arrowheads to the 1^{13} bivalent.

Ubi-H2A accumulates on unsynapsed chromosomal regions in XY and XO oocytes

In XO females, the single X chromosome remains unpaired during meiotic prophase. In XY^{tdmy} mice, the sex determining gene *Sry* is deleted, and therefore all these animals develop as females (Lovell-Badge and Robertson, 1990). During the meiotic prophase in embryonic ovaries of XY^{tdmy} mice, the X and Y chromosomes pair in approximately 19% of the cells, but no XY body-like structure has been observed (Turner et al., 2000). In pachytene oocytes from these XO and XY^{tdmy} mice, we found accumulation of ubi-H2A and Rad18 in a single subnuclear region in a large fraction of cells (Figure 5A, B; Table I). FISH analysis was used to detect the X and Y chromosomes. For Rad18 and ubi-H2A, immunoeexpression colocalized with the X-chromosome signal in approximately 50% of XY pachytene oocyte nuclei (n=14 for each antibody). In the same group of nuclei, the univalent Y chromosome signal colocalized with immunoeexpression of Rad18 and ubi-H2A, when Rad18 was absent from the X chromosome. In some nuclei, the X and Y chromosome are partially synapsed. In this situation, the immunoeexpression covered both sex chromosomes, or mainly localized to the X chromosome (Figure 5A). We observed one nucleus with accumulation of ubi-H2A on both sex chromosomes, while X and Y were clearly separated (not shown). In XO oocytes, Rad18 immunoeexpression colocalized with the X chromosome in all nuclei analyzed (not shown). Local accumulation of Rad18 and ubi-H2A is rarely detected in XX oocytes. If present, the signal covers chromatin that shows aberrant SC patterns indicating partial synapsis or heterologous synapsis (Figure 5C). Double immunostaining of XY and XO oocytes using anti-ubiH2A and anti-Rad18 showed that Rad18 signal is observed in a larger percentage of the nuclei (Table 1), but ubi-H2A always colocalizes with Rad18.

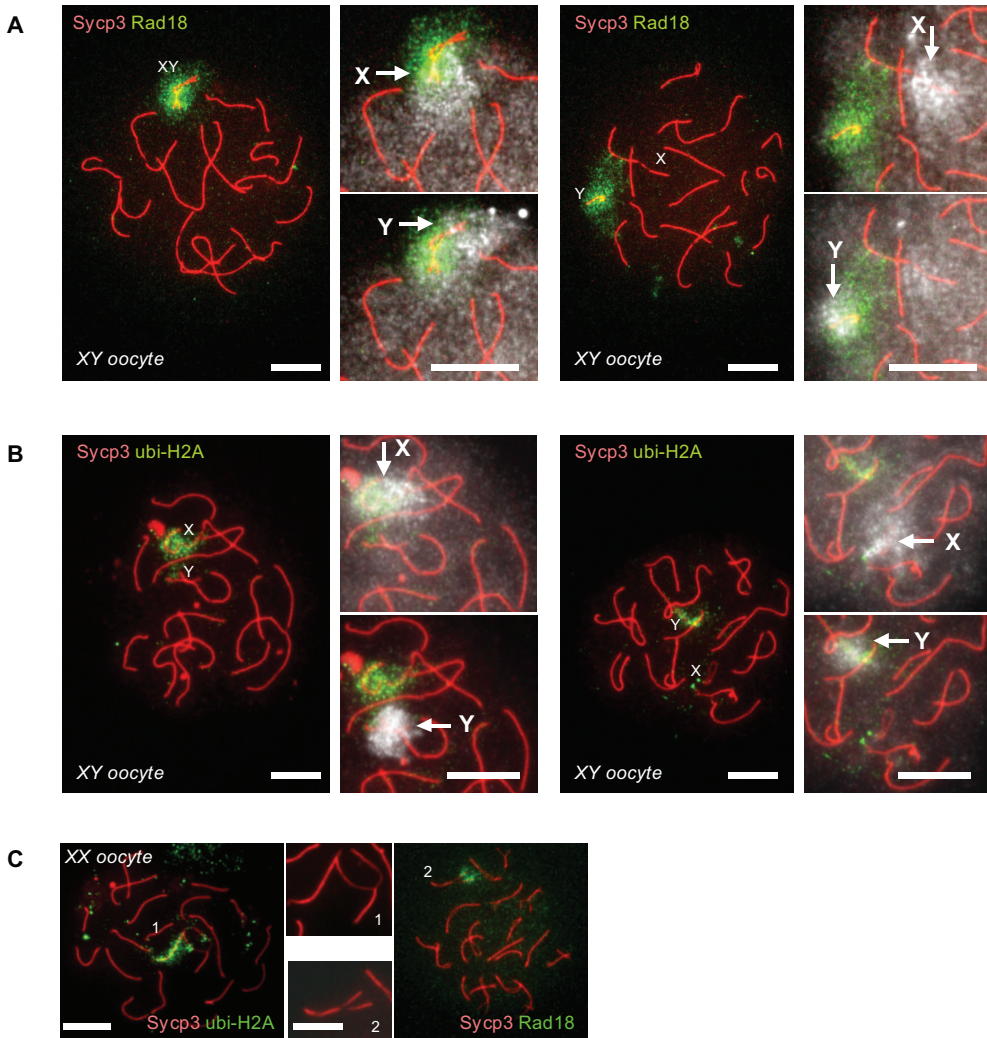


Figure 5: Ubi-H2A and Rad18 mark unsynapsed chromosome regions in oocytes. A: Two XY oocyte spread nuclei immunostained with anti-Rad18 (green) and anti-Sycp3 (red). The location of the X (X) and Y chromosomes (Y) is indicated. The smaller panels to the right of each nucleus show enlargements of the X and Y chromosomal areas with the white FISH signals for either X (top, arrow) or Y (bottom, arrow). In the nucleus shown on the left, X and Y are partially synapsed and Rad18 mainly accumulates on X-chromosomal chromatin. In the nucleus shown on the right, X and Y have separated, and Rad18 accumulation is observed only on the Y chromosome. Note that some X-FISH signal is still visible after Y-FISH (see Materials and Methods). B: Two XY oocyte spread nuclei immunostained with anti-ubi-H2A (green) and anti-Sycp3 (red). The smaller panels to the right of each nucleus show enlargements of the X and Y chromosomal areas with the white FISH signals for either X (top, arrow) or Y (bottom, arrow). In both nuclei, X and Y have separated, but ubi-H2A marks the X chromosome in the left panel and the Y chromosome in the right panel. C: XX oocyte spread nucleus immunostained with anti-Sycp3 (red) and either anti-ubi-H2A (left panel; green) or anti-Rad18 (right panel; green). The two images in the middle show enlargements (scale bar represents 10 μm) of the aberrant synaptonemal complex morphology (Sycp3 staining) in the respective ubi-H2A (1) and Rad18 (2) positive regions. All scale bars represent 20 μm unless otherwise indicated.

Incomplete chromosome synapsis leads to transcriptional silencing in oocytes

Similar to the observed silencing of unpaired chromatin regions in T/T' spermatocytes, we found that the immunoeexpression of RNA polymerase II in XO and XY oocytes was frequently lower in an area covering the single X and/or Y chromosome, as determined by presence of thinner SC axes (Figure 6A). In addition, co-immunostaining of anti-Rad18 and anti-RNA polymerase II of XY and XO oocytes revealed that areas with lower RNA-polymerase II immunoeexpression colocalized with regions of intense Rad18 signal (Figure 6B). In accordance with these data, colocalization of ubi-H2A with γ -H2AX was observed (Figure 6C). Based on γ -H2AX accumulation as a marker for transcriptional silencing, it appears that X and/or Y do not undergo silencing in all pachytene oocytes (Table 1).

	XO	XY
ubi-H2A	37 (18.5%)	73 (36.5%)
Rad18	104 (52%)	119 (59.5%)
γ -H2AX	93 (46.5%)	140 (70%)

Table 1: Immunoeexpression of ubi-H2A, Rad18, and γ -H2AX in XO and XY pachytene oocytes. Numbers (and percentages) of nuclei with a single positive staining area (200 nuclei were counted for each antibody and genotype).

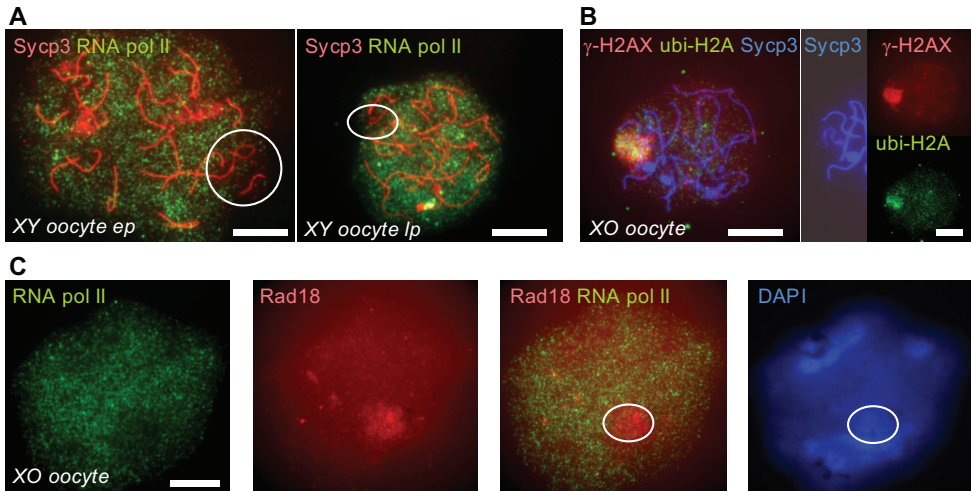


Figure 6: Transcriptional repression of XY chromosomes in XO and XY^{tdym1} oocytes. A: Early (ep) and late (lp) pachytene spermatocyte spread nuclei immunostained with anti-Sycp3 (red) and anti-RNAPolIII (green). The area with unsynapsed synaptonemal complex axes and low RNAPolIII immunoeexpression is encircled. B: Pachytene XO oocyte spread nucleus with accumulation of γ -H2AX (red) and ubi-H2A (green) on the unsynapsed X chromosome. Immunostaining of Sycp3 is shown in blue. The middle panel shows the region that contains the unsynapsed X chromosome. The panels on the right show the single γ -H2AX (red) and ubi-H2A (green) immunostainings. C: The four panels show one XO oocyte spread nucleus. RNA polIII immunoeexpression (green) is relatively low in regions with intense DAPI staining (blue) and in addition in a Rad18 positive region (red). This region is encircled in the merge and DAPI panels. All scale bars represent 20 μ m.

Discussion

Histone H2A and H2B ubiquitination

Ubiquitination of H2B in yeast is involved in gene activation, as it takes part in trans-histone control of trimethylation of H3 at lysines 4 and 79 (Daniel et al., 2004). Paradoxically, H2B ubiquitination is also required for gene silencing. It has been suggested that, when H2B ubiquitination is inhibited, reduced formation of active chromatin leads to loss of silencing proteins from regions that are normally heterochromatic (Henry et al., 2003). In addition, H2B ubiquitination is necessary for sporulation (Robzyk et al., 2000). In yeast, ubiquitination of H2A has not been shown, and site-directed mutagenesis of the putative ubiquitination site of H2A revealed no phenotype (Swerdlow et al., 1990). The function of histone ubiquitination in mammalian cells is unknown. The data presented in this manuscript show for the first time that ubi-H2A generally marks inactive chromatin regions in mammalian cells.

In XX pre-granulosa cells, we see accumulation of ubi-H2A on the Barr body of most but not all nuclei. It has been shown that a general deubiquitination of histones precedes mitosis, followed by re-ubiquitination in the daughter cells. This may explain why a proportion of the nuclei show no Barr body-associated ubi-H2A accumulation.

In the present study, we observed accumulation of ubi-H2A on the Barr body. It has been shown that a general deubiquitination of histones precedes mitosis, followed by re-ubiquitination in the daughter cells (Matsui et al., 1979; Wu et al., 1981). This may explain why a proportion of the nuclei show no Barr body-associated ubi-H2A accumulation.

Inactivation of one of the two X chromosomes in female somatic cells during embryonic development requires a functional Xist locus. However, Xist function is not essential for inactivation of the X and Y chromosomes during the male meiotic prophase (Turner et al., 2002). Therefore, the mechanisms of Barr body formation and XY body formation are essentially different. However, parts of these two inactivation mechanisms may still overlap. Increased methylation of H3 at lysines 9 and/or 27 is a relatively early event in somatic X inactivation, and has also been reported for the XY body (Mermoud et al., 2002; Peters et al., 2001; Plath et al., 2003). In addition, macroH2A1 variants are enriched in the Barr body and the XY body (Costanzi and Pehrson, 1998; Hoyer-Fender et al., 2000).

In the XY body of mouse spermatocytes, ubiquitination of H2A appears to be a relatively late event, as compared to accumulation of γ -H2AX and Rad18. This finding may indicate that ubi-H2A is not involved in the formation of silent chromatin, but rather in the maintenance of the inactive chromatin state.

We also found increased ubiquitination of H2A at silent chromatin regions of telomeric sites in late pachytene and early diplotene spermatocyte nuclei. Focal sites of ubi-H2A formation in other unidentified regions of the nuclei are also apparent.

Together, these data indicate that ubi-H2A marks several regions of silent chromatin, although it needs to be emphasized that not all silent chromatin carries the ubi-H2A mark. It will be of interest to study the relation between H2A ubiquitination and other histone modifications, to obtain more insight in possible roles of H2A ubiquitination in regulation of the histone code in vertebrates.

In this report we show that Rad18, another ubiquitin ligase that can associate with Ube2a/b, colocalizes with ubi-H2A in meiotic cells. In yeast, mutation of

RAD18 does not lead to defects in histone ubiquitination (Sun and Allis, 2002). Rather, RAD18 is thought to function specifically in replicative damage bypass, a mechanism that allows replication of damaged DNA. Based on these findings in yeast, functional involvement of Rad18 in histone ubiquitination in mouse is not expected, but it cannot be formally excluded. It appears more likely that Ube2a/b, together with Rad18 acts to ubiquitinate an as yet unknown protein substrate that might be functionally involved in silencing of unpaired DNA, as described below.

The present findings show reduced levels of RNA polymerase II and increased accumulation of the XY body markers γ -H2AX, Rad18 and ubi-H2A, on unsynapsed chromatin regions in spermatocytes and oocytes. We conclude that meiotic prophase cells are capable of detecting unpaired chromatin regions, and that this activates a mechanism leading to transcriptional silencing.

Meiotic Silencing of Unpaired DNA (MSUD) in mammalian meiosis

Recent data have pointed to the existence of a general mechanism that leads to meiotic silencing of unpaired DNA (MSUD) in *N. crassa* (Shiu and Metzberg, 2002; Shiu et al., 2001) and *C. elegans* (Bean et al., 2004). This mechanism is thought to have evolved as part of a genome surveillance system that is operative in mitotic and meiotic cells. The idea is that foreign DNA (transposon, virus), or translocated DNA, can be recognized because these sequences will not have a pairing partner during the meiotic prophase. The capacity of the cell to detect unpaired DNA can be viewed as a means to trace foreign or translocated DNA, and subsequent silencing of such DNA may render it harmless. For *C. elegans*, it has been shown that multiple copies of a transgene are often silenced during meiosis (Kelly and Fire, 1998). In addition, the X chromosome of XO *C. elegans* males is silenced during the meiotic prophase, and an epigenetic modification is maintained as an imprint during fertilization and subsequent embryo development (Bean et al., 2004; Kelly et al., 2002). Since the presence of a single X chromosome is the normal situation in male *C. elegans* worms, it appears that MSUD has been adapted to cope with the heterologous nature of sex chromosomes.

Herein, we provide evidence that MSUD also occurs during male and female meiosis in mice. This sheds new light on the evolutionary origin of the XY body. In essence, the mammalian XY body appears to be an example of naturally occurring MSUD. In addition, the XY body requires specialized mechanisms to ensure that the sex chromosomes pair and recombine, but only in the PARs.

It remains to be determined to what extent the molecular mechanisms of MSUD in *N. crassa*, *C. elegans*, and mouse are evolutionarily conserved. For *N. crassa*, components of the RNAi machinery are necessary to achieve MSUD, and it occurs at the single gene level (Hynes and Todd, 2003). Since we have shown in this report that transcriptional inactivation of the 1¹³ bivalent in T/T' mouse spermatocytes depends on the degree of desynapsis, there may be a threshold length of unpaired DNA that is required to activate MSUD.

An early and detailed investigation of monovalent translocation chromosomes closely associated with the XY body in pachytene spermatocytes, in combination with analysis of transcriptional activity, showed that these regions contained residual transcriptional activity, that is not present in normal XY bodies (Speed, 1986). Such residual transcriptional activity may signify that XY silencing precedes silencing of other unpaired chromatin. This would be in accordance with the finding that γ -H2AX and also Rad18 are found exclusively on the XY body in some T/T' nuclei, whereas accumulation on the 1¹³ bivalent is always detected in

association with enhanced levels in the XY body of γ -H2AX and Rad18.

Alternatively, silencing of aberrant unpaired chromatin in meiotic prophase might be less effective than XY silencing in a normal XY body. We found that Rad18 and ubi-H2A often accumulate only on the X or the Y chromosome in XY^{tdym1} oocytes, and no such accumulation was observed in approximately 50% of the nuclei. This was also observed for the single X in XO oocytes. These findings would be in agreement with a more solid inactivation of XY in the XY body, as compared to inactivation of other unpaired chromatin regions.

In addition, unpaired chromatin regions may undergo self-synapsis or heterologous synapsis, which could lead to an escape from a MSUD mechanism.

Our findings suggest that XY body formation is related to MSUD, a process in *N. crassa* that uses proteins that function in RNAi. For formation of the Barr body, noncoding RNAs from the Xist locus are essential. Thus, another similarity between Barr body and XY body formation could be the involvement of non-coding RNAs, derived from the Xist locus to initiate Barr body formation, and from an unknown site for XY body formation. The XY body and the Barr body have recently been shown to be functionally related in a different sense, more in terms of a father to daughter relation. Meiotic X inactivation may generate an epigenetic imprint that is carried on to the next generation, evidenced by preferential inactivation of Xp (the paternal X) in early female mouse embryos. Later during gestation, this inactivation is reversed in cells of the inner cell mass, and random X inactivation occurs (Huynh and Lee, 2003; Mak et al., 2004; Okamoto et al., 2004). From this perspective, it will be of interest to study H2A ubiquitination during early embryonic development.

Acknowledgements

We are very thankful to Dr. Paul Burgoyne and Dr. Shanti Mahadevaiah for their XY^{tdym1} and XO mice, Dr. Christa Heyting (Wageningen University, The Netherlands) for the anti-Sycp3 antibodies, and Dr. Mark Zijlmans (Erasmus MC Rotterdam, The Netherlands) for the telomere probe. This work was supported by the Dutch Science Foundation (NWO) through GB-MW (Medical Sciences), and by the Dutch Cancer Society (EUR 99-2003).

References

- Baarends, W. M., Hoogerbrugge, J. W., Roest, H. P., Ooms, M., Vreeburg, J., Hoeijmakers, J. H. J., and Grootegoed, J. A.** (1999). Histone ubiquitination and chromatin remodeling in mouse spermatogenesis. *Dev. Biol.* **207**, 322-333.
- Bailly, V., Lamb, J., Sung, P., Prakash, S., and Prakash, L.** (1994). Specific complex formation between yeast RAD6 and RAD18 proteins: a potential mechanism for targeting RAD6 ubiquitin-conjugating activity to DNA damage sites. *Genes Dev* **8**, 811-820.
- Barr, M. L., and Bertram, E. G.** (1949). A morphological distinction between neurones of the male and female, and the behaviour of the nucleolar satellite during accelerated nucleoprotein synthesis. *Nature* **163**, 676-677.
- Bean, C. J., Schaner, C. E., and Kelly, W. G.** (2004). Meiotic pairing and imprinted X chromatin assembly in *Caenorhabditis elegans*. *Nat Genet* **36**, 100-105.
- Briggs, S. D., Xiao, T., Sun, Z. W., Caldwell, J. A., Shabanowitz, J., Hunt, D. F., Allis, C. D., and Strahl, B. D.** (2002). Gene silencing: trans-histone regulatory pathway in chromatin. *Nature* **418**, 498.

- Chen, H. Y., Sun, J. M., Zhang, Y., Davie, J. R., and Meistrich, M. L.** (1998). Ubiquitination of histone H3 in elongating spermatids of rat testes. *J. Biol. Chem.* **273**, 13165-13169.
- Costanzi, C., and Pehrson, J. R.** (1998). Histone macroH2A1 is concentrated in the inactive X chromosome of female mammals. *Nature* **393**, 599-601.
- Daniel, J. A., Torok, M. S., Sun, Z. W., Schieltz, D., Allis, C. D., Yates, J. R., 3rd, and Grant, P. A.** (2004). Deubiquitination of histone H2B by a yeast acetyltransferase complex regulates transcription. *J Biol Chem* **279**, 1867-1871.
- Davie, J. R.** (1982). Two-dimensional gel systems for rapid histone analysis for use in minislab polyacrylamide gel electrophoresis. *Anal. Biochem.* **120**, 276-281.
- de Boer, P., Searle, A. G., van der Hoeven, F. A., de Rooij, D. G., and Beechey, C. V.** (1986). Male pachytene pairing in single and double translocation heterozygotes and spermatogenic impairment in the mouse. *Chromosoma* **93**, 326-336.
- Dover, J., Schneider, J., Boateng, M. A., Wood, A., Dean, K., Johnston, M., and Shilatifard, A.** (2002). Methylation of histone H3 by COMPASS requires ubiquitination of histone H2B by RAD6. *J. Biol. Chem.* **277**, 28368-28371.
- Fernandez-Capetillo, O., Mahadevaiah, S. K., Celeste, A., Romanienko, P. J., Camerini-Otero, R. D., Bonner, W. M., Manova, K., Burgoyne, P., and Nussenzweig, A.** (2003). H2AX is required for chromatin remodeling and inactivation of sex chromosomes in male mouse meiosis. *Dev Cell* **4**, 497-508.
- Henry, K. W., Wyce, A., Lo, W. S., Duggan, L. J., Emre, N. C., Kao, C. F., Pillus, L., Shilatifard, A., Osley, M. A., and Berger, S. L.** (2003). Transcriptional activation via sequential histone H2B ubiquitylation and deubiquitylation, mediated by SAGA-associated Ubp8. *Genes Dev* **17**, 2648-2663.
- Heyting, C.** (1996). Synaptonemal complexes: structure and function. *Curr. Opin. Cell. Biol.* **8**, 389-396.
- Hoyer-Fender, S., Costanzi, C., and Pehrson, J. R.** (2000). Histone macroH2A1.2 is concentrated in the XY-body by the early pachytene stage of spermatogenesis. *Exp Cell Res* **258**, 254-260.
- Huynh, K. D., and Lee, J. T.** (2003). Inheritance of a pre-inactivated paternal X chromosome in early mouse embryos. *Nature* **426**, 857-862.
- Hynes, M. J., and Todd, R. B.** (2003). Detection of unpaired DNA at meiosis results in RNA-mediated silencing. *Bioessays* **25**, 99-103.
- Kelly, W. G., and Fire, A.** (1998). Chromatin silencing and the maintenance of a functional germline in *Caenorhabditis elegans*. *Development* **125**, 2451-2456.
- Kelly, W. G., Schaner, C. E., Dernburg, A. F., Lee, M. H., Kim, S. K., Villeneuve, A. M., and Reinke, V.** (2002). X-chromosome silencing in the germline of *C. elegans*. *Development* **129**, 479-492.
- Lammers, J. H., Offenberger, H. H., van Alderen, M., Vink, A. C., Dietrich, A. J., and Heyting, C.** (1994). The gene encoding a major component of the lateral elements of synaptonemal complexes of the rat is related to X-linked lymphocyte-regulated genes. *Mol Cell Biol* **14**, 1137-1146.
- Lawrence, C.** (1994). The *RAD6* repair pathway in *Saccharomyces cerevisiae*: what does it do, and how does it do it? *BioEssays* **16**, 253-258.
- Lovell-Badge, R., and Robertson, E.** (1990). XY female mice resulting from a heritable mutation in the primary testis-determining gene, *Tdy*. *Development* **109**, 635-646.
- Mahadevaiah, S. K., Turner, J. M., Baudat, F., Rogakou, E. P., de Boer, P., Blanco-Rodriguez, J., Jasin, M., Keeney, S., Bonner, W. M., and Burgoyne, P. S.** (2001). Recombinational DNA double-strand breaks in mice precede synapsis. *Nat Genet* **27**, 271-276.
- Mak, W., Nesterova, T. B., de Napoles, M., Appanah, R., Yamanaka, S., Otte, A. P., and Brockdorff, N.** (2004). Reactivation of the paternal X chromosome in early mouse embryos. *Science* **303**, 666-669.
- Matsui, S., Sandberg, A. A., Negoro, S., Seon, B. K., and Goldstein, G.** (1982). Isopeptidase: a novel eukaryotic enzyme that cleaves isopeptide bonds. *Proc. Natl. Acad. Sci. USA* **79**, 1535-1539.
- Matsui, S. I., Seon, B. K., and Sandberg, A. A.** (1979). Disappearance of a structural chromatin protein A24 in mitosis: implications for molecular basis of chromatin condensation. *Proc. Natl. Acad. Sci. USA* **76**, 6386-6390.
- Mermoud, J. E., Popova, B., Peters, A. H., Jenuwein, T., and Brockdorff, N.** (2002). Histone H3 lysine 9 methylation occurs rapidly at the onset of random X chromosome inactivation. *Curr Biol* **12**, 247-251.
- Monesi, V.** (1965). Differential rate of ribonucleic acid synthesis in the autosomes and sex chromosomes during male meiosis in the mouse. *Chromosoma* **17**, 11-21.
- Okamoto, I., Otte, A. P., Allis, C. D., Reinberg, D., and Heard, E.** (2004). Epigenetic dynamics of imprinted X inactivation during early mouse development. *Science* **303**, 644-649.
- Peters, A. H., O'Carroll, D., Scherthan, H., Mechtler, K., Sauer, S., Schofer, C., Weipoltshammer, K., Pagani, M., Lachner, M., Kohlmaier, A., Opravil, S., Doyle, M., Sibilia, M., and Jenuwein, T.** (2001). Loss of the Suv39h histone methyltransferases impairs mammalian heterochromatin and genome stability. *Cell* **107**, 323-337.
- Peters, A. H., Plug, A. W., and de Boer, P.** (1997a). Meiosis in carriers of heteromorphic bivalents: sex differences and implications for male fertility. *Chromosome Res.* **5**, 313-324.
- Peters, A. H., Plug, A. W., van Vugt, M. J., and de Boer, P.** (1997b). A drying-down technique for the spreading of mammalian meocytes from the male and female germline. *Chromosome Res.* **5**, 66-68.
- Pickart, C. M.** (2004). Back to the future with ubiquitin. *Cell* **116**, 181-190.

- Pickart, C. M., and Cohen, R. E.** (2004). Proteasomes and their kin: proteases in the machine age. *Nat Rev Mol Cell Biol* **5**, 177-187.
- Plath, K., Fang, J., Mlynarczyk-Evans, S. K., Cao, R., Worringer, K. A., Wang, H., de la Cruz, C. C., Otte, A. P., Panning, B., and Zhang, Y.** (2003). Role of histone H3 lysine 27 methylation in X inactivation. *Science* **300**, 131-135.
- Robzyk, K., Recht, J., and Osley, M. A.** (2000). Rad6-dependent ubiquitination of histone H2B in yeast. *Science* **287**, 501-504.
- Roest, H. P., Klaveren van, J., Wit de, J., Gulp van, C. G., Koken, M. H. M., Vermey, M., Roijen van, J. H., Vreeburg, J. T. M., Baarends, W. M., Bootsma, D., Grootegoed, J. A., and Hoeijmakers, J. H. J.** (1996). Inactivation of the HR6B ubiquitin-conjugating DNA repair enzyme in mice causes a defect in spermatogenesis associated with chromatin modification. *Cell* **86**, 799-810.
- Roest, H. P., Baarends, W. M., de Wit, J., van Klaveren, J. W., Wassenaar, E., Hoogerbrugge, J. W., van Cappellen, W. A., Hoeijmakers, J. H., and Grootegoed, J. A.** (2004). The ubiquitin-conjugating DNA repair enzyme HR6A is a maternal factor essential for early embryonic development in mice. *Molecular and Cellular Biology* **In press**.
- Rogakou, E. P., Pilch, D. R., Orr, A. H., Ivanova, V. S., and Bonner, W. M.** (1998). DNA double-stranded breaks induce histone H2AX phosphorylation on serine 139. *J Biol Chem* **273**, 5858-5868.
- Shiu, P. K., and Metzberg, R. L.** (2002). Meiotic silencing by unpaired DNA: properties, regulation and suppression. *Genetics* **161**, 1483-1495.
- Shiu, P. K., Raju, N. B., Zickler, D., and Metzberg, R. L.** (2001). Meiotic silencing by unpaired DNA. *Cell* **107**, 905-916.
- Speed, R. M.** (1986). Abnormal RNA synthesis in sex vesicles of tertiary trisomic male mice. *Chromosoma* **93**, 267-270.
- Strahl, B. D., and Allis, C. D.** (2000). The language of covalent histone modifications. *Nature* **403**, 41-45.
- Sun, Z. W., and Allis, C. D.** (2002). Ubiquitination of histone H2B regulates H3 methylation and gene silencing in yeast. *Nature* **418**, 104-108.
- Swerdlow, P. S., Schuster, T., and Finley, D.** (1990). A conserved sequence in histone H2A which is a ubiquitination site in higher eucaryotes is not required for growth in *Saccharomyces cerevisiae*. *Mol. Cell. Biol.* **10**, 4905-4911.
- Thiriet, C., and Albert, P.** (1995). Rapid and effective western blotting of histones from acid-urea-Triton and sodium dodecyl sulfate polyacrylamide gels: two different approaches depending on the subsequent qualitative or quantitative analysis. *Electrophoresis* **16**, 357-361.
- Turner, J. M., Mahadevaiah, S. K., Benavente, R., Offenberg, H. H., Heyting, C., and Burgoyne, P. S.** (2000). Analysis of male meiotic "sex body" proteins during XY female meiosis provides new insights into their functions. *Chromosoma* **109**, 426-432.
- Turner, J. M., Mahadevaiah, S. K., Elliott, D. J., Garchon, H. J., Pehrson, J. R., Jaenisch, R., and Burgoyne, P. S.** (2002). Meiotic sex chromosome inactivation in male mice with targeted disruptions of Xist. *J Cell Sci* **115**, 4097-4105.
- van der Laan, R., Roest, H., Hoogerbrugge, J., Smit, E., Slater, R., Baarends, W., Hoeijmakers, J., and Grootegoed, J.** (2000). Characterization of mRAD18Sc, a mouse homolog of the yeast post-replication repair gen RAD18. *Genomics* **69**, 86-94.
- van der Laan, R., Baarends, W. M., Wassenaar, E., Roest, H. P., Hoeijmakers, J. H., and Grootegoed, J. A.** (2004). DNA lesion bypass proteins in spermatogenesis. *International Journal of Andrology* **In press**.
- Vassilev, A. P., Rasmussen, H. H., Christensen, E. I., Nielsen, S., and Celis, J. E.** (1995). The levels of ubiquitinated histone H2A are highly upregulated in transformed human cells: partial colocalization of uH2A clusters and PCNA/cyclin foci in a fraction of cells in S-phase. *J. Cell Sci.* **108**, 1205-1215.
- Wu, R. S., Kohn, K. W., and Bonner, W. M.** (1981). Metabolism of ubiquitinated histones. *J. Biol. Chem.* **256**, 5916-5920.
- Zhang, Y.** (2003). Transcriptional regulation by histone ubiquitination and deubiquitination. *Genes Dev* **17**, 2733-2740.



Chapter 7

Concluding remarks and future prospects

Concluding Remarks and Future Prospects

Introduction

In yeast, Replicative Damage Bypass (RDB) has two key players: the ubiquitin-conjugating enzyme (E2 enzyme) RAD6 and the ubiquitin ligase (E3 enzyme) RAD18. These two proteins interact, and function together with an ubiquitin-activating E1 enzyme as an enzymatic complex that can ubiquitinate protein substrates. Most likely, RAD18 targets the ubiquitination complex to specific protein substrates involved in RDB. In addition to its interaction with RAD18, RAD6 can also interact with other E3 enzymes. Moreover, RAD6 is known to have functions outside the context of RDB, including roles in sporulation, transcriptional silencing and chromatin modification (Dover et al., 2002; Lawrence, 1994; Robzyk et al., 2000; Singh et al., 1998; Sun and Allis, 2002; Sun and Hampsey, 1999). Genetic and biochemical data have provided some insight in mechanisms of action of several proteins involved in RDB in yeast. However, studying RDB in mammals remains a challenge, and to gain more insight into this specific mechanism, an *in vivo* approach is required. In this thesis, the identification of the mouse homolog of yeast *RAD18*, designated *mRAD18Sc*, is one of the first steps towards unraveling RDB in mammals. Two mammalian *RAD6* homologs, *HR6A* and *HR6B* have been previously identified (Koken et al., 1991).

Recent advances in high resolution microscopy adapted for live cell microscopy have opened the very interesting field of bio-imaging research. As described in the present thesis, we have studied subcellular localization and dynamics of fluorescently tagged HR6B and mRAD18Sc. The data obtained provide information about the temporal and spatial organization of these RDB proteins in the nucleus, in relation to locally induced DNA damage. In this chapter we aim to discuss the impact of these data on current RDB models. In addition, cross talk between RDB and other DNA repair mechanisms will be discussed. Finally, the expression pattern of mRAD18Sc protein during spermatogenesis will be placed in the context of possible RDB-associated and novel functions of mRAD18Sc during gametogenesis.

HR6B and mRAD18Sc in mammalian Replicative Damage Bypass

RDB is an important DNA damage response mechanism that allows replication over damaged templates. To discuss the mechanism of RDB in mammalian cells, it is necessary to briefly describe the current model for RDB in yeast. In general, two RDB strategies are available to prevent termination of DNA replication at encountered lesions. The first strategy involves translesion synthesis (TLS), and in this pathway a polymerase from a subset of specific TLS polymerases temporarily takes over from the replicative DNA polymerase. The lesion specificity spectrum is different for each TLS polymerase, and each TLS polymerase has its own specificity of base insertion opposite to lesions. In addition, the extension capability of TLS polymerases depends on the lesion (Kannouche and Stary, 2003). In some cases, TLS polymerases can insert nucleotides and extend a short stretch of DNA, while in other cases the insertion and extension is achieved through cooperation of

two different TLS polymerases, and this is referred to as 'the two-polymerase affair' (Prakash and Prakash, 2002).

Damage avoidance (DA) is the second strategy of RDB, where the lesion is bypassed using homology from the non-damaged, newly made, daughter strand. This process is referred to as template-switching. Alternatively, information from the undamaged homologous chromosome can be used to bypass the lesion via recombination (Baynton and Fuchs, 2000). Biochemical data support the mechanism of TLS described here, but models for DA are largely hypothetical, and the proteins involved have been identified through genetic analyses (Baynton and Fuchs, 2000; Friedberg et al., 2002).

In yeast, RAD6 and RAD18 are essential for both RDB strategies. Apart from RAD6-RAD18, another ubiquitin-conjugating complex is important in RDB. It consists of the ubiquitin-conjugating enzyme UBC13, the ubiquitin-conjugating-like enzyme MMS2, and the ubiquitin ligase RAD5. This complex is required only for DA, not for TLS. Recently, proliferating cell nuclear antigen (PCNA) has been identified as the first functionally relevant target for ubiquitination in the RDB pathway. PCNA is a trimeric ring-shaped protein complex that encircles the DNA and forms a sliding clamp for replicative DNA polymerases. It also functions as platform for recruitment of regulatory factors (Spence et al., 1995). RAD18 is capable of self-interaction, and a tetramer composed of two RAD18 and two RAD6 molecules is thought to mediate mono-ubiquitination of PCNA at lysine residue 164 in response to DNA damage (Hoege et al., 2002; Ulrich and Jentsch, 2000). Furthermore, RAD18 also interacts with RAD5 (Ulrich and Jentsch, 2000) which is relevant for lysine-63-linked poly-ubiquitination of PCNA by the RAD6-RAD18-RAD5-MMS2-UBC13 complex (Figure 1). The functional relevance of ubiquitination of PCNA has been proposed to involve initiation of TLS when PCNA is mono-ubiquitinated, and DA after lysine 63-linked poly-ubiquitination (Stelter and Ulrich, 2003).

Lysines 127 and 164 of PCNA can also be modified by covalent linkage to the small ubiquitin-related modifier (SUMO), and thus become sumoylated (Hoege et al., 2002; Muller et al., 2001). Sumoylation and ubiquitination complexes appear to compete for modification of lysine 164 of PCNA. SUMO modification of lysine 164 and/or 127 can result in activation of the TLS polymerase $\text{pol}\zeta$, to replicate DNA that is refractory to the normal polymerase in the absence of DNA damage (Stelter and Ulrich, 2003). Finally, PCNA that is not modified at lysine 164 is most likely involved in processive DNA replication. Through these mechanisms, ubiquitination and sumoylation of PCNA change the PCNA mode of action from replication to replicative damage bypass, and vice versa. This may provide a system that allows regulation of switches between replicative and translesion-synthesis polymerases (Figure 1).

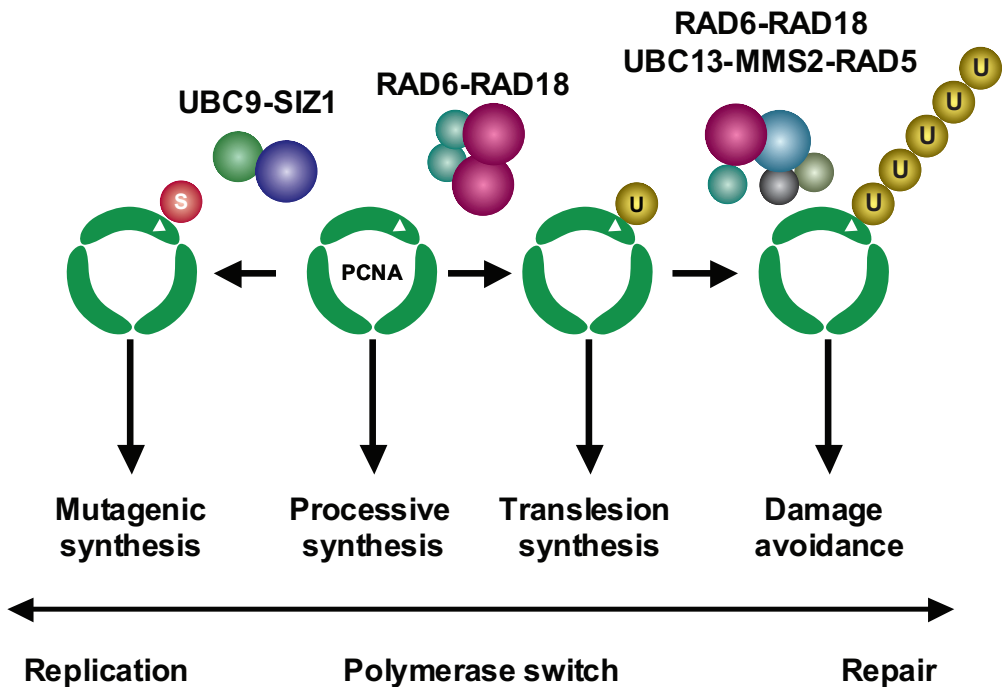


Figure 1. Model for switching between different PCNA modes in replication, mutagenesis, and replicative damage bypass mechanisms, by ubiquitination and sumoylation. PCNA is modified by ubiquitination at lysine residue (K) 164 (white triangle) in response to DNA damage. Mono-ubiquitination requires a heterotetrameric RAD6-RAD18 complex and stimulates translesion synthesis carried out by pol η and pol ζ . DNA damage also induces nuclear import of UBC13-MMS2 and, together with RAD5 and the RAD6-RAD18 heterodimer, these proteins enforce the formation of lysine 63 poly-ubiquitin chains on K164 (white triangle) of PCNA. This modification somehow promotes error-free lesion bypass through damage avoidance strategies. During normal replication, sumoylation by UBC9-SIZ1 of PCNA at K164 (white triangle) stimulates mutagenic DNA synthesis by pol ζ in the absence of DNA damage. Reversible exchange between the different PCNA modes would require relevant isopeptidases. U indicates ubiquitin and S indicates SUMO.

Inactivation of either one of the mammalian *RAD6* homologs, *HR6A* or *HR6B*, does not result in a severe somatic phenotype, and does not affect UV-sensitivity of mouse embryonic fibroblasts (MEFs), indicating that *HR6A* and *HR6B* have redundant activities in RDB (Roest et al., 1996; Roest et al., 2004). However, inactivation of both *HR6A* and *HR6B* is a lethal condition even at the cellular level, indicating the importance of these proteins in mammalian cells (Roest et al., 1996; Roest et al., 2004). The mammalian *RAD18* homolog, *mRAD18Sc* is essential for RDB as well (Tateishi et al., 2000; Tateishi et al., 2003), and overexpression in human cells of a mutant human *RAD18* cDNA interferes with the normal human *RAD18* interaction with *HR6A* and *HR6B* resulting in an increased sensitivity to various DNA damaging agents compared to wild type cells (Tateishi et al., 2000).

Fluorescence-based technology provides powerful tools to analyze fluorescently tagged proteins in living cells, and can help to answer the question how *HR6A/B* and *mRAD18Sc* control RDB in mammalian cells. We have shown that the mammalian homologs *mRAD18Sc* and *HR6B* are associated with the

replication machinery and that both proteins accumulate at subnuclear regions containing UV-induced DNA lesions. Similar observations have been reported for pol η and pol ι (Kannouche et al., 2001; Kannouche et al., 2002). Interestingly, DNA damage-dependent ubiquitination of PCNA at lysine residue 164 is also observed in mammalian cells (Hoege et al., 2002; Kannouche and Stary, 2003). Based on these observations, we strongly feel that mRAD18Sc and HR6A/B are involved in ubiquitination of PCNA. We have shown that the nuclear distribution of mRAD18Sc and HR6B changes during the cell cycle, and it would be very informative to combine time-lapse analysis of these proteins with fluorescently tagged PCNA. The degree of colocalization between mRAD18Sc or HR6A/B and PCNA increases in mid-late S phase cells, suggesting that mRAD18Sc-HR6A/B plays a role in replication of DNA stretches that are intrinsically difficult to replicate due to local chromatin conformation, towards the end of the S phase.

Five TLS polymerases, and perhaps more, that have been identified to operate in mammalian cells most likely require a precise regulation as well. Similar approaches as described above could be applied to study the behavior of different TLS polymerases following induction of specific DNA lesions. To visualize switching between PCNA modes throughout the cell cycle, or in response to DNA damage, sumoylation and ubiquitination of PCNA may be assayed in living cells using combinations of spectral GFP variants linked to PCNA, ubiquitin and SUMO. This approach may also reveal whether an additional level of control exists, whereby the three subunits of PCNA are differentially modified by ubiquitin and/or SUMO with specific implications for replication and RDB. In addition, these fluorescence-based *in vivo* studies could gain insight in the composition of replication foci during normal replication and in the presence of DNA damage.

A new approach using infrared laser light to introduce UV-lesions with great precision is described in Chapter 4. This method is very useful for analysis of *de novo* assembly of fluorescently tagged RDB proteins on damaged chromatin. In the same chapter, we have shown that the diffusion coefficients of mRAD18Sc and HR6B are very similar, suggesting that both proteins physically interact or at least reside in the same multi-protein complex. Nuclear mobility analysis by fluorescence recovery after photobleaching (FRAP) or fluorescence correlation spectroscopy (FCS) of other fluorescently tagged RDB proteins could be used to identify additional components of mRAD18Sc-HR6A/B-complexes in different situations.

By static light scattering measurements of purified His₆-HR6B-mRAD18Sc, it was found that the mRAD18Sc-HR6B complex is a dimeric (2:2) assembly of mRAD18Sc-HR6B, and that this interaction is achieved through connection between two mRAD18Sc molecules (Dr. V. Notenboom, personal communication). Dimerization of mRAD18Sc can also be studied in living cells, for example by fluorescence resonance energy transfer (FRET). It would be of great interest to determine changes in the degree of mRAD18Sc dimerization in response to different types of DNA damage. A relative loss of mRAD18Sc dimerization might point to interaction of mRAD18Sc with mammalian RAD5, taking part in assembling of a different protein complex leading to initiation of DA.

Interplay of Replicative Damage Bypass with DNA repair mechanisms

Certain types of DNA lesions require action of more than one DNA repair mechanism to be recognized, and to be removed. For example, when a lesion that is encountered during mitotic DNA replication has activated the DA-subpathway of RDB, this will require actions of proteins that are involved in homologous recombination repair. This is due to the fact that during each of the two DA strategies (template switch and recombinational repair) strand invasion and/or exchange occurs, to recruit the non-damaged template. Since these mechanisms are still largely hypothetical, it would be very interesting to study cooperation of RDB proteins with proteins involved in homologous recombination by live cell microscopy. In this respect, dynamic aspects of RAD51, the central protein in homologous recombination that is involved in strand invasion, will be of interest to study, since this protein is present in replication foci after DNA damage induction (Haaf et al., 1995), which suggests that RAD51 is recruited to non-repaired lesions during DNA replication which may be bypassed via DA.

Repair of interstrand crosslinks (ICLs), also requires a number of proteins involved in multiple DNA repair pathways. These include nucleotide excision repair (NER), RDB and homology-mediated double strand break (DSB) repair (Dronkert and Kanaar, 2001). A wide range of chemicals, including many of the most successful anti-cancer chemotherapeutics, induce ICLs. ICL is a class of damage in which two DNA bases on opposite strands become covalently linked. These lesions are very toxic since they prevent strand separation, which is a prerequisite for transcription and replication. Formation of ICLs first requires modification of one strand of DNA, followed by reaction with the second strand (Hartley et al., 1991). Thus, ICL-damaged DNA always contains a mixture of lesions and therefore proteins operating in different repair mechanisms are needed to achieve accurate removal of ICLs. *Rad6* and *rad18* yeast mutants are sensitive to ICL-inducing agents (Henriques and Moustacchi, 1981; McHugh et al., 2000), and *in vivo* studies of mammalian cells using fluorescently tagged proteins involved in NER, DSB repair and RDB could reveal insight into the involvement of these mechanisms in ICL repair.

HR6A/B and mRAD18Sc in mammalian gametogenesis

HR6B and mRAD18Sc show high expression of mRNA and protein in mouse spermatocytes and spermatids. In addition, *HR6A* and *HR6B* possess a sexual dimorphic function in gametogenesis. *HR6A* mutation has no effect on male fertility, but leads to maternal factor infertility with a block at the two-cell stage of embryonic development. In *HR6B* knockout mice, there is no such maternal factor infertility, but male mice show defective spermatogenesis, leading to infertility (Roest et al., 1996; Roest et al., 2004). The sex-specificity of the phenotype of *HR6A* and *HR6B* single knockout mice most likely can be explained by differences in expression levels of HR6A and HR6B proteins in male versus female gametogenic cells. The ratio HR6A:HR6B is higher than 1 in oocytes and lower than 1 in spermatocytes. The findings suggest an important function for HR6A/B, possibly in complex with mRAD18Sc, in mouse gametogenesis. The observed fertility phenotypes of *HR6A* and *HR6B* single knockout mice may be caused by functions of HR6A/B outside the context of RDB.

Several other mammalian RDB genes also show elevated expression in testis as compared to other tissues (McDonald et al., 1999; Murakumo et al., 2000; van Sloun et al., 1999; Velasco-Miguel et al., 2003; Yamada et al., 2000). However, no defects in fertility have been observed in knockout mouse models for two TLS polymerases, *poli* and *polk* (McDonald et al., 2003; Schenten et al., 2002). TLS polymerases are probably not essential for fertility, but might be involved in generation of genetic variability in the male germline (Baarends et al., 2001; Friedberg et al., 2002).

In yeast, RAD6 is required for ubiquitination of histone H2B, and lack of H2B ubiquitination affects sporulation. RAD6-dependent ubiquitination of histone H2B is a prerequisite for methylation of histone H3 at lysine residues 4 and 79 in yeast, and these H3 modifications are not affected in *rad18* mutant yeast strains (Sun and Allis, 2002). Modifications of histones such as methylation and acetylation, but also phosphorylation and ubiquitination, are involved in regulation of chromatin structure. Combination of different modifications that are present on the histones of the nucleosome core is referred to as the histone code (Strahl and Allis, 2000). In mammalian cells, methylation of lysine 4 of histone H3 is generally associated with gene activation, whereas for example methylated lysine 9 of H3 is a marker of transcriptionally silenced chromatin. Thus far, no defects in histone ubiquitination have been observed in somatic and gametogenic cells of *HR6A* and *HR6B* single knockout mice (Baarends et al., 1999; Baarends et al., unpublished results). However, proper tools to investigate histone ubiquitination in single cells are lacking (also see below). Detailed investigation of meiotic prophase in nuclei of *HR6B* knockout mice has revealed several aberrations that point to a role of HR6B in regulation of meiotic chromatin structure. Analysis of synaptonemal complex (SC) structure in HR6B-deficient spermatocytes has revealed that SC structure is abnormal. Compared to wild type spermatocytes, in HR6B-deficient spermatocytes SCs are longer and thinner, and depletion of SC proteins from near-telomeric regions was observed in late pachytene spermatocytes (Baarends et al., 2003). Furthermore, in HR6B-deficient spermatocytes, meiotic recombination frequency is elevated (Baarends et al., 2003).

Recent development of antibodies that specifically recognize different modified histone variants has stimulated research in this field. However, antibodies that specifically recognize ubiquitinated histone H2B are not yet available. This precludes analysis of H2B ubiquitination in single gametogenic cells during gametogenesis in the *HR6A*- and *HR6B*-deficient mouse models. A monoclonal antibody that recognizes ubiquitinated H2A (ubi-H2A) is available, but the pattern of ubi-H2A expression during spermatogenesis was found to be similar in wild type and *HR6B* knockout mice (Baarends et al., 1999). A defect in H2B ubiquitination in gametogenic cells may result in a change of the histone code, and therefore we are currently analyzing different histone modifications in spermatogenic cells of wild type and *HR6B* knockout mice, as well as in wild type and *HR6A* knockout oocytes and zygotes. The most recent data indicate that *HR6A* knockout oocytes and early embryos show no detectable aberrations of the histone code (Roest et al., 2004).

Function(s) of mRAD18Sc in spermatogenesis may be related to functions of HR6B in regulation of chromatin structure. However, it is also possible that function(s) of mRAD18Sc is not expressed in *HR6B* knockout spermatogenic cells, due to presence of HR6A which may compensate HR6B. The fact that the localization pattern of mRAD18Sc is not changed in *HR6B* knockout spermatocytes, supports this hypothesis (Baarends et al., unpublished results). It is interesting that mRAD18Sc

shows marked localization in a subnuclear region containing the partially synapsed X and Y chromosomes in pachytene spermatocytes, referred to as the sex body (XY body). Furthermore, mRAD18Sc also localizes to unpaired chromatin regions of aberrant autosomal chromosomes in pachytene spermatocytes. mRAD18Sc in spermatocytes, is likely involved in roles outside the context of RDB since PCNA and other proteins involved in RDB ($pol\eta$, $pol\iota$ and UBC13) do not localize to these unpaired chromosomal regions (Figure 2). These observations suggest that in normal spermatocytes, mRAD18Sc, together with HR6A/B might be involved in a mechanism that is associated with the largely unpaired X and Y chromosomes in the sex body and other unpaired chromosomal regions.

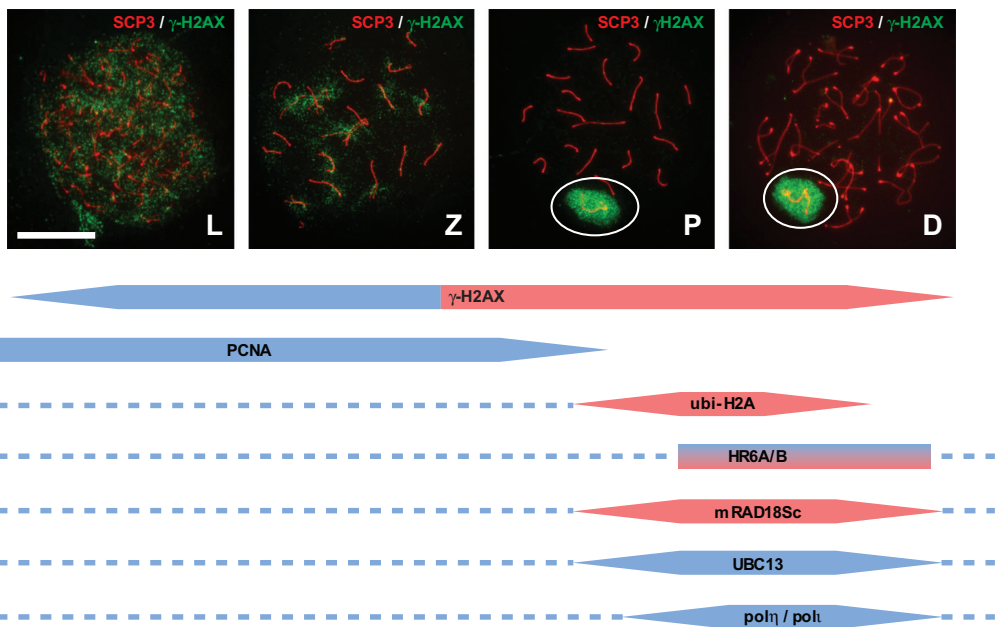


Figure 2. Meiotic nuclear spread preparations immunostained for SCP3 (red) and γ -H2AX (green). Formation of the sex body starts in late zygotene and is represented by the white circle (pachytene and diplotene). Phosphorylation of histone H2AX (γ -H2AX) is associated with Spo11 induced double strand breaks in leptotene and zygotene, but specifically marks the sex body chromatin in subsequent stages of the meiotic prophase. Proliferating nuclear cell antigen (PCNA) is allied to pre-meiotic S phase and DNA repair-related DNA synthesis, and diminishes in early pachytene (based on immunohistochemistry). Ubiquitinated histone H2A (ubi-H2A) also marks the sex body chromatin specifically in pachytene and diplotene. The RDB proteins HR6A/B (based on immunohistochemistry) and mRAD18Sc are highly expressed in pachytene and diplotene spermatocytes. mRAD18Sc localizes mainly to the sex body, and HR6A/B is present in the sex body as well as in the rest of the nucleus. Other RDB factors, $pol\eta$, $pol\iota$ and UBC13 are largely excluded from sex body chromatin. Blue bars indicate localization covering the entire the nucleus, but not the sex body when present. Red bars point to sex body specific association, and dotted blue lines represent low expression levels. L: leptotene; Z: zygotene; P: pachytene and D: diplotene. Scale bar: 20 μ m.

In the last few decades, localization of multiple proteins to the sex body has been reported in literature, but their biological significance for sex body function remains unclear (Hoyer-Fender, 2003). Also, several meiotic recombination proteins show different dynamics in appearance and disappearance from the sex body compared to autosomal bivalents in meiotic prophase in the mouse (Baarends and Grootegoed, 2003). The transcriptional silencing of genes on the XY bivalent

in male meiotic prophase is accompanied by the activation of several testis-specific autosomal homologs of X-chromosomal genes (Wang, 2004). The mechanism by which this compensatory autosomal gene activation is achieved after transcriptional silencing of the X chromosome in the sex body in primary spermatocytes, is unknown. It can be imagined that proteins localizing to the XY bivalent are involved in control of transcription. Following completion of the meiotic division, re-expression of several X-chromosomal genes occurs in haploid spermatids (Hendriksen et al., 1995). The reason why the sex body is transcriptionally silenced remains an open question. Several hypotheses have been proposed in the past, including inactivation of genes encoding proteins that would be 'toxic' for male meiosis, protection of the non-PAR regions of the X and Y chromosomes for non-homologous recombination, and promotion of homology search to allow pairing of the small PARs (Jablonka and Lamb, 1988; Lifschytz and Lindsley, 1972; McKee and Handel, 1993; Turner et al., 2000). In addition, transcriptional silencing might provide a mechanism to escape a checkpoint that detects unpaired chromatin regions in mid-pachytene (Jablonka and Lamb, 1988).

Recently, detailed analysis of the sequence of the male specific region (MSY) of the human Y-chromosome revealed the presence of extended palindromic sequences that contain multiple copies of testis-specific genes with a high degree of sequence homology (Skaletsky et al., 2003). The sophisticated and highly organized structure of these Y chromosomal regions is presumably the result of gene conversion events by intrachromosomal recombination (Skaletsky et al., 2003). The biological significance of this phenomenon is not known, and for the mouse such data are not yet available, but it may be viewed as a strategy to maintain the integrity of the Y chromosome in amammalian population in the absence of a homologous meiotic pairing partner, and regulation of this process likely requires regulation of chromatin dynamics.

In this thesis, we have used several mouse models that display meiotic pairing problems in males and/or females, to study whether accumulation of mRAD18Sc on sex body chromatin is triggered by the presence of unsynapsed chromosomal regions. It appears that mRAD18Sc is associated with all large unsynapsed chromosomal regions during the male and female meiotic prophase. Our data also indicate that such chromosomal regions are transcriptionally silenced. This silencing mechanism may be analogous to 'Meiotic Silencing of Unpaired DNA' (MSUD), a process that is operational in *N. crassa* (Shiu et al., 2001). These findings indicate that mRAD18Sc may be involved in detecting unpaired DNA, in protecting this DNA from meiotic recombination, and/or in mediating transcriptional repression of the unpaired DNA. In somatic cells, H2AX becomes phosphorylated (γ -H2AX) at sites where a DSB has occurred, and in this situation γ -H2AX most likely attracts proteins involved in recombination to the DSB site (Rogakou et al., 1998). In meiosis during leptotene, DSBs are introduced in a controlled manner by the topoisomerase Spo11, and these sites can be visualized by immunostaining of meiotic spread nuclei using γ -H2AX antibodies (Bergerat et al., 1997; Mahadevaiah et al., 2001)(Figure 2). In pachytene, γ -H2AX staining is enhanced in the sex body, and this staining pattern does not disappear in primary spermatocytes from Spo11-deficient mice, indicating that phosphorylation of H2AX in the sex body serves another function and is independent of DSB formation by Spo11 (Fernandez-Capetillo et al., 2003). In fact, γ -H2AX is required for formation and transcriptional silencing of the sex body (Fernandez-Capetillo et al., 2003). Because γ -H2AX, like

mRAD18Sc, accumulates on unsynapsed translocation bivalents that contain a non-homologous region, its function may be related to that of mRAD18Sc. However, the appearance of γ -H2AX in the sex body precedes that of mRAD18Sc (Figure 2), indicating that a functional interaction, if present, may not be direct.

From the above it becomes evident that the sex body may have a broader functional significance than previously anticipated. At this point, and in the context of this thesis, it will be most interesting to design experiments that will help to unravel possible links between meiotic chromosome pairing, transcriptional silencing of unpaired chromosomal, and regulation of recombination. Generation of a conditional knockout mouse model for *mRAD18Sc* will provide a model that may allow discovery of new aspects of the function of mRAD18Sc in RDB and gametogenesis. The impact of RDB on mutagenesis and carcinogenesis in mammals can also be studied with a conditional knockout mouse model. In addition, such a mouse model will be required to determine whether functions of mRAD18Sc in mammalian meiosis are analogous to RAD18 functions in yeast, or whether a novel role of mRAD18Sc has evolved.

References

- Baarends, W. M., Hoogerbrugge, J. W., Roest, H. P., Ooms, M., Vreeburg, J., Hoeijmakers, J. H., and Grootegoed, J. A.** (1999). Histone ubiquitination and chromatin remodeling in mouse spermatogenesis. *Dev Biol* **207**, 322-333.
- Baarends, W. M., van der Laan, R., and Grootegoed, J. A.** (2001). DNA repair mechanisms and gametogenesis. *Reproduction* **121**, 31-39.
- Baarends, W. M., Wassenaar, E., Hoogerbrugge, J. W., van Cappellen, G., Roest, H. P., Vreeburg, J., Ooms, M., Hoeijmakers, J. H., and Grootegoed, J. A.** (2003). Loss of HR6B ubiquitin-conjugating activity results in damaged synaptonemal complex structure and increased crossing-over frequency during the male meiotic prophase. *Mol Cell Biol* **23**, 1151-1162.
- Baarends, W. M., and Grootegoed, J. A.** (2003). Chromatin dynamics in the male meiotic prophase. *Cytogenet Genome Res* **103**, 225-234.
- Baynton, K., and Fuchs, R. P.** (2000). Lesions in DNA: hurdles for polymerases. *Trends Biochem Sci* **25**, 74-79.
- Bergerat, A., de Massy, B., Gabelle, D., Varoutas, P. C., Nicolas, A., and Forterre, P.** (1997). An atypical topoisomerase II from Archaea with implications for meiotic recombination. *Nature* **386**, 414-417.
- Dover, J., Schneider, J., Boateng, M. A., Wood, A., Dean, K., Johnston, M., and Shilatifard, A.** (2002). Methylation of histone H3 by COMPASS requires ubiquitination of histone H2B by RAD6. *J. Biol. Chem.* **277**, 28368-28371
- Dronkert, M. L., and Kanaar, R.** (2001). Repair of DNA interstrand cross-links. *Mutat Res* **486**, 217-247.
- Fernandez-Capetillo, O., Mahadevaiah, S. K., Celeste, A., Romanienko, P. J., Camerini-Otero, R. D., Bonner, W. M., Manova, K., Burgoyne, P., and Nussenzweig, A.** (2003). H2AX is required for chromatin remodeling and inactivation of sex chromosomes in male mouse meiosis. *Dev Cell* **4**, 497-508.
- Friedberg, E. C., Wagner, R., and Radman, M.** (2002). Specialized DNA polymerases, cellular survival, and the genesis of mutations. *Science* **296**, 1627-1630.
- Haaf, T., Golub, E. I., Reddy, G., Radding, C. M., and Ward, D. C.** (1995). Nuclear foci of mammalian Rad51 recombination protein in somatic cells after DNA damage and its localization in synaptonemal complexes. *Proc Natl Acad Sci USA* **92**, 2298-2302.
- Hartley, J. A., Berardini, M. D., and Souhami, R. L.** (1991). An agarose gel method for the determination of DNA interstrand crosslinking applicable to the measurement of the rate of total and "second-arm" crosslink reactions. *Anal Biochem* **193**, 131-134.
- Hendriksen, P. J., Hoogerbrugge, J. W., Themmen, A. P., Koken, M. H., Hoeijmakers, J. H., Oostra, B. A., van der Lende, T., and Grootegoed, J. A.** (1995). Postmeiotic transcription of X and Y chromosomal genes during spermatogenesis in the mouse. *Dev Biol* **170**, 730-733.
- Henriques, J. A., and Moustacchi, E.** (1981). Interactions between mutations for sensitivity to psoralen photoaddition (pso) and to radiation (rad) in *Saccharomyces cerevisiae*. *J Bacteriol* **148**, 248-256.
- Hoeghe, C., Pfander, B., Moldovan, G. L., Pyrowolakis, G., and Jentsch, S.** (2002). RAD6-dependent DNA repair is linked to modification of PCNA by ubiquitin and SUMO. *Nature* **419**, 135-141.

- Hoyer-Fender, S.** (2003). Molecular aspects of XY body formation. *Cytogenet Genome Res* **103**, 245-255.
- Jablunka, E., and Lamb, M. J.** (1988). Meiotic pairing constraints and the activity of sex chromosomes. *J Theor Biol* **133**, 23-36.
- Kannouche, P., Broughton, B. C., Volker, M., Hanaoka, F., Mullenders, L. H., and Lehmann, A. R.** (2001). Domain structure, localization, and function of DNA polymerase eta, defective in xeroderma pigmentosum variant cells. *Genes Dev* **15**, 158-172.
- Kannouche, P., Fernandez de Henestrosa, A. R., Coull, B., Vidal, A. E., Gray, C., Zicha, D., Woodgate, R., and Lehmann, A. R.** (2002). Localization of DNA polymerases eta and iota to the replication machinery is tightly co-ordinated in human cells. *Embo J* **21**, 6246-6256.
- Kannouche, P., and Stary, A.** (2003). Xeroderma pigmentosum variant and error-prone DNA polymerases. *Biochimie* **85**, 1123-1132.
- Koken, M. H., Reynolds, P., Jaspers-Dekker, I., Prakash, L., Prakash, S., Bootsma, D., and Hoeijmakers, J. H.** (1991). Structural and functional conservation of two human homologs of the yeast DNA repair gene RAD6. *Proc. Natl. Acad. Sci. USA* **88**, 8865-8869.
- Lawrence, C.** (1994). The RAD6 repair pathway in *Saccharomyces cerevisiae*: what does it do, and how does it do it? *BioEssays* **16**, 253-258.
- Lifschytz, E., and Lindsley, D. L.** (1972). The role of X chromosome inactivation during spermatogenesis. *Proc Natl Acad Sci USA* **69**, 182-186.
- Mahadevaiah, S. K., Turner, J. M., Baudat, F., Rogakou, E. P., de Boer, P., Blanco-Rodriguez, J., Jasin, M., Keeney, S., Bonner, W. M., and Burgoyne, P. S.** (2001). Recombinational DNA double-strand breaks in mice precede synapsis. *Nat Genet* **27**, 271-276.
- McDonald, J. P., Frank, E. G., Plosky, B. S., Rogozin, I. B., Masutani, C., Hanaoka, F., Woodgate, R., and Gearhart, P. J.** (2003). 129-derived strains of mice are deficient in DNA polymerase iota and have normal immunoglobulin hypermutation. *J Exp Med* **198**, 635-643.
- McDonald, J. P., Rapic-Otrin, V., Epstein, J. A., Broughton, B. C., Wang, X., Lehmann, A. R., Wolgemuth, D. J., and Woodgate, R.** (1999). Novel human and mouse homologs of *Saccharomyces cerevisiae* DNA polymerase eta. *Genomics* **60**, 20-30.
- McHugh, P. J., Sones, W. R., and Hartley, J. A.** (2000). Repair of intermediate structures produced at DNA interstrand cross-links in *Saccharomyces cerevisiae*. *Mol Cell Biol* **20**, 3425-3433.
- McKee, B. D., and Handel, M. A.** (1993). Sex chromosomes, recombination, and chromatin conformation. *Chromosoma* **102**, 71-80.
- Muller, S., Hoege, C., Pyrowolakis, G., and Jentsch, S.** (2001). SUMO, ubiquitin's mysterious cousin. *Nat Rev Mol Cell Biol* **2**, 202-210.
- Murakumo, Y., Roth, T., Ishii, H., Rasio, D., Numata, S., Croce, C. M., and Fishel, R.** (2000). A human REV7 homolog that interacts with the polymerase zeta catalytic subunit hREV3 and the spindle assembly checkpoint protein hMAD2. *J Biol Chem* **275**, 4391-4397.
- Prakash, S., and Prakash, L.** (2002). Translesion DNA synthesis in eukaryotes: a one- or two-polymerase affair. *Genes Dev* **16**, 1872-1883.
- Robzyk, K., Recht, J., and Osley, M. A.** (2000). Rad6-dependent ubiquitination of histone H2B in yeast. *Science* **287**, 501-504.
- Roest, H. P., Baarends, W. M., de Wit, J., van Klaveren, J. W., Wassenaar, E., Hoogerbrugge, J. W., van Cappellen, W. A., Hoeijmakers, J. A., and Grootegoed, J. A.** (2004). The Ubiquitin-conjugating DNA repair enzyme HR6A is a maternal factor essential for early embryonic development in mice. *Mol Cell Biol* in press.
- Rogakou, E. P., Pilch, D. R., Orr, A. H., Ivanova, V. S., and Bonner, W. M.** (1998). DNA double-stranded breaks induce histone H2AX phosphorylation on serine 139. *J Biol Chem* **273**, 5858-5868.
- Schenten, D., Gerlach, V. L., Guo, C., Velasco-Miguel, S., Hladik, C. L., White, C. L., Friedberg, E. C., Rajewsky, K., and Esposito, G.** (2002). DNA polymerase kappa deficiency does not affect somatic hypermutation in mice. *Eur J Immunol* **32**, 3152-3160.
- Shiu, P. K., Raju, N. B., Zickler, D., and Metzberg, R. L.** (2001). Meiotic silencing by unpaired DNA. *Cell* **107**, 905-916.
- Singh, J., Goel, V., and Klar, A. J.** (1998). A novel function of the DNA repair gene rhp6 in mating-type silencing by chromatin remodeling in fission yeast. *Mol. Cell. Biol.* **18**, 5511-5522.
- Skaletsky, H., Kuroda-Kawaguchi, T., Minx, P. J., Cordum, H. S., Hillier, L., Brown, L. G., Repping, S., Pyntikova, T., Ali, J., Bieri, T., Chinwalla, A., Delehaunty, A., Delehaunty, K., Du, H., Fewell, G., Fulton, L., Fulton, R., Graves, T., Hou, S. F., Latrielle, P., Leonard, S., Mardis, E., Maupin, R., McPherson, J., Miner, T., Nash, W., Nguyen, C., Ozersky, P., Pepin, K., Rock, S., Rohlfing, T., Scott, K., Schultz, B., Strong, C., Tin-Wollam, A., Yang, S. P., Waterston, R. H., Wilson, R. K., Rozen, S., and Page, D. C.** (2003). The male-specific region of the human Y chromosome is a mosaic of discrete sequence classes. *Nature* **423**, 825-837.
- Spence, J., Sadis, S., Haas, A. L., and Finley, D.** (1995). A ubiquitin mutant with specific defects in DNA repair and multiubiquitination. *Mol Cell Biol* **15**, 1265-1273.
- Stelter, P., and Ulrich, H. D.** (2003). Control of spontaneous and damage-induced mutagenesis by SUMO and ubiquitin conjugation. *Nature* **425**, 188-191.
- Strahl, B. D., and Allis, C. D.** (2000). The language of covalent histone modifications. *Nature* **403**, 41-45.

- Sun, Z. W., and Allis, C. D.** (2002). Ubiquitination of histone H2B regulates H3 methylation and gene silencing in yeast. *Nature* **418**, 104-108.
- Sun, Z. W., and Hampsey, M.** (1999). A general requirement for the Sin3-Rpd3 histone deacetylase complex in regulating silencing in *Saccharomyces cerevisiae*. *Genetics* **152**, 921-932.
- Tateishi, S., Niwa, H., Miyazaki, J., Fujimoto, S., Inoue, H., and Yamaizumi, M.** (2003). Enhanced genomic instability and defective postreplication repair in RAD18 knockout mouse embryonic stem cells. *Mol Cell Biol* **23**, 474-481.
- Tateishi, S., Sakuraba, Y., Masuyama, S., Inoue, H., and Yamaizumi, M.** (2000). Dysfunction of human Rad18 results in defective postreplication repair and hypersensitivity to multiple mutagens. *Proc Natl Acad Sci USA* **97**, 7927-7932.
- Turner, J. M., Mahadevaiah, S. K., Benavente, R., Offenberger, H. H., Heyting, C., and Burgoyne, P. S.** (2000). Analysis of male meiotic "sex body" proteins during XY female meiosis provides new insights into their functions. *Chromosoma* **109**, 426-432.
- Ulrich, H. D., and Jentsch, S.** (2000). Two RING finger proteins mediate cooperation between ubiquitin-conjugating enzymes in DNA repair. *Embo J* **19**, 3388-3397.
- van Sloun, P. P., Romeijn, R. J., and Eeken, J. C.** (1999). Molecular cloning, expression and chromosomal localisation of the mouse Rev3l gene, encoding the catalytic subunit of polymerase zeta. *Mutat Res* **433**, 109-116.
- Velasco-Miguel, S., Richardson, J. A., Gerlach, V. L., Lai, W. C., Gao, T., Russell, L. D., Hladik, C. L., White, C. L., and Friedberg, E. C.** (2003). Constitutive and regulated expression of the mouse Dinb (Polkappa) gene encoding DNA polymerase kappa. *DNA Repair (Amst)* **2**, 91-106.
- Wang, P. J.** (2004). X chromosomes, retrogenes and their role in male reproduction. *Trends Endocrinol Metab* **15**, 79-83.
- Yamada, A., Masutani, C., Iwai, S., and Hanaoka, F.** (2000). Complementation of defective translesion synthesis and UV light sensitivity in xeroderma pigmentosum variant cells by human and mouse DNA polymerase eta. *Nucleic Acids Res* **28**, 2473-2480.

Summary

DNA is constantly challenged by endogenous and exogenous agents that react with the chemical structure of the double helix and thereby interfere with DNA metabolism including transcription and replication. Persistent DNA lesions may induce mutations and contribute to development of malignancies. Fortunately, several DNA damage response and repair mechanisms operate to remove or bypass DNA lesions accurately.

In **Chapter 1**, these DNA response and repair mechanisms are described briefly. Replicative damage bypass (RDB) is a damage tolerance system that prevents termination when the replication machinery encounters a blocking lesion. This is achieved by recruitment of a subset of highly specialized DNA polymerases that temporarily take over from the replication machinery, referred to as translesion synthesis. Alternatively, the actual damage is avoided and non-damaged homology is used to bypass the lesion through template switching or recombination. After damage bypass, normal replication is reinitiated. In yeast, genes encoding proteins active in RDB are members of the RAD6 epistasis group, and mammalian homologs have been identified. RAD6 and RAD18 are key regulators of this mechanism in yeast, and this thesis focuses on their mammalian homologs, designated HR6A, HR6B and mRAD18Sc. HR6A and HR6B are ubiquitin-conjugating enzymes that can interact with the ubiquitin ligase RAD18, and several relevant aspects of the ubiquitin system are described. Finally, all known mammalian RDB genes show elevated expression in testis, and possible roles of these RDB proteins in spermatogenesis are discussed.

We have studied properties of RDB proteins using advanced fluorescence microscopy. **Chapter 2** provides a schematic overview of fluorescence microscopy and fluorescence based technology. The discovery of the green fluorescent protein (GFP) made it possible to study the behavior of fluorescently tagged proteins in living cells. First, fluorescence microscopy is introduced and compared to high-resolution confocal microscopy. Furthermore, several techniques to visualize multiple fluorescent markers in a single specimen are presented, and methods to study protein dynamics and interactions between proteins are described. Finally, a method to perform single molecule analysis in a living cell is presented.

In **Chapter 3**, identification of the mouse *RAD18* gene, designated *mRAD18Sc* is presented. *mRAD18Sc* encodes a 509 amino acid polypeptide, and this protein shows a high percentage of amino acid similarity to its yeast homolog. The N-terminus of mRAD18Sc contains a RING-zinc-finger, and a classical zinc-finger is located in the middle of the polypeptide. These 2 domains are present in all known RAD18 homologs, including the fungal proteins NuvA and Uvs-2. *mRAD18Sc* mRNA is ubiquitous expressed in most if not all mouse tissues, and the highest mRNA expression is found in testis. Northern blot analysis of mRNA from different germ cell types shows that the high testicular *mRAD18Sc* mRNA level mainly originates from expression in spermatocytes. Expression of GFP-mRAD18Sc protein in HeLa cells shows that mRAD18Sc is a nuclear protein. Finally, the *mRAD18Sc* gene was mapped in the mouse genome to chromosome 6F, by fluorescent *in situ* hybridization.

The subcellular localization of fluorescently tagged mRAD18Sc is further studied in **Chapter 4**. We show that YFP-mRAD18Sc colocalizes with HR6B-CFP, and that both proteins are present in replication foci. Nuclear mobility studies reveal that GFP-mRAD18Sc and HR6B-GFP diffuse with a similar speed, indicating that they either physically interact or at least reside in the same multi-protein complex. Furthermore, the localization pattern of both proteins changes throughout the cell cycle. After UV-C treatment, GFP-mRAD18Sc and HR6B-GFP redistribute to numerous discrete nuclear foci that persist for at least 8 hours after the irradiation, suggesting that mRAD18Sc and HR6B are recruited to damage-stalled replication sites. Immunofluorescence on cells that had been locally irradiated with UV-C showed that mRAD18Sc and HR6B indeed accumulate to sites of UV-induced DNA lesions. In addition, a new approach to induce UV lesions in specific selected subnuclear regions revealed that mRAD18Sc and HR6B accumulation in exposed areas is not limited to the S phase of the cell cycle. Finally, this new method makes it possible to study kinetics of *de novo* assembly of chromatin associated processes in living cells.

The relative high *mRAD18Sc* mRNA expression level in mouse testis and in particular in pachytene spermatocytes suggests a role for the encoded ubiquitin ligase in spermatogenesis. Antibodies directed against parts of the mRAD18Sc polypeptide were used to study subcellular localization of mRAD18Sc in spermatogenic cells. The results from these studies are presented in **Chapter 5**. Interestingly, the mRAD18Sc protein heavily marks the XY body in pachytene and diplotene spermatocytes. The XY body is a subnuclear structure that contains the partly synapsed and transcriptionally silenced X and Y chromosomes in male meiotic prophase. The absence of other RDB proteins (UBC13 and pol η) and PCNA from the XY body suggests that mRAD18Sc plays a role in meiosis outside the context of RDB. Finally, we found that a high level of mRAD18Sc protein correlates with a low level of RNA pol II in the XY body, and this was also observed for other unpaired chromosomal regions in primary spermatocytes, suggesting that a mechanism exists that silences unpaired DNA, in which mRAD18Sc may have a function in meiotic prophase.

In **Chapter 6**, accumulation of ubiquitinated histone H2A (ubi-H2A) on silenced chromatin regions during meiosis is presented. Ubi-H2A shows a localization pattern in primary spermatocytes that is very similar to that of mRAD18Sc. During pachytene stage, the mRAD18Sc signal precedes ubi-H2A accumulation in the XY body, and mRAD18Sc also persists somewhat longer. Silencing of unpaired chromatin regions is a phenomenon that may also occur in female meiotic prophase. Therefore, we also studied immunostaining of mRAD18Sc and ubi-H2A in relation to local presence of RNA polymerase II, oocytes of XO mice and XY^{tdym1} mice, that are sex reversed due to a mutation of the testis determining gene. Both mRAD18Sc and ubi-H2A localize on unpaired sex chromosomes in association with very low levels of RNA pol II, in pachytene XO and (sex reversed) XY^{tdym1} oocytes. In wild type (XX) pachytene oocytes accumulation of mRAD18Sc and ubi-H2A occurs rarely, only in situations of aberrant synapsis. Phosphorylation of histone H2AX is required for formation and silencing of the XY body in spermatocytes. We show that this modification is also associated with unpaired chromatin regions in male and female meiosis. Together, these results indicate that unpaired chromatin regions are transcriptionally silenced in male and female meiotic prophase. This

mechanism is reminiscent of Meiotic Silencing of Unpaired DNA (MSUD), a term that is used to describe a similar phenomenon in *Neurospora crassa*. Finally, accumulation of ubi-H2A is a general feature of silenced chromatin, and it also marks the transcriptionally silenced X chromosome, named Barr body in female somatic cells.

Chapter 7, the final chapter, discusses the research outlined in this thesis and provides several future prospects. Possible functions for HR6A/B and mRAD18Sc in RDB are described, and several suggestions are given to further study regulation of mammalian RDB in living cells, mainly by fluorescence-based *in vivo* approaches. Furthermore, possible functions for RDB proteins and in particular mRAD18Sc in gametogenesis are discussed. The work presented in this thesis gives some insights in RDB in mammalian cells and provides indications for a function of RDB proteins outside the context of RDB, in particular for MSUD in male and female gametogenesis.

Samenvatting

DNA wordt constant bedreigd door endogene en exogene factoren die met de chemische structuur van de dubbelhelix kunnen reageren en het daardoor kunnen beschadigen. DNA schades beïnvloeden DNA metabolisme op uiteenlopende wijze met grote invloed op onder andere transcriptie en replicatie. Tevens kunnen DNA schades mutaties induceren en bijdragen tot ontwikkeling van kanker, en kunnen ze leiden tot celdood en veroudering bevorderen. Gelukkig zijn een aantal DNA herstelmechanismen actief om deze DNA beschadigingen te verwijderen.

In **Hoofdstuk 1**, worden de voornaamste DNA herstelmechanismen kort beschreven. Daarnaast wordt uitgebreid ingegaan op het proces van 'Replicative Damage Bypass' (RDB), dat het hoofdonderwerp van het hier beschreven promotieonderzoek is. RDB is een schade-tolerantie systeem dat beëindiging van het replicatieproces verhindert wanneer de replicatie stuit op een blokkerende DNA schade. Dit doel wordt bereikt door rekrutering van zeer gespecialiseerde polymerasen die DNA synthese tijdelijk van de normale replicatiemachine overnemen, om voorbij het beschadigde stuk te komen met een zo klein mogelijke kans op fouten. Deze vorm van RDB wordt translesie-synthese genoemd. Als alternatief kan de daadwerkelijke DNA schade vermeden worden door gebruik te maken van de intacte homologe streng via een mechanisme van 'template switching' of recombinatie. Normale replicatie wordt opnieuw opgestart na de schadeomleiding. Gist RDB genen zijn ondergebracht in de RAD6 epistasisgroep, en in hogere eukaryoten zijn homologen van deze gistgenen geïdentificeerd. RAD6 en RAD18 zijn de hoofdrolspelers van het RDB systeem. In dit proefschrift worden de zoogdierhomologen, genaamd HR6A en HR6B (beide homologen van RAD6), en mRAD18Sc (het enige bekende homoloog van RAD18) behandeld. HR6A en HR6B zijn ubiquitine-conjugerende enzymen die een interactie aangaan met het ubiquitine ligase RAD18. Vanwege de relatie met ubiquitine systeem, worden relevante aspecten van dit systeem eveneens beschreven. Alle tot nu toe bekende RDB genen in zoogdiercellen vertonen een verhoogde relatieve expressie in de testis, en de mogelijke rol van RDB eiwitten in spermatogenese wordt belicht.

In het experimentele werk beschreven in dit proefschrift worden enkele eigenschappen van RDB eiwitten bestudeerd met behulp van geavanceerde lichtmicroscopie. **Hoofdstuk 2** geeft een schematisch overzicht van fluorescentiemicroscopie en daaraan verwante technologieën. De ontdekking van het groen fluorescerende eiwit (GFP) maakte het mogelijk om het gedrag van fluorescent gemerkte eiwitten in levende cellen te bestuderen. De fluorescentiemicroscopie wordt geïntroduceerd en vergeleken met hoge resolutie confocale microscopie. Vervolgens komen verscheidene technieken aan de orde die worden gebruikt om meerdere fluorescente eiwitten tegelijkertijd in één enkel specimen te visualiseren. Tot slot worden methodes voor het bestuderen van eiwitdynamica, eiwit-eiwit interacties, en 'single molecule' analyse in levende cellen besproken.

In **Hoofdstuk 3** wordt de identificatie van het muizen *RAD18* gen, *mRAD18Sc* beschreven. *mRAD18Sc* codeert voor een polipeptide van 509 aminozuren en dit eiwit heeft een grote mate van gelijkenis met de aminozuurvolgorde van het gisthomoloog. Aan het begin van mRAD18Sc zit een RING-zink-vinger en meer in

het midden van het polipeptide zit een klassieke zink-vinger. Deze 2 domeinen zijn aanwezig in alle bekende RAD18 homologen, waaronder de schimmel-eiwitten NuvA en Uvs-2. Het *mRAD18Sc* mRNA komt tot expressie in diverse muizenweefsels, maar het hoogste mRNA expressieniveau is gevonden in testis. Northern blot analyse van verschillende celtypen uit testis toont aan dat het *mRAD18Sc* mRNA niveau met name verhoogd is in spermatocyten. Expressie van het GFP-mRAD18Sc eiwit in HeLa cellen laat zien dat mRAD18Sc een kerneiwit is. Tot slot wordt de lokalisatie van het *mRAD18Sc* gen op chromosoom 6F in het muizengenoom beschreven.

De subcellulaire lokalisatie van fluorescent gemerkt mRAD18Sc werd verder bestudeerd, zoals beschreven in **Hoofdstuk 4**. YFP-mRAD18Sc en HR6B-CFP zitten op dezelfde plaatsen in de celkern en beide eiwitten zijn aanwezig in replicatiespots. Mobiliteitsstudies van GFP-mRAD18Sc en HR6B-GFP in de celkern geven een vergelijkbare diffusiesnelheid voor beide eiwitten. Dit resultaat wijst erop, dat deze twee eiwitten een fysieke interactie met elkaar aangaan of in ieder geval aanwezig zijn in hetzelfde multi-eiwit complex. Voorts verandert het lokalisatiepatroon van beide eiwitten gedurende de celcyclus. Na UV-C bestraling herverdelen GFP-mRAD18Sc en HR6B-GFP zich in talrijke spots in de kern en dit patroon blijft ten minste 8 uren na de straling voortduren. Het lijkt erop dat mRAD18Sc en HR6B lokaliseren op plaatsen waar de replicatie is geblokkeerd. Immunofluorescentie op cellen die plaatselijk met UV-C zijn bestraald toont inderdaad aan dat mRAD18Sc en HR6B aangetrokken worden naar plaatsen waar zich UV-geïnduceerde DNA beschadigingen bevinden. Een nieuwe methode voor het lokaal introduceren van UV-schades laat zien dat mRAD18Sc en HR6B accumuleren op blootgestelde gebieden en dat dit onafhankelijk is van de fase van de celcyclus. Deze nieuwe methode maakt het eveneens mogelijk om de kinetiek van *de novo* assemblage van chromatine geassocieerde processen in levende cellen te bestuderen.

Het relatief hoge mRNA expressieniveau in de muizentestis en in het bijzonder in pachyteen spermatocyten duidt op een rol voor mRAD18Sc in spermatogenese. Antilichamen die tegen het mRAD18Sc polipeptide zijn gericht, werden gebruikt om de subcellulaire lokalisatie van mRAD18Sc in spermatogene cellen te bestuderen. De resultaten van deze studies worden in **Hoofdstuk 5** weergegeven. Het mRAD18Sc eiwit markeert de 'XY body' in pachyteen en diploten spermatocyten. De XY body is een subnucleaire structuur die bestaat uit de gedeeltelijk ongepaarde en transcriptioneel geïnactiverde X en Y chromosomen in de mannelijke meiotische profase. De afwezigheid van andere RDB eiwitten (UBC13 en pol η) en PCNA in de XY body geeft aan dat mRAD18Sc in meiose waarschijnlijk een rol speelt buiten de context van RDB. Tot slot vonden wij dat een hoge concentratie van mRAD18Sc eiwit correleert met laag niveau van RNA polymerase II, in de XY body en in andere ongepaarde chromosomale gebieden in primaire spermatocyten. Het mRAD18Sc eiwit is mogelijk betrokken bij een mechanisme dat ongepaard DNA transcriptioneel inactieveert tijdens meiotische profase.

In **Hoofdstuk 6** wordt de lokalisatie van geubiquitineerd histon H2A (ubi-H2A) op transcriptioneel geïnactiverde chromosomale gebieden tijdens meiose beschreven. Ubi-H2a vertoont een lokalisatiepatroon vergelijkbaar aan dat van mRAD18Sc in primaire spermatocyten. Tijdens het pachyteen loopt het mRAD18Sc

signaal voor op ubi-H2A markering in de XY body, en mRAD18Sc blijft ook langer aanwezig. Inactiviteit van ongepaarde chromosomale gebieden is een fenomeen dat zich ook in de vrouwelijke meiotische profase manifesteert. Daarom hebben wij immunoexpressie van mRAD18Sc en ubi-H2A met betrekking tot RNA polymerase II bestudeerd in oocyten van XO muizen en van XY^{tdym1} muizen, de laatstgenoemde met een omgekeerd geslacht vanwege een mutatie van het testisbepalende gen. Zowel mRAD18Sc als ubi-H2A lokaliseren op ongepaarde geslachtschromosomen in pachyteen XO en XY^{tdym1} (omgekeerd geslacht) oocyten die tevens geassocieerd zijn met een zeer lage concentratie van RNA polymerase II. In normale (XX) pachyteen oocyten is accumulatie van mRAD18Sc en ubi-H2A zelden zichtbaar, maar alleen in situaties waarin zich paringsproblemen voordoen. Fosforylering van histon H2AX is vereist voor vorming en inactiviteit van de XY body in spermatocyten. Wij hebben aangetoond dat deze modificatie ook voorkomt op ongepaarde chromosomale regio's in mannelijke en vrouwelijke meiose. Samen wijzen deze resultaten erop dat ongepaarde chromosomale regio's worden geïnactiveerd in zowel mannelijke als vrouwelijke meiotische profase. Dit mechanisme lijkt op 'Meiotic Silencing of Unpaired DNA' (MSUD), een definitie die gebruikt is om een gelijkwaardig fenomeen te beschrijven in *Neurospora crassa*. Accumulatie van ubi-H2A is een algemene eigenschap van inactief chromatine, en ubi-H2A markeert ook het transcriptioneel inactieve X chromosoom, genaamd Barr body, in vrouwelijke somatische cellen.

Het laatste **Hoofdstuk (7)** bespreekt het onderzoek in dit proefschrift als geheel en geeft verscheidene toekomstige onderzoeksrichtingen aan. De mogelijke functies van HR6A/B en mRAD18Sc in RDB worden beschreven, en verder worden suggesties gegeven voor studie van regulatie van RDB in levende cellen voornamelijk met *in vivo* fluorescentie technieken. Vervolgens worden functies van RDB eiwitten, en in het bijzonder mRAD18Sc, in gametogenese besproken. Het werk dat in dit proefschrift wordt beschreven, geeft enig inzicht van RDB in zoogdiercellen en verstrekt aanwijzingen voor functie van RDB eiwitten buiten de context van RDB, in het bijzonder voor MSUD in mannelijke en vrouwelijke gametogenese.

List of abbreviations

(6-4)PP	(6-4) pyrimidine-pyrimidone photoproduct
γ-H2AX	phosphorylated histone H2A
BER	base excision repair
Bp	base pair(s)
C/G/YFP	cyan/green/yellow fluorescent protein
CAF1	chromatin assembly factor 1
CCD	charge-coupled device
cDNA	complementary deoxyribonucleic acid
CPD	cyclobutane pyrimidine dimer
DA	damage avoidance
DSB	double strand break
DUB	deubiquitination enzyme
E1	ubiquitin-activating enzyme
E2	ubiquitin-conjugating enzyme
E3	ubiquitin ligase
EJ	end-joining
FACS	fluorescence activated cell sorting
FCS	fluorescence correlation spectroscopy
FLIM	fluorescence lifetime imaging
FLIP	fluorescence loss in photobleaching
FRAP	fluorescence recovery after photobleaching
FRET	Förster (fluorescence) resonance energy transfer
HA	hemagglutinin
HeLa	human cervix carcinoma cell line
HR	homologous recombination
HR6A/B	mammalian homologs of <i>S. cerevisiae</i> RAD6 (Ube2a/b in MGI and HUGO)
ICL	interstrand crosslink
kDa	kilodalton
LSM	laser scanning microscopy
Lys (K)	lysine residue
MEF	mouse embryonic fibroblast
MMR	mismatch repair
mRAD18Sc	mouse homolog of <i>S. cerevisiae</i> RAD18 (RAD18 in MGI and HUGO)
mRNA	messenger ribonucleic acid
MSUD	meiotic silencing of unpaired DNA
MSY	male specific region on the Y-chromosome
NA	numerical aperture
NER	nucleotide excision repair
NLS	nuclear localization signal
PAR	pseudoautosomal region
PCNA	proliferating cell nuclear antigen
PMT	photomultiplier tube
pol	polymerase
RAD	radiation sensitive
RDB	replicative damage bypass
RING	really interesting new gene
SC	synaptonemal complex
SUMO	small ubiquitin-related modifier
TCR	transcription coupled repair
TLS	translesion synthesis
Ubi	ubiquitin
UBP	ubiquitin-specific processing protease
UCH	ubiquitin carboxyl-terminal hydrolase
Ubi-H2A	ubiquitinated histone H2A
UV	ultraviolet
XPV	xeroderma pigmentosum variant

List of publications

Baarends, W. M., **van der Laan, R.**, and Grootegoed, J. A. (2000). Specific aspects of the ubiquitin system in spermatogenesis. *J. Endocrinol. Invest.* **23**, 597-604.

Van der Laan, R., Roest, H. P., Hoogerbrugge, J. W., Smit, E. M., Slater, R., Baarends, W. M., Hoeijmakers, J. H., and Grootegoed, J. A. (2000). Characterization of mRAD18Sc, a mouse homolog of the yeast postreplication repair gene RAD18. *Genomics* **69**, 86-94.

J.A. Grootegoed, **R. van der Laan**, H.P. Roest, W.M. Baarends (2000). Aspects moléculaires de la spermatogenèse: la réparation post-réplication de l'ADN et la système ubiquitine. *Andrologie* **10**, 239-242

Baarends, W. M., **van der Laan, R.**, and Grootegoed, J. A. (2001). DNA repair mechanisms and gametogenesis. *Reproduction* **121**, 31-39.

List of presentations

November 15 2001

Invited by Dr. Roger Woodgate

National Institutes of Health Section on DNA Replication, Repair and Mutagenesis,
Bethesda, MD, USA

Characterization of mRAD18Sc, the mammalian homolog of the yeast post replication repair gene RAD18

November 26 2002

Invited by Dr. Fumio Hanaoka

Institute for Molecular and Cellular Biology Osaka University
Osaka, Japan

The mRAD18Sc protein interacts with HR6B and localizes to UV induced DNA damages and replication foci

August 7 2003

Invited by Dr. Jan Vijg

The University of Texas Health Science Center at San Antonio Department of
Physiology
San Antonio, Texas, USA

The mRAD18Sc is highly expressed in pachytene spermatocytes and the mRAD18Sc protein interacts with HR6B protein at replication foci and UV induced DNA lesions in HeLa cells stably expressing GFP fusions

December 5 2003

Invited by Dr. Laura J. Niedernhofer

University of Pittsburgh Cancer Institute Hillman Cancer Center
Pittsburgh, PA, USA

Post-replication repair protein mRAD18Sc: Subcellular localization during spermatogenesis, UV damage repair and replication

List of meetings

November, 1999

American Society of Microbiology, **Conference on DNA Repair and Mutagenesis**, Hilton Head Island, SC, USA

May 2000

European Molecular Biology Organization, **workshop, Ubiquitin-proteasome pathway and cellular regulation**, Driebergen, The Netherlands

June 2000

Cold Spring Harbor Laboratory, **65th Symposium on Quantitative Biology "Biological Responses to DNA Damage"**, Cold Spring Harbor, NY, USA

Poster presentation: *Characterization of mRAD18Sc, a mouse homolog of the yeast post-replication repair gene RAD18*

January 2001

Gordon Research Conferences workshop, **Mammalian DNA Repair**, Ventura, CA, USA

Poster presentation: *The mRAD18Sc protein localizes to the sex body and forms foci after UV irradiation*

February 2001

Workshop DNA Repair Interplay with other Cellular Processes, Noordwijkerhout, The Netherlands

March 2002

Gordon Research Conferences, **workshop Mutagenesis and Carcinogenesis**, Ventura, CA, USA

Poster presentation: *The mRAD18Sc protein colocalizes with the HR6B protein at UV induced DNA lesions and replication foci*

April 2002

12th European Workshop on Molecular and Cellular Endocrinology of the Testis, Doorwerth, The Netherlands

Mini poster and oral presentation: *The mRAD18Sc protein localizes to the sex body and forms foci after UV irradiation*

August 2003

Microscopy and Microanalysis, San Antonio, TX, USA

Poster presentation: *Dynamics and interaction of the post replication repair proteins mRAD18Sc and HR6B*

Microbeam Analysis Society Distinguished Student Award

Microscopy Society of America Student Poster Award, Biological Applications of Microscopy and Microanalysis – First Place

List of courses

Radiation hygiene expertise level 5B, Award February, 1998

Interfaculty Reactor Institute, Delft University of Technology, Delft, The Netherlands

Laboratory animal skills course Art. 9, Award November, 1998

Erasmus University Rotterdam, The Netherlands

Oncogenesis and Tumor Biology, May, 1999

Safe Laboratory Techniques, May, 1999

DNA damage, DNA Repair and Biological Consequences, February, 2000

Medical Genetics Center and Molecular Medicine postgraduate school, Rotterdam and Leiden, The Netherlands

The Oxford Examination in English as a Foreign Language, Award May 2000

University of Oxford, Delegacy of Local Examinations, Oxford, United Kingdom

EMBO Practical Course Light microscopy of live specimens, May, 2002

European Molecular Biology Laboratory, Heidelberg, Germany

Joint A-IMBN/EMBO Course on Fluorescence Microscopy of Living Cells,

November, 2002

Kansai Advanced Research Center, Kobe, Japan

Curriculum vitae

Roald van der Laan was born on November 6th 1973 in Tholen, the Netherlands. He graduated in 1993 from secondary school (VWO), the 'Regional Comprehensive School 't Rijks', Bergen op Zoom, the Netherlands. The same year he began a bachelors degree program in biochemistry and microbiology at the laboratory school 'Hogeschool West Brabant', Etten-Leur, the Netherlands, which was completed in 1997. As part of this degree, he participated in a one year practical training period entitled 'Post replication repair', in the Department of Cell Biology and Genetics (Erasmus MC, Rotterdam, The Netherlands) under supervision of Dr. Jan H.J. Hoeijmakers and Dr. Henk P. Roest in close collaboration with the Department of Reproduction and Development (Erasmus MC, Rotterdam, under supervision of Dr. J. Anton Grootegoed and Dr. Willy M. Baarends).

Subsequently, Roald obtained his Masters degree in Biology in 1999 from Leiden Univeristy. During this program, he trained in two laboratories. First, again with Dr. Jan H.J. Hoeijmakers at Erasmus MC, cloning and expressing *mRAD18Sc*, a mouse homolog of the yeast post replication DNA repair gene *RAD18*. Second, at the Evolutionary Biology Section of the Biology Institute at Leiden University, Leiden, the Netherlands (under the supervision of Dr. Paul M. Brakefield) studying sperm competition in the African butterfly *Bicyclus anynana*. In addition, he traveled to Uganda, East Africa to follow a five week course on tropical biology organized by the Tropical Biology Association, Cambridge, UK. Roald also participated in a five week exchange program between Leiden University and Kent State University, Kent, Ohio, USA. The short research project entitled 'Intracytoplasmic sperm injection in the mouse' was supervised by Dr. Douglas Kline at Department of Biological Sciences, Kent State University.

From April 1999 to October 2003, Roald conducted his Ph.D. studies entitled 'mRAD18Sc: a multifunctional protein in replicative damage bypass and gametogenesis' in the Department of Cell Biology and Genetics (Erasmus MC) under the supervision of Dr. Jan H.J. Hoeijmakers and Dr. Henk P. Roest and in the Department of Reproduction and Development (Erasmus MC) under the supervision of Dr. J. Anton Grootegoed and Dr. Willy M. Baarends.

In January 2004 a grant application for a UICC International Cancer Technology Transfer Fellowship was awarded by the International Union Against Cancer (UICC) for the project entitled 'Local induction of interstrand crosslinks using a multiphoton laser'. In April 2004, Roald went to the University of Pittsburgh Cancer Institute to begin this fellowship. The project was supervised by Dr. Laura J. Niedernhofer (Department of Molecular Genetics and Biochemistry, University of Pittsburgh, Pittsburgh, PA, USA).

Acknowledgements

Finally, I came to the last page of my thesis. Before I stop touching the keyboard of my laptop computer, I would like to thank many people who contributed to the realization of my thesis.

First of all, I am very grateful to my 'promotor' Prof. dr. Jan H.J. Hoeijmakers. Dear Jan, I thank you for your endless enthusiasm in particular for new innovative technology, and a fantastic instructive period under your supervision. Furthermore, I am very obliged to Prof. dr. J. Anton Grootegoed. Dear Anton, I thank you for the enormous amount of time you invested in my thesis and the opportunity to write a review together. Next, I am very grateful to my two 'copromotors' Henk and Willy. Dear Henk, you supervised me from the very beginning when I walked into the medical faculty as a naïve (but opinionated) student and I would like to thank you for your patience and everything that you taught me in all those years. In addition, I enjoyed our conversations about soccer and trips to 'de Kuip' a lot. I wish you all the best in your current position and if I ever want to know something about transplantation surgery, I will definitely knock on your door. Dear Willy, I also learned a great deal from you, especially that there is so much more to spermatogenesis than is generally known. I would like to wish you all the best in the future and I will keep looking on PubMed to learn what else you will do with the sex body. Finally, this thesis, as you see it now, would not exist without all of your aid. Many thanks to you all for going through those piles of paper that I dumped into your offices.

The research outlined in this thesis would not have been possible without the help of several people especially Dr. Gert A. van Cappellen. Dear Gert, you taught me everything about confocal microscopy and I would like to thank you for your enormous input in my project and spending all those hours with me behind the confocal. Furthermore, I would like to thank two additional fluorescence enthusiasts, Dr. Wim Vermeulen and Dr. Adriaan B. Houtsmuller. Wim, the first GFP vector I got from you and as you can see, I made extensive use of it. Thank you for your help with writing the GFP manuscript. Dear Adriaan, thank you for your stimulating scientific support and I really enjoyed the sake and fugu in Kobe, Japan.

Special thanks to many people for their scientific contribution. Without your input, the number of figures presented in this thesis would be dramatically decreased. Evert-Jan, my fellow PhD student, I appreciate our extensive collaboration very much and I look forward to your thesis. Shehu, thank you for introducing me to FCS, and I wish you success with your own PhD. Dear Evelyne, Jos, Hanny, Yvette, Esther, Yvonne, Jorie thank you for all your essential experimental help. And, I am very happy with my 'paranymphs', Evelyne and Yvette, I could not wish for better help. Furthermore, I would like to acknowledge my lab mates, Alex, Magda, Esther, Jan, Michel, Marja and Mark, for their support, the friendly lab atmosphere and lots of fun. I apologize if I have forgotten a lot of names, but this is a consequence of traveling between 6 labs on 4 floors. I would like to thank everybody that spent some time in labs 730, 575, 585, 1058, 1069 and 659. Next, I would like to thank all my colleagues from the department of Cell Biology and Genetics, the department of Reproduction and Development and the former department of Endocrinology and Reproduction. In particular, I am very grateful to Tom de Vries Lentsch. Dear Tom your effort in providing the layout of this thesis was indispensable. Finally, Jasperina, Marieke and Rita from the secretariat, thank you for your happy smiles

and organizing my travels.

In the last section I would like to thank my family and friends for their support and interest in everything I am doing. The last sentence is for you Léonie, thank you for always being there.

It was fun,

Roald

